Electronic Thesis and Dissertation Repository

8-8-2016 12:00 AM

Assisted Reproductive Technologies Disrupt Genomic Imprinting in Human and Mitochondria in Mouse Embryos

Carlee R. White
The University of Western Ontario

Supervisor
Dr. Mellissa Mann
The University of Western Ontario

Graduate Program in Biochemistry
A thesis submitted in partial fulfillment of the requirements for the degree in Doctor of Philosophy
© Carlee R. White 2016

Abstract

Infertile couples worldwide use assisted reproductive technologies (ARTs) to help conceive their own biological child. Due to the rising use of ARTs, there is continual emergence of new techniques implemented in human fertility clinics. When treatment is successful, there is an increased risk even within singletons for perinatal complications including preterm birth, intrauterine growth restriction, low and high birth weight and genomic imprinting disorders Beckwith Wiedemann Syndrome, Angelman Syndrome, and Silver-Russel Syndrome. Consequently, there is a need to investigate the effects of these treatments on the manipulated oocyte and preimplantation embryo. To address this, I first analyzed the combined effects of multiple ARTs on imprinted DNA methylation in human day 3 (6 to 8 cells) and blastocyst-stage embryos. As imprinted DNA methylation is acquired during gametogenesis and maintained throughout preimplantation development, I hypothesized that ARTs disrupt this regulation in donated, good quality, human preimplantation embryos. I observed that seventy-six percent of day 3 embryos and fifty percent of blastocysts exhibited perturbed imprinted methylation at the *SNRPN*, *KCNQ1OT1* and/or *H19* domains. This frequency was similar to that previously observed in the mouse, and importantly demonstrated that extended culture did not pose a greater risk for imprinting errors. Overall, human preimplantation embryos generated with ARTs possessed a high frequency of imprinted methylation errors. Next, I hypothesized that a single, indispensible ART treatment, ovarian stimulation, disrupts mitochondria in mouse oocytes and preimplantation embryos. Ovarian stimulation led to a decreased total and active mitochondrial pool in high hormone-treated oocytes, and an increase in the percentage of oocytes displaying mislocalization of active mitochondria. Although the total mitochondrial pool was unchanged in hormone-treated preimplantation embryos compared to controls, the active mitochondrial pool was decreased in hormone-treated 1-cell, 2-cell, morula and blastocysts. Ultimately, the lower active mitochondrial pool in treated embryos was associated with a decreased percentage of outer blastomeres containing high amounts of active mitochondria in morula and blastocysts. In blastocysts, this was associated with increased superoxide levels. Overall, my results provide novel insight onto ARTs-induced disruption of imprinted DNA methylation and mitochondria in human and mouse preimplantation embryos, respectively.

Keywords

Assisted reproductive technology, genomic imprinting, mitochondria, superovulation, ovarian stimulation, oocyte, preimplantation embryo, mouse, human

Co-Authorship Statement

Chapter 2: White, C. R., Denomme, M.M., Tekpetey, F. R., Feyles, V., Power, S.G.A., and Mann, M.R.W. (2015). High Frequency of Imprinted Methylation Errors in Human Preimplantation Embryos, Sci Rep 5, 17311.

I completed all experimental work, analyzed data and wrote manuscript.

Dr. Michelle M. Denomme thawed the human preimplantation embryos and provided assistance with the single embryo bisulfite experiments.

Dr. Francis R. Tekpetey provided clinical samples and patients' data, coordinated the patient consent process and contributed to scientific discussion

Dr. Valter Feyles provided clinical samples and contributed to scientific discussion

Dr. Stephen G.A. Power participated in study design, provided clinical samples and participated as clinical PI

Dr. Mellissa R.W. Mann designed and supervised research, interpreted data, participated as PI, coordinated the research study and wrote manuscript. All authors reviewed and approved the manuscript.

Chapter 3: Carlee R. White and Mellissa R.W. Mann. Superovulation disrupts mitochondria in mouse oocytes and preimplantation embryos, manuscript in preparation.

I completed all of the experimental work in this project.

Dr. Mellissa Mann conceived the project and experiments.

Acknowledgments

First I would like to acknowledge my supervisor, Dr. Mellissa Mann. Thank you for your guidance, your open door, your conversations about research and about life, and thank you for all of the opportunities you have provided me with. You have challenged me to achieve more out of my PhD than I thought imaginable, and for that I will be forever grateful.

I would also like to acknowledge the members of my graduate committee: Dr. David Rodenhiser, Dr. Victor Han and Dr. Gerald Kidder. Thank you for your insightful discussions and critical analyses of my results. Thank you for all of your ideas that have guided me throughout the past five years. A special thanks to Dr. David Rodenhiser, not only for reading and editing my thesis but also for your open door, especially this past year.

To the past and present members of the Mann Lab, thank you for your friendship, discussions, ideas, and understanding. A special thank you to Dr. Michelle Denomme, for her training and friendship at the beginning of my graduate career, and to Dr. Will Macdonald, for his constant willingness to lend a helping hand.

Lastly, I would like to thank my family, for their continued support and love since the very beginning. Thank you for believing in me and helping me succeed. And to my fiancé Brian Bates, thank you for your understanding, your support through all of the late nights and early mornings, for standing beside me and being my soundboard during all of the ups and downs.

Ethics Approval

Chapter 2: Research ethics approval was obtained through the Western University's Health Science Research Ethics Board (102659) and the methods were carried out in accordance with the approved guidelines. Informed consent was obtained from patients donating embryos and non-patient adults providing buccal cell samples.

Chapter 3: Experiments were performed in compliance with the guidelines set by the Canadian Council for Animal Care and the policies and procedures approved by the University of Western Ontario Council on Animal Care.

Table of Contents

List of Tables

List of Figures

List of Abbreviations

%	Percent
ºC	Degrees Celsius
5caC	5-carboxylcytosine
5fC	5-formylcytosine
5hmC	5-hydroxymethylcysosine
5mC	5-methylcytosine
A	Abnormal
ACL	ATP-citrate lyase
ADB	Antibody dilution buffer
AMA	Advanced maternal age
ANOV	Anovulatory
ARTs	Assisted reproductive technologies
AS	Angelman Syndrome
AS-IC	Angelman Syndrome imprinting centre
Ascl2	Achaete-scute complex homolog 2
Asym	Asymmetric
AUGMENT	Autologous germline mitochondrial energy transfer
B	Blastocyst
B6	C57BL/6
B6(CAST7p6)	C57BL6/CAST7p6
BADH	Betaine aldehyde dehydrogenase
BER	Base excision repair
BHMT	Betaine-homocysteine methyltransferase
BM	Blastocyst Medium
Brav	Bravelle® (Urofollitropin)
Bravelle®	Urofollitropin
BTO	Bilateral tubal obstruction/occlusion
Bu	Buccal cell
BW	Birth weight
BWS	Beckwith Wiedemann Syndrome
C	Cleavage
CAST	*Castaneus*
Cd81	CD81 antigen
Cdkn1c	Cyclin-Dependent Kinase Inhibitor 1C (P57, Kip2)
CH_3	Methyl group
CHDH	Choline dehydrogenase
CTCF	CCCTC-binding factor (zinc finger protein)
Ctrl	Control
DMG	Dimethylglycine
DNMT	DNA methyltransferase
CoQ10	Coenzyme Q10
dpc	Days post coitus/coitum
dpp	Days post partum
DPPA3	Developmental pluripotency associated factor 3
E_2	Estrogen

E8.0	Embryonic day 8.0
eCG	Equine chorionic gonadotropin
EHMT	Euchromatic histone lysine methyltransferase
ELBW	Extremely low birth weight
ENDO	Endometriosis
eSET	Elective single embryo transfer
ET	Embryos transferred
FAD$^+$	Flavin adenine dinucleotide
FBS	Fetal Bovine Serum
FDA	Food and Drug Agency
Fert	Fertinorm® (Urofollitrophin)
FPES	Fresh/frozen percutaneous epididymal/testicular sperm aspiration
Frat3	Frequently rearranged in advanced T-cell lymphomas 3
G-F	Gonal-F® (Follitropin-alpha)
gDMR	Germline differentially methylated region
Gonal-F®	Follitropin-alpha
GVBD	Germinal vesicle breakdown
H1	Histone 1
H2A	Histone 2A
H2AK119	Histone 2A Lysine 119
H2B	Histone 2B
H2BK120	Histone 2B Lysine 120
H3	Histone 3
H3K27me3	Histone 3 Lysine 27 trimethylation
H3K36me3	Histone 3 Lysine 36 trimethylation
H3K4me2	Histone 3 Lysine 4 dimethylation
H3K4me3	Histone 3 Lysine 4 trimethylation
H3K9me2	Histone 3 Lysine 9 dimethylation
H3K9me3	Histone 3 Lysine 9 trimethylation
H3S10	Histone 3 Serine 10
H4	Histone 4
H4K20me3	Histone 4 Lysine 20 trimethylation
HATs	Histone acetyltransferases
hCG	Human chorionic gonadotropin
HDACs	Histone deacetylases
HDMs	Histone demethylases
hESCs	Human embryonic stem cells
ICM	Inner cell mass
ICRs	Imprinting control regions
ICSI	Intracytoplasmic sperm injection
IDIO	Idiopathic
Igf2	Insulin-like growth factor 2
Ins2	Insulin II
Ip	Intraperitoneally
Ipw	Imprinted in Prader-Willi Syndrome
IVF	*In vitro* fertilization
Kcnq1	Potassium voltage-gated channel, subfamily Q, member 1
KCNQ1OT1	*KCNQ1 overlapping transcript 1*

KRAB-ZFPs	KRAB-containing zinc finger proteins
KS	Kolmogorov-Smirnov
LBW	Low birth weight
lncRNA	Long noncoding RNA
Lup	Lupron® (Leuprolide Acetate)
Magel2	Melanoma antigen-like 2
MAR3	Matrix attachment region 3
Mat	Maternal
MAT	Methionine transferase
Men	Menopur® (Menotropins)
Methylene THF	Methylene tetrahydrofolate
MF	Male factor
MI	Metaphase I
MII	Metaphase II
Mkrn3	Makorin ring finger protein 3
MRT	Mitochondrial replacement therapy
MTHFR	Methylene tetrahydrofolate reductase
N	Normal
N-terminal	Amino (N)-terminal
Na^+/K^+-ATPase	Sodium-potassium adenosine triphosphatase
NAD^+	Nicotinamide adenine dinucleotide
NBW	Normal birth weight
ncRNA	Non-coding RNA
Ndn	Necdin
NGS	Normal goat serum
Org	Orgalutran® (Ganirelix Acetate)
Orgalutran®	Ganirelix Acetate
Osbpl5	Oxysterol binding protein-like 5
P0.5	Postnatal day 0.5
P1	Preimplantation stage 1
Pat	Paternal
PB	Polar body
PBS	Phosphate-Buffered Saline
PCOS	Polycystic ovarian syndrome
Peg1	Paternally expressed gene 1
Peg10	Paternally expressed gene 10
Peg3	Paternally expressed gene 3
PGC	Primordial germ cells
PGD	Preimplantation genetic diagnosis
Phlda2	Pleckstrin homology-like domain, family A, member 2
PN3	Pronuclear stage 3
Pur	Puregon® (Follitropin-beta)
PWS	Prader-Willi Syndrome
PWS-IC	Prader-Willi Syndrome IC
Rasgrf1	Ras Protein-Specific Guanine Nucleotide-Releasing Factor 1
Rep	Repronex® (Menotropins)
RFU	Relative fluorescence units
RNAi	RNA interference

ROI	Region of interest
ROS	Reactive oxygen species
RTG	Ready-To-Go
SAM	S-adenosylmethionine
SEM	Standard error of the mean
SETDB1	SET domain bifurcated 1
SHMT	Serine hydroxymethyltransferase
slC	slight C
Slc22a18	Solute carrier family 22, member 18
SNP	Single nucleotide polymorphism(s)
Snrpn/SNRPN	*Small nuclear ribonucleoprotein N*
Snrpnlt	*Snrpn* lncRNA transcript
Snurf-Snrpn	*Snrpn* upstream reading frame-*Snrpn*
SRS	Silver-Russell Syndrome
Sym	Symmetric
Syn	Synarel® (Nafarelin)
Synarel®	Nafarelin
TCA	Tricarboxylic acid
TCART	Toronto Centre for Advanced Reproductive Technology
TD	Tubal disease
TDG	Thymine-DNA glycosylase
TE	Trophectoderm
TET	Ten eleven translocation
TET1, TET2	Ten-eleven translocation 1 and 2
Th	Tyrosine-hydroxylase
THF	Tetrahydrofolate
TOM20	Translocase of outer membrane 20
TRIM28	Tripartite motif 28 protein
Tssc4	Tumor-suppressing subchromosomal transferable fragment 4
Ube3a-as	*Ube3a* antisense transcript
Ube3a/UBE3A	Ubiquitin protein ligase E3A
UHRF1	Ubiquitin-like with PHD and ring finger domain 1
UK	United Kingdom
UPDs	Uniparental disomies
VLBW	Very low birth weight
XIST	X-inactive specific transcript
ZFP57	Zinc finger protein 57

Chapter 1

1   Introduction

1.1   Epigenetics

1.1.1   General Introduction

The term epigenotype was originally proposed by CH Waddington (1905-1975) to represent the whole complex of developmental processes that form the connection between genotype and phenotype (Waddington, 2012). Waddington also suggested that the name 'epigenetics' be used for the studies aimed at discovering the mechanisms behind the epigenotype. In this context, epigenetics governs numerous developmental processes, including cellular differentiation, where cells with identical genotypes exhibit distinct patterns of gene expression and consequently, cellular function (Goldberg et al., 2007).

The modern definition of epigenetics is a heritable mechanism of transcriptional control that does not involve a change to the DNA sequence (Rodenhiser and Mann, 2006). Epigenetic changes that influence gene expression act by modifying overall chromatin structure. This is accomplished by the addition of covalent and/or non-covalent modifications to the histone proteins (1.1.2) and DNA sequence (1.1.3) contained within the nucleosome. Such modifications act to change the local microenvironment by modifying charge or affecting binding of regulatory proteins. Additionally, long non-coding RNAs have also been identified to play an epigenetic role in mediating gene expression (1.1.4). Epigenetic changes to the chromatin that lead to condensation will render a gene as silent or inactivated, whereas activating modifications generating open (decondensed) chromatin will lead to gene activation or render a gene poised for expression (Goldberg et al., 2007; Rodenhiser and Mann, 2006). Overall, it is only fitting that the study of these modifications be referred to as epi- (translating to "above") genetics.

1.1.2   Histone Modification

Chromatin is composed of DNA (147 base pairs) wrapped around a core octamer of histone proteins to generate a nucleosome structure. The histone protein octamer is comprised of 2 molecules each of histone 2A (H2A), histone 2B (H2B), histone 3 (H3) and

histone 4 (H4). Linker DNA connects nucleosomes together to form chromatin, which can be further compacted by incorporation into polynucleosome fibers that are stabilized by histone 1 (H1) binding (Quina et al., 2006).

Chromatin can be modified to form heterochromatin, which is highly condensed and contains transcriptionally inactive genes, or euchromatin, which is decondensed and contains actively transcribed genes (Quina et al., 2006; Rodenhiser and Mann, 2006). Chromatin compaction and decompaction is controlled through post-translational modification to histone tails. Specifically amino (N)-terminal tails protrude from the nucleosome and are modified to affect inter-nucleosomal interactions in addition to recruiting chromatin-remodeling enzymes that are involved in nucleosome repositioning (Bannister and Kouzarides, 2011). Different classes of modifications identified on histone tails include but are not limited to acetylation, phosphorylation, lysine and arginine methylation, ubiquitylation, sumoylation and deimination (Kouzarides, 2007). Among these modifications, acetylation, phosphorylation and methylation are the most commonly studied. Histone acetylation neutralizes positive charges, disrupting the stabilizing interactions between DNA and histone proteins, which leads to open chromatin conformation (Bannister and Kouzarides, 2011; Campos and Reinberg, 2009). This functions similarly to serine, threonine and tyrosine phosphorylation, which adds negative charge to the histone structure and leads to gene activation (Bannister and Kouzarides, 2011). In contrast, the covalent addition of methyl groups to amino acids does not alter histone charge, and lysine residues subjected to methylation can be mono-, di-, or tri-methylated while arginine residues can be mono- or di-methylated (Bannister and Kouzarides, 2011). Histone methylation can be activating or repressive depending on the residue onto which it is deposited on the histone tail.

In general, active modifications to histone tails include histone acetylation (Bernstein et al., 2005; Kim et al., 2005; Roh et al., 2005), H3K4 di- and tri-methylation (H3K4me2 and H3K4me3) (Barski et al., 2007; Bernstein et al., 2002; Lauberth et al., 2013; Ruthenburg et al., 2007), H3K36me3 (Bannister et al., 2005; Barski et al., 2007), H2BK120 ubiquitylation (Thorne et al., 1987; Zhu et al., 2005) and H3S10 phosphorylation (Anest et al., 2003; Sassone-Corsi, 1999). In contrast, transcriptional repression is generally accompanied by lack of histone acetylation (Bannister and Kouzarides, 2011), H3K9me2 and H3K9me3

(Bannister et al., 2001; Barski et al., 2007), H3K27me3 (Barski et al., 2007; Boyer et al., 2006; Lee et al., 2006; Roh et al., 2006), H4K20me3 (Kalakonda et al., 2008; Kourmouli et al., 2004), H2AK119 ubiquitylation (Wang et al., 2004a), deimination of H3 and H4 arginine to citrulline (Cuthbert et al., 2004; Wang et al., 2004b), and sumoylation (Nathan et al., 2006; Shiio and Eisenman, 2003). Overall, the combined effects of multiple active or repressive histone modifications will partition the genome into areas of euchromatin and heterochromatin, respectively (Figure 1-1).
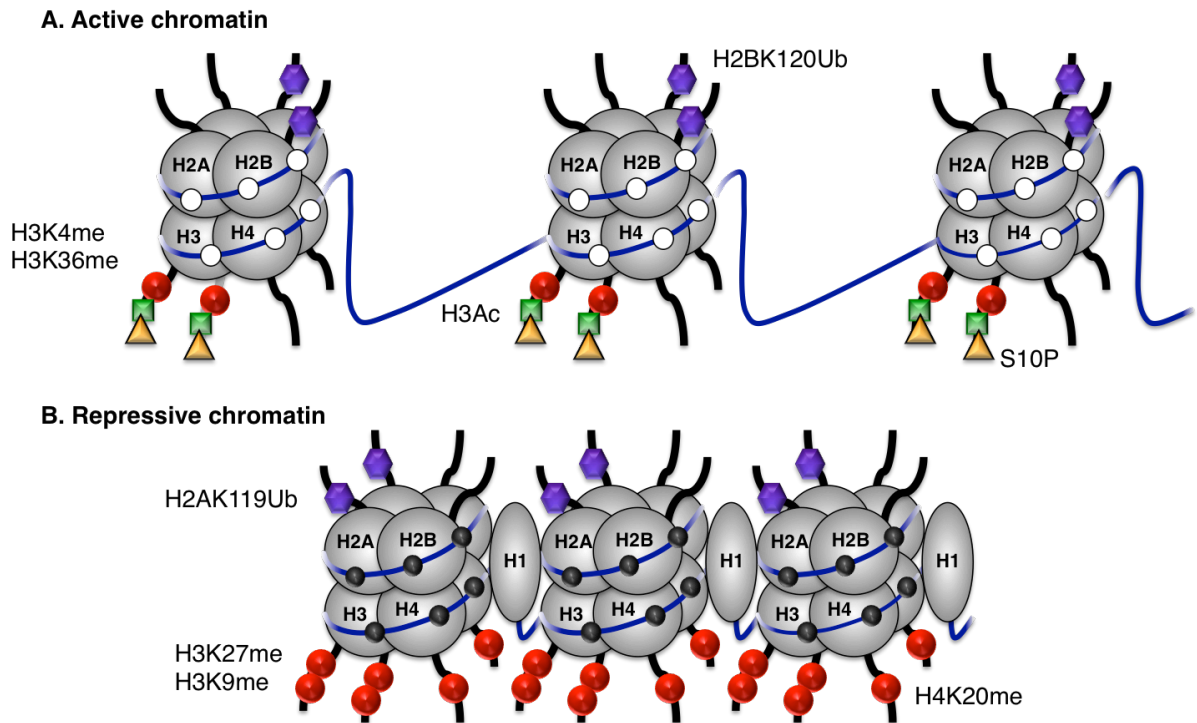
Figure 1-1: Activating and repressive histone modifications

Each nucleosome is composed of 147 bp of DNA (blue lines) wrapped around a protein octamer containing 2 molecules of histone 2A (H2A), H2B, H3 and H4 (grey circles). Linker DNA is shown as a blue line. Active chromatin modifications (A) to N-terminal histone tails (wavy black lines) include H3K4 methylation (H3K4me2, H3K4me3), H3K36me3 (red circles), H3 and H4 acetylation (H3Ac, green squares), H3S10 phosphorylation (orange triangles), ubiquitinated H2BK120 (purple octagons) and unmethylated CpGs (small white dots). Repressive modifications (B) include H3K9me2/3, H3K27me3, H4K20me3 (red circles), ubiquitinated H2AK119 (purple octagons) and methylated CpGs (black dots). Each nucleosome in repressive chromatin is linked by histone H1 (grey oval) and linker DNA (blue line).

1.1.3   DNA Methylation

DNA methylation is the most widely studied epigenetic modification that controls gene expression.   DNA methylation occurs at cytosine residues primarily within CpG dinucleotides.   DNA methyltransferase (DNMT) enzymes regulate the acquisition and maintenance of 5-methylcytosine (5mC). Specifically, the *de novo* DNMTs, DNMT3A and DNMT3B (Okano et al., 1999), catalyze the establishment of 5mC at unmethylated cytosines along with cofactor DNMT3L (Hata et al., 2002), whereas DNMT1 is the maintenance methyltransferases that binds to hemi-methylated DNA during replication to maintain 5mC on daughter strands (Figure 1-2). The cofactor UHRF1 (ubiquitin-like with PHD and ring finger domain 1; NP95) recognizes hemi-methylated DNA at the replication fork and recruits DNMT1 to these sites (Arita et al., 2008; Rottach et al., 2010; Sharif and Koseki, 2011; Sharif et al., 2007). Mutations in DNMTs lead to early embryonic lethality (Li et al., 1992; Okano et al., 1999). CpG methylation controls gene expression by altering association with chromatin binding proteins and transcriptional regulatory factors.

In general, CpG dinucleotides are infrequent within the genome (roughly 28 million CpGs exist within the human genome), and less than 10% occur in dense regions identified as CpG islands (Smith and Meissner, 2013). CpG islands generally occur at transcriptional start sites of housekeeping and developmental regulatory genes and are largely unmethylated. However, CpG island methylation is essential for processes including chromosome alignment, stabilization and integrity, silencing of repetitive elements, X-chromosome inactivation and acquisition and maintenance of genomic imprinting (Smith and Meissner, 2013). It is important to note that the number of CpG islands per haploid genome and their genomic positions (intergenic, intragenic, transcriptional start sites) are conserved between mouse and human, indicating functional significance (Deaton and Bird, 2011; Illingworth et al., 2010).
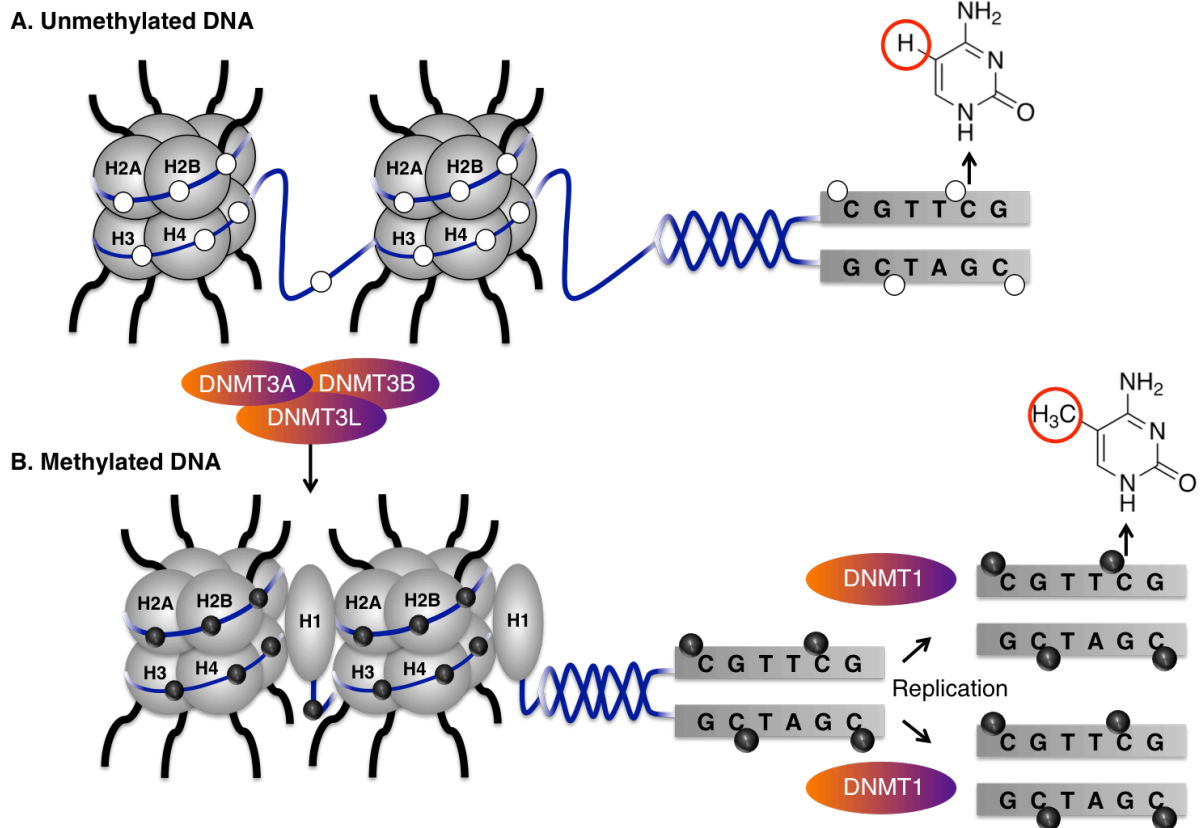
Figure 1-2: DNA methylation

Unmethylated CpG dinucleotides (white circles) within active euchromatic regions can be *de novo* methylated by DNMT3A/DNMT3B and cofactor DNMT3L to generate a repressive chromatin structure composed of methylated CpGs (black circles). DNA methylation is maintained during replication by DNMT1 and UHRF1. The difference between cytosine and methylated cytosine, circled in red, is the addition of a methyl (CH$_3$) group to the 5th carbon in the pyrimidine ring.

While DNMTs establish DNA methylation at CpG dinucleotides, counteracting mechanisms of DNA demethylation exist to remove methylation marks. DNA demethylation can occur passively in a replication-dependent manner via loss of DNMT1 maintenance, or through active DNA demethylation catalyzed by the ten eleven translocation (TET) family of dioxygenases. TET proteins specifically catalyze oxidation of 5mC to 5-hydroxymethylcysosine (5hmC) and subsequently generate 5-formylcytosine (5fC) and 5-carboxylcytosine (5caC) (Gu et al., 2011; Inoue and Zhang, 2011; Inoue et al., 2011). This is then followed by replication-dependent loss to unmethylated cytosine (Inoue and Zhang, 2011), although it has also been shown that 5caC can be excised via the thymine-DNA glycosylase (TDG)-mediated base excision repair (BER) pathway (He et al., 2011).

1.1.4   Non-coding RNA

Approximately 70-90% of the genome is transcribed into non-coding RNA (ncRNA) molecules greater than 100 nucleotides in length (Lee, 2012). These ncRNAs have recently been shown to play a role in epigenetic regulation. RNA-mediated epigenetic control has primarily been observed during X-inactivation (mediated by X-inactive specific transcript *(XIST)* ncRNA), genomic imprinting (imprinted ncRNAs) and gene silencing by RNA interference (RNAi) (Bernstein, 2005; Goldberg et al., 2007). Evidence suggests that ncRNAs function by providing a scaffold to recruit protein complexes that catalyze the addition of DNA and histone modifications to a specific genomic location (Khalil et al., 2009; Koziol and Rinn, 2010; Mercer and Mattick, 2013). This recruitment can occur in *trans*, whereby chromatin proteins are guided to multiple sites spread across the genome (Rinn et al., 2007), or in *cis*, such as at imprinted domains (Mohammad et al., 2009; Nagano et al., 2008; Zhang et al., 2014) and the inactive X-chromosome (Pinter et al., 2012; Wutz, 2011), where chromatin-modifying enzymes are thought to be recruited to modify their surrounding epigenetic neighborhood. In addition to protein recruitment, ncRNAs can regulate expression by mediating intrachromosomal loop formation (Zhang et al., 2014). Finally, studies at imprinted domains suggest that transcription of long ncRNAs (lncRNA) though antisense promoters, rather than the lncRNA itself, mediates gene expression through transcriptional interference mechanisms (Golding et al., 2011; Latos et al., 2012; Pauler et al., 2007; Santoro and Pauler, 2013). Overall, the ability for ncRNAs to mediate gene expression provides an additional layer of targeting specificity to epigenetic gene regulation.

1.2   Genomic Imprinting

1.2.1   General Introduction

Genomic imprinting is a consequence of epigenetic gene regulation whereby expression of a gene is restricted to one parental allele (Bartolomei and Ferguson-Smith, 2011).   Imprinting was originally discovered through experimental work aimed at understanding failed mammalian parthenogenesis (Kaufman et al., 1977).   Elegant pronuclear transplantation studies demonstrated that gynogenetic diploid embryos derived from two maternal pronuclei can develop up to 10 days post coitus (dpc). However, these embryos exhibit extremely poor development of extraembryonic lineages with relatively normal embryonic development (Barton et al., 1984; McGrath and Solter, 1983; 1984; Surani et al., 1984).   In contrast, androgenetic embryos with two paternal genomes have well-developed extraembryonic tissues but exhibit poor embryonic development, dying shortly after implantation (Barton et al., 1984; McGrath and Solter, 1983; 1984; Surani et al., 1984). Both genetic conditions are lethal.   Consequently, it was established that maternal and paternal contributions to embryo development are functionally non-equivalent, as both parental genomes are required for complete embryogenesis.   This developmental failure has been attributed to the absence or overexpression of imprinted genes.

To identify and map the specific chromosomal regions that are subjected to parental-specific regulation, reciprocal translocation experimentation was used to produce mice with uniparental disomies (UPDs) (Cattanach, 1986; Cattanach and Kirk, 1985; Searle and Beechey, 1978; 1990).   For example, mice with maternal UPD for the central region of chromosome 7 (7qB5) exhibit hypotonia, poor suckling response and postnatal lethality between days 3-8, while paternal UPD for the same region produces postnatal growth restriction, hyperactivity and brain pathologies (Gabriel et al., 1999; Leff et al., 1992; Tsai et al., 1999).   In humans, regions syntenic to those in mouse produce pathological disorders known as imprinting syndromes. Maternal and paternal deletions and UPD for 15q11-13 result in Prader-Willi Syndrome and Angelman Syndrome, respectively, producing similar pathologies to that seen for mouse 7qB5 (Knoll et al., 1989; Nicholls et al., 1989). These and other UPDs further demonstrate the non-equivalence of parental contributions.

1.2.2   Imprinted domains

The discovery of the first imprinted genes in 1990-1991 (Bartolomei et al., 1991; DeChiara et al., 1990) paved the way for subsequent identification of numerous imprinted genes in both mouse and human. Imprinted genes often reside in clusters that are regulated by a germline CpG island differentially methylated region (gDMR) [reviewed in (Macdonald and Mann, 2014)]. A subset of gDMRs have been identified as imprinting control regions (ICRs), since experimental or congenital gDMR deletions cause loss of imprinted gene expression (Spahn and Barlow, 2003). Differential chromatin modifications at the gDMR, including CpG methylation, modulate allelic expression (Macdonald and Mann, 2014) (Figure 1-3). In the mouse, there are 24 known imprinted gDMRs: 21 are maternal-in-origin, where DNA methylation is established on the maternal alleles during oogenesis; while 3 are paternal-in-origin, where DNA methylation is acquired on paternal alleles during spermatogenesis (Macdonald and Mann, 2014). These differential methylation marks are subsequently maintained throughout preimplantation development (discussed in detail in section 1.3). Of the 24 mouse gDMRs, 17 exhibit differential methylation in human gametes and/or tissues, 1 has no human orthologue and 6 have not been fully ascertained. Examples of conservation include mouse chromosome 7 and human chromosome 11p15.5, which harbor the *H19* and *KCNQ1OT1* (*KCNQ1 overlapping transcript 1*) imprinted domains (Mancini-DiNardo et al., 2003; Pandey et al., 2008; Srivastava et al., 2000), and mouse chromosome 7 and human chromosome 15q11-13 that contain the *Small nuclear ribonucleoprotein N* (*SNRPN*) domain (Bourc'his et al., 2001; El-Maarri et al., 2001; Geuns et al., 2003; Horsthemke, 1997; Shemer et al., 1997; Yang et al., 1998). These domains will be discussed below. Importantly, abnormal CpG methylation levels at the ICRs of these domains leads to genomic imprinting disorders.
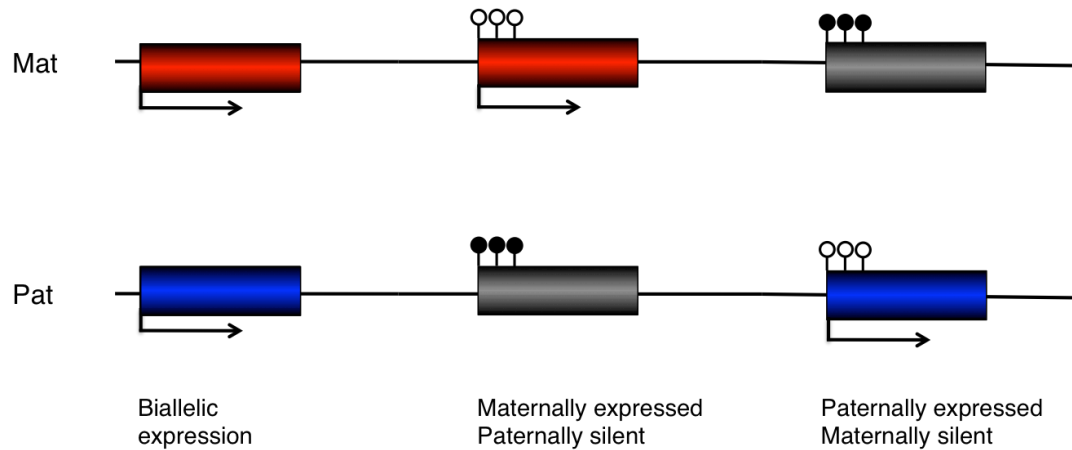
Figure 1-3: Genomic imprinting

Expression of most genes occurs biallelically (red box; maternal expression, blue box; paternal expression). Imprinted genes can be maternally-expressed and paternally-silent (grey box; silenced allele), or paternally-expressed and maternally-silent. Generally, methylated CpGs (filled black circles) mark the silent allele, whereas unmethylated CpGs (unfilled white circles) occur on the expressed allele.

1.2.2.1   *H19* imprinted domain

The *H19* imprinted domain was one of the first imprinted regions identified (Bartolomei et al., 1991) and is currently one of the best characterized. It resides on distal chromosome 7 in the mouse and chromosome 11p15.5 in human. In both mouse and human, the *H19* gDMR acquires methylation on the paternal allele during spermatogenesis while the maternal allele is unmethylated in oocytes (Bartolomei et al., 1991; Borghol et al., 2006; Ibala-Romdhane et al., 2011; Jinno et al., 1996). Genes in this domain include *H19*, Insulin-like growth factor 2 (*Igf2*), and Insulin II (*Ins2*). Insulin-like growth factor 2 (*Igf2*) is protein-coding gene that promotes fetal and placental growth (Constância et al., 2002; DeChiara et al., 1990), *H19* is a non-coding RNA that also modulates growth (Gabory et al., 2009; Keniry et al., 2012) and tumor suppression (Yoshimizu et al., 2008), while *Ins2* is involved in blood glucose regulation (Deltour et al., 1995; Duvillié et al., 1998; Giddings et al., 1994). The paternally-expressed *Igf2* and *Ins2* genes are located 90 kb upstream of the maternally-expressed *H19* gene (Bartolomei et al., 1991; DeChiara et al., 1991) and share common enhancer sequences located downstream *H19* (Tremblay et al., 1997). Imprinted expression of *Igf2*, *Ins2* and *H19* is regulated by an enhancer-insulator mechanism (Figure 1-4).

The *H19* ICR is located 2 to 4 kb upstream from the *H19* transcriptional start site and contains binding sites for the insulator protein CTCF [CCCTC-binding factor (zinc finger protein)] (Hark et al., 2000; Li et al., 2008a). CTCF controls higher-order chromatin conformation by directing intrachromosomal loop formation through blocking, or insulating, interactions between promoter and enhancer elements. Binding of CTCF is dependent on allelic ICR methylation. CTCF binding to the unmethylated maternal *H19* ICR blocks ("insulates") interactions between the enhancer regulatory element and *Igf2* and *Ins2*, consequently permitting interaction with the maternal *H19* promoter (Hark et al., 2000; Kurukuti et al., 2006; Li et al., 2008a). In contrast, *H19* ICR methylation on the paternal allele prevents CTCF binding, enabling intrachromosomal enhancer looping to the *Igf2/Ins2* control elements (Hark et al., 2000; Li et al., 2008a). In addition to ICR-mediated regulation, *Igf2* and *Ins2* expression is also controlled by two additional somatic paternally methylated DMRs, DMR1 and DMR2. DMR1 is located proximal to *Igf2* and functions as a silencer of *Igf2* expression in mesodermal tissues on the maternal allele, potentially through a tight loop structure generated by *H19* ICR and matrix attachment region 3 (MAR3) interactions

(Constância et al., 2000; Kurukuti et al., 2006) (Figure 1-4). Matrix attachment regions are DNA loci that localize to the nuclear matrix and are associated with repressed and active chromatin (Macdonald et al., 2015). In contrast, DMR2 is located within the sixth *Igf2* exon where it functions as an methylated enhancer on the paternal allele to enable paternal *Igf2* transcription (Murrell et al., 2001). The *H19* ICR is required for monoallelic expression of *H19* and *Igf2*. A maternally inherited deletion of the ICR that prevents CTCF binding leads to biallelic *Igf2* expression while paternal deletion results in biallelic *H19* expression (Engel et al., 2006; Thorvaldsen et al., 1998; Tremblay et al., 1997). Furthermore, mutating CpG dinucleotides within the ICR prevents paternal imprinted methylation and enables CTCF binding that results in insulator activity and biallelic *H19* expression (Engel et al., 2004).

Genetic and epigenetic errors at the *H19* domain cause the imprinting disorder Beckwith-Wiedemann Syndrome (BWS) (OMIM #130650). BWS is an overgrowth disorder with clinical features that include macrosomia, macroglossia, abdominal wall defects, hemihyperplasia, visceromegaly and predisposition to malignancies (Choufani et al., 2010; 2013; Weksberg et al., 2010). In the general population, BWS incidence is estimated to be 1 in 13, 700 (Weksberg et al., 2010). Microdeletions/microduplications, cytogenetic alterations and point mutations at chromosome 11p15 account for ~15% of BWS cases (Choufani et al., 2010; 2013). An imprinting defect at the *H19* ICR can also lead to BWS. Five percent of BWS cases are due to an abnormal gain of methylation (hypermethylation) of the maternal *H19* ICR (Choufani et al., 2010; Weksberg et al., 2010).

In addition to BWS, abnormal loss of methylation (hypomethylation) at the *H19* ICR leads to a growth restricted imprinting disorder, Silver Russell Syndrome (SRS) (OMIM #180860). SRS is a severe intrauterine growth restriction disorder associated with poor postnatal growth, craniofacial features that include pronounced forehead and triangular shaped face, and other minor malformations (Begemann et al., 2011; Eggermann et al., 2006; 2010). Hypomethylation of the paternal *H19* ICR leads to SRS in >38% of patients (Begemann et al., 2011; Eggermann et al., 2006; Hannula et al., 2001). Maternal UPD of chromosome 11p15 has also been documented. In contrast, 10% of SRS cases demonstrate uniparental disomy at another imprinted domain, *Peg1* (paternally expressed gene 1), located on human chromosome 7q32 (mouse chromosome 6) (Begemann et al., 2011).
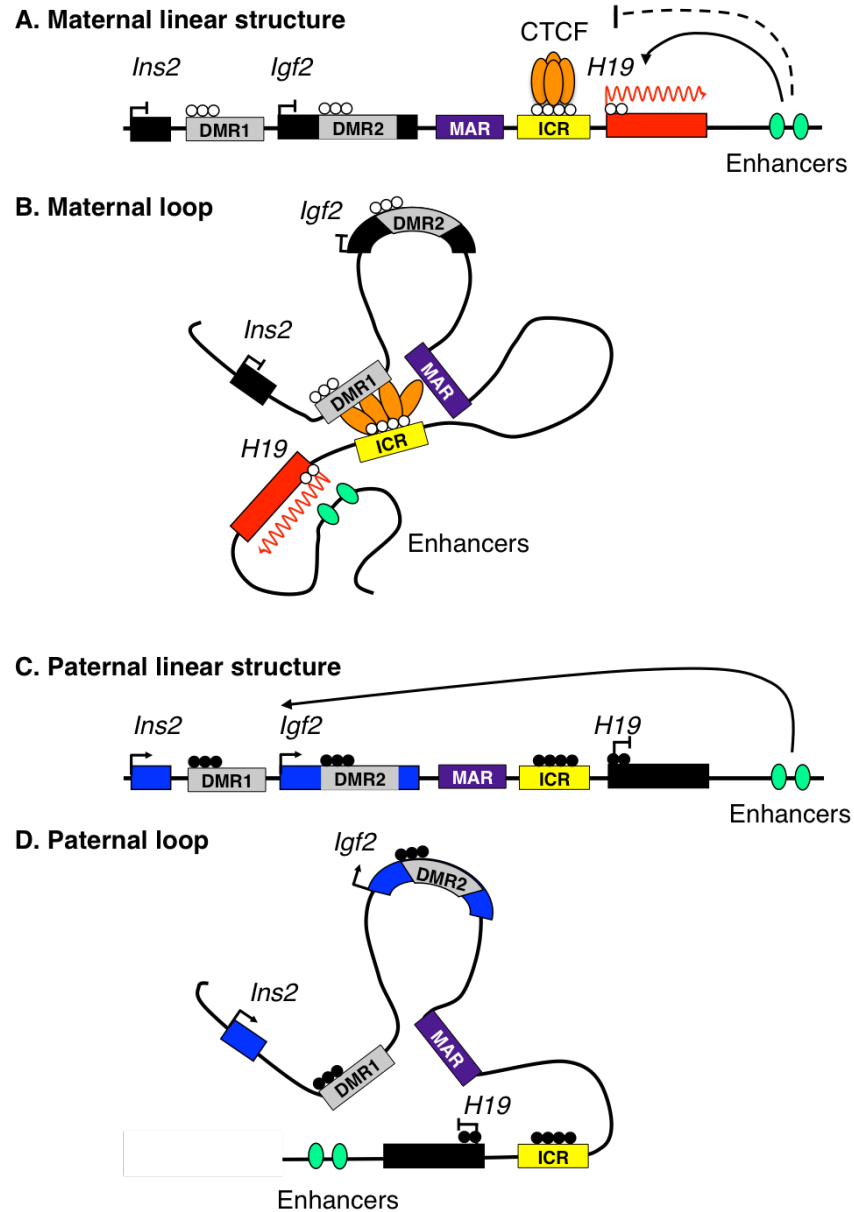
Figure 1-4: Structure and regulation of the *H19* domain

On the maternal allele (A, B), *H19* ICR is unmethylated, allowing for CTCF binding and intrachromosomal loop formation. The ICR, DMR1 and MAR regions interact in a tight loop formation, excluding *Igf2/Ins2* and bringing the enhancer elements to the *H19* promoter. In contrast on the paternally methylated allele (C, D), CTCF is unable to bind, generating a loop formation that brings the enhancer elements to the *Igf2/Ins2* region, and preventing *H19* expression. Somatic DMRs, DMR1 and DMR2, function in maternal *Igf2* silencing and paternal *Igf2* expression, respectively.

1.2.2.2 *Kcnq1ot1* imprinted domain

The *Kcnq1ot1/KCNQ1OT1* imprinted domain is also located on the distal portion of mouse chromosome 7 and human chromosome 11p15.5. This domain includes the paternally expressed *Kcnq1ot1* lncRNA, 9 maternally expressed protein-coding genes, and 6 biallelic genes that escape imprinted regulation (Figure 1-5). Of the 9 maternally expressed genes, 5 exhibit placental-specific imprinted expression (oxysterol binding protein-like 5, *Osbpl5;* tumor-suppressing subchromosomal transferable fragment 4*, Tssc4;* CD81 antigen, *Cd81;* achaete-scute complex homolog 2, *Ascl2; and* tyrosine-hydroxylase, *Th*) while the remaining 4 are imprinted in both placental and embryonic lineages (pleckstrin homology-like domain, family A, member 2, *Phlda2;* solute carrier family 22, member 18, *Slc22a18;* cyclin-dependent kinase inhibitor 1C, *Cdkn1c;* and potassium voltage-gated channel, subfamily Q, member 1, *Kcnq1*) (Golding et al., 2011; Lewis et al., 2004; Mohammad et al., 2012; Umlauf et al., 2004).

The *Kcnq1ot1* domain contains an ICR, within which the *Kcnq1ot1* promoter is embedded. In the mouse and human, this ICR is methylated during oogenesis, unmethylated in sperm, and maintains maternal methylation during embryogenesis (Beatty et al., 2006; Khoueiry et al., 2008; 2012). On the maternal allele, methylation at the *Kcnq1ot1* ICR prevents *Kcnq1ot1* transcription, thereby allowing expression of the 9 maternally transcribed genes. On the paternal allele, the *Kcnq1ot1* ICR is unmethylated and *Kcnq1ot1* is expressed, producing a 471 kb transcript that is involved in paternal repression of surrounding genes (Golding et al., 2011). The complete mechanisms responsible for imprinting at the *Kcnq1ot1* cluster are not fully elucidated. However, it has been demonstrated that both the *Kcnq1ot1* ICR and *Kcnq1ot1* long ncRNA (lncRNA)-mediated repression are important. Loss of maternal methylation at the *Kcnq1ot1* ICR results in biallelic *Kcnq1ot1* expression and silencing of the normally expressed maternal alleles of the imprinted genes (Fitzpatrick et al., 2002; Lewis et al., 2004; Smilinich et al., 1999). In contrast, deletion of the maternal *Kcnq1ot1* ICR recapitulates the wildtype situation where a maternally methylated *Kcnq1ot1* ICR or a deleted *Kcnq1ot1* ICR (and *Kcnq1ot1* promoter) prevent production of the *Kcnq1ot1* lncRNA, thereby permitting expression of maternally transcribed genes (Fitzpatrick et al., 2002). Paternal inheritance of a deleted *Kcnq1ot1* ICR also results in loss of *Kcnq1ot1* expression, consequently re-activating the normally silent paternal alleles of

imprinted genes in the domain (Fitzpatrick et al., 2002; 2007; Mancini-DiNardo et al., 2003; Shin et al., 2008). These data suggest that the *Kcnq1ot1* ICR mediates imprinting at this domain by regulating expression of the *Kcnq1ot1* lncRNA, although the exact role of the *Kcnq1ot1* lncRNA in mediating the regulation of imprinting at this domain is still under debate. Some studies suggest the *Kcnq1ot1* lncRNA acts by coating the domain and preventing transcription by recruiting repressive complexes to the promoter regions of silent paternal alleles of imprinted genes within the domain (Mager et al., 2003; Pandey et al., 2008; Terranova et al., 2008; Umlauf et al., 2004; Wagschal et al., 2008). Furthermore, activation of paternally silent imprinted genes occurs when *Kcnq1ot1* stability is decreased, paternal *Kcnq1ot1* is truncated and repressive epigenetic marks are lost (Fitzpatrick et al., 2002; Lewis et al., 2004; Mancini-DiNardo et al., 2006; Pandey et al., 2008; Shin et al., 2008; Thakur et al., 2003; 2004). Finally, a study conducted in our lab suggests that the act of transcription rather than the transcript itself is involved in domain regulation in embryo-derived stem cells (Golding et al., 2011).

Genetic and epigenetic errors at the *KCNQ1OT1* domain also cause the imprinting disorder Beckwith-Wiedemann Syndrome (BWS) (OMIM #130650). Here, 50% of BWS cases result from hypomethylation of the maternal *KCNQ1OT1* ICR (Choufani et al., 2010; 2013; Horike et al., 2000). An additional 5-10% of BWS patients have mutations within *CDKN1C,* a maternally expressed gene in the *KCNQ1OT1* cluster. Finally, 20% of cases consist of paternal uniparental disomy (UPD) involving chromosome 11p15, involving both the *KCNQ1OT1* and *H19* domains (Choufani et al., 2010; 2013).
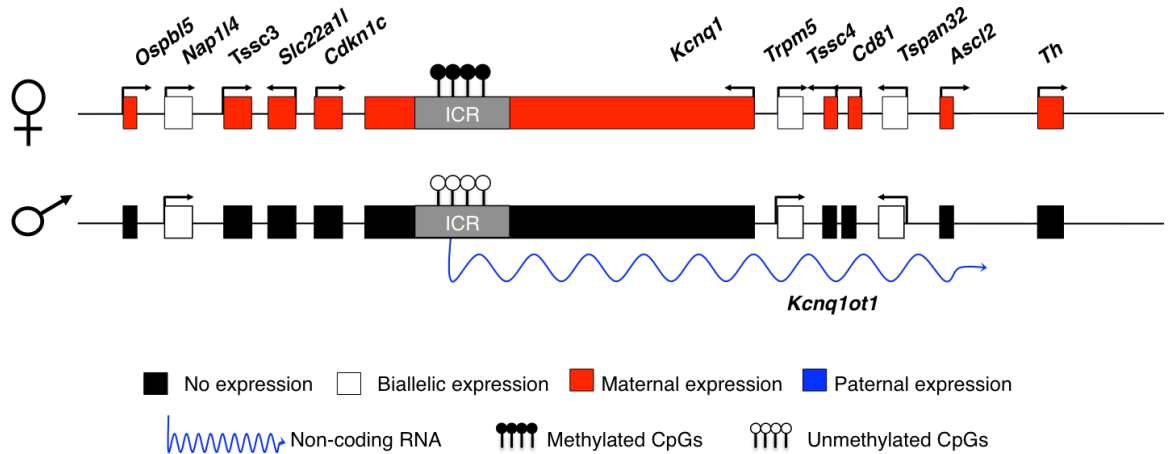
Figure 1-5: Structure and regulation of the *Kcnq1ot1* domain

Imprinting at the *Kcnq1ot1* domain is controlled by differential methylation at the maternal (upper strand) and paternal (bottom strand) ICRs. Maternal methylation of the ICR represses *Kcnq1ot1* transcription, permitting maternal expression of surrounding genes. On the paternal allele, the ICR is unmethylated, the *Kcnq1ot1* lncRNA is expressed and surrounding genes are repressed.

1.2.2.3 *Snrpn* imprinted domain

The small nuclear ribonucleoprotein N (*Snrpn/SNRPN*) imprinted domain is located on the central region of mouse chromosome 7 and human chromosome 15q11-q13. The *Snrpn/SNRPN* ICR within the promoter and exon 1 is methylated during oogenesis, unmethylated in sperm, and maintains maternal-specific methylation throughout preimplantation (El-Maarri et al., 2003; Geuns et al., 2003; Shemer et al., 1997). This imprinted cluster contains numerous genes expressed exclusively from the paternal chromosome, including *Snurf-Snrpn* (*Snrpn* upstream reading frame-*Snrpn*), *Frat3* (frequently rearranged in advanced T-cell lymphomas 3), *Mkrn3 (*makorin ring finger protein 3)*, *Magel2* (melanoma antigen-like 2)*, *Ndn* (Necdin)*, *Ipw* (imprinted in Prader-Willi Syndrome), over 70 *snoRNA* genes and a *Snrpn* lncRNA transcript (*Snrpnlt*) (Figure 1-6). This lncRNA, which is over 470 kb in human and 1,000 kb in mouse, includes *Snrpn* and extends through *Ipw*, the *snoRNAs* and *Ube3a* (ubiquitin protein ligase E3A), also known as the *Ube3a* antisense transcript, *Ube3a-as* (Horsthemke and Wagstaff, 2008; Landers et al., 2005; Runte et al., 2001) (Figure 1-6). Maternal-specific expression of the *Ube3a/UBE3A* gene is restricted to the brain in both human and mouse, maternal expression of *ATP10C* (ATPase, class V, type 10C) is imprinted in human brain and fibroblasts (Herzing et al., 2001; Meguro et al., 2001), although there are conflicting reports as to whether *Atp10c* is imprinted in the mouse (Kashiwagi et al., 2003; Kayashima et al., 2003).

The *Snrpn* ICR is located in the *Snrpn* promoter and extends into exon 1. Regulation of the *Snrpn* imprinted domain is not fully understood; however, both the *Snrpn* ICR and *Snrpnlt* are likely required. A PWS family with paternal *SNRPN* ICR deletions exhibited loss of *MKRN3*, *MAGEL2*, *NDN* and *SNRPN* expression (Bielinska et al., 2000). This effect was recapitulated in a mouse model harboring a similar deletion (Bielinska et al., 2000) as well as in mice inheriting a paternal 42 kb deletion covering *Snrpn* exons 1-6 and 23 kb upstream (Yang et al., 1998). In contrast, a smaller 0.9 kb microdeletion including the majority of the mouse *Snrpn* promoter and exon 1 did not affect *Mkrn3*, *Ndn*, *Magel2 and Ube3a* expression, while a small deletion (4.8 kb) produced mosaic effects. With respect to the *Snrpnlt* lncRNA, it is thought that imprinted expression of *Ube3a/UBE3A* is the result of transcriptional interference of the *Snrpnlt*, but this still remains to be validated (Chamberlain and Brannan, 2001; Chamberlain et al., 2014; Rougeulle et al., 1998; Runte et al., 2001).
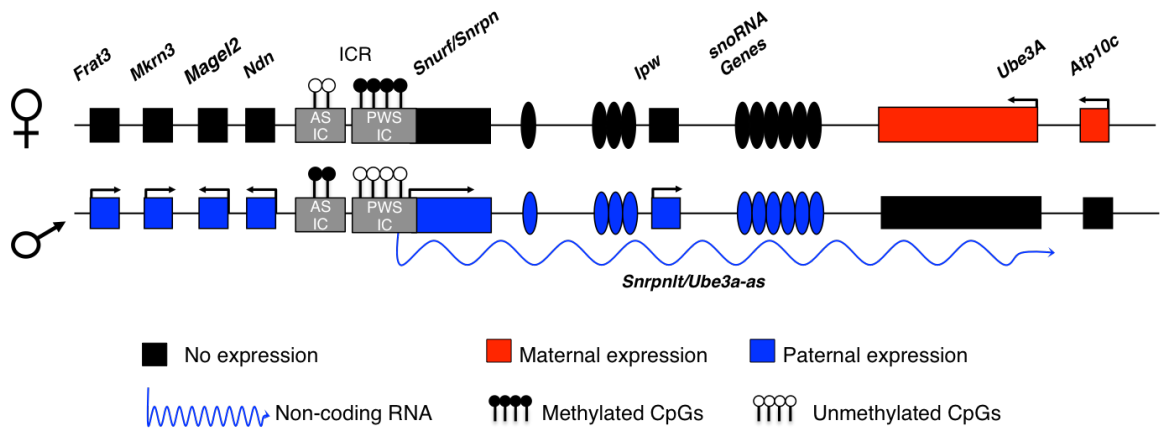
Figure 1-6: Structure and regulation of the *Snrpn* domain

The *Snrpn* domain consists of a bipartite ICR (AS-IC and PWS-IC). On the paternal allele, the unmethylated PWS-IC region of the ICR permits *Snrpnlt* expression and enables paternal transcription of surrounding genes *Frat3*, *Mkrn3*, *Magel2*, *Ndn*, *Snrpn*, *Ipw*, and *snoRNA* genes, and represses *Ube3a* and *Atp10c*. In contrast, on the maternal allele, *Snrpn* ICR methylation at PWS-IC prevents *Snrpnlt* transcription and enables *Ube3a* and *Atp10c* expression in a brain-specific manner.

On the paternal allele, the *Snrpn* ICR is unmethylated, the *Snrpn* lncRNA is transcribed, directing expression of other paternally expressed genes, while interfering with transcription of *Ube3a* and *Atp10c* (Horsthemke and Wagstaff, 2008). In contrast, on the maternal allele, the *Snrpn* ICR is methylated, the *Snrpn* lncRNA is not transcribed and *Ube3a* and *Atp10c* are expressed in a brain-specific manner (El-Maarri et al., 2001; Horsthemke and Wagstaff, 2008). For this domain, ICR regulation is more complicated since the *Snrpn/SNRPN* ICR has a bipartite structure, containing two specific regions termed the Angelman Syndrome imprinting centre (AS-IC) and Prader-Willi Syndrome IC (PWS-IC) (Horsthemke, 1997). The PWS-IC is a 4.3 kb sequence located around the *SNRPN* promoter/exon1 (Ohta et al., 1999), while the AS-IC is 880 bp and is located approximately 35 kb upstream of the *SNRPN* transcriptional start site (Buiting et al., 1999). On the maternal allele, exons within the unmethylated AS-IC are transcribed, which leads to methylation at the PWS-IC (Horsthemke and Wagstaff, 2008; Kantor et al., 2004; Shemer et al., 2000). This in turn silences the *Snrpnlt* lncRNA and permits expression of *Ube3a* and *Atp10c* (Horsthemke and Wagstaff, 2008). On the paternal allele, AS-IC is methylated, blocking transcription of exons within the AS-IC (Horsthemke and Wagstaff, 2008; Kantor et al., 2004; Shemer et al., 2000). Thus, PWS-IC is unmethylated, enabling *Frat3*, *Mkrn3*, *Magel2*, *Ndn*, *Snrpn*, *Snrpnlt*, *Ipw*, snoRNAs and transcription, and silencing *Ube3a* and *Atp10c* (El-Maarri et al., 2001).

Genetic and epigenetic errors at the *SNRPN* domain cause the imprinting disorders Angelman Syndrome (AS) (OMIM #105830) and Prader-Willi Syndrome (PWS) (OMIM #176279). Angelman Syndrome is a neurological syndrome characterized by severe intellectual and motor retardation, limited speech, ataxia, hypotonia and unusual facies such as open-mouthed expression (Van Buggenhout and Fryns, 2009). Its incidence is approximately 1 in 15,000 newborns (Horsthemke, 1997; Van Buggenhout and Fryns, 2009). Maternal deletions of the 15q11.2-q13 region (including AS-IC microdeletions, 60-75%), paternal UPD (2-5%) and mutations in the *UBE3A* gene (10%) cause AS (Van Buggenhout and Fryns, 2009). Less than 5% of cases result from loss of maternal methylation at the *SNRPN* ICR (Horsthemke, 1997; Van Buggenhout and Fryns, 2009). In contrast to AS, Prader-Willi Syndrome is characterized by intellectual disability, decreased fetal activity, obesity, small hands and feet, muscular hypotonia, short stature and

hypogonadotropic hypogonadism. The incidence of PWS is about 1 in 20,000 and results from a lack of paternal-specific gene expression from the domain due to paternal 15q11.2-q13 deletions (including PWS-IC microdeletions, 65-75%), maternal UPD (20-30%) and gain of methylation at the paternal *SNRPN* ICR (1-3%) (Cassidy et al., 2012).

1.2.3   Evolution of genomic imprinting and the placenta

The importance of imprinted genes in fetal and placental growth and development was originally identified by nuclear transplantation experiments as well as uniparental disomies of specific chromosomal regions containing imprinted genes (Cattanach, 1986; Cattanach and Kirk, 1985; Searle and Beechey, 1990) (see 1.2.1). Failed embryo development in androgenetic and gynogenetic embryos, in part due to defects in the trophoblast, indicated that imprinted genes likely play a role in placental development and function. Furthermore, there is an evolutionary link between imprinted genes and the placenta, as existence of imprinting seemingly evolved at the same time Therian mammals (marsupial and placental mammals) separated from egg-laying monotremes (Ager et al., 2007; Killian et al., 2000; Renfree and Pask, 2011; Smits et al., 2008; Suzuki et al., 2011; Weidman et al., 2004). Consequently numerous theories have arisen regarding the emergence genomic of imprinting. The parental conflict theory states that imprinting arose to balance the opposing interests between maternal and paternal genomes with respect to maternal-fetal nutrient transfer (Moore and Haig, 1991). In contrast, another theory suggests that imprinting evolved to protect the female from trophoblast invasion, or ectopic trophoblast (Hall, 1990; Varmuza and Mann, 1994). The latter theory relates to the fact that the trophoblast must invade the uterine epithelium for successful pregnancy. This theory states that genomic imprinting protects females from excessive trophoblast invasion in the ovary when oocytes spontaneously activate by suppressing maternal genes involved in placental development (Hall, 1990; Varmuza and Mann, 1994). Irrespective of their differences, the above theories suggest that a subset of genes must be appropriately regulated by imprinting to balance proper embryonic and placental development, and maternal survival.

The specific functions of a numerous imprinted genes in the placenta have been determined (Figure 1-7) (Tunster et al., 2013). For example, both the *H19* and *Kcnq1ot1* imprinted domains play an important role in placental function and resulting growth (Tunster

et al., 2013). With respect to the *H19* domain, loss of paternal *Igf2* expression results in reduced placental weight and growth restriction while elevated *Igf2*/loss of expression of *H19* results in fetal overgrowth (Angiolini et al., 2011; Lefebvre, 2012; Sandovici et al., 2012). The role of the *H19* domain in placental function and growth is conserved in the human and also causes growth deficiencies or overgrowth abnormalities in human babies (Bouwland-Both et al., 2013; Demetriou et al., 2014; Gonzalez-Rodriguez et al., 2016; Kappil et al., 2015; McMinn et al., 2006) including Beckwith-Wiedemann Syndrome (Aoki et al., 2011) and Silver Russell Syndrome (Yamazawa et al., 2008). Furthermore, numerous genes within the *Kcnq1ot1* cluster have been implicated in placental function. Specifically, 5 out of the 9 maternally expressed genes in this domain exhibit placental-specific imprinted expression (*Osbpl5*, *Tssc4*, *Cd81*, *Ascl2* and *Th*) while the remaining 4 genes are imprinted in both the placenta and embryo (*Phlda2*, *Slc22a18*, *Cdkn1c*, *Kcnq1*) (Golding et al., 2011; Lewis et al., 2004; Mohammad et al., 2012; Umlauf et al., 2004). The roles of *Ascl2*, *Cdkn1c* and *Phlda2* in placental function have been analyzed (Fitzpatrick et al., 2002; Mancini-DiNardo et al., 2006). Briefly, decreased *Ascl2* impairs placental and in turn embryonic growth (Tunster et al., 2010), loss of *Cdkn1c* results in placental and fetal overgrowth (Takahashi et al., 2000) while *Phlda2* overexpression impairs fetal growth during late gestation (Tunster et al., 2010). Similar to the *H19* domain, the role of the *Kcnq1ot1* region in controlling placental growth and function has been identified in the human (Kanber et al., 2009; López-Abad et al., 2016; Mandò et al., 2014; McMinn et al., 2006), including its role in Beckwith-Wiedemann Syndrome (Bourque et al., 2011).
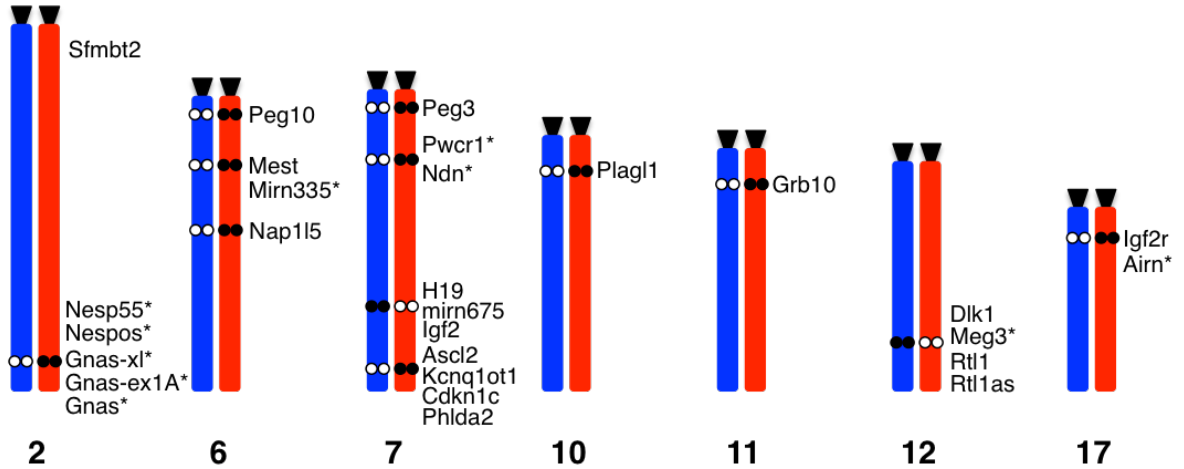
Figure 1-7: Imprinted genes with demonstrated placental function in the mouse

Mouse imprinted genes with known placental functions are shown beside identified gametic DMRs. Imprinted genes with an asterisk indicate suspected placental function. Blue rectangles, paternal allele; red rectangles, maternal allele; black triangles, centromere; white circles, unmethylated CpGs; black circles, methylated CpGs. Chromosome number is indicated below each chromosome set.

1.3   DNA methylation reprogramming in mouse and human

As mentioned above, imprinted gDMRs acquire allele-specific methylation during gametogenesis, which is then maintained throughout preimplantation development. In general, global and imprinted DNA methylation marks are dynamically regulated during early mammalian development (Bartolomei and Ferguson-Smith, 2011). There are three major waves of DNA methylation reprogramming that occur during gamete and preimplantation development (Figure 1-8). First, global and imprinted DNA methylation marks from previous generations are erased in primordial germ cells (PGCs). Subsequently, maternal and paternal-specific DNA methylation and imprints are acquired differentially during oocyte and sperm development. Finally, imprints are maintained during preimplantation development when the remainder of the genome undergoes an erasure stage to establish totipotency of the early embryo. This section describes the three phases of DNA methylation reprogramming in mouse, and concludes with a description of the conservation of these phases in the human [reviewed in (White et al., 2016)].

1.3.1   DNA methylation erasure during mouse primordial germ cell development

The first phase of epigenetic programming is DNA methylation erasure. Here, previous parental DNA methylation marks are removed in sexually uncommitted primordial germ cells (PGCs). In the mouse, global DNA methylation loss occurs in two distinct waves. In stage I, DNA methylation erasure is initiated at embryonic day 8.0 (E8.0) (Hajkova et al., 2002a; Saitou et al., 2012; Seki et al., 2005). Global 5mC levels progressively decline in a passive, replication-dependent manner to E9.0, reducing global methylation levels to ~30% (Guibert et al., 2012; Seisenberger et al., 2012; Seki et al., 2005). Although the maintenance methyltransferase *Dnmt1* remains highly expressed at these stages, its recruitment cofactor *Uhrf1/Np95* is not, likely accounting for methylation loss (Kurimoto et al., 2008). Stage II methylation erasure produces a further decline in 5mC levels between E10.5-13.5. Here, erasure occurs via active demethylation, resulting from ten-eleven translocation 1 and 2 (TET1, TET2) oxidation of 5mC to the intermediate 5-hydroxymethylcytosine (5hmC) (Hajkova et al., 2008; 2010; Piccolo et al., 2013; Yamaguchi et al., 2013) (Figure 1-9). The base excision repair pathway may also have a role in active demethylation, involving activation-induced cytidine deaminase and thymine-DNA glycosylase (TDG) (Cortellino et

al., 2011; Hajkova et al., 2010; Morgan et al., 2004; Popp et al., 2010). At E13.5, 5mC declines to its lowest levels (Guibert et al., 2012; Popp et al., 2010; Saitou et al., 2012; Seisenberger et al., 2012; Yamaguchi et al., 2013), representing the epigenetic ground state of the germline genome (Hajkova, 2011).

In comparison to the whole genome, DNA methylation erasure at imprinted gDMRs is delayed. Onset of erasure begins after E9.5 and is complete at or after E13.5 (Guibert et al., 2012; Hackett et al., 2013; Hajkova et al., 2002a; Kagiwada et al., 2013; Kobayashi et al., 2013). More specifically, of the 18 maternal gDMRs and 3 paternal gDMRs analyzed, only 7 still retain some level of methylation (~20% methylation or less) at E13.5, while demethylation is completed at the remaining 14 gDMRs (Kobayashi et al., 2013). Current studies investigating imprinted gDMR methylation loss in PGCs indicate roles for both passive and active demethylation. Passive replication-dependent demethylation, beginning at E9.5 (Kagiwada et al., 2013), is supported by repression of *Uhrf1* (Kurimoto et al., 2008). By comparison, active demethylation occurs through TET1 conversion of 5mC to 5hmC commencing at E10.5 (Hackett et al., 2013; Piccolo et al., 2013; Vincent et al., 2013) (Figure 1-9). There is little evidence for demethylation through the base excision repair pathway at imprinted gDMRs (Hackett et al., 2013; Kagiwada et al., 2013; Popp et al., 2010).

Oogenesis

Ovarian stimulation
In vitro oocyte maturation

Preimplantation development

Cryopreservation

Cryopreservation
Embryo culture

P21

IVF/ICSI

E8.0   E13.5   Birth   P3   P7

Primordial germ cell   Primordial follicle   Primary follicle   Secondary follicle   Preovulatory Follicle   MII oocyte   Sperm   1-cell   2-cell   4-cell   8-cell   Morula   Blastocyst

Fertilization

Erasure   **Acquisition**   **Maintenance**

Methylation %

E8.0   E13.5   E15   Birth   P6   P18-20 MI/MII   P20   P28   P35

Primordial germ cell   Prospg   Spg   Scy   RS   ES   Mature Spermatozoa

Spermatogenesis

- Global demethylation
- Imprinted demethylation
- Global maternal methylation
- Global paternal methylation
- Maternally imprinted allele
- Paternally imprinted allele

Figure 1-8: DNA methylation dynamics during gametogenesis and preimplantation development

Global DNA methylation (orange line) and imprinted DNA methylation (purple line) is first erased in primordial germ cells. Then, sex-specific DNA methylation is acquired both globally and at imprinted gDMRs during gametogenesis. Specifically global (dark blue) and imprinted (light blue) methylation is established early during spermatogenesis, with methylation mostly completed at birth. In contrast, DNA methylation acquisition globally (red) and at imprinted domains (pink) is delayed in oogenesis, occurring after birth and beginning in growing oocytes up to MII ovulated oocytes. Despite global DNA demethylation of the paternal (blue) and maternal (red) genomes after fertilization during preimplantation development, imprinted DNA methylation is maintained at imprinted genes (light blue, pink). Assisted reproductive technologies occur during imprint acquisition and imprint maintenance phases, with examples shown in grey italicized text. E, embryonic day; P, postnatal day; MI, meiosis I; MII, meiosis II; Prospg, prospermatogonia; Spg, spermatogonia; Scy, spermatocyte; RS, round spermatid; ES, elongating spermatid; IVF, *in vitro* fertilization; ICSI, intracytoplasmic sperm injection.

1.3.2   DNA methylation acquisition during mouse gametogenesis

Following erasure, the next phase of DNA methylation programming is DNA methylation acquisition. In males, global DNA methylation acquisition commences in E14.5-E16.5 mitotically-arrested fetal prospermatogonia, reaching 50% methylation levels by E16.5, and continues to rise through to the spermatogonia stage (Kobayashi et al., 2013), where the highest global methylation levels are present during spermatogenesis (Kobayashi et al., 2013; Niles et al., 2011; Seisenberger et al., 2012; Vlachogiannis et al., 2015). In mature sperm, ~80% of cytosines are methylated (Kobayashi et al., 2012). This pattern was recently confirmed in a genome-wide DNA methylation study, where overall 5mC levels increased from 30% in E16.5 prospermatogonia to 76%, ~77% and 79% in postnatal day 0.5 (P0.5) prospermatogonia, P7.5 spermatogonia and adult spermatozoa, respectively (Kubo et al., 2015). In mature sperm, ~78-90% of cytosines are methylated (Kobayashi et al., 2012; Kubo et al., 2015; Smith et al., 2012; Wang et al., 2014). Mechanistically, DNA methylation acquisition occurs through the *de novo* DNA methyltransferases, DNMT3A and DNMT3B, and accessory protein DNMT3L (Kato et al., 2007) (Figure 1-9).

In contrast to male germ cells, E16.5 diplotene stage female germ cells (Ewen and Koopman, 2010) remain globally hypomethylated (Kobayashi et al., 2012). Instead, acquisition of global *de novo* methylation is delayed until oocytes enter the growth phase (Smallwood et al., 2011). By the time oocytes are at the germinal-vesicle and mature MII stages, acquisition of DNA methylation is complete (Kobayashi et al., 2012; Shirane et al., 2013; Smallwood et al., 2011; Smith et al., 2012; Tomizawa et al., 2011). Globally, ~40-55% of cytosines are methylated in oocytes (Kobayashi et al., 2012; Smallwood et al., 2011; Smith et al., 2012; Wang et al., 2014). Mechanistically, DNMT3A and DNMT3L are indispensable for DNA methylation acquisition in female germ cells (Kobayashi et al., 2012; Smallwood et al., 2011) (Figure 1-9).

Recently, CpG island DNA methylation acquisition in oocytes has also been linked to transcription (Veselovska et al., 2015).   Transcription initiating from alternative transcriptional start sites throughout oogenesis is highly correlated with hypermethylated CpG domains in fully grown GV oocytes (Veselovska et al., 2015). This occurs in part during transcription elongation where disposition of histone 3 lysine 36 trimethylation

(H3K36me3) enhances DNMT3A activity (Dhayalan et al., 2010; Veselovska et al., 2015; Zhang et al., 2010).

For imprinted DNA methylation, acquisition occurs with similar timing to that of the whole genome. In the male germline, imprinted methylation acquisition at *H19*, *Gtl2* and *Rasgrf1* has begun by E14.5, increasing progressively through to E18.5 in fetal prospermatogonia until being completed in P0 mitotically arrested spermatogonia (Davis et al., 2000; Kaneda et al., 2004; Kato et al., 2007; Kobayashi et al., 2013; Lee et al., 2010; Lucifero et al., 2002; Ueda et al., 2000). The two parental alleles undergo differential methylation acquisition, with *de novo* methylation initiating earlier (E14.5) on the previous paternally-methylated *H19, Gtl2* and *Rasgrf1* alleles than on the previous maternally-unmethylated alleles (E16.5) (Davis et al., 2000; 1999; Kato et al., 2007; Ueda et al., 2000). This differential acquisition indicates that some previous parental identity is retained in the absence of DNA methylation. *H19* and *Gtl2* imprinted methylation acquisition during spermatogenesis is dependent on DNMT3A and DNMT3L, while *Rasgrf1* additionally requires DNMT3B (Bourc'his and Bestor, 2004; Hirasawa et al., 2008; Kaneda et al., 2004; Kato et al., 2007; Vlachogiannis et al., 2015; Webster et al., 2005) (Figure 1-9).

In E16.5 female germ cells, imprinted gDMRs have low methylation levels (Kobayashi et al., 2013). DNA methylation acquisition at the *Snrpn*, *Igf2r*, *Peg1*, *Peg3*, *Kcnq1ot1, Zac1, Meg1* and *Impact* gDMRs is delayed compared to male imprint acquisition, which occurs prenatally. Instead, DNA methylation is acquired during oocyte growth in a size-dependent manner from the primary to antral follicle stage, and is completed by the ovulated metaphase II (MII) stage (Denomme et al., 2012; Hiura et al., 2006; Lucifero, 2004; Lucifero et al., 2002; Obata and Kono, 2002). In oocytes, as in sperm, allelic identity also influences DNA methylation acquisition. Specifically, *de novo* methylation is initiated earlier (P10) on the previous maternally-methylated *Snrpn*, *Zac1* and *Peg1* alleles than on the previous paternally-unmethylated alleles (P15) (Davis et al., 2000; Hiura et al., 2006; Kato et al., 2007; Lee et al., 2010; Lucifero, 2004). This again indicates that epigenetic memory of parental identity is DNA methylation-independent. Expression of *de novo* methyltransferases, *Dnmt3A*, *Dnmt3B* and *Dnmt3L,* occurs during 10-25 days post partum (dpp), increasing co-ordinately with oocyte diameter (Lucifero et al., 2007) and DNA methylation acquisition (Lucifero, 2004). However, imprinted DNA methylation

establishment is dependent on DNMT3A and DNMT3L (Bourc'his et al., 2001; Hata et al., 2002; Kaneda et al., 2010; Lucifero, 2004; Lucifero et al., 2002; Obata and Kono, 2002) but not DNMT3B (Kaneda et al., 2010) (Figure 1-9). Similar to global DNA methylation acquisition, imprinted DNA methylation acquisition at gDMRs within the oocyte is dependent on transcription through gDMRs, as shown for *Snrpn* (Smith et al., 2011), *Gnas* (Chotalia et al., 2009), and *Zac1*/*Plagl1* (Veselovska et al., 2015).

1.3.3 DNA methylation dynamics during mouse preimplantation development

Preimplantation development represents the third epigenetic reprogramming phase where DNA methylation loss occurs globally through the zygote to blastocyst stages, albeit not to the epigenomic ground state level seen in PGCs. Following fertilization, there is active loss of DNA methylation globally in zygotes (Okamoto et al., 2016; Smith et al., 2012) and 2-cell embryos (Wang et al., 2014). As the latter study did not analyze zygotes (Wang et al., 2014), active DNA methylation loss was hypothesized to occur at the 1-cell stage, consistent with loss of global 5mC staining in the paternal pronucleus 4-6 hours following in vitro fertilization (Santos et al., 2002; 2013). Based on 5hmC staining and DNA methylation analyses of *Tet3*-deficient zygotes, active demethylation of the paternal pronucleus occurs via TET3-mediated 5mC conversion to 5hmC (Gu et al., 2011; Guo et al., 2014a; Inoue and Zhang, 2011; Inoue et al., 2011; Iqbal et al., 2011; Wossidlo et al., 2011) (Figure 1-9). Consistent with this, *Tet3* mRNA is more abundant than *Tet1* and *Tet2* transcripts in oocytes and zygotes (Okae et al., 2014; Wossidlo et al., 2011), and TET3 protein along with 5hmC levels are restricted to/overabundant in the paternal compared to maternal pronucleus (Gu et al., 2011; Inoue and Zhang, 2011; Inoue et al., 2011; Shen et al., 2014; Wang et al., 2014). Having said this, TET3 hydroxylation and the spike in 5hmC levels may be restricted to S-phase (pronuclear stage 3, PN3) (Santos et al., 2013), which occurs subsequent to initiation of DNA demethylation (Amouroux et al., 2016; Okamoto et al., 2016), indicating a role for additional mechanisms in this initial demethylation event. In fact, abrogated 5hmC formation via small molecule TET inhibitors or oocyte *Tet3* deletion had no effect on paternal 5mC loss in early PN3 zygotes (Amouroux et al., 2016). Thus, additional mechanisms are likely involved in pre-replicative active DNA demethylation of the paternal pronucleus (Amouroux et al., 2016). In post-replicative PN3 to PN4 zygotes,

genome-wide CpG sites exhibited methylation loss both actively (TET3-dependent) and/or passively (replication-dependent) (Guo et al., 2014a). The latter includes repetitive elements, where DNA demethylation in the paternal pronucleus possessed hemimethylated CpG dinucleotides due to replication-dependent dilution, with minor replication-independent active demethylation (Amouroux et al., 2016; Arand et al., 2015). Interestingly, production of 5hmC by TET3 is linked to DNMT1 and DNMT3A in late P4 zygotes, suggesting that *de novo* methylated cytosines may be targets of hydroxylation (Amouroux et al., 2016). Overall, such evidence supports both active and passive pathways in paternal pronuclear demethylation.

In comparison to the paternal pronucleus, the maternal pronucleus is protected from 5mC demethylation. Protection from DNA demethylation is accomplished via maternal effect proteins, which are synthesized by the oocyte and required in the preimplantation embryo. In zygotes, the maternal effect protein developmental pluripotency associated factor 3 (DPPA3/Stella/PGC7) binds to maternal chromatin containing histone 3 lysine 9 dimethylation (H3K9me2), thereby inhibiting TET3 activity (Nakamura et al., 2007; 2012; Nakatani et al., 2015) (Figure 1-9). DPPA3 binding to chromatin may be dependent on the H3K9me2 methyltransferase protein euchromatic histone lysine methyltransferase 2 (EHMT2/G9a) as well as on its heterodimeric partner, EHMT1/GLP, since their deletion in embryonic stem cells results in reduced DNA methylation at promoter regions (Nakamura et al., 2012; Zhang et al., 2016). Despite this protection, active demethylation may lead to partial DNA methylation loss on the maternal genome, since low 5hmC levels are present in maternal pronuclei of zygotes (Salvaing et al., 2012; Wossidlo et al., 2011). In support of this, haploid parthenogenetic embryos (only maternal genome) display pre-S-phase 5mC depletion 6 hours post-activation (Amouroux et al., 2016; Okamoto et al., 2016); and *Tet3*-deficient zygotes show impaired DNA demethylation on both paternal and maternal pronuclei (Guo et al., 2014a).

After the first cleavage division, demethylation of the majority of the maternal genome is initiated in a passive, replication-coupled manner. Thus, DNA methylation loss of ~50% at each cell cycle leads to the lowest levels by the early blastocyst stage (Mayer et al., 2000; Oswald et al., 2000; Santos et al., 2002). The absence of highly concentrated oocyte-specific DNMT1o in nuclei, except for at the 8-cell stage, and the presence of small amounts

of the somatic DNMT (DNMT1s) in nuclei during preimplantation development, are the contributing factors to passive DNA demethylation (Cirio et al., 2008a; 2008b; Hirasawa et al., 2008). However, DNA methylation loss may not occur solely through replication dilution. A recent genome-wide, allele-specific study has documented 5mC, 5hmC, and subsequent oxidized derivatives 5fC and 5caC in 2-cell to 4-cell embryos, identifying a role for active demethylation of the paternal and maternal genome at these stages (Wang et al., 2014). Thus, passive replicative dilution of maternal DNA methylation may be delayed until the 4-cell stage. However, the loss of paternal genomic 5hmC is controversial as evidence has been presented for active BER pathways (Guo et al., 2014a; He et al., 2011; Santos et al., 2013) as well as passive replication-dependent dilution (Arand et al., 2015; Guo et al., 2014a; Inoue and Zhang, 2011; Inoue et al., 2011; Shen et al., 2014). For the latter, there is a progressive decline in asymmetric 5hmC, 5fC and 5caC staining on the presumptive paternal metaphase chromatids from the 2-cell to 8-cell stage, pointing to passive replication-dependent dilution of these oxidized derivatives (Inoue and Zhang, 2011; Inoue et al., 2011; Shen et al., 2014). Future studies are needed to uncover the mechanisms and dynamics of demethylation during preimplantation development.

Genome-wide data have reported higher than expected DNA methylation levels in the blastocyst if subjected to passive demethylation (Kobayashi et al., 2012). This is attributed to maintenance methylation at oocyte gDMRs, imprinted gDMRs and repetitive elements, which retain DNA methylation though preimplantation development. For imprinted gDMRs, several proteins have been identified that maintain/protect imprinted methylation during preimplantation development. In zygotes, maternally (*Peg1*, *Peg3* and *Peg10*) and paternally [*H19* and *Rasgrf1* (Ras protein-specific guanine nucleotide-releasing factor 1)] imprinted gDMRs are protected from TET3 demethylation of 5mC to 5hmC by maternally-derived DPPA3 binding to H3K9me2 (Nakamura et al., 2007; 2012) (Figure 1-9). After the 1-cell stage, maternal and embryonic zinc finger protein 57 (ZFP57) likely protects imprinted gDMRs from passive demethylation by binding to CpG methylation (Li et al., 2008b; Quenneville et al., 2011; Zuo et al., 2012) and recruiting repressive complex machinery, that includes tripartite motif 28 protein (TRIM28), the H3K9me3 histone methyltransferase SET domain bifurcated 1 (SETDB1), and DNMT1s/1o (Alexander et al., 2015; Bilodeau et al., 2009; Cirio et al., 2008a; 2008b; Howell et al., 2001; Kurihara et al., 2008; Li et al., 2008b;

Lorthongpanich et al., 2013; Messerschmidt et al., 2012; Quenneville et al., 2011; Ratnam et al., 2002; Schultz et al., 2002; Zuo et al., 2012) (Figure 1-9). As studies involving ZFP57 have been performed in later stage embryos (E11.5) and ES cells, future studies are required to validate this mechanism in preimplantation embryos. Overall, current evidence indicates that imprinted gDMRs are protected from both active and passive forms of demethylation during preimplantation development by maternal effect DNA methylation protector proteins. Further investigations are also required to elucidate the mechanisms and dynamics of methylation maintenance at non-imprinted oocyte gDMRs and repetitive elements.
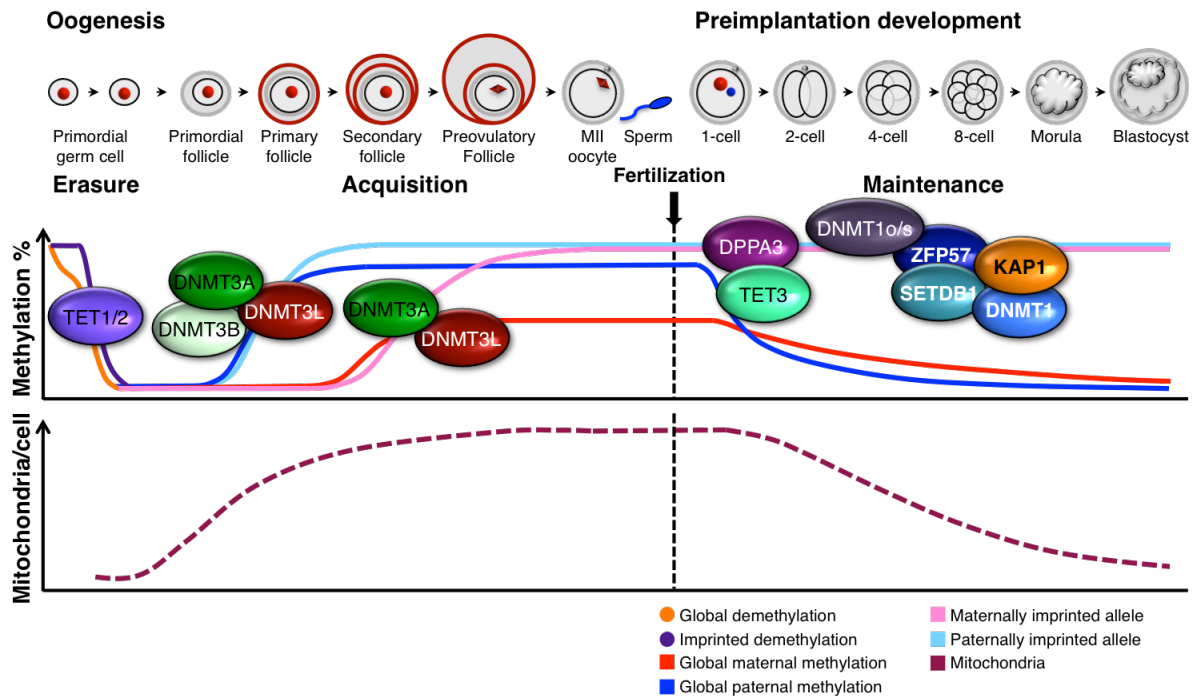
Figure 1-9: Maternal effect products

Upon erasure of methylation marks from the previous generation by TET1/TET2 (light purple circle), imprints are established differentially by DNMT3A/DNMT3L/DNMT3B (light green circle) in spermatocytes and DNMT3A (green circle)/DNMT3L (maroon circle) in oocytes. During this period of imprint establishment during oogenesis, mitochondria numbers rapidly increase from a small progenitor pool in PGCs (maroon dotted line). After fertilization DPPA3 (dark purple circle) protects the maternal genome and paternally methylated ICRs from TET3 (bright green circle)-catalyzed active demethylation of the paternal genome. DNMT1 (DNMT1o/s, grey circle) maintains imprinted methylation during the S-phase of cleavage divisions while ZFP57 (dark blue circle) and additional complex members regulate methylation maintenance beginning at the 8-cell stage. Mitochondrial DNA is not replicated during preimplantation development, suggesting that total mitochondrial numbers remain relatively constant though preimplantation. Consequently, mitochondrial numbers per blastomere would be halved after each cell division.

1.3.4   Conservation of DNA methylation dynamics between mouse and human

While a greater body of data exists on DNA methylation dynamics during gamete and preimplantation development for the mouse compared to the human, available data in the human highlight striking similarities between these species.

1.3.4.1   Conservation of DNA methylation erasure in human PGCs

Prior to comparing DNA methylation erasure in mouse and human, it is important to correlate developmental time points. PGC development takes place between E6.25-E13.5 in the mouse, with PGC development occurring during weeks 2-9 of gestation in humans (De Felici, 2013; Ewen and Koopman, 2010; Leitch et al., 2013; Tang et al., 2015). More specifically, PGC migration and colonization of the developing genital ridge occurs between E8-E10.5 in mouse, which corresponds to ~3-5 weeks gestation in humans (Park et al., 2009; Tang et al., 2015). Mouse PGCs at E11.5-12.5 were most similar to week 7-9 human PGCs (Tang et al., 2015).   At E13.5 in mouse and after week 9 in human, germ cell sexual differentiation has produced oogonia and prospermatogonia in female and male gonads, respectively (Ewen and Koopman, 2010; Kocer et al., 2009; Tang et al., 2015). To study earlier stages of PGC development, human PGC-like cells have been generated from embryonic stem cells and are representative of E6.5-E7.5 premigratory mouse PGCs (Tang et al., 2015).

Overall, studies on PGC methylation erasure dynamics in human have yielded comparable results to mouse.   Stage I of methylation erasure in mouse occurring prior to E10.5 (Guibert et al., 2012; Hajkova et al., 2002b; Saitou et al., 2012; Seisenberger et al., 2012; Seki et al., 2005) likely initiates prior to week 5.5 gestation in human (Tang et al., 2015). Similar stage II methylation erasure events have been reported globally in human 5-19 week PGCs (Driscoll and Migeon, 1990; Gkountela et al., 2015; Guo et al., 2015; Tang et al., 2015; Wermann et al., 2010), corresponding to stage II of methylation erasure in mouse E10.5-13.5 PGCs (Hajkova et al., 2008; 2010; Piccolo et al., 2013; Yamaguchi et al., 2013). Globally for both mouse and human, this erasure produces the greatest loss of DNA methylation throughout development (Gkountela et al., 2015; Guo et al., 2015; Hajkova, 2011; Tang et al., 2015). Mechanistically, active demethylation may contribute to erasure of

stage I and/or II global methylation in human since TET1 protein, 5hmC, and BER pathway members are present (Gkountela et al., 2015; 2013; Guo et al., 2015; Tang et al., 2015). This indicates a potential conserved role to mouse for TET1, 5hmC (Hajkova et al., 2008; 2010; Piccolo et al., 2013; Yamaguchi et al., 2013) and BER (Cortellino et al., 2011; Hajkova et al., 2010; Morgan et al., 2004; Popp et al., 2010) in PGC methylation erasure. For DNA methylation erasure dynamics at imprinted domains in humans, one group showed similar delayed DNA methylation erasure (Gkountela et al., 2013; 2015) as in mouse (Kobayashi et al., 2013), while other studies reported DNA methylation erasure initiating coincident with global erasure (Guo et al., 2015; Tang et al., 2015). In both cases, imprinted methylation erasure was more protracted than global erasure. Like mouse (Hackett et al., 2013; Piccolo et al., 2013; Vincent et al., 2013), imprinted gDMR methylation loss in PGCs may occur by active DNA demethylation, since oxidation of 5mC to 5hmC was evident at *H19* and *GNAS* ICRs (Tang et al., 2015), and at the *PEG3* DMR (Gkountela et al., 2013). The role of passive demethylation has not been investigated.

1.3.4.2 Conservation of DNA methylation acquisition in human gametes

Regarding methylation acquisition in gametes, available data point to spatial, temporal and mechanistic conservation of global and imprinted methylation acquisition in sperm and oocytes between mouse and human (Guo et al., 2014b; Kobayashi et al., 2012; Okae et al., 2014; Smallwood et al., 2011; Smith et al., 2012; 2014; Wang et al., 2014). Both species establish global DNA methylation profiles prenatally during spermatogenesis (Kobayashi et al., 2013; Wermann et al., 2010) and postnatally during oocyte growth (Kobayashi et al., 2012; Shirane et al., 2013; Smallwood et al., 2011; Smith et al., 2012; Tomizawa et al., 2011; Wermann et al., 2010). Similarly, imprinted DNA methylation acquisition is already fully acquired in human adult spermatogonia, spermatocytes, round and elongating spermatids and mature ejaculated spermatozoa (Boissonnas et al., 2010; Kerjean et al., 2000; Kobayashi et al., 2007; Marques et al., 2008; 2011; Sato et al., 2011), and therefore likely occurs prior to birth as in mouse (Davis et al., 2000; Kaneda et al., 2004; Kato et al., 2007; Kobayashi et al., 2013; Lee et al., 2010; Lucifero et al., 2002; Ueda et al., 2000). Maternal imprint acquisition in human occurs in an oocyte size-dependent manner (Arima and Wake, 2006; Sato et al., 2007), similar to the mouse (Arima and Wake, 2006;

Denomme et al., 2012; Lucifero, 2004; Sato et al., 2007). With respect to mechanistic conservation, mouse and human gametes possess *DNMT3A* and *DNMT3B* transcripts at similar levels in comparative oocyte analysis (Okae et al., 2014) and corresponding DNMT3A and DNMT3B protein products have been detected in human (Petrussa et al., 2014). However, unlike the mouse (Kato et al., 2007; La Salle et al., 2007; Niles et al., 2013), *DNMT3L* transcripts/protein have not been detected in human spermatogenic cells or oocytes (Huntriss et al., 2004; Okae et al., 2014; Petrussa et al., 2014), suggesting divergence in its role in global and imprinted methylation acquisition. Further investigations should also be aimed at the specific roles of DNMT3A, DNMT3B and DNMT3L in human sperm and pre-GV methylation acquisition in oocytes.

1.3.4.3 Conservation of DNA methylation programming during preimplantation development

In the preimplantation embryo, DNA methylation dynamics are more complex than expected. Globally in zygotes, active DNA demethylation of the paternal genome by the TET family likely occurs in both species, with potential for roles at maternal genomes (Beaujean et al., 2004; Fulka et al., 2008; 2004; Gu et al., 2011; Guo et al., 2014b; Inoue and Zhang, 2011; Inoue et al., 2011; Iqbal et al., 2011; Pendina et al., 2011; Wossidlo et al., 2011). Both mouse and human oocytes express elevated *Tet3*/*TET3* compared to *Tet1*/*TET1* and *Tet2*/TET2, in addition to expressing the protective *Dppa3*/*DPPA3* factor (Kobayashi et al., 2012; Okae et al., 2014; Wossidlo et al., 2011; Yan et al., 2013). A confirmed role for these proteins in human zygotes remains to be elucidated. However, since the human maternal pronucleus harbors greater 5mC and lower 5hmC than the paternal pronucleus, it is likely that at least a portion of the maternal genome must be protected from active demethylation (Fulka et al., 2004; 2008; Pendina et al., 2011). During cleavage divisions, DNA methylation and hydroxymethylation marks display an asymmetric chromatid localization, which are passively diluted though replication in both species (Efimova et al., 2015; Inoue and Zhang, 2011; Inoue et al., 2011; Shen et al., 2014; Wang et al., 2014). However, a role for active demethylation also exists for both mouse (Smith et al., 2012) and human (Efimova et al., 2015), possibly in a stage-specific and sequence-specific manner. Mechanistically in mouse, passive loss of DNA methylation during preimplantation development was attributed to DNMT1o exclusion from nuclei (except at the 8-cell stage) and low nuclear DNMT1s levels

at all preimplantation stages (Cirio et al., 2008a; 2008b; Hirasawa et al., 2008; Howell et al., 2001; Kurihara et al., 2008; Ratnam et al., 2002). In humans, DNMT1o nuclear localization occurs throughout preimplantation, while nuclear localization of DNMT1s is restricted to nuclei of 6-cell to morula stage embryos (Petrussa et al., 2014). Not withstanding this difference, it appears that DNMT1o and DNMT1s are present at sufficient levels to maintain imprinted methylation during mouse and human preimplantation development. Further research is required to delineate the functions of these DNMT1 isoforms.

With regards to imprinted DNA methylation, genome-wide methylation studies of human gametes and preimplantation embryos indicate preservation of maintenance of DNA methylation at imprinted gDMRs (Guo et al., 2014b; Kobayashi et al., 2012; Okae et al., 2014). As in mouse (Nakamura et al., 2007; 2012), high abundance of *DPPA3* in human oocytes (Goto et al., 2002; Kobayashi et al., 2012; Yan et al., 2013) suggests a conserved role for this protein in protecting imprinted gDMRs from active DNA methylation loss in zygotes. During cleavage division, the presence of *DNMT1o*/DNMT1o and *DNMT1s*/DNMT1s and nuclear localization of DNMT1o/DNMT1s during human preimplantation development (Huntriss et al., 2004; Petrussa et al., 2014) suggests conservation to mouse (Cirio et al., 2008a; 2008b) in maintaining DNA methylation at imprinted gDMRs. With regard to the DNMT1 interacting partner ZFP57, limited data exists for its role in human embryos. However, to assess its function, mouse embryonic stem cells were transfected with human *ZFP57*. The mouse and human ZFP57 proteins are interchangeable in maintaining imprinted DNA methylation as well as binding to TRIM28 (Takikawa et al., 2013). In line with this, in human embryonic stem cells, TRIM28 is recruited to the majority of human imprinted DMRs by KRAB-containing zinc finger proteins (KRAB-ZFPs)(Jacobs et al., 2014; Turelli et al., 2014) (Table 1). Since ZFP57 and TRIM28 are maternal effect proteins in mouse, their expression has also been examined in human oocytes. Although *TRIM28* mRNA abundance was similar between human and mouse oocytes (Okae et al., 2014), human oocytes were reported to lack *ZFP57* transcripts (Okae et al., 2014; Yan et al., 2013), with embryonic *ZFP57* expression commencing at the morula stage (Yan et al., 2013). This requires further validation since *ZFP57* protein levels were not assessed. Overall, current evidence indicates that imprinted gDMRs are maintained during human preimplantation development, with

potential conservation of DNA methylation protector proteins that bar active and passive demethylation.

In conclusion, regulation of DNA methylation dynamics during gamete and preimplantation development is complex. While a greater body of data exists for the mouse compared to the human, available data highlight striking similarities between these species. Regardless of differences that may exist, in both species it is evident that proper regulation of imprinted DNA methylation dynamics is necessary for successful preimplantation embryo development. Consequently, any disruption of imprinted DNA methylation dynamics during this period could lead to aberrant or failed development or genomic imprinting disorders.

1.4   Mitochondria

Mitochondrial dysfunction has confirmed roles in mitochondrial disease, failed reproductive success and age-related infertility. Many studies have confirmed the vital role mitochondria play as important determinants of developmental competence throughout oocyte and preimplantation embryo growth. As mitochondria are dynamically regulated and critically required during this early period of development, defects in mitochondrial distribution, quantity, and/or activity have negative developmental consequences in multiple species, including mouse and human (Ge et al., 2012; Thouas et al., 2004; Van Blerkom et al., 1995; 2000; Van Blerkom, 2004; 2008; 2009; 2011; Wakefield et al., 2011).

1.4.1   Mitochondrial dynamics during oogenesis and preimplantation development

At fertilization in the fully grown mature oocyte, the mitochondrial complement has been derived from approximately 10-20 mitochondria in PGCs that increases rapidly via mitochondrial biogenesis and mitochondrial DNA replication during mouse and human oocyte growth up to the MII stage (Cummins, 2002; Jansen, 2000; St John et al., 2010; Van Blerkom, 2011). In the human, mitochondrial numbers reach about 100,000 to 400,000 in the mature MII oocyte (Cummins, 2002; Jansen, 2000; Jansen and de Boer, 1998; Jansen and Burton, 2004), similar to the $92,500 \pm 7000$ identified in the mouse egg (Pikó and Matsumoto, 1976). This oocyte mitochondrial pool represents the sole source of mitochondria present during oogenesis, preimplantation development and throughout life.

After fertilization in both human and mouse, mitochondrial DNA molecules are not replicated until the blastocyst stage of preimplantation development (Larsson et al., 1998; Pikó and Chase, 1973; Pikó and Taylor, 1987; Thundathil et al., 2005). Thus, mitochondrial numbers are anticipated to remain relatively constant within the preimplantation embryo. This would mean that mitochondrial numbers decrease by half per blastomere with each successive cleavage division (Motta et al., 2000; Sathananthan and Trounson, 2000; St John et al., 2010; Thundathil et al., 2005; Van Blerkom, 2011; Zamboni, 1971) (Figure 1-9). After implantation, the molecular machinery for mitochondrial DNA replication becomes active, with mitochondrial DNA copy number and mitochondrial biogenesis increasing first primarily in trophectodermal cells then subsequently in the epiblast (Assou et al., 2006; Larsson et al., 1998; St John et al., 2010; Thundathil et al., 2005).

Although mitochondria are in a state of replicative senescence during preimplantation development, the organelles undergo dynamic changes in morphology. In oocytes and early embryos, mitochondria are small, spherical and structurally underdeveloped but still functional and active in generating ATP (Motta et al., 2000; Pikó and Chase, 1973). As preimplantation development continues, mitochondria elongate, increase cristae numbers, and by the expanded blastocyst stage they begin to resemble forms present in differentiated somatic cells, again predominantly in trophectoderm (Motta et al., 2000; Pikó and Chase, 1973; Van Blerkom et al., 1973). These structural changes occur in parallel to increased respiration to meet the energy demands for blastocyst formation and the development of the fluid filled cavity by trophectoderm cells (Houghton, 2006). Most of the energy produced in blastocyst trophectoderm is hypothesized to drive and support activity of the ATP-dependent Na^+/K^+-ATPase (sodium-potassium adenosine triphosphatase) (Houghton, 2006; Van Blerkom, 2008), which is known to be vital for blastocyst formation/cavitation (Madan et al., 2007; Watson et al., 2004).

In addition to dynamic morphological changes, mitochondria also actively translocate to specific regions of the cytoplasm during oogenesis and preimplantation development. Perinuclear translocation of active mitochondria occurs during meiosis, with nuclear localization coinciding with bursts of ATP production specifically during nuclear maturation (germinal vesicle break down (GVBD), metaphase I (MI) spindle migration, MI to MII transition, and polar body (PB) extrusion) (Van Blerkom, 1991; Yu et al., 2010). At the

ovulated MII stage, both perinuclear mitochondrial localization (Kan et al., 2011; Nagai et al., 2006) and a homogenous distribution throughout the cytoplasm (Tokura et al., 1993; Van Blerkom, 2004; Yu et al., 2010) has been documented. In addition to this distribution of active mitochondria during oogenesis, a persistent subcortical high potential mitochondrial ring in the oocyte exists and is required for sperm penetration, fertilization and meiotic maturation (Van Blerkom and Davis, 2007). The localization of mitochondria during preimplantation development is less characterized. However, perinuclear localization at the 2-cell stage (Van Blerkom et al., 2000; Van Blerkom, 2009), symmetrical distribution of mitochondria between pronuclei/blastomeres from the pronuclear 1-cell to 8-cell stage (Van Blerkom et al., 2000), and higher mitochondrial activity in trophectoderm cells (TE) versus inner cell mass (ICM) cells in blastocysts (Houghton, 2006) have all been reported.

1.4.2   The role of mitochondria in developmental competence

Recently, many studies performed in mouse and human have concentrated on analyzing mitochondrial parameters with respect to reproductive success of the oocyte and preimplantation embryo.   With regards to oocyte competence, nuclear and meiotic maturation (and consequently fertilization) are dependent on ATP generation (Dumollard et al., 2004; St John et al., 2010; Yu et al., 2010). Those oocytes with sufficient ATP and mitochondria numbers generate higher-quality blastocyst embryos (Takeuchi et al., 2005) and exhibit an increased potential for continued embryogenesis, implantation (Van Blerkom et al., 1995), and postimplantation development (Wai et al., 2010). Perinuclear accumulation of active mitochondria is also necessary for oocyte competence (Van Blerkom, 1991; Van Blerkom and Runner, 1984; Yu et al., 2010).

As during oogenesis, mitochondrial function and the ability to generate sufficient ATP is required for successful cleavage throughout preimplantation development (Liu et al., 2000; May-Panloup et al., 2005; Thouas et al., 2004). Upon successful fertilization, failure to accumulate mitochondria to the perinuclear region in zygotes is associated with decreased blastocyst developmental rates (Zhao et al., 2009). Furthermore, decreased ATP content occurs in mouse embryos undergoing a 2-cell block in development (Wang et al., 2009). With regard to mitochondrial distribution, 1-cell zygote to 8-cell stage preimplantation embryos exhibiting an asymmetrical segregation of mitochondria surrounding pronuclei and

between blastomeres undergo increased developmental arrest, with lysis of blastomeres inheriting lower amounts of mitochondria (Van Blerkom et al., 2000). Finally, mitochondrial inhibition during preimplantation development leads to impaired ATP production, incrementally reduced blastocyst development, decreased blastocyst ICM and TE cell numbers, and reduced fetal and placental growth, thus highlighting the importance of mitochondria both during preimplantation and postimplantation development (Wakefield et al., 2011).

In conclusion, appropriate regulation of mitochondrial dynamics is critical for successful development of human and mouse oocytes and preimplantation embryos. Consequently, perturbations in mitochondrial dynamics during this critical period have the potential to negatively impact developmental outcomes.

1.5 Assisted Reproductive Technologies (ARTs)

1.5.1 Infertility and ART

Infertility is generally defined as the inability to conceive naturally after 1 year of unprotected sex. Recent figures alarmingly estimate that approximately 48.6 million couples worldwide are unable to conceive after 5 years of unprotected sex (Mascarenhas et al., 2012). In Canada and the United States, infertility affects 16% and 10-15% of couples, respectively, tripling Canadian rates since 1984 (5.4%) (Bushnik et al., 2012; Chandra et al., 2013). Medically assisted reproductive technologies (ARTs) represent infertility treatment methods that give infertile/subfertile couples the best chance to conceive. These techniques include ovarian stimulation, *in vitro* oocyte maturation, *in vitro* fertilization (IVF), intracytoplasmic sperm injection (ICSI), *in vitro* embryo culture, blastocyst hatching, preimplantation genetic diagnosis (PGD), embryo transfer, oocyte and embryo cryopreservation, and recently mitochondrial replacement therapy and AUGMENT (discussed in section 1.5.3).

Due to the rising prevalence of infertility, since the birth of Louise Brown, the first human infant conceived through ARTs in July of 1978 (Steptoe and Edwards, 1978), the use of ARTs has drastically increased. Now, the proportion of infants born following ARTs is approximately 1.6% of all births in the United States (Sunderam et al., 2015), reaching as high as 4.5% of births in developed countries (Ferraretti et al., 2013). In Canada, 32 of 33

clinics reported completion of approximately 16, 062 ART cycles in 2013, with an overall live birth rate of 25% (Human Assisted Reproduction 2014). However, when treatment is successful (< 40%), it carries an increased risk of perinatal complications even within singleton pregnancies, including; (1) preterm birth; (2) intrauterine growth restriction; (3) low birth weight (Helmerhorst et al., 2004; Jackson et al., 2004; McGovern et al., 2004; Okun and Sierra, 2014; Reddy et al., 2007; Savage et al., 2011; Schieve et al., 2002; Sunderam et al., 2014; Wisborg et al., 2010); (4) large for gestational age (Hansen and Bower, 2014; Ishihara et al., 2014; Korosec et al., 2014; 2016; Li et al., 2014; Pinborg et al., 2014; Sazonova et al., 2012; Wennerholm et al., 2013); and (5) higher incidences of the genomic imprinting disorders, (a) Beckwith-Wiedemann Syndrome (DeBaun et al., 2003; Doornbos et al., 2007; Gicquel et al., 2003; Maher et al., 2003a; Sutcliffe et al., 2006; Vermeiden and Bernardus, 2013), (b) Angelman Syndrome (Cox et al., 2002; Doornbos et al., 2007; Ludwig et al., 2005; Maher et al., 2003a; Ørstavik et al., 2003), and (c) Silver-Russell Syndrome (SRS) (Bliek et al., 2006; Chiba et al., 2013; Chopra et al., 2010; Cocchi et al., 2013; Hiura et al., 2012; Kagami et al., 2007; Lammers et al., 2012; Vermeiden and Bernardus, 2013).

1.5.2 ART and imprinting disorders

The overall risk for an imprinting disorder such as BWS, AS or SRS after ART is approximately 1 in 5,000 children (Okun and Sierra, 2014). This is compared to the low risk in the general population for BWS (1 in 13,700), AS (1 in 15,000) and SRS (unknown prevalence). Specifically, the risk of BWS is 3-16 times greater in ART-conceived children compared to the general population (DeBaun et al., 2003; Gicquel et al., 2003; Gosden et al., 2003; Halliday et al., 2004; Hiura et al., 2012; Lim et al., 2009; Lucifero et al., 2004; Maher et al., 2003a; 2003b; Rossignol et al., 2006; Sutcliffe et al., 2006; van Montfoort et al., 2012; Vermeiden and Bernardus, 2013). Within BWS patients conceived by ART, imprinted methylation errors occur at a greater frequency, with over 90% of ART cases showing *KCNQ1OT1* hypomethylation compared to 50% in the general population (DeBaun et al., 2003; Gicquel et al., 2003; Gosden et al., 2003; Halliday et al., 2004; Hiura et al., 2012; Lim et al., 2009; Maher et al., 2003a; 2003b; Rossignol et al., 2006; Sutcliffe et al., 2006), and conversely, 17% of ART cases showing *H19* hypermethylation compared to 5% in general (DeBaun et al., 2003; Lennerz et al., 2010; Rossignol et al., 2006). Likewise for AS, 46% of

patients conceived by ARTs possessed imprinting defects at the *SNRPN* ICR (Cox et al., 2002; Ludwig et al., 2005; Ørstavik et al., 2003) compared to 5% in general (Horsthemke and Wagstaff, 2008; Van Buggenhout and Fryns, 2009) while for SRS, 11 out of 12 (92%) ART patients harboured *H19* hypomethylation (Bliek et al., 2009; Chopra et al., 2010; Cocchi et al., 2013; Hiura et al., 2012; Kagami et al., 2007; Lammers et al., 2012; Vermeiden and Bernardus, 2013) compared to 40% in the general population (Chiba et al., 2013). Overall, studies suggest that ARTs increase imprinting disorders, likely through alterations in epigenetic regulation of imprinted gene expression. Specifically, one explanation for this risk is that gamete and embryo manipulations disrupt acquisition and/or maintenance of genomic imprints during gametogenesis and preimplantation development. It is therefore essential to determine where imprinted methylation errors are occurring and which aspect(s) of ARTs lead to these adverse epigenetic effects.

1.5.2.1   Mouse model system

Much of what we know regarding imprinting disorders and ARTs has been discovered using the mouse model system. This system has specifically been instrumental in the investigation of the effects of individual ARTs on genomic imprint acquisition during gametogenesis and maintenance throughout preimplantation development. Additionally, the mouse model allows for controlled studies without issues of confounding infertility that are unavoidable when studying human assisted conception. Major findings from mouse studies indicate that imprinted methylation acquisition is not perturbed by superovulation (Denomme et al., 2011) or *in vitro* oocyte maturation in oocytes (Anckaert et al., 2009; 2010; Geuns et al., 2003; 2007), but instead imprint maintenance in preimplantation embryos is disrupted by superovulation (Hajj et al., 2011; Market-Velker et al., 2010b), *in vitro* fertilization (IVF) (Fauque et al., 2010), *in vitro* embryo culture (Li et al., 2005; Mann et al., 2004; Market-Velker et al., 2010a; 2012) and oocyte vitrification (Cheng et al., 2014). Within these studies, imprinted methylation errors in preimplantation embryos occurred at a relatively high frequency, with errors present in 10-90% of embryos analyzed. Studies in our lab have specifically analyzed the effect of ovarian stimulation, or superovulation, on imprinted methylation at both low (6.25 IU) and high (10 IU) hormone doses. Superovulation using high and low hormone-doses did not perturb imprinted methylation acquisition in individual oocytes at *Snrpn*, *Peg3*, *Kcnq1ot1* or *H19* (Denomme et al., 2011). In contrast, individual

blastocyst-stage embryos derived from superovulated females exhibited a dose-dependent loss of methylation at imprinted domains, specifically *Snrpn*, *Peg3*, *Kcnq1ot1* and *H19* (Market-Velker et al., 2010b). Consequently, we demonstrated that superovulation alone perturbs imprinted methylation in blastocyst embryos at a high frequency. This finding is additionally supported by two studies in human that discovered patients receiving ovarian stimulation alone as an ART gave birth to BWS and AS children (Chang et al., 2005; Ludwig et al., 2005).

1.5.2.2   Discrepancy between human and mouse

Disparity has arisen concerning the frequency of imprinting errors produced by ARTs in humans compared to mice. When comparing the overall risk for an imprinting disorder, 10-90% of treated preimplantation mouse embryos show abnormal imprint maintenance (Fauque et al., 2010; Hajj et al., 2011; Market-Velker et al., 2010b; 2012), while only 1 in 5, 000 ART children are at risk for BWS, AS or SRS (Okun and Sierra, 2014). Overtly, it would therefore appear that the mouse is more sensitive than the human with respect to the incidence of ART-induced imprinting errors. This has lead to questioning whether the effects of ARTs on imprint regulation in the mouse recapitulate those processes involved in humans. However, one key difference in studies between these species is the time of analysis. The majority of mouse studies have focused on preimplantation or mid-gestation development, while human studies are primarily retrospective studies of ART children with imprinting disorders. Although few studies on human preimplantation embryos exist (Chen et al., 2010; Geuns et al., 2003; 2007; Ibala-Romdhane et al., 2011; Khoueiry et al., 2012; Shi et al., 2014), most embryos that have been analyzed were poor quality embryos unsuitable for transfer. Therefore it becomes essential to identify the risk for imprinting errors in high quality human preimplantation embryos.

1.5.3   Mitochondria in Assisted Reproductive Technologies

The importance of mitochondria during gametogenesis and preimplantation has recently been acknowledged in human Assisted Reproductive Technologies (ARTs; discussed in detail section 1.5). Fertility clinics around the world are now actively addressing the role mitochondria play during preimplantation development by utilizing novel techniques to overcome perturbed mitochondrial function. For example, dietary coenzyme

Q10, or CoQ10, an essential component of the electron transport chain, is used in human clinics to increase mitochondrial activity with the intention of improving oocyte quality (Ben-Meir et al., 2015; Bentov et al., 2010; 2014; Chappel, 2013; Meldrum et al., 2016). Additionally, more invasive procedures are also being implemented. Specifically, mitochondrial replacement therapy (MRT) is currently being used in the United Kingdom (UK) to circumvent the inheritance of mitochondrial DNA mutations and mitochondrial disease to offspring of affected mothers (Reinhardt et al., 2013). In this technology, pronuclear DNA of the intended parents is injected into an enucleated donor oocyte containing "mutation-free" mitochondria. This technique was originally performed in mice (Sato et al., 2005), and before implementation in human was also used to produce macaque babies (Tachibana et al., 2009). Currently, juvenile macaque offspring born through mitochondrial replacement therapy are seemingly healthy with normal metabolic profiles (Tachibana et al., 2013). However as of now, concern from the United States Food and Drug Agency (FDA) has prevented the use of this technology until more data are available to support its safety (Couzin-Frankel, 2015). Consistent with this, results in the mouse suggest that MRT could potentially alter respiration, growth, and exercise and learning ability in adults (Nagao et al., 1998; Roubertoux et al., 2003). This could be due to disrupted cross-talk between genes encoded in the nucleus and the mitochondria, as coordinated interactions between mitochondria and nuclear alleles are favored, and these are disrupted by MRT (Muir et al., 2016; Reinhardt et al., 2013; Woodson and Chory, 2008). Nonetheless, although controversial, MRT is currently being used in the UK to avoid inherited mitochondrial disease.

Another mitochondrial treatment has recently been made available to assist conception in women of advanced reproductive age or in couples with repetitive failed *in vitro* fertilization (IVF) cycles. The US-based company OvaScience developed a new fertility treatment, termed Autologous Germline Mitochondrial Energy Transfer (AUGMENT), and it is based on improving oocyte quality through supplying the egg with a supposedly germline-derived source of mitochondria from the ovarian cortex (Woods and Tilly, 2015). Again, the FDA has prohibited its current use in the US. However, it is offered at the Toronto Centre for Advanced Reproductive Technology (TCART) clinic in Canada, as well in London UK, Istanbul, Japan, Panama, Spain, Turkey and Dubai (Motluk, 2015). This

technique is different from the MRT technique that is used for disease prevention, since AUGMENT does not require donor mitochondria but depends on the existence of controversial (Zhang et al., 2012), patient-matched cells that are extracted from the ovary (Bukovsky et al., 2004; Johnson et al., 2004; Pacchiarotti et al., 2010; Virant-Klun et al., 2013; White et al., 2012; Zou et al., 2009). These putative cells are in the ovarian cortex and studies in mouse have shown that when reintroduced into adult ovaries they can produce mature oocytes and viable preimplantation embryos, including blastocysts (White et al., 2012). Additionally, a separate group that transfected these ovarian cells with a GFP virus reported production of live offspring that inherited the GFP transgene, birthed from transplanted infertile females (Zou et al., 2009). Importantly, the role of these cells in normal folliculogenesis is unknown (Begum et al., 2008). The AUGMENT technique isolates mitochondria from a patient's own cells extracted from the ovary and injects them into the oocyte at the time of intracytoplasmic sperm injection (ICSI) (Tilly and Sinclair, 2013; Woods and Tilly, 2015). Although controversial, the world's first AUGMENT baby was born in Toronto over 1 year ago, on April 13th, 2015.

1.5.3.1   Effects of ARTs on mitochondria

Many studies have focused on mitochondrial dynamics during gametogenesis and the preimplantation period. However, much of what we know is based on samples obtained by assisted reproductive technologies (ARTs). ART treatments coincide with critical time points where mitochondria are drastically increased during oogenesis, translocated to provide stage-specific spatial ATP requirements, and sustained in a non-replicative state during preimplantation development while still functioning as the primary ATP source. Few studies in mouse and human have addressed the effect of ARTs on mitochondrial dynamics and function, with the majority of these focusing on oocyte freezing. Albeit, a few studies have analyzed the effect of ovarian stimulation on mitochondria in mouse (Combelles and Albertini, 2003; Ge et al., 2012; Shu et al., 2015) and macaque (Gibson et al., 2005). These studies have shown that ovarian stimulation decreases mitochondrial DNA copy number, ATP levels and mitochondrial membrane potential in resulting mouse oocytes (Combelles and Albertini, 2003; Ge et al., 2012; Shu et al., 2015) and increases mitochondrial DNA deletions in macaque oocytes (Gibson et al., 2005).

1.6   Rationale

With the use of ARTs rising worldwide (Dyer et al., 2016), there is a continual emergence of new techniques being implemented in human IVF, including mitochondrial replacement therapy (Reinhardt et al., 2013; Wolf et al., 2015) and AUGMENT (Woods and Tilly, 2015). Furthermore, due to the announcement of ART funding in Ontario, which was implemented December 2015 (Motluk, 2016), and the absence of strict regulation of ARTs in Canada (Assisted Human Reproduction Act), it is becoming increasingly important for researchers to investigate the effects of these treatments on the manipulated oocyte and preimplantation embryo. This is especially important as ART techniques coincide with critical time points where imprinted DNA methylation marks are being maintained and mitochondria are very dynamic (Figure 1-9). As discrepancy in the field exists between risk for imprinting disorders in preimplantation mouse embryos and human infants born through ARTs, it is essential to identify the risk for imprinting abnormalities in early human embryos. Furthermore, with the advent of novel treatments targeting mitochondria, the effects of widely used ARTs on mitochondria, such as the indispensible procedure of ovarian stimulation, must be determined.

1.7   Hypothesis

My overall hypothesis is that imprinted DNA methylation maintenance and mitochondrial dynamics are disrupted by ARTs during preimplantation development. Specifically, I hypothesize that imprinted methylation errors occur at similar frequencies in donated, good quality, human preimplantation embryos compared to those identified in mouse. Furthermore, I hypothesize that ovarian stimulation disrupts maternally derived mitochondria in oocytes and preimplantation embryos derived from hormone-treated females.

1.8   Objectives

1. To determine the effect of ARTs on imprinted DNA methylation in human preimplantation embryos. Specifically, this objective will address whether donated human ART-produced preimplantation embryos harbour aberrant imprinted methylation at similar incidences to that observed in the mouse.

a. Determine baseline imprinted DNA methylation levels at *SNRPN*, *KCNQ1OT1* and *H19* in untreated human buccal cell samples.

b. Determine whether imprinted methylation errors occur in human day 3 (~6-8 cells) and blastocyst-stage embryos, and whether short or extended culture produces a greater frequency of imprinted methylation errors.

c. Determine whether aberrant imprinted methylation in human day 3 and blastocyst embryos correlates with parental biometrics or clinical treatment.

2. My second objective further extends analyses on the effects of ART treatments on resulting embryos by analyzing the effects of ovarian simulation on mitochondria in the oocyte and throughout preimplantation development.

a. Determine whether superovulation disrupts the pool of total mitochondria, active mitochondria, and mitochondrial distribution in oocytes and during preimplantation development

b. Determine whether resulting blastocyst embryos exhibit perturbed mitochondrial function.

1.9 References

Ager, E., Suzuki, S., Pask, A., Shaw, G., Ishino, F., and Renfree, M.B. (2007). Insulin is imprinted in the placenta of the marsupial, Macropus eugenii. Dev. Biol. *309*, 317–328.

Alexander, K.A., Wang, X., Shibata, M., Clark, A.G., and García-García, M.J. (2015). TRIM28 Controls Genomic Imprinting through Distinct Mechanisms during and after Early Genome-wide Reprogramming. Cell Rep *13*, 1194–1205.

Amouroux, R., Nashun, B., Shirane, K., Nakagawa, S., Hill, P.W.S., D'Souza, Z., Nakayama, M., Matsuda, M., Turp, A., Ndjetehe, E., et al. (2016). De novo DNA methylation drives 5hmC accumulation in mouse zygotes. Nat. Cell Biol. *18*, 225–233.

Anckaert, E., Adriaenssens, T., Romero, S., Dremier, S., and Smitz, J. (2009). Unaltered imprinting establishment of key imprinted genes in mouse oocytes after in vitro follicle culture under variable follicle-stimulating hormone exposure. Int. J. Dev. Biol. *53*, 541–548.

Anckaert, E., Romero, S., Adriaenssens, T., and Smitz, J. (2010). Effects of low methyl donor levels in culture medium during mouse follicle culture on oocyte imprinting establishment. Biol. Reprod. *83*, 377–386.

Anest, V., Hanson, J.L., Cogswell, P.C., Steinbrecher, K.A., Strahl, B.D., and Baldwin, A.S. (2003). A nucleosomal function for IκB kinase-α in NF-κB-dependent gene expression. Nature *423*, 659–663.

Angiolini, E., Coan, P.M., Sandovici, I., Iwajomo, O.H., Peck, G., Burton, G.J., Sibley, C.P., Reik, W., Fowden, A.L., and Constância, M. (2011). Developmental adaptations to increased fetal nutrient demand in mouse genetic models of Igf2-mediated overgrowth. Faseb J. *25*, 1737–1745.

Aoki, A., Shiozaki, A., Sameshima, A., Higashimoto, K., Soejima, H., and Saito, S. (2011). Beckwith-Wiedemann syndrome with placental chorangioma due to H19-differentially methylated region hypermethylation: a case report. J. Obstet. Gynaecol. Res. *37*, 1872–1876.

Arand, J., Wossidlo, M., Lepikhov, K., Peat, J.R., Reik, W., and Walter, J. (2015). Selective impairment of methylation maintenance is the major cause of DNA methylation reprogramming in the early embryo. Epigenetics Chromatin *8*, 1.

Arima, T., and Wake, N. (2006). Establishment of the primary imprint of the HYMAI/PLAGL1 imprint control region during oogenesis. Cytogenet. Genome Res. *113*, 247–252.

Arita, K., Ariyoshi, M., Tochio, H., Nakamura, Y., and Shirakawa, M. (2008). Recognition of hemi-methylated DNA by the SRA protein UHRF1 by a base-flipping mechanism. Nature *455*, 818–821.

Assou, S., Anahory, T., Pantesco, V., Le Carrour, T., Pellestor, F., Klein, B., Reyftmann, L., Dechaud, H., De Vos, J., and Hamamah, S. (2006). The human cumulus--oocyte complex gene-expression profile. Human Reproduction *21*, 1705–1719.

Bannister, A.J., Zegerman, P., Partridge, J.F., Miska, E.A., Thomas, J.O., Allshire, R.C., and Kouzarides, T. (2001). Selective recognition of methylated lysine 9 on histone H3 by the HP1 chromo domain. Nature *410*, 120–124.

Bannister, A.J., and Kouzarides, T. (2011). Regulation of chromatin by histone modifications. Cell Res. *21*, 381–395.

Bannister, A.J., Schneider, R., Myers, F.A., Thorne, A.W., Crane-Robinson, C., and Kouzarides, T. (2005). Spatial distribution of di- and tri-methyl lysine 36 of histone H3 at active genes. J. Biol. Chem. *280*, 17732–17736.

Barski, A., Cuddapah, S., Cui, K., Roh, T.-Y., Schones, D.E., Wang, Z., Wei, G., Chepelev, I., and Zhao, K. (2007). High-resolution profiling of histone methylations in the human genome. Cell *129*, 823–837.

Bartolomei, M.S., Zemel, S., and Tilghman, S.M. (1991). Parental imprinting of the mouse H19 gene. Nature *351*, 153–155.

Bartolomei, M.S., and Ferguson-Smith, A.C. (2011). Mammalian genomic imprinting. Cold Spring Harb Perspect Biol *3*.

Barton, S.C., Surani, M.A., and Norris, M.L. (1984). Role of paternal and maternal genomes in mouse development. Nature *311*, 374–376.

Beatty, L., Weksberg, R., and Sadowski, P.D. (2006). Detailed analysis of the methylation patterns of the KvDMR1 imprinting control region of human chromosome 11. Genomics *87*, 46–56.

Beaujean, N., Hartshorne, G., Cavilla, J., Taylor, J., Gardner, J., Wilmut, I., Meehan, R., and Young, L. (2004). Non-conservation of mammalian preimplantation methylation dynamics. Curr. Biol. *14*, R266–R267.

Begemann, M., Spengler, S., Kanber, D., Haake, A., Baudis, M., Leisten, I., Binder, G., Markus, S., Rupprecht, T., Segerer, H., et al. (2011). Silver-Russell patients showing a broad range of ICR1 and ICR2 hypomethylation in different tissues. Clin. Genet. *80*, 83–88.

Begum, S., Papaioannou, V.E., and Gosden, R.G. (2008). The oocyte population is not renewed in transplanted or irradiated adult ovaries. Hum. Reprod. *23*, 2326–2330.

Ben-Meir, A., Burstein, E., Borrego-Alvarez, A., Chong, J., Wong, E., Yavorska, T., Naranian, T., Chi, M., Wang, Y., Bentov, Y., et al. (2015). Coenzyme Q10 restores oocyte mitochondrial function and fertility during reproductive aging. Aging Cell *14*, 887–895.

Bentov, Y., Esfandiari, N., Burstein, E., and Casper, R.F. (2010). The use of mitochondrial nutrients to improve the outcome of infertility treatment in older patients. Fertil. Steril. *93*, 272–275.

Bentov, Y., Hannam, T., Jurisicova, A., Esfandiari, N., and Casper, R.F. (2014). Coenzyme Q10 Supplementation and Oocyte Aneuploidy in Women Undergoing IVF-ICSI Treatment. Clin Med Insights Reprod Health *8*, 31–36.

Bernstein, B.E., Humphrey, E.L., Erlich, R.L., Schneider, R., Bouman, P., Liu, J.S., Kouzarides, T., and Schreiber, S.L. (2002). Methylation of histone H3 Lys 4 in coding regions of active genes. Proc. Natl. Acad. Sci. U.S.a. *99*, 8695–8700.

Bernstein, B.E., Kamal, M., Lindblad-Toh, K., Bekiranov, S., Bailey, D.K., Huebert, D.J., McMahon, S., Karlsson, E.K., Kulbokas, E.J., Gingeras, T.R., et al. (2005). Genomic maps and comparative analysis of histone modifications in human and mouse. Cell *120*, 169–181.

Bernstein, E. (2005). RNA meets chromatin. Genes & Development *19*, 1635–1655.

Bielinska, B., Blaydes, S.M., Buiting, K., Yang, T., Krajewska-Walasek, M., Horsthemke, B., and Brannan, C.I. (2000). De novo deletions of SNRPN exon 1 in early human and mouse embryos result in a paternal to maternal imprint switch. Nat Genet *25*, 74–78.

Bilodeau, S., Kagey, M.H., Frampton, G.M., Rahl, P.B., and Young, R.A. (2009). SetDB1 contributes to repression of genes encoding developmental regulators and maintenance of ES cell state. Genes & Development *23*, 2484–2489.

Bliek, J., Terhal, P., van den Bogaard, M.-J., Maas, S., Hamel, B., Salieb-Beugelaar, G., Simon, M., Letteboer, T., van der Smagt, J., Kroes, H., et al. (2006). Hypomethylation of the H19 gene causes not only Silver-Russell syndrome (SRS) but also isolated asymmetry or an SRS-like phenotype. Am. J. Hum. Genet. *78*, 604–614.

Bliek, J., Verde, G., Callaway, J., Maas, S.M., De Crescenzo, A., Sparago, A., Cerrato, F., Russo, S., Ferraiuolo, S., Rinaldi, M.M., et al. (2009). Hypomethylation at multiple maternally methylated imprinted regions including PLAGL1 and GNAS loci in Beckwith-Wiedemann syndrome. Eur. J. Hum. Genet. *17*, 611–619.

Boissonnas, C.C., Abdalaoui, H.E., Haelewyn, V., Fauque, P., Dupont, J.M., Gut, I., Vaiman, D., Jouannet, P., Tost, J., and Jammes, H. (2010). Specific epigenetic alterations of IGF2-H19 locus in spermatozoa from infertile men. Eur. J. Hum. Genet. *18*, 73–80.

Borghol, N., Lornage, J., Blachère, T., Sophie Garret, A., and Lefèvre, A. (2006). Epigenetic status of the H19 locus in human oocytes following in vitro maturation. Genomics *87*, 417–426.

Bourc'his, D., Xu, G.L., Lin, C.S., Bollman, B., and Bestor, T.H. (2001). Dnmt3L and the establishment of maternal genomic imprints. Science *294*, 2536–2539.

Bourc'his, D., and Bestor, T.H. (2004). Meiotic catastrophe and retrotransposon reactivation in male germ cells lacking Dnmt3L. Nature *431*, 96–99.

Bourque, D.K., Peñaherrera, M.S., Yuen, R.K.C., Van Allen, M.I., McFadden, D.E., and Robinson, W.P. (2011). The utility of quantitative methylation assays at imprinted genes for the diagnosis of fetal and placental disorders. Clin. Genet. *79*, 169–175.

Bouwland-Both, M.I., van Mil, N.H., Stolk, L., Eilers, P.H.C., Verbiest, M.M.P.J., Heijmans, B.T., Tiemeier, H., Hofman, A., Steegers, E.A.P., Jaddoe, V.W.V., et al. (2013). DNA methylation of IGF2DMR and H19 is associated with fetal and infant growth: the generation R study. PLoS ONE *8*, e81731.

Boyer, L.A., Plath, K., Zeitlinger, J., Brambrink, T., Medeiros, L.A., Lee, T.I., Levine, S.S., Wernig, M., Tajonar, A., Ray, M.K., et al. (2006). Polycomb complexes repress developmental regulators in murine embryonic stem cells. Nature *441*, 349–353.

Buiting, K., Lich, C., Cottrell, S., Barnicoat, A., and Horsthemke, B. (1999). A 5-kb imprinting center deletion in a family with Angelman syndrome reduces the shortest region of deletion overlap to 880 bp. Hum Genet *105*, 665–666.

Bukovsky, A., Caudle, M.R., Svetlikova, M., and Upadhyaya, N.B. (2004). Origin of germ cells and formation of new primary follicles in adult human ovaries. Reprod. Biol. Endocrinol. *2*, 20.

Bushnik, T., Cook, J.L., Yuzpe, A.A., Tough, S., and Collins, J. (2012). Estimating the prevalence of infertility in Canada. Hum. Reprod. *27*, 738–746.

Campos, E.I., and Reinberg, D. (2009). Histones: annotating chromatin. Annu. Rev. Genet. *43*, 559–599.

Cassidy, S.B., Schwartz, S., Miller, J.L., and Driscoll, D.J. (2012). Prader-Willi syndrome. Genet. Med. *14*, 10–26.

Cattanach, B.M. (1986). Parental origin effects in mice. J Embryol Exp Morphol *97 Suppl*, 137–150.

Cattanach, B.M., and Kirk, M. (1985). Differential activity of maternally and paternally derived chromosome regions in mice. Nature *315*, 496–498.

Chamberlain, S.J., and Brannan, C.I. (2001). The Prader-Willi syndrome imprinting center activates the paternally expressed murine Ube3a antisense transcript but represses paternal Ube3a. Genomics *73*, 316–322.

Chamberlain, S.J., Germain, N.D., Chen, P.-F., Hsiao, J.S., and Glatt-Deeley, H. (2014). Modeling Genomic Imprinting Disorders Using Induced Pluripotent Stem Cells. Methods Mol. Biol.

Chandra, A., Copen, C.E., and Stephen, E.H. (2013). Infertility and impaired fecundity in the United States, 1982-2010: data from the National Survey of Family Growth. Natl Health Stat Report 1–18–1pfollowing19.

Chang, A.S., Moley, K.H., Wangler, M., Feinberg, A.P., and DeBaun, M.R. (2005). Association between Beckwith-Wiedemann syndrome and assisted reproductive technology: a case series of 19 patients. Fertil. Steril. *83*, 349–354.

Chappel, S. (2013). The role of mitochondria from mature oocyte to viable blastocyst. Obstet Gynecol Int *2013*, 183024–183024.

Chen, S.-L., Shi, X.-Y., Zheng, H.-Y., Wu, F.-R., and Luo, C. (2010). Aberrant DNA methylation of imprinted H19 gene in human preimplantation embryos. Fertil. Steril. *94*, 2356–8–2358.e1.

Cheng, K.-R., Fu, X.-W., Zhang, R.-N., Jia, G.-X., Hou, Y.-P., and Zhu, S.-E. (2014). Effect of oocyte vitrification on deoxyribonucleic acid methylation of H19, Peg3, and Snrpn differentially methylated regions in mouse blastocysts. Fertil. Steril. *102*, 1183–1190.e1183.

Chiba, H., Hiura, H., Okae, H., Miyauchi, N., Sato, F., Sato, A., and Arima, T. (2013). DNA methylation errors in imprinting disorders and assisted reproductive technology. Pediatr Int *55*, 542–549.

Chopra, M., Amor, D.J., Sutton, L., Algar, E., and Mowat, D. (2010). Russell-Silver syndrome due to paternal H19/IGF2 hypomethylation in a patient conceived using intracytoplasmic sperm injection. Reprod. Biomed. Online *20*, 843–847.

Chotalia, M., Smallwood, S.A., Ruf, N., Dawson, C., Lucifero, D., Frontera, M., James, K., Dean, W., and Kelsey, G. (2009). Transcription is required for establishment of germline methylation marks at imprinted genes. Genes & Development *23*, 105–117.

Choufani, S., Shuman, C., and Weksberg, R. (2010). Beckwith-Wiedemann syndrome. Am. J. Med. Genet. *154C*, 343–354.

Choufani, S., Shuman, C., and Weksberg, R. (2013). Molecular findings in Beckwith-

Wiedemann syndrome. Am. J. Med. Genet. *163C*, 131–140.

Cirio, M.C., Martel, J., Mann, M., Toppings, M., Bartolomei, M., Trasler, J., and Chaillet, J.R. (2008a). DNA methyltransferase 1o functions during preimplantation development to preclude a profound level of epigenetic variation. Dev. Biol. *324*, 139–150.

Cirio, M.C., Ratnam, S., Ding, F., Reinhart, B., Navara, C., and Chaillet, J.R. (2008b). Preimplantation expression of the somatic form of Dnmt1 suggests a role in the inheritance of genomic imprints. BMC Dev. Biol. *8*, 9.

Cocchi, G., Marsico, C., Cosentino, A., Spadoni, C., Rocca, A., De Crescenzo, A., and Riccio, A. (2013). Silver-Russell syndrome due to paternal H19/IGF2 hypomethylation in a twin girl born after in vitro fertilization. Am. J. Med. Genet. A *161A*, 2652–2655.

Combelles, C.M.H., and Albertini, D.F. (2003). Assessment of oocyte quality following repeated gonadotropin stimulation in the mouse. Biol. Reprod. *68*, 812–821.

Constância, M., Dean, W., Lopes, S., Moore, T., Kelsey, G., and Reik, W. (2000). Deletion of a silencer element in Igf2 results in loss of imprinting independent of H19. Nat Genet *26*, 203–206.

Constância, M., Hemberger, M., Hughes, J., Dean, W., Ferguson-Smith, A., Fundele, R., Stewart, F., Kelsey, G., Fowden, A., Sibley, C., et al. (2002). Placental-specific IGF-II is a major modulator of placental and fetal growth. Nature *417*, 945–948.

Cortellino, S., Xu, J., Sannai, M., Moore, R., Caretti, E., Cigliano, A., Le Coz, M., Devarajan, K., Wessels, A., Soprano, D., et al. (2011). Thymine DNA glycosylase is essential for active DNA demethylation by linked deamination-base excision repair. Cell *146*, 67–79.

Couzin-Frankel, J. (2015). Reproductive medicine. Eggs' power plants energize new IVF debate. Science *348*, 14–15.

Cox, G.F., Bürger, J., Lip, V., Mau, U.A., Sperling, K., Wu, B.-L., and Horsthemke, B. (2002). Intracytoplasmic sperm injection may increase the risk of imprinting defects. Am. J. Hum. Genet. *71*, 162–164.

Cummins, J.M. (2002). The role of maternal mitochondria during oogenesis, fertilization and embryogenesis. Reprod. Biomed. Online *4*, 176–182.

Cuthbert, G.L., Daujat, S., Snowden, A.W., Erdjument-Bromage, H., Hagiwara, T., Yamada, M., Schneider, R., Gregory, P.D., Tempst, P., Bannister, A.J., et al. (2004). Histone deimination antagonizes arginine methylation. Cell *118*, 545–553.

Davis, T.L., Trasler, J.M., Moss, S.B., Yang, G.J., and Bartolomei, M.S. (1999). Acquisition of the H19 methylation imprint occurs differentially on the parental alleles during spermatogenesis. Genomics *58*, 18–28.

Davis, T.L., Yang, G.J., McCarrey, J.R., and Bartolomei, M.S. (2000). The H19 methylation

imprint is erased and re-established differentially on the parental alleles during male germ cell development. Hum. Mol. Genet. *9*, 2885–2894.

De Felici, M. (2013). Origin, Migration, and Proliferation of Human Primordial Germ Cells. In Oogenesis, G. Coticchio, D.F. Albertini, and L. De Santis, eds. (Springer London), pp. 19–37.

Deaton, A.M., and Bird, A. (2011). CpG islands and the regulation of transcription. Genes & Development *25*, 1010–1022.

DeBaun, M.R., Niemitz, E.L., and Feinberg, A.P. (2003). Association of in vitro fertilization with Beckwith-Wiedemann syndrome and epigenetic alterations of LIT1 and H19. Am. J. Hum. Genet. *72*, 156–160.

DeChiara, T.M., Efstratiadis, A., and Robertson, E.J. (1990). A growth-deficiency phenotype in heterozygous mice carrying an insulin-like growth factor II gene disrupted by targeting. Nature *345*, 78–80.

DeChiara, T.M., Robertson, E.J., and Efstratiadis, A. (1991). Parental imprinting of the mouse insulin-like growth factor II gene. Cell *64*, 849–859.

Deltour, L., Montagutelli, X., Guenet, J.L., Jami, J., and Pàldi, A. (1995). Tissue- and developmental stage-specific imprinting of the mouse proinsulin gene, Ins2. Dev. Biol. *168*, 686–688.

Demetriou, C., Abu-Amero, S., Thomas, A.C., Ishida, M., Aggarwal, R., Al-Olabi, L., Leon, L.J., Stafford, J.L., Syngelaki, A., Peebles, D., et al. (2014). Paternally expressed, imprinted insulin-like growth factor-2 in chorionic villi correlates significantly with birth weight. PLoS ONE *9*, e85454.

Denomme, M.M., White, C.R., Gillio-Meina, C., Macdonald, W.A., Deroo, B.J., Kidder, G.M., and Mann, M.R.W. (2012). Compromised fertility disrupts Peg1 but not Snrpn and Peg3 imprinted methylation acquisition in mouse oocytes. Front Genet *3*, 1–11.

Denomme, M.M., Zhang, L., and Mann, M.R.W. (2011). Embryonic imprinting perturbations do not originate from superovulation-induced defects in DNA methylation acquisition. Fertil. Steril. *96*, 734–738.e2.

Dhayalan, A., Rajavelu, A., Rathert, P., Tamas, R., Jurkowska, R.Z., Ragozin, S., and Jeltsch, A. (2010). The Dnmt3a PWWP domain reads histone 3 lysine 36 trimethylation and guides DNA methylation. J. Biol. Chem. *285*, 26114–26120.

Doornbos, M.E., Maas, S.M., McDonnell, J., Vermeiden, J.P.W., and Hennekam, R.C.M. (2007). Infertility, assisted reproduction technologies and imprinting disturbances: a Dutch study. Human Reproduction *22*, 2476–2480.

Driscoll, D.J., and Migeon, B.R. (1990). Sex difference in methylation of single-copy genes in human meiotic germ cells: implications for X chromosome inactivation, parental imprinting, and origin of CpG mutations. Somat. Cell Mol. Genet. *16*, 267–282.

Dumollard, R., Marangos, P., FitzHarris, G., Swann, K., Duchen, M., and Carroll, J. (2004). Sperm-triggered [Ca2+] oscillations and Ca2+ homeostasis in the mouse egg have an absolute requirement for mitochondrial ATP production. Development *131*, 3057–3067.

Duvillié, B., Bucchini, D., Tang, T., Jami, J., and Pàldi, A. (1998). Imprinting at the mouse Ins2 locus: evidence for cis- and trans-allelic interactions. Genomics *47*, 52–57.

Dyer, S., Chambers, G.M., de Mouzon, J., Nygren, K.G., Zegers-Hochschild, F., Mansour, R., Ishihara, O., Banker, M., and Adamson, G.D. (2016). International Committee for Monitoring Assisted Reproductive Technologies world report: Assisted Reproductive Technology 2008, 2009 and 2010. Hum. Reprod.

Efimova, O.A., Pendina, A.A., Tikhonov, A.V., Fedorova, I.D., Krapivin, M.I., Chiryaeva, O.G., Shilnikova, E.M., Bogdanova, M.A., Kogan, I.Y., Kuznetzova, T.V., et al. (2015). Chromosome hydroxymethylation patterns in human zygotes and cleavage-stage embryos. Reproduction *149*, 223–233.

Eggermann, T., Schönherr, N., Meyer, E., Obermann, C., Mavany, M., Eggermann, K., Ranke, M.B., and Wollmann, H.A. (2006). Epigenetic mutations in 11p15 in Silver-Russell syndrome are restricted to the telomeric imprinting domain. J. Med. Genet. *43*, 615–616.

Eggermann, T., Spengler, S., Bachmann, N., Baudis, M., Mau-Holzmann, U.A., Singer, S., and Rossier, E. (2010). Chromosome 11p15 duplication in Silver-Russell syndrome due to a maternally inherited translocation t(11;15). Am. J. Med. Genet. A *152A*, 1484–1487.

El-Maarri, O., Buiting, K., Peery, E.G., Kroisel, P.M., Balaban, B., Wagner, K., Urman, B., Heyd, J., Lich, C., Brannan, C.I., et al. (2001). Maternal methylation imprints on human chromosome 15 are established during or after fertilization. Nat Genet *27*, 341–344.

El-Maarri, O., Seoud, M., Coullin, P., Herbiniaux, U., Oldenburg, J., Rouleau, G., and Slim, R. (2003). Maternal alleles acquiring paternal methylation patterns in biparental complete hydatidiform moles. Hum. Mol. Genet. *12*, 1405–1413.

Engel, N., Thorvaldsen, J.L., and Bartolomei, M.S. (2006). CTCF binding sites promote transcription initiation and prevent DNA methylation on the maternal allele at the imprinted H19/Igf2 locus. Hum. Mol. Genet. *15*, 2945–2954.

Engel, N., West, A.G., Felsenfeld, G., and Bartolomei, M.S. (2004). Antagonism between DNA hypermethylation and enhancer-blocking activity at the H19 DMD is uncovered by CpG mutations. Nat Genet *36*, 883–888.

Ewen, K.A., and Koopman, P. (2010). Mouse germ cell development: from specification to sex determination. Molecular and Cellular Endocrinology *323*, 76–93.

Fauque, P., Mondon, F., Letourneur, F., Ripoche, M.-A., Journot, L., Barbaux, S., Dandolo, L., Patrat, C., Wolf, J.-P., Jouannet, P., et al. (2010). In vitro fertilization and embryo culture strongly impact the placental transcriptome in the mouse model. PLoS ONE *5*, e9218.

Ferraretti, A.P., Goossens, V., Kupka, M., Bhattacharya, S., de Mouzon, J., Castilla, J.A.,

Erb, K., Korsak, V., Nyboe Andersen, A., European IVF-Monitoring (EIM) Consortium for the European Society of Human Reproduction and Embryology (ESHRE) (2013). Assisted reproductive technology in Europe, 2009: results generated from European registers by ESHRE. Hum. Reprod. *28*, 2318–2331.

Fitzpatrick, G.V., Pugacheva, E.M., Shin, J.-Y., Abdullaev, Z., Yang, Y., Khatod, K., Lobanenkov, V.V., and Higgins, M.J. (2007). Allele-specific binding of CTCF to the multipartite imprinting control region KvDMR1. Molecular and Cellular Biology *27*, 2636–2647.

Fitzpatrick, G.V., Soloway, P.D., and Higgins, M.J. (2002). Regional loss of imprinting and growth deficiency in mice with a targeted deletion of KvDMR1. Nat Genet *32*, 426–431.

Fulka, H., Barnetova, I., Mosko, T., and Fulka, J. (2008). Epigenetic analysis of human spermatozoa after their injection into ovulated mouse oocytes. Hum. Reprod. *23*, 627–634.

Fulka, H., Mrazek, M., Tepla, O., and Fulka, J. (2004). DNA methylation pattern in human zygotes and developing embryos. Reproduction *128*, 703–708.

Gabory, A., Ripoche, M.-A., Le Digarcher, A., Watrin, F., Ziyyat, A., Forné, T., Jammes, H., Ainscough, J.F.X., Surani, M.A., Journot, L., et al. (2009). H19 acts as a trans regulator of the imprinted gene network controlling growth in mice. Development *136*, 3413–3421.

Gabriel, J.M., Merchant, M., Ohta, T., Ji, Y., Caldwell, R.G., Ramsey, M.J., Tucker, J.D., Longnecker, R., and Nicholls, R.D. (1999). A transgene insertion creating a heritable chromosome deletion mouse model of Prader-Willi and angelman syndromes. Proc. Natl. Acad. Sci. U.S.a. *96*, 9258–9263.

Ge, H., Tollner, T.L., Hu, Z., Da, M., Li, X., Guan, H., Shan, D., Lu, J., Huang, C., and Dong, Q. (2012). Impaired mitochondrial function in murine oocytes is associated with controlled ovarian hyperstimulation and in vitro maturation. Reprod. Fertil. Dev. *24*, 945–952.

Geuns, E., De Rycke, M., Van Steirteghem, A., and Liebaers, I. (2003). Methylation imprints of the imprint control region of the SNRPN-gene in human gametes and preimplantation embryos. Hum. Mol. Genet. *12*, 2873–2879.

Geuns, E., De Temmerman, N., Hilven, P., Van Steirteghem, A., Liebaers, I., and De Rycke, M. (2007). Methylation analysis of the intergenic differentially methylated region of DLK1-GTL2 in human. Eur. J. Hum. Genet. *15*, 352–361.

Gibson, T.C., Kubisch, H.M., and Brenner, C.A. (2005). Mitochondrial DNA deletions in rhesus macaque oocytes and embryos. Mol. Hum. Reprod. *11*, 785–789.

Gicquel, C., Gaston, V., Mandelbaum, J., Siffroi, J.-P., Flahault, A., and Le Bouc, Y. (2003). In vitro fertilization may increase the risk of Beckwith-Wiedemann syndrome related to the abnormal imprinting of the KCN1OT gene. Am. J. Hum. Genet. *72*, 1338–1341.

Giddings, S.J., King, C.D., Harman, K.W., Flood, J.F., and Carnaghi, L.R. (1994). Allele

specific inactivation of insulin 1 and 2, in the mouse yolk sac, indicates imprinting. Nat Genet *6*, 310–313.

Gkountela, S., Li, Z., Vincent, J.J., Zhang, K.X., Chen, A., Pellegrini, M., and Clark, A.T. (2013). The ontogeny of cKIT+ human primordial germ cells proves to be a resource for human germ line reprogramming, imprint erasure and in vitro differentiation. Nat. Cell Biol. *15*, 113–122.

Gkountela, S., Zhang, K.X., Shafiq, T.A., Liao, W.-W., Hargan-Calvopiña, J., Chen, P.-Y., and Clark, A.T. (2015). DNA Demethylation Dynamics in the Human Prenatal Germline. Cell *161*, 1425–1436.

Goldberg, A.D., Allis, C.D., and Bernstein, E. (2007). Epigenetics: a landscape takes shape. Cell *128*, 635–638.

Golding, M.C., Magri, L.S., Zhang, L., Lalone, S.A., Higgins, M.J., and Mann, M.R.W. (2011). Depletion of Kcnq1ot1 non-coding RNA does not affect imprinting maintenance in stem cells. Development *138*, 3667–3678.

Gonzalez-Rodriguez, P., Cantu, J., O'Neil, D., Seferovic, M.D., Goodspeed, D.M., Suter, M.A., and Aagaard, K.M. (2016). Alterations in expression of imprinted genes from the H19/IGF2 loci in a multigenerational model of intrauterine growth restriction (IUGR). Am. J. Obstet. Gynecol. *214*, 625.e1–625.e11.

Gosden, R., Trasler, J., Lucifero, D., and Faddy, M. (2003). Rare congenital disorders, imprinted genes, and assisted reproductive technology. Lancet *361*, 1975–1977.

Goto, T., Jones, G.M., Lolatgis, N., Pera, M.F., Trounson, A.O., and Monk, M. (2002). Identification and characterisation of known and novel transcripts expressed during the final stages of human oocyte maturation. Mol. Reprod. Dev. *62*, 13–28.

Gu, T.-P., Guo, F., Yang, H., Wu, H.-P., Xu, G.-F., Liu, W., Xie, Z.-G., Shi, L., He, X., Jin, S.-G., et al. (2011). The role of Tet3 DNA dioxygenase in epigenetic reprogramming by oocytes. Nature *477*, 606–610.

Guibert, S., Forné, T., and Weber, M. (2012). Global profiling of DNA methylation erasure in mouse primordial germ cells. Genome Res. *22*, 633–641.

Guo, F., Li, X., Liang, D., Li, T., Zhu, P., Guo, H., Wu, X., Wen, L., Gu, T.-P., Hu, B., et al. (2014a). Active and passive demethylation of male and female pronuclear DNA in the mammalian zygote. Cell Stem Cell *15*, 447–458.

Guo, F., Yan, L., Guo, H., Li, L., Hu, B., Zhao, Y., Yong, J., Hu, Y., Wang, X., Wei, Y., et al. (2015). The Transcriptome and DNA Methylome Landscapes of Human Primordial Germ Cells. Cell *161*, 1437–1452.

Guo, H., Zhu, P., Yan, L., Li, R., Hu, B., Lian, Y., Yan, J., Ren, X., Lin, S., Li, J., et al. (2014b). The DNA methylation landscape of human early embryos. Nature *511*, 606–610.

Hackett, J.A., Sengupta, R., Zylicz, J.J., Murakami, K., Lee, C., Down, T.A., and Surani, M.A. (2013). Germline DNA demethylation dynamics and imprint erasure through 5-hydroxymethylcytosine. Science *339*, 448–452.

Hajj, El, N., Trapphoff, T., Linke, M., May, A., Hansmann, T., Kuhtz, J., Reifenberg, K., Heinzmann, J., Niemann, H., Daser, A., et al. (2011). Limiting dilution bisulfite (pyro)sequencing reveals parent-specific methylation patterns in single early mouse embryos and bovine oocytes. Epigenetics *6*, 1176–1188.

Hajkova, P. (2011). Epigenetic reprogramming in the germline: towards the ground state of the epigenome. Philosophical Transactions of the Royal Society B: Biological Sciences *366*, 2266–2273.

Hajkova, P., Ancelin, K., Waldmann, T., Lacoste, N., Lange, U.C., Cesari, F., Lee, C., Almouzni, G., Schneider, R., and Surani, M.A. (2008). Chromatin dynamics during epigenetic reprogramming in the mouse germ line. Nature *452*, 877–881.

Hajkova, P., El-Maarri, O., Engemann, S., Oswald, J., Olek, A., and Walter, J. (2002a). DNA-methylation analysis by the bisulfite-assisted genomic sequencing method. Methods Mol. Biol. *200*, 143–154.

Hajkova, P., Erhardt, S., Lane, N., Haaf, T., El-Maarri, O., Reik, W., Walter, J., and Surani, M.A. (2002b). Epigenetic reprogramming in mouse primordial germ cells. Mech. Dev. *117*, 15–23.

Hajkova, P., Jeffries, S.J., Lee, C., Miller, N., Jackson, S.P., and Surani, M.A. (2010). Genome-wide reprogramming in the mouse germ line entails the base excision repair pathway. Science *329*, 78–82.

Hall, J.G. (1990). Genomic imprinting. Arch. Dis. Child. *65*, 1013–1015.

Halliday, J., Oke, K., Breheny, S., Algar, E., and Amor, D.J. (2004). Beckwith-Wiedemann syndrome and IVF: a case-control study. Am. J. Hum. Genet. *75*, 526–528.

Hannula, K., Lipsanen-Nyman, M., Kontiokari, T., and Kere, J. (2001). A narrow segment of maternal uniparental disomy of chromosome 7q31-qter in Silver-Russell syndrome delimits a candidate gene region. Am. J. Hum. Genet. *68*, 247–253.

Hansen, M., and Bower, C. (2014). The impact of assisted reproductive technologies on intra-uterine growth and birth defects in singletons. Semin Fetal Neonatal Med *19*, 228–233.

Hark, A.T., Schoenherr, C.J., Katz, D.J., Ingram, R.S., Levorse, J.M., and Tilghman, S.M. (2000). CTCF mediates methylation-sensitive enhancer-blocking activity at the H19/Igf2 locus. Nature *405*, 486–489.

Hata, K., Okano, M., Lei, H., and Li, E. (2002). Dnmt3L cooperates with the Dnmt3 family of de novo DNA methyltransferases to establish maternal imprints in mice. Development *129*, 1983–1993.

He, Y.-F., Li, B.-Z., Li, Z., Liu, P., Wang, Y., Tang, Q., Ding, J., Jia, Y., Chen, Z., Li, L., et al. (2011). Tet-mediated formation of 5-carboxylcytosine and its excision by TDG in mammalian DNA. Science *333*, 1303–1307.

Helmerhorst, F.M., Perquin, D.A.M., Donker, D., and Keirse, M.J.N.C. (2004). Perinatal outcome of singletons and twins after assisted conception: a systematic review of controlled studies. Bmj *328*, 261.

Herzing, L.B., Kim, S.J., Cook, E.H., and Ledbetter, D.H. (2001). The human aminophospholipid-transporting ATPase gene ATP10C maps adjacent to UBE3A and exhibits similar imprinted expression. Am. J. Hum. Genet. *68*, 1501–1505.

Hirasawa, R., Chiba, H., Kaneda, M., Tajima, S., Li, E., Jaenisch, R., and Sasaki, H. (2008). Maternal and zygotic Dnmt1 are necessary and sufficient for the maintenance of DNA methylation imprints during preimplantation development. Genes & Development *22*, 1607–1616.

Hiura, H., Obata, Y., Komiyama, J., Shirai, M., and Kono, T. (2006). Oocyte growth-dependent progression of maternal imprinting in mice. Genes Cells *11*, 353–361.

Hiura, H., Okae, H., Miyauchi, N., Sato, F., Sato, A., Van De Pette, M., John, R.M., Kagami, M., Nakai, K., Soejima, H., et al. (2012). Characterization of DNA methylation errors in patients with imprinting disorders conceived by assisted reproduction technologies. Hum. Reprod. *27*, 2541–2548.

Horike, S., Mitsuya, K., Meguro, M., Kotobuki, N., Kashiwagi, A., Notsu, T., Schulz, T.C., Shirayoshi, Y., and Oshimura, M. (2000). Targeted disruption of the human LIT1 locus defines a putative imprinting control element playing an essential role in Beckwith-Wiedemann syndrome. Hum. Mol. Genet. *9*, 2075–2083.

Horsthemke, B. (1997). Structure and function of the human chromosome 15 imprinting center. J. Cell. Physiol. *173*, 237–241.

Horsthemke, B., and Wagstaff, J. (2008). Mechanisms of imprinting of the Prader-Willi/Angelman region. Am. J. Med. Genet. *146A*, 2041–2052.

Houghton, F.D. (2006). Energy metabolism of the inner cell mass and trophectoderm of the mouse blastocyst. Differentiation *74*, 11–18.

Howell, C.Y., Bestor, T.H., Ding, F., Latham, K.E., Mertineit, C., Trasler, J.M., and Chaillet, J.R. (2001). Genomic imprinting disrupted by a maternal effect mutation in the Dnmt1 gene. Cell *104*, 829–838.

Huntriss, J., Hinkins, M., Oliver, B., Harris, S.E., Beazley, J.C., Rutherford, A.J., Gosden, R.G., Lanzendorf, S.E., and Picton, H.M. (2004). Expression of mRNAs for DNA methyltransferases and methyl-CpG-binding proteins in the human female germ line, preimplantation embryos, and embryonic stem cells. Mol. Reprod. Dev. *67*, 323–336.

Ibala-Romdhane, S., Al-Khtib, M., Khoueiry, R., Blachère, T., Guérin, J.F., and Lefèvre, A.

(2011). Analysis of H19 methylation in control and abnormal human embryos, sperm and oocytes. Eur. J. Hum. Genet. *19*, 1138–1143.

Illingworth, R.S., Gruenewald-Schneider, U., Webb, S., Kerr, A.R.W., James, K.D., Turner, D.J., Smith, C., Harrison, D.J., Andrews, R., and Bird, A.P. (2010). Orphan CpG islands identify numerous conserved promoters in the mammalian genome. PLoS Genet *6*, e1001134.

Inoue, A., and Zhang, Y. (2011). Replication-dependent loss of 5-hydroxymethylcytosine in mouse preimplantation embryos. Science *334*, 194.

Inoue, A., Shen, L., Dai, Q., He, C., and Zhang, Y. (2011). Generation and replication-dependent dilution of 5fC and 5caC during mouse preimplantation development. Cell Res. *21*, 1670–1676.

Iqbal, K., Jin, S.-G., Pfeifer, G.P., and Szabó, P.E. (2011). Reprogramming of the paternal genome upon fertilization involves genome-wide oxidation of 5-methylcytosine. Proceedings of the National Academy of Sciences *108*, 3642–3647.

Ishihara, O., Araki, R., Kuwahara, A., Itakura, A., Saito, H., and Adamson, G.D. (2014). Impact of frozen-thawed single-blastocyst transfer on maternal and neonatal outcome: an analysis of 277,042 single-embryo transfer cycles from 2008 to 2010 in Japan. Fertil. Steril. *101*, 128–133.

Jackson, R.A., Gibson, K.A., Wu, Y.W., and Croughan, M.S. (2004). Perinatal outcomes in singletons following in vitro fertilization: a meta-analysis. Obstet Gynecol *103*, 551–563.

Jacobs, F.M.J., Greenberg, D., Nguyen, N., Haeussler, M., Ewing, A.D., Katzman, S., Paten, B., Salama, S.R., and Haussler, D. (2014). An evolutionary arms race between KRAB zinc-finger genes ZNF91/93 and SVA/L1 retrotransposons. Nature *516*, 242–245.

Jansen, R.P. (2000). Germline passage of mitochondria: quantitative considerations and possible embryological sequelae. Human Reproduction *15 Suppl 2*, 112–128.

Jansen, R.P., and de Boer, K. (1998). The bottleneck: mitochondrial imperatives in oogenesis and ovarian follicular fate. Molecular and Cellular Endocrinology *145*, 81–88.

Jansen, R.P.S., and Burton, G.J. (2004). Mitochondrial dysfunction in reproduction. Mitochondrion *4*, 577–600.

Jinno, Y., Sengoku, K., Nakao, M., Tamate, K., Miyamoto, T., Matsuzaka, T., Sutcliffe, J.S., Anan, T., Takuma, N., Nishiwaki, K., et al. (1996). Mouse/human sequence divergence in a region with a paternal-specific methylation imprint at the human H19 locus. Hum. Mol. Genet. *5*, 1155–1161.

Johnson, J., Canning, J., Kaneko, T., Pru, J.K., and Tilly, J.L. (2004). Germline stem cells and follicular renewal in the postnatal mammalian ovary. Nature *428*, 145–150.

Kagami, M., Nagai, T., Fukami, M., Yamazawa, K., and Ogata, T. (2007). Silver-Russell

syndrome in a girl born after in vitro fertilization: partial hypermethylation at the differentially methylated region of PEG1/MEST. J Assist Reprod Genet *24*, 131–136.

Kagiwada, S., Kurimoto, K., Hirota, T., Yamaji, M., and Saitou, M. (2013). Replication-coupled passive DNA demethylation for the erasure of genome imprints in mice. Embo J. *32*, 340–353.

Kalakonda, N., Fischle, W., Boccuni, P., Gurvich, N., Hoya-Arias, R., Zhao, X., Miyata, Y., Macgrogan, D., Zhang, J., Sims, J.K., et al. (2008). Histone H4 lysine 20 monomethylation promotes transcriptional repression by L3MBTL1. Oncogene *27*, 4293–4304.

Kan, R., Yurttas, P., Kim, B., Jin, M., Wo, L., Lee, B., Gosden, R., and Coonrod, S.A. (2011). Regulation of mouse oocyte microtubule and organelle dynamics by PADI6 and the cytoplasmic lattices. Dev. Biol. *350*, 311–322.

Kanber, D., Buiting, K., Zeschnigk, M., Ludwig, M., and Horsthemke, B. (2009). Low frequency of imprinting defects in ICSI children born small for gestational age. Eur. J. Hum. Genet. *17*, 22–29.

Kaneda, M., Hirasawa, R., Chiba, H., Okano, M., Li, E., and Sasaki, H. (2010). Genetic evidence for Dnmt3a-dependent imprinting during oocyte growth obtained by conditional knockout with Zp3-Cre and complete exclusion of Dnmt3b by chimera formation. Genes Cells.

Kaneda, M., Okano, M., Hata, K., Sado, T., Tsujimoto, N., Li, E., and Sasaki, H. (2004). Essential role for de novo DNA methyltransferase Dnmt3a in paternal and maternal imprinting. Nature *429*, 900–903.

Kantor, B., Kaufman, Y., Makedonski, K., Razin, A., and Shemer, R. (2004). Establishing the epigenetic status of the Prader-Willi/Angelman imprinting center in the gametes and embryo. Hum. Mol. Genet. *13*, 2767–2779.

Kappil, M.A., Green, B.B., Armstrong, D.A., Sharp, A.J., Lambertini, L., Marsit, C.J., and Chen, J. (2015). Placental expression profile of imprinted genes impacts birth weight. Epigenetics *10*, 842–849.

Kashiwagi, A., Meguro, M., Hoshiya, H., Haruta, M., Ishino, F., Shibahara, T., and Oshimura, M. (2003). Predominant maternal expression of the mouse Atp10c in hippocampus and olfactory bulb. J. Hum. Genet. *48*, 194–198.

Kato, Y., Kaneda, M., Hata, K., Kumaki, K., Hisano, M., Kohara, Y., Okano, M., Li, E., Nozaki, M., and Sasaki, H. (2007). Role of the Dnmt3 family in de novo methylation of imprinted and repetitive sequences during male germ cell development in the mouse. Hum. Mol. Genet. *16*, 2272–2280.

Kaufman, M.H., Barton, S.C., and Surani, M.A. (1977). Normal postimplantation development of mouse parthenogenetic embryos to the forelimb bud stage. Nature *265*, 53–55.

Kayashima, T., Yamasaki, K., Joh, K., Yamada, T., Ohta, T., Yoshiura, K.-I., Matsumoto, N., Nakane, Y., Mukai, T., Niikawa, N., et al. (2003). Atp10a, the mouse ortholog of the human imprinted ATP10A gene, escapes genomic imprinting. Genomics *81*, 644–647.

Keniry, A., Oxley, D., Monnier, P., Kyba, M., Dandolo, L., Smits, G., and Reik, W. (2012). The H19 lincRNA is a developmental reservoir of miR-675 that suppresses growth and Igf1r. Nat. Cell Biol. *14*, 659–665.

Kerjean, A., Dupont, J.M., Vasseur, C., Le Tessier, D., Cuisset, L., Pàldi, A., Jouannet, P., and Jeanpierre, M. (2000). Establishment of the paternal methylation imprint of the human H19 and MEST/PEG1 genes during spermatogenesis. Hum. Mol. Genet. *9*, 2183–2187.

Khalil, A.M., Guttman, M., Huarte, M., Garber, M., Raj, A., Rivea Morales, D., Thomas, K., Presser, A., Bernstein, B.E., van Oudenaarden, A., et al. (2009). Many human large intergenic noncoding RNAs associate with chromatin-modifying complexes and affect gene expression. Proceedings of the National Academy of Sciences *106*, 11667–11672.

Khoueiry, R., Khoureiry, R., Ibala-Rhomdane, S., Méry, L., Blachère, T., Guérin, J.-F., Lornage, J., and Lefèvre, A. (2008). Dynamic CpG methylation of the KCNQ1OT1 gene during maturation of human oocytes. J. Med. Genet. *45*, 583–588.

Khoueiry, R., Ibala-Romdhane, S., Al-Khtib, M., Blachère, T., Lornage, J., Guérin, J.F., and Lefèvre, A. (2012). Abnormal methylation of KCNQ1OT1 and differential methylation of H19 imprinting control regions in human ICSI embryos. Zygote 1–10.

Killian, J.K., Byrd, J.C., Jirtle, J.V., Munday, B.L., Stoskopf, M.K., MacDonald, R.G., and Jirtle, R.L. (2000). M6P/IGF2R imprinting evolution in mammals. Molecular Cell *5*, 707–716.

Kim, T.H., Barrera, L.O., Zheng, M., Qu, C., Singer, M.A., Richmond, T.A., Wu, Y., Green, R.D., and Ren, B. (2005). A high-resolution map of active promoters in the human genome. Nature *436*, 876–880.

Knoll, J.H., Nicholls, R.D., Magenis, R.E., Graham, J.M., Lalande, M., and Latt, S.A. (1989). Angelman and Prader-Willi syndromes share a common chromosome 15 deletion but differ in parental origin of the deletion. Am. J. Med. Genet. *32*, 285–290.

Kobayashi, H., Sakurai, T., Imai, M., Takahashi, N., Fukuda, A., Yayoi, O., Sato, S., Nakabayashi, K., Hata, K., Sotomaru, Y., et al. (2012). Contribution of intragenic DNA methylation in mouse gametic DNA methylomes to establish oocyte-specific heritable marks. PLoS Genet *8*, e1002440.

Kobayashi, H., Sakurai, T., Miura, F., Imai, M., Mochiduki, K., Yanagisawa, E., Sakashita, A., Wakai, T., Suzuki, Y., Ito, T., et al. (2013). High-resolution DNA methylome analysis of primordial germ cells identifies gender-specific reprogramming in mice. Genome Res. *23*, 616–627.

Kobayashi, H., Sato, A., Otsu, E., Hiura, H., Tomatsu, C., Utsunomiya, T., Sasaki, H., Yaegashi, N., and Arima, T. (2007). Aberrant DNA methylation of imprinted loci in sperm

from oligospermic patients. Hum. Mol. Genet. *16*, 2542–2551.

Kocer, A., Reichmann, J., Best, D., and Adams, I.R. (2009). Germ cell sex determination in mammals. Mol. Hum. Reprod. *15*, 205–213.

Korosec, S., Ban Frangez, H., Verdenik, I., Kladnik, U., Kotar, V., Virant-Klun, I., and Vrtacnik Bokal, E. (2014). Singleton pregnancy outcomes after in vitro fertilization with fresh or frozen-thawed embryo transfer and incidence of placenta praevia. Biomed Res Int *2014*, 431797.

Korosec, S., Frangez, H.B., Steblovnik, L., Verdenik, I., and Bokal, E.V. (2016). Independent factors influencing large-for-gestation birth weight in singletons born after in vitro fertilization. J Assist Reprod Genet *33*, 9–17.

Kourmouli, N., Jeppesen, P., Mahadevhaiah, S., Burgoyne, P., Wu, R., Gilbert, D.M., Bongiorni, S., Prantera, G., Fanti, L., Pimpinelli, S., et al. (2004). Heterochromatin and tri-methylated lysine 20 of histone H4 in animals. J. Cell. Sci. *117*, 2491–2501.

Kouzarides, T. (2007). Chromatin modifications and their function. Cell *128*, 693–705.

Koziol, M.J., and Rinn, J.L. (2010). RNA traffic control of chromatin complexes. Curr. Opin. Genet. Dev. *20*, 142–148.

Kubo, N., Toh, H., Shirane, K., Shirakawa, T., Kobayashi, H., Sato, T., Sone, H., Sato, Y., Tomizawa, S.-I., Tsurusaki, Y., et al. (2015). DNA methylation and gene expression dynamics during spermatogonial stem cell differentiation in the early postnatal mouse testis. BMC Genomics *16*, 624.

Kurihara, Y., Kawamura, Y., Uchijima, Y., Amamo, T., Kobayashi, H., Asano, T., and Kurihara, H. (2008). Maintenance of genomic methylation patterns during preimplantation development requires the somatic form of DNA methyltransferase 1. Dev. Biol. *313*, 335–346.

Kurimoto, K., Yabuta, Y., Ohinata, Y., Shigeta, M., Yamanaka, K., and Saitou, M. (2008). Complex genome-wide transcription dynamics orchestrated by Blimp1 for the specification of the germ cell lineage in mice. Genes & Development *22*, 1617–1635.

Kurukuti, S., Tiwari, V.K., Tavoosidana, G., Pugacheva, E., Murrell, A., Zhao, Z., Lobanenkov, V., Reik, W., and Ohlsson, R. (2006). CTCF binding at the H19 imprinting control region mediates maternally inherited higher-order chromatin conformation to restrict enhancer access to Igf2. Proc. Natl. Acad. Sci. U.S.a. *103*, 10684–10689.

La Salle, S., Oakes, C.C., Neaga, O.R., Bourc'his, D., Bestor, T.H., and Trasler, J.M. (2007). Loss of spermatogonia and wide-spread DNA methylation defects in newborn male mice deficient in DNMT3L. BMC Dev. Biol. *7*, 104.

Lammers, T.H.M., van Haelst, M.M., Alders, M., and Cobben, J.M. (2012). Het Silver-Russell-syndroom in Nederland. Tijdschr. Kindergeneeskunde *80*, 86–91.

Landers, M., Calciano, M.A., Colosi, D., Glatt-Deeley, H., Wagstaff, J., and Lalande, M. (2005). Maternal disruption of Ube3a leads to increased expression of Ube3a-ATS in trans. Nucleic Acids Res. *33*, 3976–3984.

Larsson, N.G., Wang, J., Wilhelmsson, H., Oldfors, A., Rustin, P., Lewandoski, M., Barsh, G.S., and Clayton, D.A. (1998). Mitochondrial transcription factor A is necessary for mtDNA maintenance and embryogenesis in mice. Nat Genet *18*, 231–236.

Latos, P.A., Pauler, F.M., Koerner, M.V., Şenergin, H.B., Hudson, Q.J., Stocsits, R.R., Allhoff, W., Stricker, S.H., Klement, R.M., Warczok, K.E., et al. (2012). Airn transcriptional overlap, but not its lncRNA products, induces imprinted Igf2r silencing. Science *338*, 1469–1472.

Lauberth, S.M., Nakayama, T., Wu, X., Ferris, A.L., Tang, Z., Hughes, S.H., and Roeder, R.G. (2013). H3K4me3 interactions with TAF3 regulate preinitiation complex assembly and selective gene activation. Cell *152*, 1021–1036.

Lee, D.-H., Singh, P., Tsai, S.Y., Oates, N., Spalla, A., Spalla, C., Brown, L., Rivas, G., Larson, G., Rauch, T.A., et al. (2010). CTCF-dependent chromatin bias constitutes transient epigenetic memory of the mother at the H19-Igf2 imprinting control region in prospermatogonia. PLoS Genet *6*, e1001224.

Lee, J.T. (2012). Epigenetic Regulation by Long Noncoding RNAs. Science *338*, 1435–1439.

Lee, T.I., Jenner, R.G., Boyer, L.A., Guenther, M.G., Levine, S.S., Kumar, R.M., Chevalier, B., Johnstone, S.E., Cole, M.F., Isono, K.-I., et al. (2006). Control of developmental regulators by Polycomb in human embryonic stem cells. Cell *125*, 301–313.

Lefebvre, L. (2012). The placental imprintome and imprinted gene function in the trophoblast glycogen cell lineage. Reprod. Biomed. Online *25*, 44–57.

Leff, S.E., Brannan, C.I., Reed, M.L., Ozçelik, T., Francke, U., Copeland, N.G., and Jenkins, N.A. (1992). Maternal imprinting of the mouse Snrpn gene and conserved linkage homology with the human Prader-Willi syndrome region. Nat Genet *2*, 259–264.

Leitch, H.G., Tang, W.W.C., and Surani, M.A. (2013). Chapter Five - Primordial Germ-Cell Development and Epigenetic Reprogramming in Mammals. In Epigenetics and Development, E. Heard, ed. (Academic Press), pp. 149–187.

Lennerz, J.K., Timmerman, R.J., Grange, D.K., DeBaun, M.R., Feinberg, A.P., and Zehnbauer, B.A. (2010). Addition of H19 "loss of methylation testing" for Beckwith-Wiedemann syndrome (BWS) increases the diagnostic yield. J Mol Diagn *12*, 576–588.

Lewis, A., Mitsuya, K., Umlauf, D., Smith, P., Dean, W., Walter, J., Higgins, M., Feil, R., and Reik, W. (2004). Imprinting on distal chromosome 7 in the placenta involves repressive histone methylation independent of DNA methylation. Nat Genet *36*, 1291–1295.

Li, E., Bestor, T.H., and Jaenisch, R. (1992). Targeted mutation of the DNA methyltransferase gene results in embryonic lethality. Cell *69*, 915–926.

Li, T., Hu, J.-F., Qiu, X., Ling, J., Chen, H., Wang, S., Hou, A., Vu, T.H., and Hoffman, A.R. (2008a). CTCF regulates allelic expression of Igf2 by orchestrating a promoter-polycomb repressive complex 2 intrachromosomal loop. Molecular and Cellular Biology *28*, 6473–6482.

Li, T., Vu, T.H., Ulaner, G.A., Littman, E., Ling, J.-Q., Chen, H.-L., Hu, J.-F., Behr, B., Giudice, L., and Hoffman, A.R. (2005). IVF results in de novo DNA methylation and histone methylation at an Igf2-H19 imprinting epigenetic switch. Mol. Hum. Reprod. *11*, 631–640.

Li, X., Ito, M., Zhou, F., Youngson, N., Zuo, X., Leder, P., and Ferguson-Smith, A.C. (2008b). A maternal-zygotic effect gene, Zfp57, maintains both maternal and paternal imprints. Developmental Cell *15*, 547–557.

Li, Z., Wang, Y.A., Ledger, W., and Sullivan, E.A. (2014). Birthweight percentiles by gestational age for births following assisted reproductive technology in Australia and New Zealand, 2002-2010. Hum. Reprod. *29*, 1787–1800.

Lim, D., Bowdin, S.C., Tee, L., Kirby, G.A., Blair, E., Fryer, A., Lam, W., Oley, C., Cole, T., Brueton, L.A., et al. (2009). Clinical and molecular genetic features of Beckwith-Wiedemann syndrome associated with assisted reproductive technologies. Hum. Reprod. *24*, 741–747.

Liu, L., Trimarchi, J.R., and Keefe, D.L. (2000). Involvement of mitochondria in oxidative stress-induced cell death in mouse zygotes. Biol. Reprod. *62*, 1745–1753.

Lorthongpanich, C., Cheow, L.F., Balu, S., Quake, S.R., Knowles, B.B., Burkholder, W.F., Solter, D., and Messerschmidt, D.M. (2013). Single-cell DNA-methylation analysis reveals epigenetic chimerism in preimplantation embryos. Science *341*, 1110–1112.

López-Abad, M., Iglesias-Platas, I., and Monk, D. (2016). Epigenetic Characterization of CDKN1C in Placenta Samples from Non-syndromic Intrauterine Growth Restriction. Front Genet *7*, 62.

Lucifero, D. (2004). Gene-specific timing and epigenetic memory in oocyte imprinting. Hum. Mol. Genet. *13*, 839–849.

Lucifero, D., Chaillet, J.R., and Trasler, J.M. (2004). Potential significance of genomic imprinting defects for reproduction and assisted reproductive technology. Human Reproduction Update *10*, 3–18.

Lucifero, D., La Salle, S., Bourc'his, D., Martel, J., Bestor, T.H., and Trasler, J.M. (2007). Coordinate regulation of DNA methyltransferase expression during oogenesis. BMC Dev. Biol. *7*, 36.

Lucifero, D., Mertineit, C., Clarke, H.J., Bestor, T.H., and Trasler, J.M. (2002). Methylation dynamics of imprinted genes in mouse germ cells. Genomics *79*, 530–538.

Ludwig, M., Katalinic, A., Gross, S., Sutcliffe, A., Varon, R., and Horsthemke, B. (2005). Increased prevalence of imprinting defects in patients with Angelman syndrome born to

subfertile couples. J. Med. Genet. *42*, 289–291.

Macdonald, W.A., and Mann, M.R.W. (2014). Epigenetic regulation of genomic imprinting from germ line to preimplantation. Mol. Reprod. Dev. *81*, 126–140.

Macdonald, W.A., Sachani, S.S., White, C.R., and Mann, M.R.W. (2015). A role for chromatin topology in imprinted domain regulation. Biochem. Cell Biol. 1–13.

Madan, P., Rose, K., and Watson, A.J. (2007). Na/K-ATPase beta1 subunit expression is required for blastocyst formation and normal assembly of trophectoderm tight junction-associated proteins. J. Biol. Chem. *282*, 12127–12134.

Mager, J., Montgomery, N.D., de Villena, F.P.-M., and Magnuson, T. (2003). Genome imprinting regulated by the mouse Polycomb group protein Eed. Nat Genet *33*, 502–507.

Maher, E.R., Afnan, M., and Barratt, C.L. (2003a). Epigenetic risks related to assisted reproductive technologies: epigenetics, imprinting, ART and icebergs? Human Reproduction *18*, 2508–2511.

Maher, E.R., Brueton, L.A., Bowdin, S.C., Luharia, A., Cooper, W., Cole, T.R., Macdonald, F., Sampson, J.R., Barratt, C.L., Reik, W., et al. (2003b). Beckwith-Wiedemann syndrome and assisted reproduction technology (ART). J. Med. Genet. *40*, 62–64.

Mancini-DiNardo, D., Steele, S.J.S., Ingram, R.S., and Tilghman, S.M. (2003). A differentially methylated region within the gene Kcnq1 functions as an imprinted promoter and silencer. Hum. Mol. Genet. *12*, 283–294.

Mancini-DiNardo, D., Steele, S.J.S., Levorse, J.M., Ingram, R.S., and Tilghman, S.M. (2006). Elongation of the Kcnq1ot1 transcript is required for genomic imprinting of neighboring genes. Genes & Development *20*, 1268–1282.

Mandò, C., De Palma, C., Stampalija, T., Anelli, G.M., Figus, M., Novielli, C., Parisi, F., Clementi, E., Ferrazzi, E., and Cetin, I. (2014). Placental mitochondrial content and function in intrauterine growth restriction and preeclampsia. Am. J. Physiol. Endocrinol. Metab. *306*, E404–E413.

Mann, M.R.W., Lee, S.S., Doherty, A.S., Verona, R.I., Nolen, L.D., Schultz, R.M., and Bartolomei, M.S. (2004). Selective loss of imprinting in the placenta following preimplantation development in culture. Development *131*, 3727–3735.

Market-Velker, B.A., Fernandes, A.D., and Mann, M.R.W. (2010a). Side-by-side comparison of five commercial media systems in a mouse model: suboptimal in vitro culture interferes with imprint maintenance. Biol. Reprod. *83*, 938–950.

Market-Velker, B.A., Denomme, M.M., and Mann, M.R.W. (2012). Loss of genomic imprinting in mouse embryos with fast rates of preimplantation development in culture. Biol. Reprod. *86*, 143–1–16.

Market-Velker, B.A., Zhang, L., Magri, L.S., Bonvissuto, A.C., and Mann, M.R.W. (2010b).

Dual effects of superovulation: loss of maternal and paternal imprinted methylation in a dose-dependent manner. Hum. Mol. Genet. *19*, 36–51.

Marques, C.J., Costa, P., Vaz, B., Carvalho, F., Fernandes, S., Barros, A., and Sousa, M. (2008). Abnormal methylation of imprinted genes in human sperm is associated with oligozoospermia. Mol. Hum. Reprod. *14*, 67–74.

Marques, C.J., João Pinho, M., Carvalho, F., Bièche, I., Barros, A., and Sousa, M. (2011). DNA methylation imprinting marks and DNA methyltransferase expression in human spermatogenic cell stages. Epigenetics *6*, 1354–1361.

Mascarenhas, M.N., Flaxman, S.R., Boerma, T., Vanderpoel, S., and Stevens, G.A. (2012). National, regional, and global trends in infertility prevalence since 1990: a systematic analysis of 277 health surveys. PLoS Med. *9*, e1001356.

May-Panloup, P., Chretien, M.F., Jacques, C., Vasseur, C., Malthièry, Y., and Reynier, P. (2005). Low oocyte mitochondrial DNA content in ovarian insufficiency. Human Reproduction *20*, 593–597.

Mayer, W., Niveleau, A., Walter, J., Fundele, R., and Haaf, T. (2000). Demethylation of the zygotic paternal genome. Nature *403*, 501–502.

McGovern, P.G., Llorens, A.J., Skurnick, J.H., Weiss, G., and Goldsmith, L.T. (2004). Increased risk of preterm birth in singleton pregnancies resulting from in vitro fertilization–embryo transfer or gamete intrafallopian transfer: A meta-analysis. Fertil. Steril. *82*, 1514–1520.

McGrath, J., and Solter, D. (1983). Nuclear transplantation in mouse embryos. J. Exp. Zool. *228*, 355–362.

McGrath, J., and Solter, D. (1984). Completion of mouse embryogenesis requires both the maternal and paternal genomes. Cell *37*, 179–183.

McMinn, J., Wei, M., Schupf, N., Cusmai, J., Johnson, E.B., Smith, A.C., Weksberg, R., Thaker, H.M., and Tycko, B. (2006). Unbalanced placental expression of imprinted genes in human intrauterine growth restriction. Placenta *27*, 540–549.

Meguro, M., Kashiwagi, A., Mitsuya, K., Nakao, M., Kondo, I., Saitoh, S., and Oshimura, M. (2001). A novel maternally expressed gene, ATP10C, encodes a putative aminophospholipid translocase associated with Angelman syndrome. Nat Genet *28*, 19–20.

Meldrum, D.R., Casper, R.F., Diez-Juan, A., Simón, C., Domar, A.D., and Frydman, R. (2016). Aging and the environment affect gamete and embryo potential: can we intervene? Fertil. Steril. *105*, 548–559.

Mercer, T.R., and Mattick, J.S. (2013). Structure and function of long noncoding RNAs in epigenetic regulation. Nat. Struct. Mol. Biol. *20*, 300–307.

Messerschmidt, D.M., de Vries, W., Ito, M., Solter, D., Ferguson-Smith, A., and Knowles,

B.B. (2012). Trim28 is required for epigenetic stability during mouse oocyte to embryo transition. Science *335*, 1499–1502.

Mohammad, F., Mondal, T., and Kanduri, C. (2009). Epigenetics of imprinted long noncoding RNAs. Epigenetics *4*, 277–286.

Mohammad, F., Pandey, G.K., Mondal, T., Enroth, S., Redrup, L., Gyllensten, U., and Kanduri, C. (2012). Long noncoding RNA-mediated maintenance of DNA methylation and transcriptional gene silencing. Development *139*, 2792–2803.

Moore, T., and Haig, D. (1991). Genomic imprinting in mammalian development: a parental tug-of-war. Trends Genet. *7*, 45–49.

Morgan, H.D., Dean, W., Coker, H.A., Reik, W., and Petersen-Mahrt, S.K. (2004). Activation-induced cytidine deaminase deaminates 5-methylcytosine in DNA and is expressed in pluripotent tissues: implications for epigenetic reprogramming. J. Biol. Chem. *279*, 52353–52360.

Motluk, A. (2015). IVF booster offered in Canada but not US. CMAJ *187*, E89–E90.

Motluk, A. (2016). Ontario funds one cycle of IVF--while supplies last. CMAJ *188*, E32.

Motta, P.M., Nottola, S.A., Makabe, S., and Heyn, R. (2000). Mitochondrial morphology in human fetal and adult female germ cells. Human Reproduction *15 Suppl 2*, 129–147.

Muir, R., Diot, A., and Poulton, J. (2016). Mitochondrial content is central to nuclear gene expression: Profound implications for human health. Bioessays *38*, 150–156.

Murrell, A., Heeson, S., Bowden, L., Constância, M., Dean, W., Kelsey, G., and Reik, W. (2001). An intragenic methylated region in the imprinted Igf2 gene augments transcription. EMBO Rep. *2*, 1101–1106.

Nagai, S., Mabuchi, T., Hirata, S., Shoda, T., Kasai, T., Yokota, S., Shitara, H., Yonekawa, H., and Hoshi, K. (2006). Correlation of abnormal mitochondrial distribution in mouse oocytes with reduced developmental competence. Tohoku J. Exp. Med. *210*, 137–144.

Nagano, T., Mitchell, J.A., Sanz, L.A., Pauler, F.M., Ferguson-Smith, A.C., Feil, R., and Fraser, P. (2008). The Air noncoding RNA epigenetically silences transcription by targeting G9a to chromatin. Science *322*, 1717–1720.

Nagao, Y., Totsuka, Y., Atomi, Y., Kaneda, H., Lindahl, K.F., Imai, H., and Yonekawa, H. (1998). Decreased physical performance of congenic mice with mismatch between the nuclear and the mitochondrial genome. Genes Genet. Syst. *73*, 21–27.

Nakamura, T., Arai, Y., Umehara, H., Masuhara, M., Kimura, T., Taniguchi, H., Sekimoto, T., Ikawa, M., Yoneda, Y., Okabe, M., et al. (2007). PGC7/Stella protects against DNA demethylation in early embryogenesis. Nat. Cell Biol. *9*, 64–71.

Nakamura, T., Liu, Y.-J., Nakashima, H., Umehara, H., Inoue, K., Matoba, S., Tachibana,

M., Ogura, A., Shinkai, Y., and Nakano, T. (2012). PGC7 binds histone H3K9me2 to protect against conversion of 5mC to 5hmC in early embryos. Nature *486*, 415–419.

Nakatani, T., Yamagata, K., Kimura, T., Oda, M., Nakashima, H., Hori, M., Sekita, Y., Arakawa, T., Nakamura, T., and Nakano, T. (2015). Stella preserves maternal chromosome integrity by inhibiting 5hmC-induced γH2AX accumulation. EMBO Rep. *16*, 582–589.

Nathan, D., Ingvarsdottir, K., Sterner, D.E., Bylebyl, G.R., Dokmanovic, M., Dorsey, J.A., Whelan, K.A., Krsmanovic, M., Lane, W.S., Meluh, P.B., et al. (2006). Histone sumoylation is a negative regulator in Saccharomyces cerevisiae and shows dynamic interplay with positive-acting histone modifications. Genes & Development *20*, 966–976.

Nicholls, R.D., Knoll, J.H., Butler, M.G., Karam, S., and Lalande, M. (1989). Genetic imprinting suggested by maternal heterodisomy in nondeletion Prader-Willi syndrome. Nature *342*, 281–285.

Niles, K.M., Yeh, J.R., Chan, D., Landry, M., Nagano, M.C., and Trasler, J.M. (2013). Haploinsufficiency of the paternal-effect gene Dnmt3L results in transient DNA hypomethylation in progenitor cells of the male germline. Hum. Reprod. *28*, 519–530.

Niles, K.M., Chan, D., La Salle, S., Oakes, C.C., and Trasler, J.M. (2011). PLOS ONE: Critical Period of Nonpromoter DNA Methylation Acquisition during Prenatal Male Germ Cell Development. PLoS ONE *6*, e24156.

Obata, Y., and Kono, T. (2002). Maternal primary imprinting is established at a specific time for each gene throughout oocyte growth. J. Biol. Chem. *277*, 5285–5289.

Ohta, T., Buiting, K., Kokkonen, H., McCandless, S., Heeger, S., Leisti, H., Driscoll, D.J., Cassidy, S.B., Horsthemke, B., and Nicholls, R.D. (1999). Molecular mechanism of angelman syndrome in two large families involves an imprinting mutation. Am. J. Hum. Genet. *64*, 385–396.

Okae, H., Chiba, H., Hiura, H., Hamada, H., Sato, A., Utsunomiya, T., Kikuchi, H., Yoshida, H., Tanaka, A., Suyama, M., et al. (2014). Genome-wide analysis of DNA methylation dynamics during early human development. PLoS Genet *10*, e1004868.

Okamoto, Y., Yoshida, N., Suzuki, T., Shimozawa, N., Asami, M., Matsuda, T., Kojima, N., Perry, A.C.F., and Takada, T. (2016). DNA methylation dynamics in mouse preimplantation embryos revealed by mass spectrometry. Sci Rep *6*, 19134.

Okano, M., Bell, D.W., Haber, D.A., and Li, E. (1999). DNA methyltransferases Dnmt3a and Dnmt3b are essential for de novo methylation and mammalian development. Cell *99*, 247–257.

Okun, N., and Sierra, S. (2014). Pregnancy outcomes after assisted human reproduction. J Obstet Gynaecol Can *36*, 64–83.

Oswald, J., Engemann, S., Lane, N., Mayer, W., Olek, A., Fundele, R., Dean, W., Reik, W., and Walter, J. (2000). Active demethylation of the paternal genome in the mouse zygote.

Curr. Biol. *10*, 475–478.

Pacchiarotti, J., Maki, C., Ramos, T., Marh, J., Howerton, K., Wong, J., Pham, J., Anorve, S., Chow, Y.-C., and Izadyar, F. (2010). Differentiation potential of germ line stem cells derived from the postnatal mouse ovary. Differentiation *79*, 159–170.

Pandey, R.R., Mondal, T., Mohammad, F., Enroth, S., Redrup, L., Komorowski, J., Nagano, T., Mancini-DiNardo, D., and Kanduri, C. (2008). Kcnq1ot1 antisense noncoding RNA mediates lineage-specific transcriptional silencing through chromatin-level regulation. Molecular Cell *32*, 232–246.

Park, T.S., Galic, Z., Conway, A.E., Lindgren, A., van Handel, B.J., Magnusson, M., Richter, L., Teitell, M.A., Mikkola, H.K.A., Lowry, W.E., et al. (2009). Derivation of primordial germ cells from human embryonic and induced pluripotent stem cells is significantly improved by coculture with human fetal gonadal cells. Stem Cells *27*, 783–795.

Pauler, F.M., Koerner, M.V., and Barlow, D.P. (2007). Silencing by imprinted noncoding RNAs: is transcription the answer? Trends Genet. *23*, 284–292.

Pendina, A.A., Efimova, O.A., Fedorova, I.D., Leont'eva, O.A., Shilnikova, E.M., Lezhnina, J.G., Kuznetzova, T.V., and Baranov, V.S. (2011). DNA methylation patterns of metaphase chromosomes in human preimplantation embryos. Cytogenet. Genome Res. *132*, 1–7.

Petrussa, L., Van de Velde, H., and De Rycke, M. (2014). Dynamic regulation of DNA methyltransferases in human oocytes and preimplantation embryos after assisted reproductive technologies. Mol. Hum. Reprod. *20*, 861–874.

Piccolo, F.M., Bagci, H., Brown, K.E., Landeira, D., Soza-Ried, J., Feytout, A., Mooijman, D., Hajkova, P., Leitch, H.G., Tada, T., et al. (2013). Different roles for Tet1 and Tet2 proteins in reprogramming-mediated erasure of imprints induced by EGC fusion. Molecular Cell *49*, 1023–1033.

Pikó, L., and Chase, D.G. (1973). Role of the mitochondrial genome during early development in mice. Effects of ethidium bromide and chloramphenicol. J. Cell Biol. *58*, 357–378.

Pikó, L., and Matsumoto, L. (1976). Number of mitochondria and some properties of mitochondrial DNA in the mouse egg. Dev. Biol. *49*, 1–10.

Pikó, L., and Taylor, K.D. (1987). Amounts of mitochondrial DNA and abundance of some mitochondrial gene transcripts in early mouse embryos. Dev. Biol. *123*, 364–374.

Pinborg, A., Henningsen, A.A., Loft, A., Malchau, S.S., Forman, J., and Andersen, A.N. (2014). Large baby syndrome in singletons born after frozen embryo transfer (FET): is it due to maternal factors or the cryotechnique? Hum. Reprod. *29*, 618–627.

Pinter, S.F., Sadreyev, R.I., Yildirim, E., Jeon, Y., Ohsumi, T.K., Borowsky, M., and Lee, J.T. (2012). Spreading of X chromosome inactivation via a hierarchy of defined Polycomb stations. Genome Res. *22*, 1864–1876.

Popp, C., Dean, W., Feng, S., Cokus, S.J., Andrews, S., Pellegrini, M., Jacobsen, S.E., and Reik, W. (2010). Genome-wide erasure of DNA methylation in mouse primordial germ cells is affected by AID deficiency. Nature *463*, 1101–1105.

Quenneville, S., Verde, G., Corsinotti, A., Kapopoulou, A., Jakobsson, J., Offner, S., Baglivo, I., Pedone, P.V., Grimaldi, G., Riccio, A., et al. (2011). In embryonic stem cells, ZFP57/KAP1 recognize a methylated hexanucleotide to affect chromatin and DNA methylation of imprinting control regions. Molecular Cell *44*, 361–372.

Quina, A.S., Buschbeck, M., and Di Croce, L. (2006). Chromatin structure and epigenetics. Biochemical Pharmacology *72*, 1563–1569.

Ratnam, S., Mertineit, C., Ding, F., Howell, C.Y., Clarke, H.J., Bestor, T.H., Chaillet, J.R., and Trasler, J.M. (2002). Dynamics of Dnmt1 methyltransferase expression and intracellular localization during oogenesis and preimplantation development. Dev. Biol. *245*, 304–314.

Reddy, U.M., Wapner, R.J., Rebar, R.W., and Tasca, R.J. (2007). Infertility, assisted reproductive technology, and adverse pregnancy outcomes: executive summary of a National Institute of Child Health and Human Development workshop. pp. 967–977.

Reinhardt, K., Dowling, D.K., and Morrow, E.H. (2013). Medicine. Mitochondrial replacement, evolution, and the clinic. Science *341*, 1345–1346.

Renfree, M.B., and Pask, A.J. (2011). Reproductive and developmental manipulation of the marsupial, the tammar wallaby Macropus eugenii. Methods Mol. Biol. *770*, 457–473.

Rinn, J.L., Kertesz, M., Wang, J.K., Squazzo, S.L., Xu, X., Brugmann, S.A., Goodnough, L.H., Helms, J.A., Farnham, P.J., Segal, E., et al. (2007). Functional demarcation of active and silent chromatin domains in human HOX loci by noncoding RNAs. Cell *129*, 1311–1323.

Rodenhiser, D., and Mann, M. (2006). Epigenetics and human disease: translating basic biology into clinical applications. Cmaj *174*, 341–348.

Roh, T.-Y., Cuddapah, S., and Zhao, K. (2005). Active chromatin domains are defined by acetylation islands revealed by genome-wide mapping. Genes & Development *19*, 542–552.

Roh, T.-Y., Cuddapah, S., Cui, K., and Zhao, K. (2006). The genomic landscape of histone modifications in human T cells. Proc. Natl. Acad. Sci. U.S.a. *103*, 15782–15787.

Rossignol, S., Steunou, V., Chalas, C., Kerjean, A., Rigolet, M., Viegas-Pequignot, E., Jouannet, P., Le Bouc, Y., and Gicquel, C. (2006). The epigenetic imprinting defect of patients with Beckwith-Wiedemann syndrome born after assisted reproductive technology is not restricted to the 11p15 region. J. Med. Genet. *43*, 902–907.

Rottach, A., Frauer, C., Pichler, G., Bonapace, I.M., Spada, F., and Leonhardt, H. (2010). The multi-domain protein Np95 connects DNA methylation and histone modification. Nucleic Acids Res. *38*, 1796–1804.

Roubertoux, P.L., Sluyter, F., Carlier, M., Marcet, B., Maarouf-Veray, F., Chérif, C., Marican, C., Arrechi, P., Godin, F., Jamon, M., et al. (2003). Mitochondrial DNA modifies cognition in interaction with the nuclear genome and age in mice. Nat Genet *35*, 65–69.

Rougeulle, C., Cardoso, C., Fontés, M., Colleaux, L., and Lalande, M. (1998). An imprinted antisense RNA overlaps UBE3A and a second maternally expressed transcript. Nat Genet *19*, 15–16.

Runte, M., Hüttenhofer, A., Gross, S., Kiefmann, M., Horsthemke, B., and Buiting, K. (2001). The IC-SNURF-SNRPN transcript serves as a host for multiple small nucleolar RNA species and as an antisense RNA for UBE3A. Hum. Mol. Genet. *10*, 2687–2700.

Ruthenburg, A.J., Allis, C.D., and Wysocka, J. (2007). Methylation of lysine 4 on histone H3: intricacy of writing and reading a single epigenetic mark. Molecular Cell *25*, 15–30.

Saitou, M., Kagiwada, S., and Kurimoto, K. (2012). Epigenetic reprogramming in mouse pre-implantation development and primordial germ cells. Development *139*, 15–31.

Salvaing, J., Aguirre-Lavin, T., Boulesteix, C., Lehmann, G., Debey, P., and Beaujean, N. (2012). 5-Methylcytosine and 5-hydroxymethylcytosine spatiotemporal profiles in the mouse zygote. PLoS ONE *7*, e38156.

Sandovici, I., Hoelle, K., Angiolini, E., and Constância, M. (2012). Placental adaptations to the maternal-fetal environment: implications for fetal growth and developmental programming. Reprod. Biomed. Online *25*, 68–89.

Santoro, F., and Pauler, F.M. (2013). Silencing by the imprinted Airn macro lncRNA: transcription is the answer. Cell Cycle *12*, 711–712.

Santos, F., Hendrich, B., Reik, W., and Dean, W. (2002). Dynamic reprogramming of DNA methylation in the early mouse embryo. Dev. Biol. *241*, 172–182.

Santos, F., Peat, J., Burgess, H., Rada, C., Reik, W., and Dean, W. (2013). Active demethylation in mouse zygotes involves cytosine deamination and base excision repair. Epigenetics Chromatin *6*, 39.

Sassone-Corsi, P. (1999). Requirement of Rsk-2 for Epidermal Growth Factor-Activated Phosphorylation of Histone H3. Science *285*, 886–891.

Sathananthan, A.H., and Trounson, A.O. (2000). Mitochondrial morphology during preimplantational human embryogenesis. Human Reproduction *15*, 148–159.

Sato, A., Otsu, E., Negishi, H., Utsunomiya, T., and Arima, T. (2007). Aberrant DNA methylation of imprinted loci in superovulated oocytes. Human Reproduction *22*, 26–35.

Sato, A., Hiura, H., Okae, H., Miyauchi, N., Abe, Y., Utsunomiya, T., Yaegashi, N., and Arima, T. (2011). Assessing loss of imprint methylation in sperm from subfertile men using novel methylation polymerase chain reaction Luminex analysis. Fertil. Steril. *95*, 129–34–134.e1–4.

Sato, A., Kono, T., Nakada, K., Ishikawa, K., Inoue, S.-I., Yonekawa, H., and Hayashi, J.-I. (2005). Gene therapy for progeny of mito-mice carrying pathogenic mtDNA by nuclear transplantation. Proc. Natl. Acad. Sci. U.S.a. *102*, 16765–16770.

Savage, T., Peek, J., Hofman, P.L., and Cutfield, W.S. (2011). Childhood outcomes of assisted reproductive technology. Hum. Reprod. *26*, 2392–2400.

Sazonova, A., Källen, K., Thurin-Kjellberg, A., Wennerholm, U.-B., and Bergh, C. (2012). Obstetric outcome in singletons after in vitro fertilization with cryopreserved/thawed embryos. Hum. Reprod. *27*, 1343–1350.

Schieve, L.A., Meikle, S.F., Ferre, C., Peterson, H.B., Jeng, G., and Wilcox, L.S. (2002). Low and very low birth weight in infants conceived with use of assisted reproductive technology. N. Engl. J. Med. *346*, 731–737.

Schultz, D.C., Ayyanathan, K., Negorev, D., Maul, G.G., and Rauscher, F.J. (2002). SETDB1: a novel KAP-1-associated histone H3, lysine 9-specific methyltransferase that contributes to HP1-mediated silencing of euchromatic genes by KRAB zinc-finger proteins. Genes & Development *16*, 919–932.

Searle, A.G., and Beechey, C.V. (1978). Complementation studies with mouse translocations. Cytogenet. Cell Genet. *20*, 282–303.

Searle, A.G., and Beechey, C.V. (1990). Genome imprinting phenomena on mouse chromosome 7. Genet. Res. *56*, 237–244.

Seisenberger, S., Andrews, S., Krueger, F., Arand, J., Walter, J., Santos, F., Popp, C., Thienpont, B., Dean, W., and Reik, W. (2012). The dynamics of genome-wide DNA methylation reprogramming in mouse primordial germ cells. Molecular Cell *48*, 849–862.

Seki, Y., Hayashi, K., Itoh, K., Mizugaki, M., Saitou, M., and Matsui, Y. (2005). Extensive and orderly reprogramming of genome-wide chromatin modifications associated with specification and early development of germ cells in mice. Dev. Biol. *278*, 440–458.

Sharif, J., and Koseki, H. (2011). Recruitment of Dnmt1 roles of the SRA protein Np95 (Uhrf1) and other factors. Prog Mol Biol Transl Sci *101*, 289–310.

Sharif, J., Muto, M., Takebayashi, S.-I., Suetake, I., Iwamatsu, A., Endo, T.A., Shinga, J., Mizutani-Koseki, Y., Toyoda, T., Okamura, K., et al. (2007). The SRA protein Np95 mediates epigenetic inheritance by recruiting Dnmt1 to methylated DNA. Nature *450*, 908–912.

Shemer, R., Birger, Y., Riggs, A.D., and Razin, A. (1997). Structure of the imprinted mouse Snrpn gene and establishment of its parental-specific methylation pattern. Proc. Natl. Acad. Sci. U.S.a. *94*, 10267–10272.

Shemer, R., Hershko, A.Y., Perk, J., Mostoslavsky, R., Tsuberi, B., Cedar, H., Buiting, K., and Razin, A. (2000). The imprinting box of the Prader-Willi/Angelman syndrome domain. Nat Genet *26*, 440–443.

Shen, L., Inoue, A., He, J., Liu, Y., Lu, F., and Zhang, Y. (2014). Tet3 and DNA replication mediate demethylation of both the maternal and paternal genomes in mouse zygotes. Cell Stem Cell *15*, 459–470.

Shi, X., Chen, S., Zheng, H., Wang, L., and Wu, Y. (2014). Abnormal DNA Methylation of Imprinted Loci in Human Preimplantation Embryos. Reprod Sci.

Shiio, Y., and Eisenman, R.N. (2003). Histone sumoylation is associated with transcriptional repression. Proc. Natl. Acad. Sci. U.S.a. *100*, 13225–13230.

Shin, J.-Y., Fitzpatrick, G.V., and Higgins, M.J. (2008). Two distinct mechanisms of silencing by the KvDMR1 imprinting control region. Embo J. *27*, 168–178.

Shirane, K., Toh, H., Kobayashi, H., Miura, F., Chiba, H., Ito, T., Kono, T., and Sasaki, H. (2013). Mouse oocyte methylomes at base resolution reveal genome-wide accumulation of non-CpG methylation and role of DNA methyltransferases. PLoS Genet *9*, e1003439.

Shu, J., Xing, L.-L., Ding, G.-L., Liu, X.-M., Yan, Q.-F., and Huang, H.-F. (2015). Effects of ovarian hyperstimulation on mitochondria in oocytes and early embryos. Reprod. Fertil. Dev.

Smallwood, S.A., Tomizawa, S.-I., Krueger, F., Ruf, N., Carli, N., Segonds-Pichon, A., Sato, S., Hata, K., Andrews, S.R., and Kelsey, G. (2011). Dynamic CpG island methylation landscape in oocytes and preimplantation embryos. Nat Genet *43*, 811–814.

Smilinich, N.J., Day, C.D., Fitzpatrick, G.V., Caldwell, G.M., Lossie, A.C., Cooper, P.R., Smallwood, A.C., Joyce, J.A., Schofield, P.N., Reik, W., et al. (1999). A maternally methylated CpG island in KvLQT1 is associated with an antisense paternal transcript and loss of imprinting in Beckwith-Wiedemann syndrome. Proc. Natl. Acad. Sci. U.S.a. *96*, 8064–8069.

Smith, E.Y., Futtner, C.R., Chamberlain, S.J., Johnstone, K.A., and Resnick, J.L. (2011). Transcription is required to establish maternal imprinting at the Prader-Willi syndrome and Angelman syndrome locus. PLoS Genet *7*, e1002422–e1002422.

Smith, Z.D., and Meissner, A. (2013). DNA methylation: roles in mammalian development. Nat Rev Genet *14*, 204–220.

Smith, Z.D., Chan, M.M., Humm, K.C., Karnik, R., Mekhoubad, S., Regev, A., Eggan, K., and Meissner, A. (2014). DNA methylation dynamics of the human preimplantation embryo : Nature : Nature Publishing Group. Nature *511*, 611–615.

Smith, Z.D., Chan, M.M., Mikkelsen, T.S., Gu, H., Gnirke, A., Regev, A., and Meissner, A. (2012). A unique regulatory phase of DNA methylation in the early mammalian embryo. Nature *484*, 339–344.

Smits, G., Mungall, A.J., Griffiths-Jones, S., Smith, P., Beury, D., Matthews, L., Rogers, J., Pask, A.J., Shaw, G., VandeBerg, J.L., et al. (2008). Conservation of the H19 noncoding RNA and H19-IGF2 imprinting mechanism in therians. Nat Genet *40*, 971–976.

Spahn, L., and Barlow, D.P. (2003). An ICE pattern crystallizes. Nat Genet *35*, 11–12.

Srivastava, M., Hsieh, S., Grinberg, A., Williams-Simons, L., Huang, S.P., and Pfeifer, K. (2000). H19 and Igf2 monoallelic expression is regulated in two distinct ways by a shared cis acting regulatory region upstream of H19. Genes & Development *14*, 1186–1195.

St John, J.C., Facucho-Oliveira, J., Jiang, Y., Kelly, R., and Salah, R. (2010). Mitochondrial DNA transmission, replication and inheritance: a journey from the gamete through the embryo and into offspring and embryonic stem cells. Human Reproduction Update *16*, 488–509.

Steptoe, P.C., and Edwards, R.G. (1978). Birth after the reimplantation of a human embryo. Lancet *2*, 366.

Sunderam, S., Kissin, D.M., Crawford, S.B., Folger, S.G., Jamieson, D.J., and Barfield, W.D. (2014). Assisted reproductive technology surveillance - United States, 2011. MMWR Surveill Summ *63 Suppl 10*, 1–28.

Sunderam, S., Kissin, D.M., Crawford, S.B., Folger, S.G., Jamieson, D.J., Warner, L., Barfield, W.D., Centers for Disease Control and Prevention (CDC) (2015). Assisted Reproductive Technology Surveillance - United States, 2013. MMWR Surveill Summ *64*, 1–25.

Surani, M.A., Barton, S.C., and Norris, M.L. (1984). Development of reconstituted mouse eggs suggests imprinting of the genome during gametogenesis. Nature *308*, 548–550.

Sutcliffe, A.G., Peters, C.J., Bowdin, S., Temple, K., Reardon, W., Wilson, L., Clayton-Smith, J., Brueton, L.A., Bannister, W., and Maher, E.R. (2006). Assisted reproductive therapies and imprinting disorders--a preliminary British survey. Human Reproduction *21*, 1009–1011.

Suzuki, S., Shaw, G., Kaneko-Ishino, T., Ishino, F., and Renfree, M.B. (2011). Characterisation of marsupial PHLDA2 reveals eutherian specific acquisition of imprinting. BMC Evol. Biol. *11*, 244.

Tachibana, M., Amato, P., Sparman, M., Woodward, J., Sanchis, D.M., Ma, H., Gutierrez, N.M., Tippner-Hedges, R., Kang, E., Lee, H.-S., et al. (2013). Towards germline gene therapy of inherited mitochondrial diseases. Nature *493*, 627–631.

Tachibana, M., Sparman, M., Sritanaudomchai, H., Ma, H., Clepper, L., Woodward, J., Li, Y., Ramsey, C., Kolotushkina, O., and Mitalipov, S. (2009). Mitochondrial gene replacement in primate offspring and embryonic stem cells. Nature *461*, 367–372.

Takahashi, K., Kobayashi, T., and Kanayama, N. (2000). p57(Kip2) regulates the proper development of labyrinthine and spongiotrophoblasts. Mol. Hum. Reprod. *6*, 1019–1025.

Takeuchi, T., Neri, Q.V., Katagiri, Y., Rosenwaks, Z., and Palermo, G.D. (2005). Effect of treating induced mitochondrial damage on embryonic development and epigenesis. Biol. Reprod. *72*, 584–592.

Takikawa, S., Wang, X., Ray, C., Vakulenko, M., Bell, F.T., and Li, X. (2013). Human and mouse ZFP57 proteins are functionally interchangeable in maintaining genomic imprinting at multiple imprinted regions in mouse ES cells. Epigenetics *8*, 1268–1279.

Tang, W.W.C., Dietmann, S., Irie, N., Leitch, H.G., Floros, V.I., Bradshaw, C.R., Hackett, J.A., Chinnery, P.F., and Surani, M.A. (2015). A Unique Gene Regulatory Network Resets the Human Germline Epigenome for Development. Cell *161*, 1453–1467.

Terranova, R., Yokobayashi, S., Stadler, M.B., Otte, A.P., van Lohuizen, M., Orkin, S.H., and Peters, A.H.F.M. (2008). Polycomb group proteins Ezh2 and Rnf2 direct genomic contraction and imprinted repression in early mouse embryos. Developmental Cell *15*, 668–679.

Thakur, N., Kanduri, M., Holmgren, C., Mukhopadhyay, R., and Kanduri, C. (2003). Bidirectional silencing and DNA methylation-sensitive methylation-spreading properties of the Kcnq1 imprinting control region map to the same regions. J. Biol. Chem. *278*, 9514–9519.

Thakur, N., Tiwari, V.K., Thomassin, H., Pandey, R.R., Kanduri, M., Göndör, A., Grange, T., Ohlsson, R., and Kanduri, C. (2004). An antisense RNA regulates the bidirectional silencing property of the Kcnq1 imprinting control region. Molecular and Cellular Biology *24*, 7855–7862.

Thorne, A.W., Sautiere, P., Briand, G., and Crane-Robinson, C. (1987). The structure of ubiquitinated histone H2B. Embo J. *6*, 1005–1010.

Thorvaldsen, J.L., Duran, K.L., and Bartolomei, M.S. (1998). Deletion of the H19 differentially methylated domain results in loss of imprinted expression of H19 and Igf2. Genes & Development *12*, 3693–3702.

Thouas, G.A., Trounson, A.O., Wolvetang, E.J., and Jones, G.M. (2004). Mitochondrial dysfunction in mouse oocytes results in preimplantation embryo arrest in vitro. Biol. Reprod. *71*, 1936–1942.

Thundathil, J., Filion, F., and Smith, L.C. (2005). Molecular control of mitochondrial function in preimplantation mouse embryos. Mol. Reprod. Dev. *71*, 405–413.

Tilly, J.L., and Sinclair, D.A. (2013). Germline energetics, aging, and female infertility. Cell Metab *17*, 838–850.

Tokura, T., Noda, Y., Goto, Y., and Mori, T. (1993). Sequential observation of mitochondrial distribution in mouse oocytes and embryos. J Assist Reprod Genet *10*, 417–426.

Tomizawa, S.-I., Kobayashi, H., Watanabe, T., Andrews, S., Hata, K., Kelsey, G., and Sasaki, H. (2011). Dynamic stage-specific changes in imprinted differentially methylated regions during early mammalian development and prevalence of non-CpG methylation in oocytes. Development *138*, 811–820.

Tremblay, K.D., Duran, K.L., and Bartolomei, M.S. (1997). A 5' 2-kilobase-pair region of

the imprinted mouse H19 gene exhibits exclusive paternal methylation throughout development. Molecular and Cellular Biology *17*, 4322–4329.

Tsai, T.F., Jiang, Y.H., Bressler, J., Armstrong, D., and Beaudet, A.L. (1999). Paternal deletion from Snrpn to Ube3a in the mouse causes hypotonia, growth retardation and partial lethality and provides evidence for a gene contributing to Prader-Willi syndrome. Hum. Mol. Genet. *8*, 1357–1364.

Tunster, S.J., Jensen, A.B., and John, R.M. (2013). Imprinted genes in mouse placental development and the regulation of fetal energy stores. Reproduction *145*, R117–R137.

Tunster, S.J., Tycko, B., and John, R.M. (2010). The imprinted Phlda2 gene regulates extraembryonic energy stores. Molecular and Cellular Biology *30*, 295–306.

Turelli, P., Castro-Diaz, N., Marzetta, F., Kapopoulou, A., Raclot, C., Duc, J., Tieng, V., Quenneville, S., and Trono, D. (2014). Interplay of TRIM28 and DNA methylation in controlling human endogenous retroelements. Genome Res. *24*, 1260–1270.

Ueda, T., Abe, K., Miura, A., Yuzuriha, M., Zubair, M., Noguchi, M., Niwa, K., Kawase, Y., Kono, T., Matsuda, Y., et al. (2000). The paternal methylation imprint of the mouse H19 locus is acquired in the gonocyte stage during foetal testis development. Genes Cells *5*, 649–659.

Umlauf, D., Goto, Y., Cao, R., Cerqueira, F., Wagschal, A., Zhang, Y., and Feil, R. (2004). Imprinting along the Kcnq1 domain on mouse chromosome 7 involves repressive histone methylation and recruitment of Polycomb group complexes. Nat Genet *36*, 1296–1300.

Van Blerkom, J. (1991). Microtubule mediation of cytoplasmic and nuclear maturation during the early stages of resumed meiosis in cultured mouse oocytes. Proc. Natl. Acad. Sci. U.S.a. *88*, 5031–5035.

Van Blerkom, J., and Runner, M.N. (1984). Mitochondrial reorganization during resumption of arrested meiosis in the mouse oocyte. Am. J. Anat. *171*, 335–355.

Van Blerkom, J., Davis, P.W., and Lee, J. (1995). ATP content of human oocytes and developmental potential and outcome after in-vitro fertilization and embryo transfer. Human Reproduction *10*, 415–424.

Van Blerkom, J., Davis, P., and Alexander, S. (2000). Differential mitochondrial distribution in human pronuclear embryos leads to disproportionate inheritance between blastomeres: relationship to microtubular organization, ATP content and competence. Human Reproduction *15*, 2621–2633.

Van Blerkom, J., Manes, C., and Daniel, J.C. (1973). Development of preimplantation rabbit embryos in vivo and in vitro. I. An ultrastructural comparison. Dev. Biol. *35*, 262–282.

Van Blerkom, J. (2004). Mitochondria in human oogenesis and preimplantation embryogenesis: engines of metabolism, ionic regulation and developmental competence. Reproduction *128*, 269–280.

Van Blerkom, J. (2008). Mitochondria as regulatory forces in oocytes, preimplantation embryos and stem cells. Reprod. Biomed. Online *16*, 553–569.

Van Blerkom, J. (2009). Mitochondria in early mammalian development. Seminars in Cell & Developmental Biology *20*, 354–364.

Van Blerkom, J. (2011). Mitochondrial function in the human oocyte and embryo and their role in developmental competence. Mitochondrion *11*, 797–813.

Van Blerkom, J., and Davis, P. (2007). Mitochondrial signaling and fertilization. Mol. Hum. Reprod. *13*, 759–770.

Van Buggenhout, G., and Fryns, J.-P. (2009). Angelman syndrome (AS, MIM 105830). Eur. J. Hum. Genet. *17*, 1367–1373.

van Montfoort, A.P.A., Hanssen, L.L.P., de Sutter, P., Viville, S., Geraedts, J.P.M., and de Boer, P. (2012). Assisted reproduction treatment and epigenetic inheritance. Human Reproduction Update *18*, 171–197.

Varmuza, S., and Mann, M. (1994). Genomic imprinting--defusing the ovarian time bomb. Trends Genet. *10*, 118–123.

Vermeiden, J.P.W., and Bernardus, R.E. (2013). Are imprinting disorders more prevalent after human in vitro fertilization or intracytoplasmic sperm injection? Fertil. Steril. *99*, 642–651.

Veselovska, L., Smallwood, S.A., Saadeh, H., Stewart, K.R., Krueger, F., Maupetit-Méhouas, S., Arnaud, P., Tomizawa, S.-I., Andrews, S., and Kelsey, G. (2015). Deep sequencing and de novo assembly of the mouse oocyte transcriptome define the contribution of transcription to the DNA methylation landscape. Genome Biol. *16*, 209.

Vincent, J.J., Huang, Y., Chen, P.-Y., Feng, S., Calvopiña, J.H., Nee, K., Lee, S.A., Le, T., Yoon, A.J., Faull, K., et al. (2013). Stage-specific roles for tet1 and tet2 in DNA demethylation in primordial germ cells. Cell Stem Cell *12*, 470–478.

Virant-Klun, I., Skutella, T., Hren, M., Gruden, K., Cvjeticanin, B., Vogler, A., and Sinkovec, J. (2013). Isolation of small SSEA-4-positive putative stem cells from the ovarian surface epithelium of adult human ovaries by two different methods. Biomed Res Int *2013*, 690415.

Vlachogiannis, G., Niederhuth, C.E., Tuna, S., Stathopoulou, A., Viiri, K., de Rooij, D.G., Jenner, R.G., Schmitz, R.J., and Ooi, S.K.T. (2015). The Dnmt3L ADD Domain Controls Cytosine Methylation Establishment during Spermatogenesis. Cell Rep.

Waddington, C.H. (2012). The epigenotype. 1942. Int J Epidemiol *41*, 10-13.

Wagschal, A., Sutherland, H.G., Woodfine, K., Henckel, A., Chebli, K., Schulz, R., Oakey, R.J., Bickmore, W.A., and Feil, R. (2008). G9a histone methyltransferase contributes to imprinting in the mouse placenta. Molecular and Cellular Biology *28*, 1104–1113.

Wai, T., Ao, A., Zhang, X., Cyr, D., Dufort, D., and Shoubridge, E.A. (2010). The role of mitochondrial DNA copy number in mammalian fertility. Biol. Reprod. *83*, 52–62.

Wakefield, S.L., Lane, M., and Mitchell, M. (2011). Impaired mitochondrial function in the preimplantation embryo perturbs fetal and placental development in the mouse. Biol. Reprod. *84*, 572–580.

Wang, H., Wang, L., Erdjument-Bromage, H., Vidal, M., Tempst, P., Jones, R.S., and Zhang, Y. (2004a). Role of histone H2A ubiquitination in Polycomb silencing. Nature *431*, 873–878.

Wang, L., Zhang, J., Duan, J., Gao, X., Zhu, W., Lu, X., Yang, L., Zhang, J., Li, G., Ci, W., et al. (2014). Programming and inheritance of parental DNA methylomes in mammals. Cell *157*, 979–991.

Wang, S., Lin, C., Shi, H., Xie, M., Zhang, W., and Lv, J. (2009). Correlation of the mitochondrial activity of two-cell embryos produced in vitro and the two-cell block in Kunming and B6C3F1 mice. Anat Rec (Hoboken) *292*, 661–669.

Wang, Y., Wysocka, J., Sayegh, J., Lee, Y.-H., Perlin, J.R., Leonelli, L., Sonbuchner, L.S., McDonald, C.H., Cook, R.G., Dou, Y., et al. (2004b). Human PAD4 regulates histone arginine methylation levels via demethylimination. Science *306*, 279–283.

Watson, A.J., Natale, D.R., and Barcroft, L.C. (2004). Molecular regulation of blastocyst formation. Animal Reproduction Science *82-83*, 583–592.

Webster, K.E., O'Bryan, M.K., Fletcher, S., Crewther, P.E., Aapola, U., Craig, J., Harrison, D.K., Aung, H., Phutikanit, N., Lyle, R., et al. (2005). Meiotic and epigenetic defects in Dnmt3L-knockout mouse spermatogenesis. Proc. Natl. Acad. Sci. U.S.a. *102*, 4068–4073.

Weidman, J.R., Murphy, S.K., Nolan, C.M., Dietrich, F.S., and Jirtle, R.L. (2004). Phylogenetic footprint analysis of IGF2 in extant mammals. Genome Res. *14*, 1726–1732.

Weksberg, R., Shuman, C., and Beckwith, J.B. (2010). Beckwith-Wiedemann syndrome. Eur. J. Hum. Genet. *18*, 8–14.

Wennerholm, U.-B., Henningsen, A.-K.A., Romundstad, L.B., Bergh, C., Pinborg, A., Skjaerven, R., Forman, J., Gissler, M., Nygren, K.-G., and Tiitinen, A. (2013). Perinatal outcomes of children born after frozen-thawed embryo transfer: a Nordic cohort study from the CoNARTaS group. Hum. Reprod. *28*, 2545–2553.

Wermann, H., Stoop, H., Gillis, A.J.M., Honecker, F., van Gurp, R.J.H.L.M., Ammerpohl, O., Richter, J., Oosterhuis, J.W., Bokemeyer, C., and Looijenga, L.H.J. (2010). Global DNA methylation in fetal human germ cells and germ cell tumours: association with differentiation and cisplatin resistance. J. Pathol. *221*, 433–442.

White, C.R., Macdonald, W.A., and Mann, M.R.W. (2016). Conservation of DNA Methylation Programming Between Mouse and Human Gametes and Preimplantation Embryos. Biol. Reprod; doi: 10.1095/biolreprod.116.140319

White, Y.A.R., Woods, D.C., Takai, Y., Ishihara, O., Seki, H., and Tilly, J.L. (2012). Oocyte formation by mitotically active germ cells purified from ovaries of reproductive-age women. Nat. Med. *18*, 413–421.

Wisborg, K., Ingerslev, H.J., and Henriksen, T.B. (2010). In vitro fertilization and preterm delivery, low birth weight, and admission to the neonatal intensive care unit: a prospective follow-up study. Fertil. Steril. *94*, 2102–2106.

Wolf, D.P., Mitalipov, N., and Mitalipov, S. (2015). Mitochondrial replacement therapy in reproductive medicine. Trends Mol Med *21*, 68–76.

Woods, D.C., and Tilly, J.L. (2015). Autologous Germline Mitochondrial Energy Transfer (AUGMENT) in Human Assisted Reproduction. Semin. Reprod. Med. *33*, 410–421.

Woodson, J.D., and Chory, J. (2008). Coordination of gene expression between organellar and nuclear genomes. Nat Rev Genet *9*, 383–395.

Wossidlo, M., Nakamura, T., Lepikhov, K., Marques, C.J., Zakhartchenko, V., Boiani, M., Arand, J., Nakano, T., Reik, W., and Walter, J. (2011). 5-Hydroxymethylcytosine in the mammalian zygote is linked with epigenetic reprogramming. Nat Commun *2*, 241.

Wutz, A. (2011). Gene silencing in X-chromosome inactivation: advances in understanding facultative heterochromatin formation. Nat Rev Genet *12*, 542–553.

Yamaguchi, S., Hong, K., Liu, R., Inoue, A., Shen, L., Zhang, K., and Zhang, Y. (2013). Dynamics of 5-methylcytosine and 5-hydroxymethylcytosine during germ cell reprogramming. Cell Res. *23*, 329–339.

Yamazawa, K., Kagami, M., Nagai, T., Kondoh, T., Onigata, K., Maeyama, K., Hasegawa, T., Hasegawa, Y., Yamazaki, T., Mizuno, S., et al. (2008). Molecular and clinical findings and their correlations in Silver-Russell syndrome: implications for a positive role of IGF2 in growth determination and differential imprinting regulation of the IGF2-H19 domain in bodies and placentas. J. Mol. Med. *86*, 1171–1181.

Yan, L., Yang, M., Guo, H., Yang, L., Wu, J., Li, R., Liu, P., Lian, Y., Zheng, X., Yan, J., et al. (2013). Single-cell RNA-Seq profiling of human preimplantation embryos and embryonic stem cells. Nat. Struct. Mol. Biol. *20*, 1131–1139.

Yang, T., Adamson, T.E., Resnick, J.L., Leff, S., Wevrick, R., Francke, U., Jenkins, N.A., Copeland, N.G., and Brannan, C.I. (1998). A mouse model for Prader-Willi syndrome imprinting-centre mutations. Nat Genet *19*, 25–31.

Yoshimizu, T., Miroglio, A., Ripoche, M.-A., Gabory, A., Vernucci, M., Riccio, A., Colnot, S., Godard, C., Terris, B., Jammes, H., et al. (2008). The H19 locus acts in vivo as a tumor suppressor. Proceedings of the National Academy of Sciences *105*, 12417–12422.

Yu, Y., Dumollard, R., Rossbach, A., Lai, F.A., and Swann, K. (2010). Redistribution of mitochondria leads to bursts of ATP production during spontaneous mouse oocyte maturation. J. Cell. Physiol. *224*, 672–680.

Zamboni, L. (1971). Fine morphology of mammalian fertilization. (New York, Evanston, San Francisco and London: Harper & Row.).

Zhang, H., Zeitz, M.J., Wang, H., Niu, B., Ge, S., Li, W., Cui, J., Wang, G., Qian, G., Higgins, M.J., et al. (2014). Long noncoding RNA-mediated intrachromosomal interactions promote imprinting at the Kcnq1 locus. J. Cell Biol. *204*, 61–75.

Zhang, H., Zheng, W., Shen, Y., Adhikari, D., Ueno, H., and Liu, K. (2012). Experimental evidence showing that no mitotically active female germline progenitors exist in postnatal mouse ovaries. Proceedings of the National Academy of Sciences *109*, 12580–12585.

Zhang, T., Termanis, A., Özkan, B., Bao, X.X., Culley, J., de Lima Alves, F., Rappsilber, J., Ramsahoye, B., and Stancheva, I. (2016). G9a/GLP Complex Maintains Imprinted DNA Methylation in Embryonic Stem Cells. Cell Rep *15*, 77–85.

Zhang, Y., Jurkowska, R., Soeroes, S., Rajavelu, A., Dhayalan, A., Bock, I., Rathert, P., Brandt, O., Reinhardt, R., Fischle, W., et al. (2010). Chromatin methylation activity of Dnmt3a and Dnmt3a/3L is guided by interaction of the ADD domain with the histone H3 tail. Nucleic Acids Res. *38*, 4246–4253.

Zhao, X.-M., Fu, X.-W., Hou, Y.-P., Yan, C.-L., Suo, L., Wang, Y.-P., Zhu, H.-B., Dinnyés, A., and Zhu, S.-E. (2009). Effect of vitrification on mitochondrial distribution and membrane potential in mouse two pronuclear (2-PN) embryos. Mol. Reprod. Dev. *76*, 1056–1063.

Zhu, B., Zheng, Y., Pham, A.-D., Mandal, S.S., Erdjument-Bromage, H., Tempst, P., and Reinberg, D. (2005). Monoubiquitination of human histone H2B: the factors involved and their roles in HOX gene regulation. Molecular Cell *20*, 601–611.

Zou, K., Yuan, Z., Yang, Z., Luo, H., Sun, K., Zhou, L., Xiang, J., Shi, L., Yu, Q., Zhang, Y., et al. (2009). Production of offspring from a germline stem cell line derived from neonatal ovaries. Nat. Cell Biol. *11*, 631–636.

Zuo, X., Sheng, J., Lau, H.-T., McDonald, C.M., Andrade, M., Cullen, D.E., Bell, F.T., Iacovino, M., Kyba, M., Xu, G., et al. (2012). Zinc finger protein ZFP57 requires its co-factor to recruit DNA methyltransferases and maintains DNA methylation imprint in embryonic stem cells via its transcriptional repression domain. J. Biol. Chem. *287*, 2107–2118.

Ørstavik, K.H., Eiklid, K., van der Hagen, C.B., Spetalen, S., Kierulf, K., Skjeldal, O., and Buiting, K. (2003). Another case of imprinting defect in a girl with Angelman syndrome who was conceived by intracytoplasmic semen injection. Am. J. Hum. Genet. *72*, 218–219.

Chapter 2

The work in this chapter originates from the following peer-reviewed article:

White, C.R., Denomme, M.M., Tekpetey, F.R., Feyles, V., Power, S.G.A., and Mann, M.R.W. (2015). High Frequency of Imprinted Methylation Errors in Human Preimplantation Embryos. Sci Rep *5*, 17311.

2 High frequency of imprinted methylation errors in human preimplantation embryos

Assisted reproductive technologies (ARTs) represent the best chance for infertile couples to conceive, although increased risks for morbidities exist, including imprinting disorders. This increased risk could arise from ARTs disrupting genomic imprints during gametogenesis or preimplantation. The few studies examining ART effects on genomic imprinting primarily assessed poor quality human embryos. Here, we examined day 3 and blastocyst stage, good to high quality, donated human embryos for imprinted *SNRPN*, *KCNQ1OT1* and *H19* methylation. Seventy-six percent of day 3 embryos and 50% of blastocysts exhibited perturbed imprinted methylation, demonstrating that extended culture did not pose greater risk for imprinting errors than short culture. Comparison of embryos with normal and abnormal methylation didn't reveal any confounding factors. Notably, two embryos from male factor infertility patients using donor sperm harboured aberrant methylation, suggesting errors in these embryos cannot be explained by infertility alone. Overall, these results indicate that ART human preimplantation embryos possess a high frequency of imprinted methylation errors.

2.1 Introduction

Alarming figures indicate that an estimated 48.5 million couples worldwide are unable to conceive after 5 years of unprotected sex (Mascarenhas et al., 2012). For these couples, medically assisted reproductive technologies (ARTs) represent the best chance to conceive. However, when treatment is successful (< 40%), there is an increased risk of perinatal

complications even within singletons, including preterm birth, intrauterine growth restriction, low birth weight (Mascarenhas et al., 2012; Okun and Sierra, 2014; Savage et al., 2011) and the genomic imprinting disorders; (1) Beckwith-Wiedemann Syndrome (BWS) (DeBaun et al., 2003; Doornbos et al., 2007; Gicquel et al., 2003; Maher et al., 2003a; Sutcliffe et al., 2006), (2) Angelman Syndrome (AS) (Cox et al., 2002; Doornbos et al., 2007; Ludwig et al., 2005; Maher et al., 2003a; Ørstavik et al., 2003), and (3) Silver-Russell Syndrome (SRS) (Bliek et al., 2006; Chiba et al., 2013; Chopra et al., 2010; Cocchi et al., 2013; Hiura et al., 2012; Kagami et al., 2007; Lammers et al., 2012).

Genomic imprinting is an epigenetic phenomenon that restricts expression to one parental allele while the other allele is in an inactivated state. Imprinted genes are regulated by a master control switch known as a gametic differentially methylated region (gDMR) or imprinting control region (ICR). Importantly, abnormal cytosine methylation levels at the ICR can lead to imprinting disorders such as BWS, AS and SRS.

Risk association studies have found increased risks of imprinting disorders in ART children. The risk of BWS is 3-16 times greater in children in the ART population compared to those in the general population (DeBaun et al., 2003; Gicquel et al., 2003; Halliday et al., 2004; Hiura et al., 2012; Lim et al., 2009; Maher et al., 2003b; Maher, 2005; Rossignol et al., 2006; Sutcliffe et al., 2006; van Montfoort et al., 2012). Epigenetic errors at *KCNQ1OT1*, namely maternal hypomethylation, are observed in more than 90% of ART BWS cases compared to 50% in the general population (DeBaun et al., 2003; Gicquel et al., 2003; Halliday et al., 2004; Hiura et al., 2012; Horike et al., 2000; Lim et al., 2009; Maher et al., 2003b; Maher, 2005; Rossignol et al., 2006; Sutcliffe et al., 2006; Weksberg et al., 2010), while *H19* maternal hypermethylation occurs in 17% of ART BWS cases compared to 5% in the general population (DeBaun et al., 2003; Lennerz et al., 2010; Rossignol et al., 2006; Weksberg et al., 2010). Of the small number of patients analyzed, 46% of AS patients conceived by ARTs possessed imprinting defects at the *SNRPN* ICR compared to 5% in the general population (Cox et al., 2002; Ludwig et al., 2005; Van Buggenhout and Fryns, 2009; Ørstavik et al., 2003), while 92% of SRS patients conceived by ARTs harboured *H19* hypomethylation compared to 40% in the general population (Bliek et al., 2006; Chiba et al., 2013; Chopra et al., 2010; Cocchi et al., 2013; Hiura et al., 2012; Kagami et al., 2007; Lammers et al., 2012). The overall risk for an imprinting disorder such as BWS, AS or SRS

in ART children is estimated to be around 1 in 5,000 (Okun and Sierra, 2014). Thus, disparity has arisen concerning the frequency of imprinting errors produced by ARTs in humans compared to mice, as mouse studies have identified between 10% to 90% of treated preimplantation embryos showing abnormal imprint maintenance (Fauque et al., 2007; Hajj et al., 2011; Mann et al., 2004; Market-Velker et al., 2012; 2010). However, one key difference in studies between these species is the time of analysis. The majority of mouse studies have focused on preimplantation or mid-gestation development, while human studies are primarily retrospective studies of ART children with imprinting disorders. Consequently, we sought to determine whether donated human ART-produced preimplantation embryos harbour aberrant imprinted methylation at similar incidences to that observed in the mouse (Fauque et al., 2007; Hajj et al., 2011; Mann et al., 2004; Market-Velker et al., 2010; 2012). Additionally, we analyzed whether short or extended culture produces a greater frequency of imprinted methylation errors, and whether aberrant imprinted methylation correlates with parental biometrics or clinical treatment. We analyzed methylation levels at *SNRPN*, *KCNQ1OT1* and *H19* ICRs in individual good to high quality day 3 cleavage and blastocyst stage ART-produced human embryos.

2.2   Materials and Methods

2.2.1   Donated human embryos

Twenty-three patients who had completed their fertility treatment at The Fertility Clinic at London Health Sciences Centre donated for research 24 day 3 cleavage and 29 blastocyst-stage human embryos that were no longer needed for their treatment. Buccal cells (B1-B4) were obtained from 4 healthy, non-patient adults (<30 years old). Research ethics approval was obtained through the Western University's Health Science Research Ethics Board (102659) and the methods were carried out in accordance with the approved guidelines. Informed consent was obtained from patients donating embryos and non-patient adults providing buccal cell samples. All embryos were cultured in the glucose/phosphate-free preimplantation stage 1 (P1) culture medium (Irvine Scientific, California) to day 3, then in Blastocyst Medium (BM) in a sequential media protocol (Irvine Scientific, California) to the blastocyst stage. Embryos were slow frozen between the years 2000-2007 and thawed between October 2013-August 2014. Slow freezing was performed according to

the Testart's (propanediol) freezing method (Testart et al., 1986) using Sydney IVF Cryopreservation Kits.

Day 3 human embryos were graded by blastomere number, and morphological fragmentation levels by either the former A through F grading system or the currently used G1 through G6 system: A, even, regular, no fragments; B, uneven, irregular, no fragments; slight C (slC), slight fragmentation; C, minor (<25%) fragmentation; D, major (between 25-50%) fragmentation; E, extensive (>50%) fragmentation; F, degenerate; or by fragmentation levels: G1, <5% fragmentation; G2, 5-10% fragmentation; G3, 11-25% fragmentation; G4, 26-50% fragmentation; G5, >50% fragmentation; and G6, degenerate (Hardy et al., 2003; Rijnders and Jansen, 1998; Sjöblom et al., 2006). Following thawing, the majority of embryos were G1-G3 grade and had an average of 4 cells (data not shown).

Blastocyst grading was according to blastocyst cavity size/hatching, inner cell mass characteristics and trophoblast cell number giving a numeric-alpha-alpha score based on the Gardner and Schoolcraft scoring system (Gardner and Schoolcraft, 1999). Cavity size or hatching score was graded as 1, early blastocyst with cavity less than half the embryo volume; 2, blastocyst with cavity greater than half the embryo volume; 3, full blastocyst, cavity full; 4, expanded blastocyst, cavity expanded beyond earlier embryo size with thinning zona; 5, hatching blastocyst; 6, hatched blastocyst. Inner cell mass (ICM) grading was A, tightly packed ICM, many cells; B, loosely grouped ICM, several cells; and C, very few cells, and trophectoderm was graded as A, many cells with cohesive epithelium; B, few cells with loose epithelium; and C, very few large cells. All embryos were immediately processed for methylation analysis following thawing.

2.2.2   Isolation of Control Cells

Buccal cells were collected using the end of a sterile 20 μL pipet tip and diluted into approximately 1000, 100, 50 and 5-10 cells in 20 μL of 1 X PBS (Phosphate-Buffered Saline). Buccal cells were then embedded into a 2:1 3% LMP agarose and lysis solution, and then subjected to imprinted DNA methylation analysis. One confluent well of a 6-well dish (~1x10^6 cells) of HES2 human ESCs (WiCell Research Institute Inc.) was washed once with 1X PBS (Sigma) and incubated in TrypLE Express (GIBCO) in Dulbecco's PBS (DPBS). Trypsin was inactivated by addition of DMEM and 10% Fetal Bovine Serum (FBS) medium.

Detached hESCs were collected, pelleted gently, washed with 1X PBS and re-suspended in 1000 μL of 1X DPBS. Approximately 1 μL of cells (~1000 cells) was embedded into a 2:1 3% LMP agarose and lysis solution, then subjected to bisulfite mutagenesis.

2.2.3   Imprinted DNA Methylation Analysis

Immediately following thawing individual embryos were embedded under mineral oil (Sigma) into 10 μL of a 2:1 mixture of 3% LMP agarose (Sigma) and lysis solution [100 mM Tris–HCl, pH 7.5 (Bioshop), 500 mM LiCl (Sigma), 10 mM EDTA, pH 8.0 (Sigma), 1% LiDS (Bioshop), and 5 mM DTT (Sigma), 1 μl 2mg/ml proteinase K (Sigma), and1 μl 10% Igepal (Sigma)]. DNA methylation analysis was performed using the bisulfite mutagenesis and clonal sequencing method as previously described (Denomme et al., 2011). Samples were placed on ice for 10 minutes to generate an agarose/lysis bead and subsequently incubated overnight in SDS lysis buffer for 20 hours in a 50°C water bath. Lysis buffer was removed and replaced with 300 μL of mineral oil and embryos were either frozen at -20°C for a maximum of 3 days or immediately processed for bisulfite mutagenesis. Briefly, for bisulfite treatment, samples were incubated at 90°C to inactivate proteinase K (Sigma) for 2.5 minutes and transferred to ice for 10 minutes. DNA denaturation was performed in 1 mL of 0.1 M NaOH at 37°C for 15 minutes. Samples were covered with 300 μL of mineral oil and 500 μL of 2.5 M bisulfite solution for a 3.5-hour bisulfite conversion at 50°C. After conversion, desulfonation was performed in 1 mL of 0.3 M NaOH at 37°C for 15 minutes. Negative controls (beads containing no embryo or buccal cell sample) were processed with each bisulfite reaction. For first round PCR amplification, agarose bead with bisulfite converted DNA (10 μL) was added directly to 15 μL of Hot Start Ready-To-Go (RTG) (GE Healthcare) PCR bead that contained 0.5 μL of each 10 μM gene-specific external primer, 1 μL of 240 ng/mL transfer RNA and water with a 25 μL mineral oil overlay. Multiplexing of *H19* and *KCNQ1OT1* was performed during the first round of PCR. *SNRPN* amplification was performed individually. Five microliters of first round PCR product was added to 20 μL of RTG beads mixed with 19 μL 0.5 μL of each 10 μM internal primer and water for nested PCR. Separate second round PCR reactions were performed for *H19* and *KCNQ1OT1*.

The KCNQ1OT1 PCR bisulfite primers were described previously (Ibala-Romdhane et al., 2011; Khoueiry et al., 2012). The *KCNQ1OT1* region analyzed contained a G

(94.7%)/A (6.3%) SNP (rs56134303). For the *H19* region (GenBank Af087017, 6161-6409), external primers used were as described previously (Khoueiry et al., 2012). Due to SNPs residing in the previously described inner primers (Khoueiry et al., 2012), newly designed forward inner primer 5'-TTGGTTGTAGTTGTGGAAT-3' and *H19* reverse inner primer 5'-AACCATAACACTAAAACCCT-3' were used for nested PCR, amplifying a 249 base pair sequence encompassing 20 CpGs and rs2071094 A (33.6%)/C (66.4%) and rs2107425 G (55.5%)/A (44.5%) common SNPs. For *SNRPN*, nested primers (UCSC, chr15:25, 200, 009-25, 200, 379) were designed to amplify a 360 base pair region encompassing 24 CpGs and a G (84.8%)/A (15.2%) SNP (rs220029) within the ICR as follows, *SNRPN* outer forward, 5'-TAGTGTTGTGGGGTTTTAGGG-3'; *SNRPN* outer reverse, 5'-TACCCACCTCCACCCATATC-3'; *SNRPN* inner forward, 5'-AGGGAGGGAGTTGGGATTT-3'; *SNRPN* inner reverse, 5'-CACAACAACAAACCTCTAAACATTC-3'. All PCR reactions were performed as previously described (Al-Khtib et al., 2011), 94°C for 10 minutes followed by 55 cycles of 94°C for 15 seconds, 56°C for 20 seconds and 72°C for 20 seconds, with a final 72°C for 10 minute extension.

PCR products were ligated into the pGEM-T EASY vector system (Promega), transformed into Z-competent DH5α *Escherichia coli* cells (Zymo Research) and following blue/white selection and colony PCR, samples were sent for sequencing at Bio Basic Inc. (Markham, ON, Canada) (Market-Velker et al., 2010). For both day 3 and blastocyst-stage embryos, 30-65 clones were sequenced per embryo per gene. Methylation patterns were determined using online software (BISMA). Identical clones (identical location and number of unconverted CpG-associated cytosines and identical location and number of unconverted non-CpG-associated cytosines) were included only once and represented one individual DNA strand. Only clones with ≥85% conversion rates were included. Total DNA methylation for each gene, or for each allele of a gene, if parental identity was assigned, was calculated as a percentage of the total number of methylated CpG/the total number of CpG dinucleotides.

2.2.4 Statistical Analysis

Student's t-test was used to examine significance between embryos with normal methylation and those with abnormal methylation for maternal age, hormone dose, and stimulation

response (E$_2$ levels). Statistical analyses for patient diagnosis, hormone induction method, fertilization method, and embryo grade was determined using the nonparametric Kolmogorov-Smirnov (KS) test to analyze differences between groups. A p-value of <0.05 was considered to be significantly different.

2.3   Results

2.3.1   Imprinted methylation in control samples

As with previous studies, non-ART-treated, human preimplantation embryos cannot be obtained for experimental purposes. I therefore determined the imprinted methylation levels in readily obtainable cells from adults as a control. Imprinted DNA methylation at the *SNRPN*, *KCNQ1OT1* and *H19* ICR was first assessed in untreated human buccal cell (Bu) samples from 4 young, non-patient adults. Bisulfite clonal sequencing was used to analyze 20-24 CpGs per gene. For all controls, a total of 30-65 clones were sequenced to obtain representative DNA strands.   Sequences with identical CpG methylation profiles and unconverted cytosines were considered to be identical and were included once to eliminate clonal bias. Each region of analysis included a single nucleotide polymorphism (s) (SNP) that when present in heterozygous samples could distinguish between parental alleles (Table 2-1). Since we did not have access to patient samples, we consider the methylated strands as the presumptive paternal *H19*, maternal *SNRPN* and maternal *KCNQ1OT1* alleles, and the unmethylated strands as the maternal *H19,* paternal *SNRPN* and paternal *KCNQ1OT1* alleles, as was done in previous studies (Ibala-Romdhane et al., 2011; Khoueiry et al., 2012).

For the *SNRPN* ICR, a 360 bp-region was analyzed comprising 24 CpGs and a G/A SNP (rs220029) that occurs at a general population frequency of 84.8% and 15.2%, respectively (Figure 2-1A). All control samples were homozygous at this SNP (Table 2-1), and thus no allelic assignment could be made. Total *SNRPN* methylation levels in buccal cell controls (~1000 cells) were Bu1-1000 46%, Bu2-1000 45%, Bu3-1000 43% and Bu4-1000 40% (Figure 2-1B). Since buccal samples exhibited a mean *SNRPN* methylation level less than anticipated (43%), we analyzed *SNRPN* methylation in human embryonic stem cells (hESCs), an undifferentiated cell type that more closely matched preimplantation embryos. In hESCs, *SNRPN* methylation levels were 41% (Figure 2-1B), consistent with those in buccal cells. To assess cell numbers similar to blastocyst and day 3 embryos, methylation

levels were analyzed in ~50 or ~100 cells (Figure 2-1C) and 5-10 cells (denoted hereafter as 10 cells) (Figure 2-1D) for Bu1 and Bu3 samples. Total *SNRPN* methylation levels were Bu1-100 39%, Bu1-50 41% (Figure 2-1C), Bu1-10 44% and 41% (Figure 2-1D), and Bu3-100 49%, Bu3-50 44% (Figure 2-1C), Bu3-10 38% and 42% (Figure 2-1D). Thus within sample, methylation level mean and standard deviation were 42.2±2.8 for Bu1 and 43.2±4.0 for Bu3.

For the *KCNQ1OT1* ICR, a 265 bp-region was analyzed encompassing 22 CpGs (Khoueiry et al., 2012) and a G (94.7%)/A (6.3%) SNP (rs56134303), that eliminated the first CpG (Figure 2-2A). All controls were homozygous at the *KCNQ1OT1* SNP (Table 2-1). Total *KCNQ1OT1* methylation levels in control samples were Bu1-1000 63%, Bu2-1000 57%, Bu3-1000 58% and Bu4-1000 65%   (Figure 2-2B). Since the mean *KCNQ1OT1* methylation level was greater than anticipated (60%), *KCNQ1OT1* methylation was assessed in hESCs. *KCNQ1OT1* methylation levels were hESC-1000 65% (Figure 2-2B), consistent with those in buccal cells. At cell numbers similar to blastocyst and day 3 embryos, *KCNQ1OT1* methylation levels were Bu1-100 57%, Bu1-50 65%, (Figure 2-2C), Bu1-10 64% and 64% (Figure 2-2D), and Bu3-100 54%, Bu3-50 57% (Figure 2-2C), Bu3-10 54% and 57% (Figure 2-2D). Thus within sample, methylation level mean and standard deviation were 62.6±3.2 for Bu1 and 56.0±1.8 for Bu3.
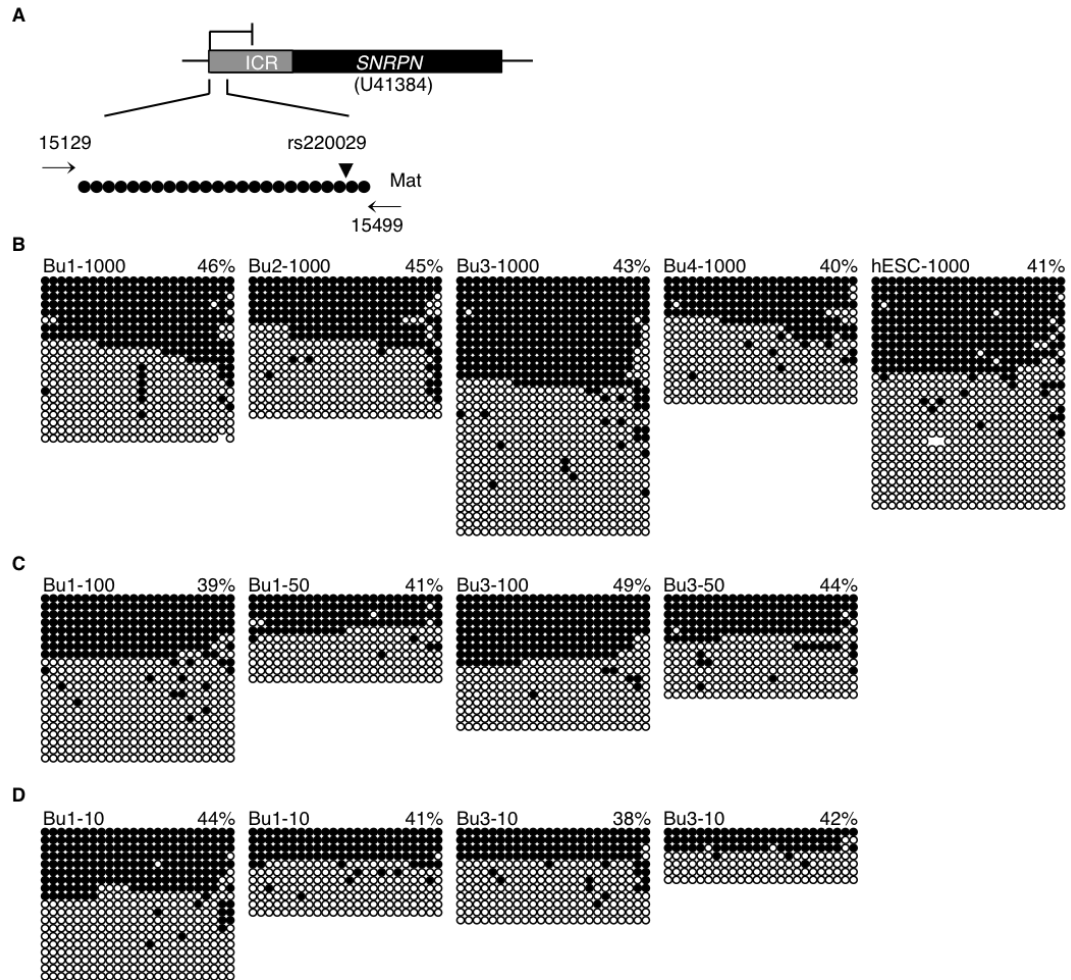
Figure 2-1: *SNRPN* **imprinted methylation in buccal cell and human embryonic stem cell (hESC) control samples.**

(A) Map of the *SNRPN* region analyzed. Accession numbers are located below genes, primer locations are marked with arrows, and SNPs are indicated by arrowheads. Methylation analyses in (B) four buccal cell (Bu1-4) and human embryonic stem cell (hESC) control samples with ~1000 cells, (C) in buccal cell samples with ~50 or ~100 cells, as indicated, representing blastocysts, and (D) with buccal cell samples ~10 cells, representing day 3 cleavage embryos. Each group of circles represents an individual human sample. Each line is an individual DNA strand. Methylated CpGs are filled black circles and unmethylated CpGs are open circles. Percent methylation is indicated above each set of DNA strands for a gene or parental allele and was calculated as the number of methylated CpGs divided by the total number of CpG dinucleotides.

Figure 2-2: *KCNQ1OT1* imprinted methylation in buccal cell and hESC control samples

(A) Map of the *KCNQ1OT1* region analyzed. Methylation analyses in (B) buccal cell (Bu) and human embryonic stem cell (hESC) control samples with ~1000 cells, (C) in buccal cell samples with ~50 or ~100 cells (as indicated), representing blastocysts, and (D) with buccal cell samples ~10 cells, representing day 3 cleavage embryos. See Figure legend 2-1 for details.

Samples assessed for *KCNQ1OT1* methylation levels were also analyzed for DNA methylation at the *H19* ICR. We initially began our analysis for a 234 bp-region within the *H19* imprinting control region that included 18 CpGs (Khoueiry et al., 2012) and a common A (33.6%)/C (66.4%) SNP (rs2071094) (Figure 2-3A). However, we observed biased allelic recovery and subsequently found two additional SNPs present in the forward and reverse inner nested primers. Thus, we designed new internal primers for a larger 249 bp-region within the *H19* ICR containing 20 CpGs, the rs2071094 (A, 33.6%; C, 66.4%) SNP and rs2107425 (G, 55.5%; A, 44.5%) SNPs (Figure 2-3A). For buccal cell samples, Bu3 was heterozygous at both *H19* SNPs, Bu4 was heterozygous at one SNP, while Bu1 and Bu2 were homozygous for both *H19* SNPs (Table 2-1). Samples Bu1-1000 and Bu2-1000 had total *H19* methylation levels of 57% and 61%, respectively. Sample Bu3-1000 had 96% methylation on the presumptive paternal *H19* allele and 11% methylation on the presumptive maternal *H19* allele (56% total methylation), while Bu4-1000 had 94% and 11% methylation on the presumptive paternal and maternal *H19* alleles, respectively (52% total methylation) (Figure 2-3B). Thus, total methylation levels fell with a mean (56%) expected for paternally methylated and maternally unmethylated alleles. For smaller cell numbers, total *H19* methylation levels were Bu1-100 55%, Bu1-50 60% (Figure 2-3C), Bu1-10 63% and 53% (Figure 2-3D), and Bu3-100 59%, Bu3-50 50% (Figure 2-3C), Bu3-10 52% and 54% (Figure 2-3D), with 94-98% and 3-12% methylation on the presumptive paternal and maternal *H19* alleles, respectively. Thus within samples, methylation level mean and standard deviation were 57.6±4.0 for Bu1 and 54.2±3.5 (Pat 95.6±1.5; Mat 8.8±3.6) for Bu3.

Given the *SNRPN*, *KCNQ1OT1* and *H19* methylation levels in all control samples, conservatively, we considered a methylation range of 4 times the standard deviations above/below the mean as a normal methylation level. For *SNRPN*, the mean methylation level was 42.2%±3.0, generating a 30%-54% normal methylation range. For *KCNQ1OT1*, the mean methylation level was 60.0%±4.4, giving a normal methylation range of 42%-78%. The mean methylation level for *H19* was 56.0%±4.1, generating a 40%-72% normal methylation range. For embryos with heterozygous SNPs, conservatively ≥70% methylation on the presumptive maternal *SNRPN*, maternal *KCNQ1OT1* and paternal *H19* alleles and ≤20% methylation on the presumptive paternal *SNRPN*, paternal *KCNQ1OT1* and maternal *H19* alleles were considered as normal methylation levels.
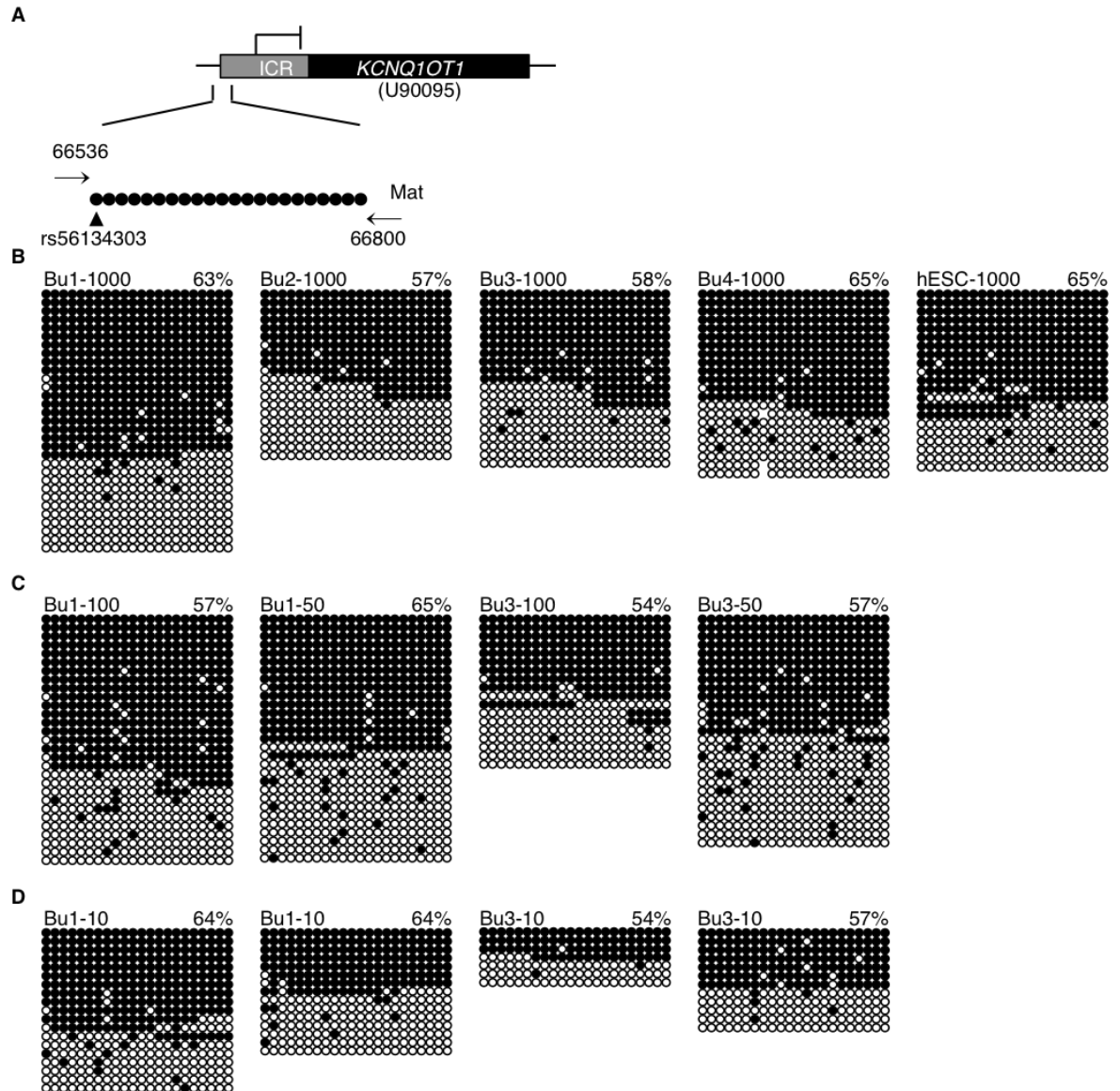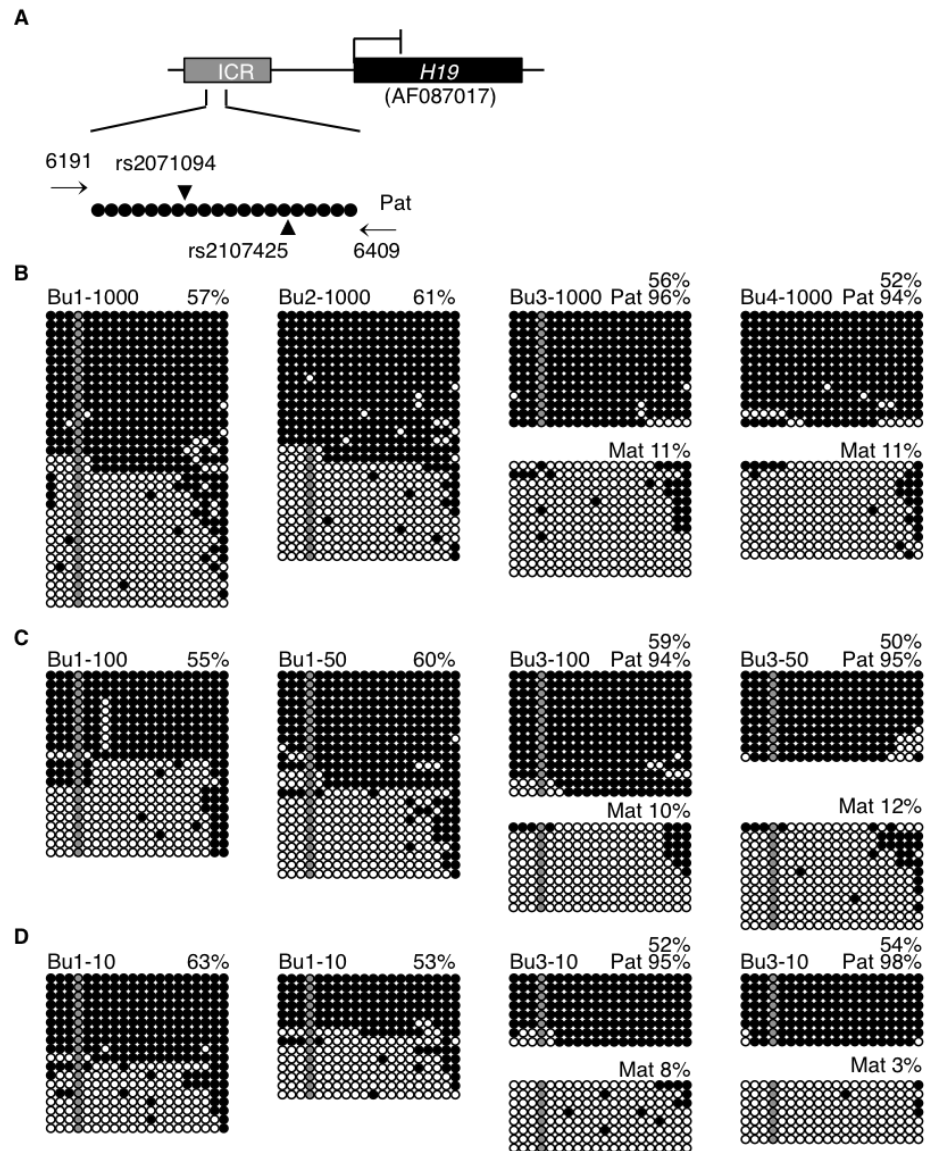
Figure 2-3: *H19* imprinted methylation in buccal cell control samples

(A) Map of the *H19* region analyzed. Methylation analyses in (B) buccal cell (Bu) and human embryonic stem cell (hESC) control samples with ~1000 cells, (C) in buccal cell samples with ~50 or ~100 cells (as indicated), representing blastocysts, and (D) with buccal cell samples ~10 cells, representing day 3 cleavage embryos. Grey circles are not included in methylation analyses as they represent a C/T SNP that cannot be distinguished following bisulfite conversion. Alleles are separated into presumptive maternal (Mat) and paternal (Pat) strands in samples with heterozygous SNPs. See Figure legend 2-1 for details.

2.3.2   Aberrant imprinted methylation in day 3 embryos

During fertility treatment, embryos were cultured to day 3, after which embryos were either transferred to the mother, or cryopreserved and stored for future cycles, or cultured to the blastocyst stage then cryopreserved and stored for future cycles. For identification purposes, embryos were given an alphanumeric ID that included patient number (1-23), freeze stage [day 3 cleavage (C) or blastocyst (B)], and embryo number (1-6), for example "9C2" represents patient 9, day 3 cleavage embryo 2. Individual, cryopreserved day 3 cleavage embryos were analyzed for maintenance of imprinted methylation. For all day 3 and blastocyst-stage embryos, a total of 30-65 clones were sequenced to obtain representative DNA strands and to sequence all possible unique DNA strands following thawing and bisulfite treatment. Data were obtained for 9 of 12 day 3 embryos for *SNRPN*; 7 of 12 day 3 embryos for *KCNQ1OT1*; and 7 of 12 day 3 embryos for *H19*.

SNRPN is normally methylated on the silent maternal allele, while the paternal allele is unmethylated. All day 3 embryos were homozygous at the rs220029 SNP (Table 2-1) and thus were examined for total methylation levels. Of the 9 day 3 cleavage embryos analyzed, normal methylation levels were observed for 4 embryos (Figure 2-4A). By comparison, 5 embryos had abnormal *SNRPN* methylation levels, with 4 embryos exhibiting aberrant hypermethylation (1C1, 62%; 1C5, 67%; 1C6, 59%; 18C1, 62%) while 1 embryo (21C1) displaying aberrant hypomethylation of 18%. Overall, 56% of day 3 cleavage embryos had abnormal *SNRPN* imprinted methylation.

KCNQ1OT1 is also normally methylated on the silent maternal allele, while the paternally inherited allele is unmethylated. All 7 day 3 embryos were homozygous at the rs56134303 SNP (Table 2-1), and thus, total methylation levels were analyzed. One embryo had methylation levels within the normal range (Figure 2-4B). Of the remaining 6 embryos, 1 embryo had abnormal hypermethylation (9C1, 80%) while 5 embryos exhibited aberrant *KCNQ1OT1* hypomethylation (12C1, 19%; 7C1, 33%; 7C2, 35%; 6C1, 22%; 4C1, 19%). In total, 86% of day 3 cleavage embryos had aberrant *KCNQ1OT1* imprinted methylation.

A

SNRPN

1C1 (3,3)   62%, A
1C2 (7,6)   42%, N
1C3 (6,5)   46%, N
1C4 (7,7)   42%, N

1C5 (4,4)   67%, A
1C6 (7,6)   59%, A
9C2 (8,0)   52%, N
18C1 (8,0)   62%, A

21C1 (7,6)   18%, A

B

KCNQ1OT1

3C1 (7,3)   65%, N
12C1 (8,8)   19%, A
7C1 (8,5)   33%, A
7C2 (7,5)   35%, A

6C1 (7,2)   22%, A
4C1 (6,5)   19%, A
9C1 (8,7)   80%, A

C

H19

3C1 (7,3)   38%, A
7C1 (8,5)   Pat 95%, A
7C2 (7,5)   Pat 94%, A
6C1 (7,2)   Pat 35%, A

Mat 85%
Mat 71%
Mat 5%

6C2 (7,1)   Pat 61%, A
4C1 (6,5)   Pat 86%, N
9C1 (8,7)   Pat 70%, N

Mat 11%
Mat 14%
Mat 5%
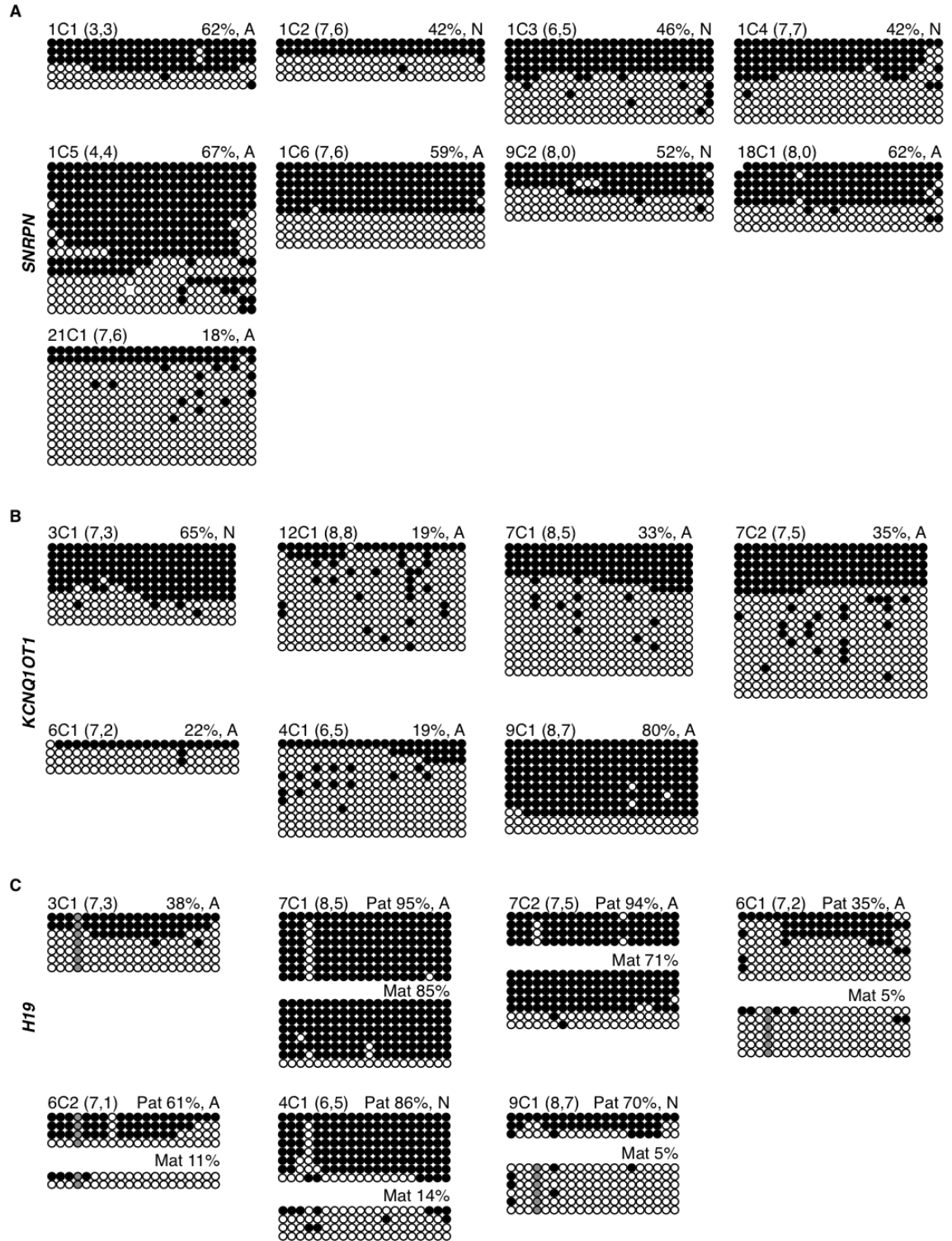
Figure 2-4: Methylation of the (A) *SNRPN,* **(B)** *KCNQ1OT1* **and (C)** *H19* **ICRs in day 3 human cleavage-stage embryos**

Each group of DNA strands is an individual day 3 embryo with embryo ID (top left), and percent methylation and presumptive maternal/paternal allele designation (top right) indicated. Normal (N) and abnormal (A) embryos are designated next to percent methylation values (top right). The pre-freeze and post-thaw cell numbers, respectively, are indicated in brackets beside each embryo name. Grey circles are not included in methylation analyses as they represent a C/T SNP that cannot be distinguished following bisulfite conversion. See Figure legend 2-1 for details.

H19 is normally methylated on the paternal allele, while the maternally inherited allele is unmethylated. Three day 3 cleavage embryos (4C1, 7C1, 7C2) were heterozygous at both rs2071094 and rs2107425, 1 embryo (6C2) was heterozygous at rs2071094 and 2 embryos (6C1, 9C1) were heterozygous at rs2107425 (Table 2-1), allowing for allelic assignment. Only one embryo (3C1) was homozygous at the rs2071094 and rs2107425 SNPs and was examined for total methylation levels. Out of 7 day 3 embryos, 2 had a normal methylation pattern with methylation ≥70% on the presumptive paternal allele and ≤20% hypomethylation on the presumptive maternal allele (Figure 2-4C). Of the remaining 5 embryos, 3 showed loss of methylation on the presumptive paternal *H19* allele (6C1, 35%; 6C2, 61%) and 2 displayed a gain of methylation on the presumptive maternal allele (7C1, 85%; 7C2, 71%). Finally, for the homozygous embryo (3C1), there was a loss of total *H19* methylation (38%). Overall, 71% of day 3 cleavage embryos were abnormally hypo- and/or hypermethylated at *H19*. Furthermore, of the 6 embryos successfully assessed for both *KCNQ1OT1* and *H19* methylation, 3 embryos (50%) displayed aberrant methylation levels at both genes (7C1; 7C2; 6C1).

2.3.3 Abnormal imprinted methylation in blastocyst stage embryos

Individual, cryopreserved blastocysts were also analyzed for maintenance of imprinted methylation. Data were obtained for 12 of 15 blastocysts for *SNRPN*; 13 of 14 blastocysts for *KCNQ1OT1*; and 14 of 14 blastocysts for *H19*. For *SNRPN*, 3 blastocyst-stage embryos (22B1, 9B2, 17B1) were heterozygous at rs220029, while the remaining 9 embryos were homozygous at the rs220029 SNP (Table 2-1). Four embryos had total methylation levels within the normal range (30%-54%) (Figure 2-5). Of the 8 remaining embryos, 3 homozygous embryos showed a gain of total *SNRPN* methylation (10B3, 63%; 14B3, 57%; and 14B4, 62%), and 2 homozygous blastocysts exhibited *SNRPN* hypomethylation (16B2, 28%; and 23B1, 15%), while 1 heterozygous blastocyst (9B2) exhibited a gain of paternal *SNRPN* methylation (24% Pat) and 2 heterozygous blastocysts possessed both a loss of maternal *SNRPN* methylation and a gain of paternal *SNRPN* methylation (17B1, 65% Mat, 26% Pat; and 22B1, 48% Mat, 26% Pat) (Figure 2-5). In total, 67% of blastocyst embryos exhibited abnormal *SNRPN* imprinted methylation.

For *KCNQ1OT1*, all embryos were homozygous at the rs56134303 SNP (Table 2-1), allowing total methylation levels to be determined. Normal *KCNQ1OT1* methylation levels (42%-78%) were observed in 9 blastocysts (Figure 2-6). For the remaining 4 blastocysts, a loss of *KCNQ1OT1* methylation was observed (14B2, 16%; 11B1, 19%; 19B1, 37%; and 2B2, 39%). Overall, 4 of 13 (31%) blastocysts had abnormal *KCNQ1OT1* methylation levels.

The same 14 embryos analyzed for *KCNQ1OT1* imprinted methylation were assessed for *H19* imprinted methylation. Three blastocysts (4B1, 8B1, 14B2) were heterozygous at rs2071094 and rs2107425, 3 blastocysts (9B1, 19B1, 2B1) were heterozygous at rs2071094, and 2 blastocysts (2B2 and 13B1) were heterozygous for rs2107425 (Table 2-1). The remaining 6 blastocysts (14B1, 11B1, 15B1, 21B1, 4B2 and 20B1) were homozygous for both *H19* SNPs (Table 2-1). All blastocysts, except 2, fell within the normal *H19* methylation range (40%-72%) (Figure 2-7). One blastocyst displayed a loss of total *H19* methylation (20B1, 29%) and one displayed abnormal gain of maternal *H19* methylation (14B2, 87% Pat, 36% Mat). Overall, 14% of blastocysts had an abnormal *H19* methylation profile. Blastocyst 20B1, with aberrant *H19* methylation, had normal *KCNQ1OT1* methylation, while blastocyst 14B2 had abnormal methylation at both *H19* and *KCNQ1OT1*. In total for all three genes, 76% day 3 embryos and 50% blastocysts exhibited abnormal imprinted methylation (Figure 2-8).
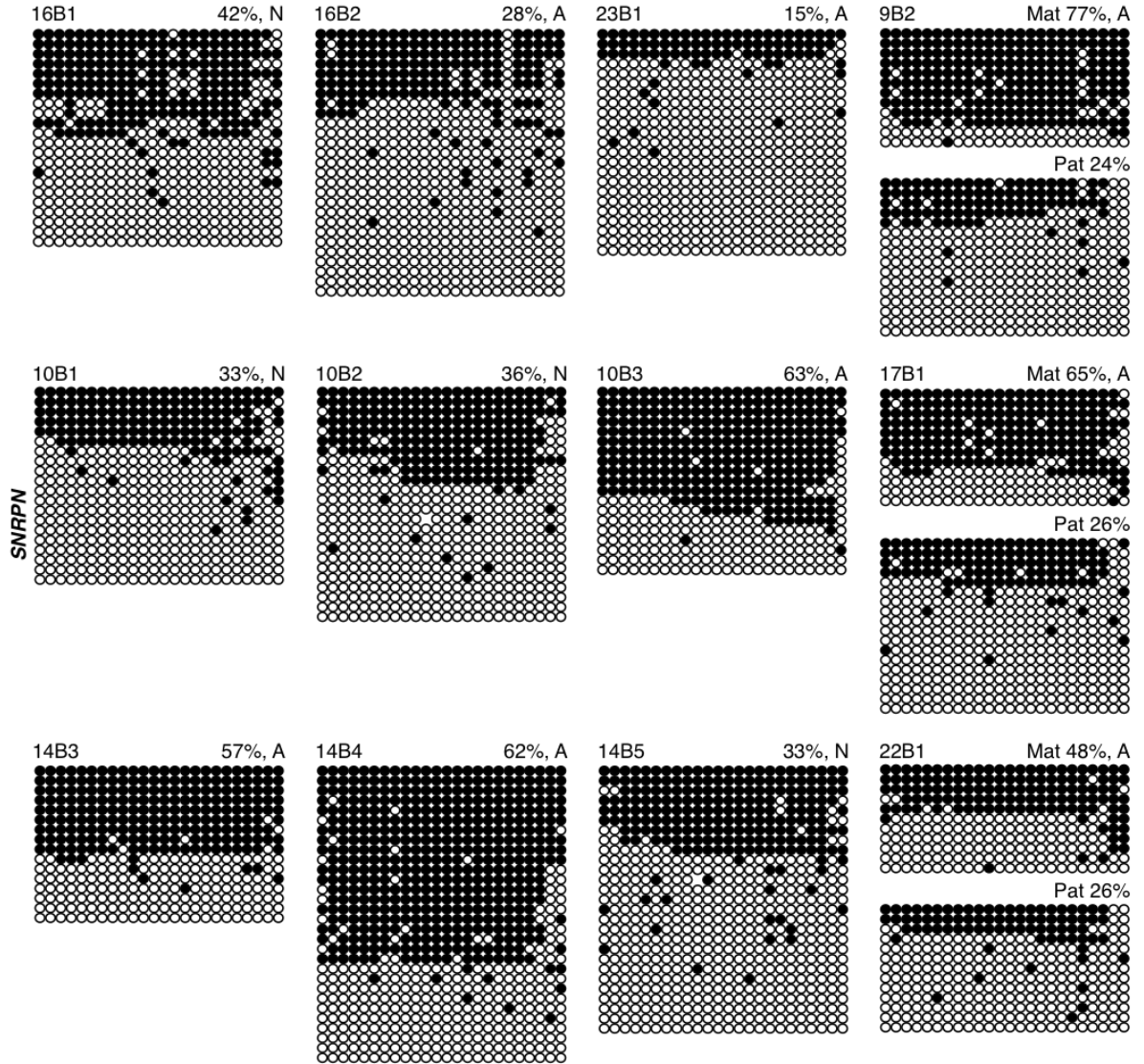
Figure 2-5: Methylation of the *SNRPN* ICR in human blastocyst-stage embryos

Each group of DNA strands is an individual blastocyst with embryo ID (top left), and percent methylation and presumptive maternal/paternal allele designation (top right) indicated. Normal (N) and abnormal (A) embryos are designated next to percent methylation values (top right). See Figure legend 2-1 for details.
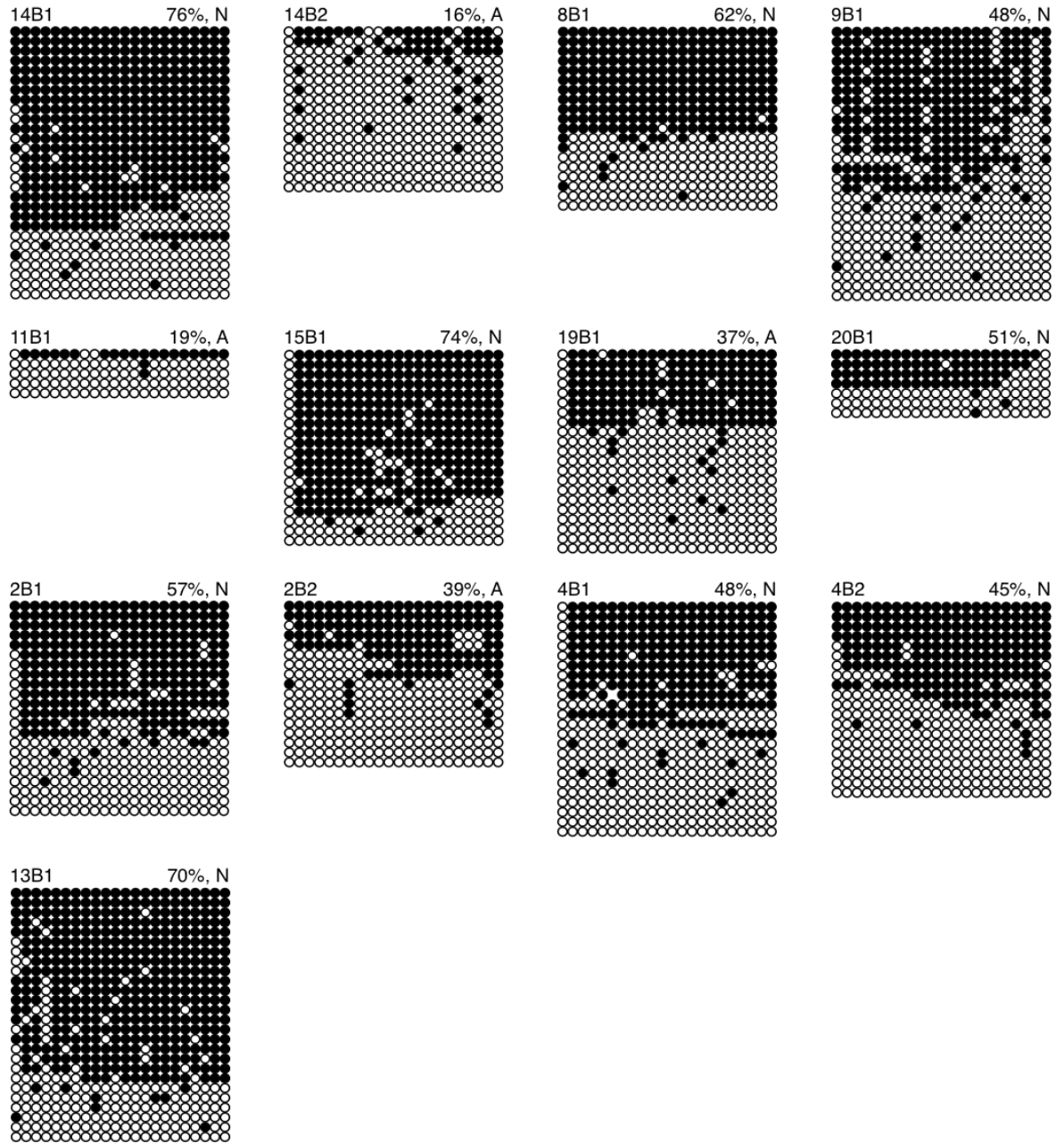
Figure 2-6: Methylation of the *KCNQ1OT1* ICR in human blastocyst-stage embryos

Each group of DNA strands is an individual blastocyst with embryo ID (top left), and percent methylation and presumptive maternal/paternal allele designation (top right) indicated. Normal (N) and abnormal (A) embryos are designated next to percent methylation values (top right). See Figure legend 2-1 for details.
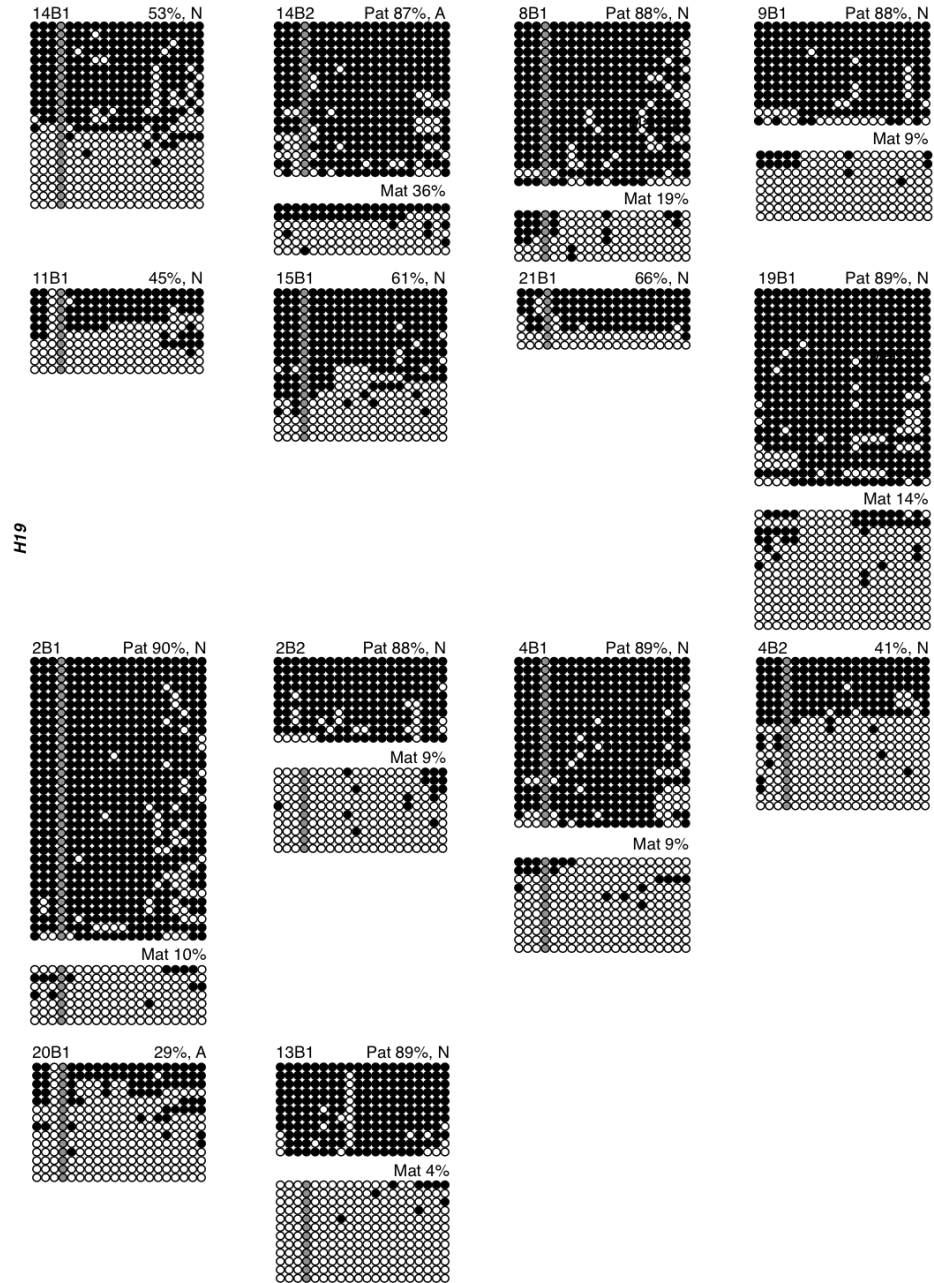
Figure 2-7: Methylation of the *H19* ICR in human blastocyst-stage embryos

Each group of DNA strands is an individual blastocyst with embryo ID (top left), and percent methylation and presumptive maternal/paternal allele designation (top right) indicated. Normal (N) and abnormal (A) embryos are designated next to percent methylation values (top right). Grey circles are not included in methylation analyses as they represent a C/T SNP that cannot be distinguished following bisulfite conversion. See Figure legend 2-1 for details.
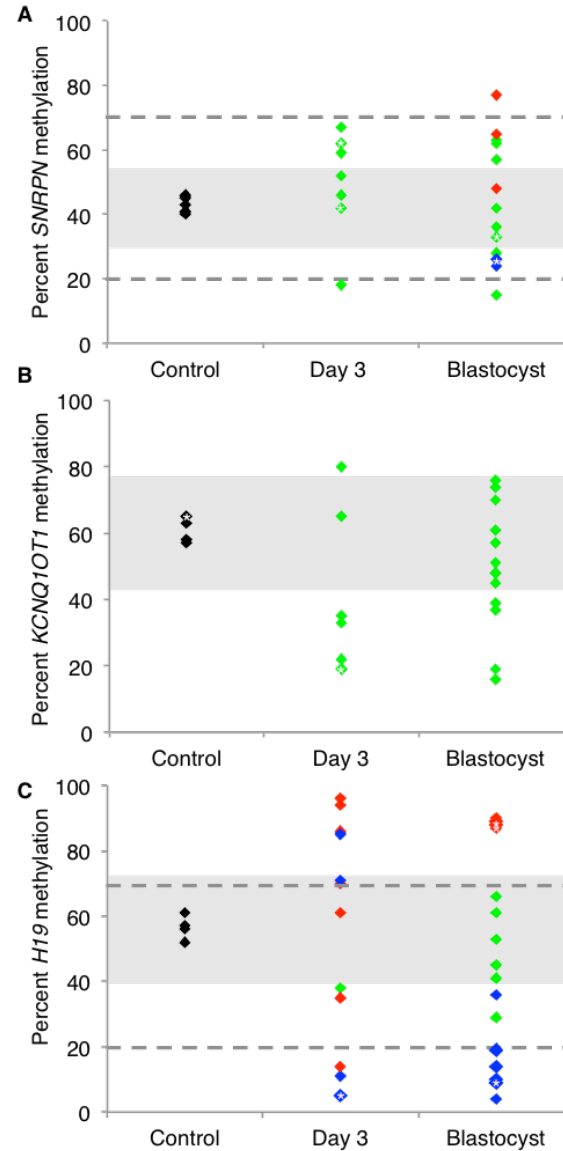
Figure 2-8: Graphical representation for (A) *SNRPN,* (B) *KCNQ1OT1* and (C) *H19* methylation levels in control buccal and ESC samples, and day 3 cleavage and blastocyst-stage embryos

Black diamonds, control sample methylation levels with grey shaded area indicating normal methylation range. Green diamonds, total methylation levels in day 3 embryos and blastocyst embryos. Red diamonds indicate presumptive *SNRPN*, *KCNQ1OT1* and *H19* maternal alleles and blue diamonds indicate presumptive *SNRPN*, *KCNQ1OT1* and *H19* paternal alleles, with grey dashed lines representing ≥70% methylation and ≤20% methylation allelic cutoffs. Asterisk (*) represents a data point for which more than one embryo exists.

2.3.4   Intra-patient comparison of imprinted methylation in embryos at different preimplantation stages

The design of this study allowed multiple embryos from the same patient to be compared for their imprinted methylation status. Out of 22 patients for whom data were obtained, 10 patients had more than one embryo analyzed (Table 2-2). For two patients, 6 and 7, all *in vitro*-produced embryos experienced perturbations in imprinted methylation (*KCNQ1OT1*/*H19* or *H19*). The remaining 8 patients had a portion of embryos with normal and a portion of embryos with abnormal methylation levels. For patient 1, 3/6 day 3 embryos had aberrant *SNRPN* imprinted methylation. For patients 2, 10, 14 and 16, 1/2 (abnormal *KCNQ1OT1*), 1/3 (abnormal *SNRPN*), 3/5 (aberrant *KCNQ1OT1*/aberrant *H19*; aberrant *SNRPN*) and 1/2 (abnormal *SNRPN*) blastocysts had aberrant methylation levels, respectively. Finally, three patients had both day 3 cleavage and blastocyst-stage embryos. For patient 21 and 4, the day 3 embryos had aberrant methylation (abnormal *SNRPN*; abnormal *KCNQ1OT1*), while the blastocysts displayed normal methylation levels. Finally, for patient 9, 1 day 3 embryo and 1 blastocyst possessed normal methylation levels, while 1 day 3 embryo and 1 blastocyst had perturbed methylation (abnormal *KCNQ1OT1*; abnormal *SNRPN*). Overall, all 10 patients had at least one embryo with aberrant imprinted methylation. Since there were embryos with and without imprinted methylation errors from the same patient, and there were genes with and without aberrant imprinted methylation in the same embryo, methylation errors were likely stochastic in nature. Furthermore, the presence of methylation errors in both day 3 cleavage and blastocyst-stage embryos indicates that methylation errors arise as early as the 6-8 cell stage, and that extended culture does not pose a greater risk for imprinting errors than short culture.

2.3.5   Correlation between parental biometrics, clinical treatment and aberrant imprinted methylation

Medical records were examined for parental biometrics, clinical treatment and pregnancy outcomes. Clinical pregnancy rates for fresh embryo transfers as determined by gestational sac by ultrasound were 65% for the same cycle in which the surplus embryos were cryopreserved and donated. Live birth rate was 61% and live births/embryo transfer was 36% (Table 2-3). Of all live births, 45% (9/20) of newborns (2 singletons, 3 sets of twins, and 1 of the triplets) were outside clinically normal birth weight, with 1 high birth weight

(>4000 g), 5 low birth weight (<2500), 1 very low birth weight (<1500 g) and 2 extremely low birth weight (<1000 g). Gestational age was not obtained. To discern any confounding factors related to parental biometrics or clinical treatment, embryos with methylation levels in the normal range were compared to embryos with aberrant methylation for maternal age, patient diagnosis, induction method, hormone dose, stimulation response (E_2 levels), fertilization method (IVF/ICSI), and embryo grade (Table 2-4). Note that for all embryos, the same conditions and reagents were used for *in vitro* culture and slow-freezing cryopreservation, and thus no comparison could be made. For this analysis, the premise was that each embryo could have a different response to influences/exposures, although we acknowledge that embryos from the same mother may have similar exposures to maternal factor treatment. To make a comparison at the patient level for maternal age, hormone dose and estrogen response, separate analyses was also done for patients with only one embryo (12/22), since the remaining 10 patients with more than one embryo had a least one embryo with abnormal methylation. Data from both stages were combined for analyses, except for embryo grade.

Maternal age range for patients in this study was 23-42 years. Mean maternal age for embryos with normal methylation levels was 34 years while that for embryos with aberrant methylation was 33 years (Figure 2-9A), which was not statistically different (p=0.21). Excluding patients with more than one embryo, maternal age for embryos with normal methylation levels was 33 years while that for embryos with abnormal methylation was 30 years (results not shown) (p=0.38). Multiple etiologies contributing to infertility were diagnosed in patients. The four most common patient diagnoses were bilateral tubal obstruction/occlusion (BTO, 29.4% normal, 26.9% abnormal), male factor (MF, 17.6% normal, 15.4% abnormal), blocked tubes with endometriosis (BTO+ENDO, 11.8% normal, 15.4% abnormal) and polycystic ovarian syndrome (PCOS, 11.8% normal, 11.5% abnormal) (Figure 2-9B). Thus, patient diagnoses were not statistically different between embryos with normal and abnormal methylation levels (p>0.99). For induction method, Nafarelin (Synarel®) and Follitropin-alpha (Gonal-F®) was the most common hormone combination for patients with both normal (70.6%) and abnormal (69.2%) embryo groups, followed by Urofollitropin (Bravelle®) and Ganirelix Acetate (Orgalutran®) (11.8% normal and 7.7% abnormal) (Figure 2-9C). Thus, no significant difference was observed for hormone

induction method (p=0.80). Mean hormone dose and estrogen response (E_2) was calculated at 2894.1 IU and 15084.4 pM/L for the normal group and at 2361.5 IU and 12484.7 pM/L for the abnormal group (Figure 2-9D,E), which was not significantly different (p=0.18 and 0.20, respectively). Excluding patients with more than one embryo, dose and estrogen response (E_2) was 4150 IU and 15394.3 pM/L for the normal group and 2233.3 IU and 11546.6 pM/L (results not shown), which was not significantly different (p=0.06 and p=0.43, respectively). For fertilization method, percentage of embryos in the normal group was 62.5% IVF and 47.5% ICSI, and in the abnormal group was 57.7% IVF and 42.3% ICSI (Figure 2-9F), which did not differ statistically (p=0.33). For day 3 embryo grade, embryos with normal methylation levels exhibited a grade of slight C/G2 (slC/G2) (3 embryos) and C/G3 (1 embryo) while those with abnormal methylation levels had a grade of A/B/G1 (4 embryos), slC/G2 (8 embryos) and C (1 embryo) (Figure 2-9G). Importantly, embryos transferred to patients (Table 2-3, 28A/B/G1, 15 slC/G2 and 12 C/G3) had similar grading information to those that were frozen. For blastocysts, 10 of the 13 embryos with normal methylation levels had grading information; 3 were AA, 1 AB, 1 BA, 2 BB, 1 BC, 1CA and 1 CB (Figure 2-9H). For embryos with abnormal methylation levels, 6 of the 13 had grading information: 5 were AA and 1 BA. These grades were not statistically different (p=0.25). A comparison of these grading criteria separately showed that for stage (all 26 embryos included), embryos with normal methylation (5 stage 2, 2 stage 3, 6 stage 4) were not significantly different (p>0.99) from embryos with abnormal methylation (1 stage 1, 7 stage 2, 3 stage 3, 2 stage 4). For ICM grade, embryos with normal methylation (4 A, 4 B, and 2 C) were not statistically different (p=0.40) than embryos with abnormal methylation levels (5 A, 1 B). For TE grade, embryos with normal methylation (5 A, 4 B, 1 C) were not statistically different (p=0.60) from embryos with abnormal methylation levels (6 A). Overall, no specific parameter was identified to have an association with abnormal imprinted methylation. Importantly, we found that embryos of the highest quality with day 3 A/B/G1 and blastocyst AA grading can have abnormal methylation.
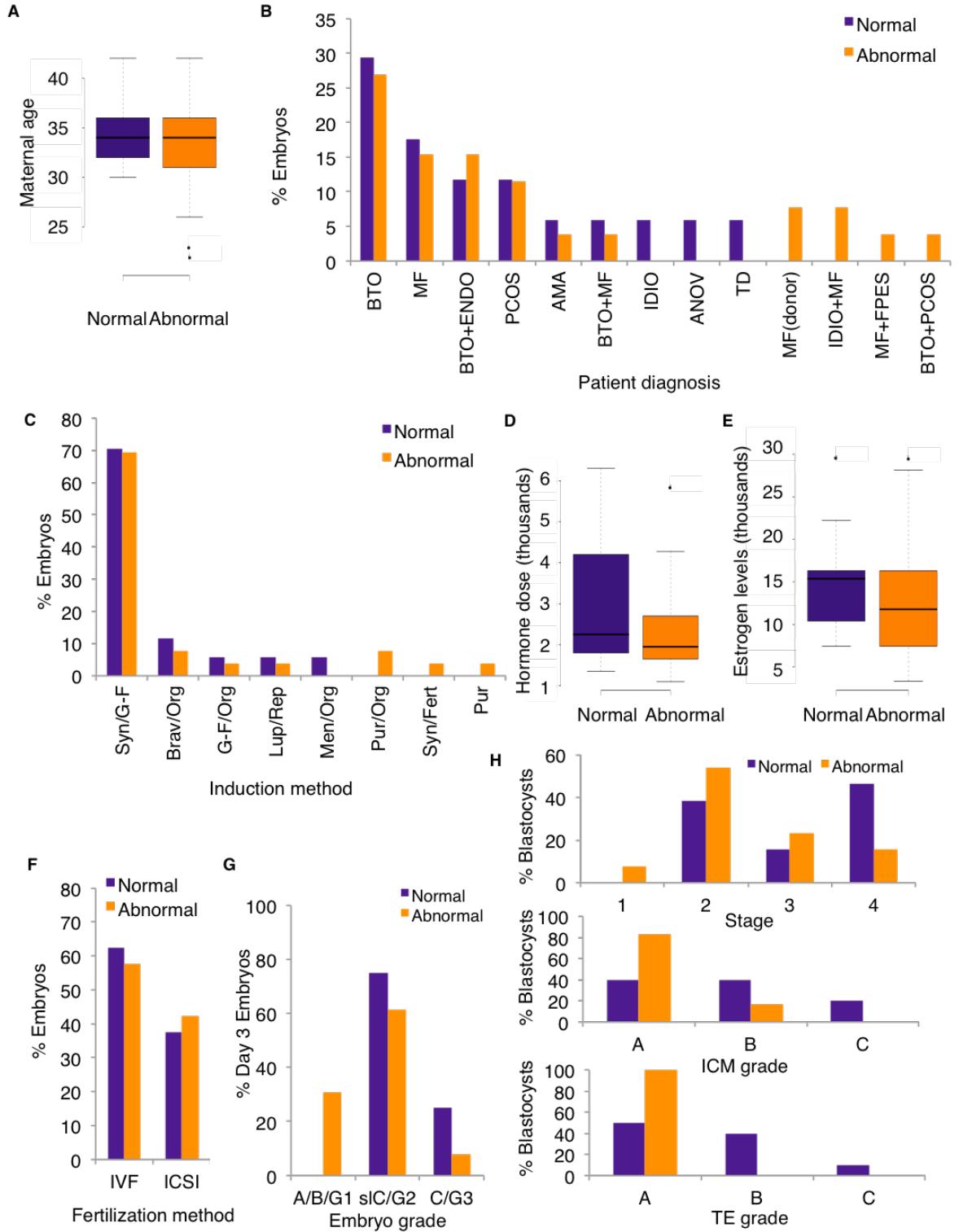
Figure 2-9: Patient characteristics and embryo outcome for embryos with normal and abnormal imprinted methylation

Day 3 cleavage and blastocyst-stage embryos exhibiting normal imprinted methylation (purple bars; n=17) were compared to those with abnormal methylation (orange bars; n=26) for (A) maternal age (t-test), (B) patient diagnosis (KS test), (C) induction method (KS test), (D) hormone dose (t-test), (E) estrogen levels (t-test), and (F) fertilization method (KS test). Means are indicated by black line for maternal age, hormone dose and estrogen levels. (G) Grading of day 3 embryos with normal (n=4) and abnormal methylation (n=13) (no statistical analysis). (H) Blastocysts with normal [n=13 (stage), n=10 (grade)] and abnormal methylation [n=13 (stage), n=6 (grade)] were compared for embryo stage and grade (KS test). No significant difference was observed for any parameter between embryos with normal and abnormal methylation. BTO, bilateral tubal obstruction/occlusion; MF, male factor; ENDO, endometriosis; PCOS, polycystic ovarian syndrome; AMA, advanced maternal age; IDIO, idiopathic; ANOV, anovulatory; TD, tubal disease; (donor), donor sperm; FPES Fresh/frozen percutaneous epididymal/testicular sperm aspiration sample; Syn, Synarel® (Nafarelin); G-F, Gonal-F® (Follitropin-alpha); Brav, Bravelle® (Urofollitropin); Org, Orgalutran® (Ganirelix Acetate); Lup, Lupron® (Leuprolide Acetate); Rep, Repronex® (Menotropins); Men, Menopur® (Menotropins); Pur, Puregon® (Follitropin-beta); Fert, Fertinorm® (Urofollitrophin); IVF, *in vitro* fertilization; ICSI intracytoplasmic sperm injection. See methods for embryo grades.

2.4   Discussion

Although mouse models have been instrumental in analyzing the effects of ARTs on genomic imprinting in oocytes and early embryos, it is important to assess the effects of these technologies in donated human counterparts. This is especially important, as imprinting errors were perceived to be more common in mouse preimplantation embryos than in ART-conceived children. In this study, we observed that 76% day 3 embryos exhibited perturbed imprinted methylation, with 56%, 86% and 71% day 3 embryos possessing aberrant *SNRPN*, *KCNQ1OT1* and *H19* imprinted methylation, respectively. Furthermore, 50% blastocyst-stage embryos exhibited abnormal methylation levels with 67%, 31% and 14% blastocysts having aberrant *SNRPN*, *KCNQ1OT1* and *H19* imprinted methylation, respectively. Both losses and gains of imprinted methylation were observed, and in some cases, both within the same embryo (ex. 17C1, 22B1). Additionally, 50% of day 3 and one blastocyst embryo exhibited both *KCNQ1OT1* and *H19* imprinted methylation perturbations (6C1, 7C1, 7C2, 14B2). This is similar to the multi-locus loss of imprinting we previously observed in the mouse (Market-Velker et al., 2010) and that others have reported in BWS and SRS children (Azzi et al., 2009; Bliek et al., 2009; Chang et al., 2005; DeBaun et al., 2003; Hiura et al., 2012; Lennerz et al., 2010; Lim et al., 2009; Rossignol et al., 2006; Turner et al., 2010).

Very few studies have examined the effects of ARTs on genomic imprinting in donated human preimplantation embryos (Chen et al., 2010; Geuns et al., 2003; 2007; Ibala-Romdhane et al., 2011; Khoueiry et al., 2012; Shi et al., 2014). Moreover, these studies were primarily performed on poor quality embryos that were unsuitable for transfer. Nevertheless, their results were similar to what is reported here. For *SNRPN*, 8/9 day 3 embryos (89%) possessed a loss or gain of methylation (Geuns et al., 2003). For *KCNQ1OT1*, 7/67 day 3 embryos (10%) (Shi et al., 2014) and 9/16 poor quality blastocysts (56%) harboured aberrant methylation (Khoueiry et al., 2012). Finally for *H19*, 3 studies reported aberrant imprinted methylation in 6/32 day 3 embryos (17%) (Chen et al., 2010), 9/21 poor quality morula-blastocysts (43%) (Ibala-Romdhane et al., 2011), and 5/60 blastocysts (8%) (Shi et al., 2014), while the remaining study did not observe any alterations in *H19* imprinted methylation in 8 low quality blastocysts (0%) (Khoueiry et al., 2012). In addition to these genes, previous studies identified 11/65 day 3 embryos (17%) with abnormal *PEG1* imprinted methylation (Shi et al., 2014) and 18/24 day 3 embryos (75%) with aberrant *GTL2* imprinted methylation

(Geuns et al., 2007). All together, our study along with previous publications demonstrate that the frequency of imprinting errors in human donated preimplantation embryos (6-89%) occurs at a similar frequency to that produced in mouse preimplantation embryos (10-90%) (Fauque et al., 2007; Hajj et al., 2011; Market-Velker et al., 2010; 2012).

Of the above studies, two examined imprinted methylation in good quality, in vitro produced embryos. For *KCNQ1OT1*, 2/5 high quality (40%) blastocysts harboured aberrant methylation (Khoueiry et al., 2012), which was similar to what we report here (4/13; 31%). For *H19*, 0/5 high quality (0%) morula-blastocysts (Ibala-Romdhane et al., 2011) and 0/5 high quality blastocysts (0%) possessed aberrant methylation (Khoueiry et al., 2012). This contrasted with our study where we observed 2/14 blastocysts (14%) with aberrant *H19* methylation. This discrepancy may relate to the number of embryos analyzed in these studies.

The design of our study allowed comparison of short culture to day 3 cleavage stages and extended culture to the blastocyst stage. Our data together with previous studies found imprinted methylation errors at both stages; *SNRPN* day 3 (56%, 89%) versus blastocysts (67%); *KCNQ1OT1* day 3 (86%, 10%) versus blastocysts (31%, 40%, 56%); and *H19* day 3 (71%, 17%) versus blastocysts (14%, 8%, 0%) (Chen et al., 2010; Ibala-Romdhane et al., 2011; Khoueiry et al., 2012; Shi et al., 2014). Thus, the presence of methylation errors in embryos undergoing both short (55% embryos) and extended (31% embryos) culture indicates that methylation errors arise as early as the 6-8 cell stage. Furthermore, extending culture from day 3 to the blastocyst stage does not appear to pose any greater risk for imprinting errors. Consequently, our study offers additional support for extended culture to the blastocyst stage to select the most developmentally competent embryos.

Although the frequency of imprinting errors was similar between mice and human preimplantation embryos, disparity still exists between frequencies of imprinting errors in human preimplantation embryos compared to frequencies of imprinting errors reported in ART children. One explanation for this discrepancy may be that imprinting errors in the early embryo lead to reduced levels of implantation or pregnancy failure. Alternatively, blastomeres with aberrant imprinted methylation may be preferentially relegated to the extraembryonic lineages. Previous studies in the mouse provide support for the latter

explanation, since we and others have observed a selective loss of imprinting in the placenta compared to the embryo in midgestation mouse embryos following preimplantation development in culture (de Waal et al., 2014; Mann et al., 2004; Rivera et al., 2008).

Infertility rates have increased around the world (Chandra et al., 2013; Mascarenhas et al., 2012). Advanced maternal age (>35 years) is directly related to this rise, consequently leading to the question of whether delayed childbearing in ART women may contribute to increased imprinting errors in ART children. Additionally, current evidence indicates that the supra-physiological hormonal milieu of ovarian stimulation may produce adverse outcomes in ART pregnancies. For example, similar incidences of low birth weight and preterm low birth weight were present in ART children produced from donor oocytes from fertile women compared to oocytes from subfertile mothers (Kalra and Barnhart, 2011). This birth weight variation in *in vitro*-conceived children may be explained by alterations in DNA methylation levels at growth-related genes, as detected in newborn cord blood and placenta (Turan et al., 2012). With respect to imprinting disorders, ovarian stimulation has also been linked to BWS and AS in ART-conceived children (Chang et al., 2005; Ludwig et al., 2005; Sutcliffe et al., 2006), and for some of these children, the only procedure used was ovarian stimulation (Chang et al., 2005; Ludwig et al., 2005). Our comparison of maternal age, induction method, hormone dosage levels and stimulation response in embryos with and without aberrant methylation revealed no significant difference between these groups. These results were not all that surprising, since embryos with and without methylation errors may have had similar exposures to maternal factor treatment and/or parental biometrics; and all embryos were generated using supra-physiological hormone dosages and the same conditions for *in vitro* culture and slow-freezing cryopreservation. Similarly, no significant difference in fertilization method (IVF/ICSI) or blastocyst grade was observed between embryos with normal or abnormal imprinted methylation. However, it should be noted that even the highest quality day 3 cleavage (A/B/G1) and blastocyst-stage (AA) embryos harbour abnormal methylation levels. This finding has significant bearing on future studies employing high quality embryos as their control group. One further observation of note was that two embryos (19B1, 20B1), produced via donor sperm for male factor infertility, possessed abnormal imprinted methylation. This suggests that imprinting errors in these embryos cannot be explained by inherent infertility, but instead may point to ART-induced errors. Further

studies are required to investigate imprinted methylation errors in *in vitro*-produced embryos using donor oocytes and sperm

There were several limitations of this study. Similar to other studies on ART human embryos, our investigation lacks naturally conceived controls, which is ethically unavoidable. Additionally, due to limited availability of donated embryos, this study and others employed small numbers in analyses. However, the statistical analyses used in this type of study remains valid within the embryo population analyzed, and may allow cumulative analysis of larger sample sizes in the future. Finally, although our study controlled for operating procedure in the clinic, donated embryos analyzed here were obtained from a single fertility clinic.

Going forward, future research should focus on determining differences between human embryos with and without imprinting errors with respect to embryo properties, the timing and origin of these errors, as well as the molecular factors responsible for inducing imprinted methylation errors in ART embryos. Animal models will be instrumental in these studies prior to investigation in human embryos.

Table 2-1: Buccal cell sample, hESCs and embryo genotype

Study ID	*SNRPN* rs220029 (Mat/Pat)*	*KCNQ1OT1* rs56134303 (Mat/Pat)*	*H19* rs2071094 (Mat/Pat)*	*H19* rs2107425 (Mat/Pat)*
Controls				
Bu1	G/G	G/G	A/A	G/G
Bu2	G/G	G/G	T/T	A/A
Bu3	G/G	G/G	T/A	A/G
Bu4	G/G	G/G	A/T	G/G
hESCs	G/G	G/G		
Day 3				
1C1	G/G			
1C2	G/G			
1C3	G/G			
1C4	G/G			
1C5	G/G			
1C6	G/G			
9C2	G/G			
18C1	G/G			
21C1	G/G			
3C1		G/G	A/A	G/G
3C2		IC	IC	IC
4C1		G/G	T/A	A/G
6C1		G/G	T/T	A/G
6C2		IC	T/A	G/G
7C1		G/G	T/A	A/G
7C2		G/G	T/A	A/G
9C1		G/G	A/A	A/G
12C1		G/G	IC	
Blastocyst				
9B2	A/G			
10B1	G/G			
10B2	G/G			
10B3	G/G			
14B3	G/G			
14B4	G/G			
14B5	G/G			
16B1	G/G			
16B2	G/G			
17B1	A/G			
22B1	G/A			
23B1	G/G			
2B1		G/G	T/A	G/G

2B2	G/G	T/T	G/A
4B1	G/G	T/A	A/G
4B2	G/G	A/A	G/G
8B1	G/G	T/A	A/G
9B1	G/G	A/T	G/G
11B1	G/G	A/A	G/G
13B1	G/G	T/T	A/G
14B1	G/G	A/A	G/G
14B2	G/G	T/A	A/G
15B1	G/G	A/A	G/G
19B1	G/G	A/T	G/G
20B1	G/G	A/A	G/G
21B1	IC	A/A	G/G

* presumptive maternal and paternal alleles

Bu, buccal cell samples; hESCs, human embryonic stem cells; Mat, maternal; Pat, paternal; C, day 3 cleavage stage embryo; B, blastocyst stage embryo; ND, not determined; IC, inconclusive.

Table 2-2: Comparison of imprinted methylation status of patients with single and multiple embryos

Patients with a single embryo											
Emb	**3**	**12**	**18**	**8**	**11**	**13**	**15**	**17**	**19**	**20**	**22**	**23**
C1	K 65 / H 38	K 19	S 62									
B1				K 62 / H 88P 9M	K 19 / H 45	K 70 / H 89P 4M	K 74 / H 61	S 65M 26P	K 37 / H 89P 14M	K 51 / H 29	S 48M 26P	S 15

Patients with multiple embryos										
Emb	**6**	**7**	**1**	**2**	**10**	**14**	**15**	**21**	**4**	**9**
C1	K 22 / H 35P 5M	K 33 / H 95P 85M	S 62					S 18	K 19 / H 86P 14M	K 80 / H 70P 5M
C2	H 61P 11M	K 35 / H 94P 71M	S 42							S 52
C3			S 46							
C4			S 42							
C5			S 67							
C6			S 59							
B1				K 57 / H 90P 10M	S 33	K 76 / H 53	S 42	H 66	K 48 / H 89P 9M	K 48 / H 88P 9M
B2				K 39 / H 88P 9M	S 36	K 16 / H 87P 36M	S 28		K 45 / H 41	S 77M 24P
B3					S 63	S 57				
B4						S 62				
B5						S 33				

Emb, embryo; S, *SNRPN*; K, *KCNQ1OT1*; H, *H19*; Numbers, % methylation; P, paternal; M, maternal; purple, normal methylation levels; orange, abnormal methylation levels.

Table 2-3: Pregnancy outcome for each patient

Patient	# ET	Embryo grade	Pregnancy	Live birth	BW (g)	Category
1	2	8B,10slC	No	-		
2	3	8B,8B,7B	No	-		
3	2	9slC,8A	Yes	Y (twins)	925, 820	EL,EL
4	2	8B, 9B	No	-		
5	3	8A,8A,8slC	Yes	Y (twins)	2240, 2466	L,L
6	3	10slC,8A,8A	Yes	Y	1185	VL
7	2	9slC,10slC	Yes	Y	3856	N
8	2	10C,8B	No	-		
9	3	8B,8slC,8A	Yes	Y (twins)	2722, 2665	N,N
10	2	8slC,9C	Yes	Y	3600	N
11	2	8slC,6slC	Yes	Y	3260	N
12	3	8A,7C,A*	Yes	Y	2920	
13	3	7C,4B,5C	No	-		
14	3	8A,8B,8B	Yes	Y (triplets)	2268, 2551, 2551	L, N, N
15	2	7C,10C	No	-		
16	2	6slC,6C	Yes	N		
17	2	7B,7slC	Yes	Y	2948	N
18	2	8B,10B	Yes	Y	4678	H
19	2	8slC,10C	No	-		
20	3	8B,8slC,8A	Yes	Y	3912	N
21	3	8C,8C,8C	Yes	Y (twins)	2325, 2041	L,L
22	2	7A,9A	Yes	Y	3515	N
23	2	10slC,8A	No	-		

ET, embryos transferred; BW, birth weight; N, normal BW; L, low BW; VL, very low BW; EL, extremely low BW. Asterisk indicates embryo was compacting. Gestational age was not obtained.

Table 2-4: Patient biometrics and clinical treatment

Emb ID	Mat Age	Diagnosis	Induction Method	Dose (IU)	E$_2$ Levels (pM/L)	IVF/ICSI	Freeze Year	Emb Grade
1C1	34	MF	Agonist, Synarel, Gonal-F	1,800	16,287	ICSI	2005	3C
1C2	34	MF	Agonist, Synarel, Gonal-F	1,800	16,287	ICSI	2005	7C
1C3	34	MF	Agonist, Synarel, Gonal-F	1,800	16,287	ICSI	2005	6slC
1C4	34	MF	Agonist, Synarel, Gonal-F	1,800	16,287	ICSI	2005	7slC
1C5	34	MF	Agonist, Synarel, Gonal-F	1,800	16,287	ICSI	2005	4slC
1C6	34	MF	Agonist, Synarel, Gonal-F	1,800	16,287	ICSI	2005	7A
3C1	30	MF	Agonist, Synarel, Gonal-F	1,650	16,305	ICSI	2006	7G2
4C1	32	BTO	Agonist, Synarel, Gonal-F	2,250	22,206	IVF	2005	6B
6C1	35	IDIO+MF	Agonist, Synarel, Gonal-F	1,950	8,934	ICSI	2006	7A
6C2	35	IDIO+MF	Agonist, Synarel, Gonal-F	1,950	8,934	ICSI	2006	7slC
7C1	26	PCOS	Antagonist, Orgalutran, Puregon	1,100	6,155	IVF	2007	8slC
7C2	26	PCOS	Antagonist, Orgalutran, Puregon	1,100	6,155	IVF	2007	7slC
9C1	36	BTO+ENDO	Antagonist, Orgalutran, Bravelle	4,200	7,446	ICSI	2006	8B
9C2	36	BTO+ENDO	Antagonist, Orgalutran, Bravelle	4,200	7,446	ICSI	2006	8slC
12C1	37	BTO+ENDO	Agonist, Synarel, Gonal-F	4,275	4,086	IVF	2007	8G2
18C1	32	BTO	Agonist, Synarel, Gonal-F	1,650	5,565	IVF	2004	8slC
21C1	42	AMA	Agonist, Lupron, Repronex	2,850	29,613	IVF	2006	7slC
2B1	38	BTO+MF	Antagonist, Orgalutran, Gonal-F	5,850	10,416	ICSI	2004	4BB
2B2	38	BTO+MF	Antagonist, Orgalutran, Gonal-F	5,850	10,416	ICSI	2004	2AA
4B1	32	BTO	Agonist, Synarel, Gonal-F	2,250	22,206	IVF	2005	3BC
4B2	32	BTO	Agonist, Synarel, Gonal-F	2,250	22,206	IVF	2005	4CA
8B1	34	TD	Agonist, Synarel, Gonal-F	1,800	18,588	IVF	2003	2--
9B1	36	BTO+ENDO	Antagonist, Orgalutran, Bravelle	4,200	7,446	ICSI	2006	1AA
9B2	36	BTO+ENDO	Antagonist, Orgalutran, Bravelle	4,200	7,446	ICSI	2006	3AA
10B1	32	PCOS	Agonist, Synarel, Gonal-F	1,350	9,118	IVF	2006	4AB
10B2	32	PCOS	Agonist, Synarel, Gonal-F	1,350	9,118	IVF	2006	4BB
10B3	32	PCOS	Agonist, Synarel, Gonal-F	1,350	9,118	IVF	2006	4BA
11B1	35	MF+FPES	Agonist, Synarel, Gonal-F	2,250	3,345	ICSI	2007	4AA
13B1	36	IDIO	Antagonist, Orgalutran, Menopur	6,300	14,882	ICSI/IVF	2007	4BA
14B1	36	BTO	Agonist, Synarel, Gonal-F	2,700	15,373	IVF	2007	4AA
14B2	36	BTO	Agonist, Synarel, Gonal-F	2,700	15,373	IVF	2007	3AA
14B3	36	BTO	Agonist, Synarel, Gonal-F	2,700	15,373	IVF	2007	2--
14B4	36	BTO	Agonist, Synarel, Gonal-F	2,700	15,373	IVF	2007	2--
14B5	36	BTO	Agonist, Synarel, Gonal-F	2,700	15,373	IVF	2007	2--
15B1	30	ANOV	Agonist, Synarel, Gonal-F	4,350	12,713	IVF	2003	2--
16B1	31	BTO	Agonist, Synarel, Gonal-F	1,800	13,057	IVF	2007	2AA
16B2	31	BTO	Agonist, Synarel, Gonal-F	1,800	13,057	IVF	2007	2AA
17B1	35	BTO+ENDO	Agonist, Synarel, Fertinorm	1,950	7,555	IVF	2000	2--
19B1	32	MF (DONOR)	Puregon, no agonist	1,300	13,158	IVF	2002	4--
20B1	33	MF (DONOR)	Agonist, Synarel, Gonal-F	3,375	10,502	ICSI	2003	2--
21B1	42	AMA	Agonist, Lupron, Repronex	2,850	29,613	IVF	2006	2CB
22B1	23	BTO+PCOS	Agonist, Synarel, Gonal-F	2,475	13,809	IVF	2003	4--
23B1	26	BTO	Agonist, Synarel, Gonal-F	1,275	28,132	IVF	2003	2--

Emb, embryo; Mat, maternal; C, day 3 cleavage stage embryo; B, blastocysts; E$_2$, serum estrogen on day of hCG trigger; ICSI, intracytoplasmic sperm injection; IVF, *in vitro* fertilization; MF, male factor; ENDO, endometriosis; BTO, bilateral tubal obstruction/occlusion; IDIO, idiopathic; PCOS, polycystic ovarian syndrome; AMA, advanced maternal age; ANOV, anovulatory; TD, tubal disease; DONOR, donor sperm; FPES, Fresh/frozen percutaneous epididymal/testicular sperm aspiration sample; --, no grade available.

2.5 References

Al-Khtib, M., Perret, A., Khoueiry, R., Ibala-Romdhane, S., Blachère, T., Greze, C., Lornage, J., and Lefèvre, A. (2011). Vitrification at the germinal vesicle stage does not affect the methylation profile of H19 and KCNQ1OT1 imprinting centers in human oocytes subsequently matured in vitro. Fertil. Steril. *95*, 1955–1960.

Azzi, S., Rossignol, S., Steunou, V., Sas, T., Thibaud, N., Danton, F., Le Jule, M., Heinrichs, C., Cabrol, S., Gicquel, C., et al. (2009). Multilocus methylation analysis in a large cohort of 11p15-related foetal growth disorders (Russell Silver and Beckwith Wiedemann syndromes) reveals simultaneous loss of methylation at paternal and maternal imprinted loci. Hum. Mol. Genet. *18*, 4724–4733.

Bliek, J., Terhal, P., van den Bogaard, M.-J., Maas, S., Hamel, B., Salieb-Beugelaar, G., Simon, M., Letteboer, T., van der Smagt, J., Kroes, H., et al. (2006). Hypomethylation of the H19 gene causes not only Silver-Russell syndrome (SRS) but also isolated asymmetry or an SRS-like phenotype. Am. J. Hum. Genet. *78*, 604–614.

Bliek, J., Verde, G., Callaway, J., Maas, S.M., De Crescenzo, A., Sparago, A., Cerrato, F., Russo, S., Ferraiuolo, S., Rinaldi, M.M., et al. (2009). Hypomethylation at multiple maternally methylated imprinted regions including PLAGL1 and GNAS loci in Beckwith-Wiedemann syndrome. Eur. J. Hum. Genet. *17*, 611–619.

Chandra, A., Copen, C.E., and Stephen, E.H. (2013). Infertility and impaired fecundity in the United States, 1982-2010: data from the National Survey of Family Growth. Natl Health Stat Report 1–18–1pfollowing19.

Chang, A.S., Moley, K.H., Wangler, M., Feinberg, A.P., and DeBaun, M.R. (2005). Association between Beckwith-Wiedemann syndrome and assisted reproductive technology: a case series of 19 patients. Fertil. Steril. *83*, 349–354.

Chen, S.-L., Shi, X.-Y., Zheng, H.-Y., Wu, F.-R., and Luo, C. (2010). Aberrant DNA methylation of imprinted H19 gene in human preimplantation embryos. Fertil. Steril. *94*, 2356–8–2358.e1.

Chiba, H., Hiura, H., Okae, H., Miyauchi, N., Sato, F., Sato, A., and Arima, T. (2013). DNA methylation errors in imprinting disorders and assisted reproductive technology. Pediatr Int *55*, 542–549.

Chopra, M., Amor, D.J., Sutton, L., Algar, E., and Mowat, D. (2010). Russell-Silver syndrome due to paternal H19/IGF2 hypomethylation in a patient conceived using intracytoplasmic sperm injection. Reprod. Biomed. Online *20*, 843–847.

Cocchi, G., Marsico, C., Cosentino, A., Spadoni, C., Rocca, A., De Crescenzo, A., and Riccio, A. (2013). Silver-Russell syndrome due to paternal H19/IGF2 hypomethylation in a twin girl born after in vitro fertilization. Am. J. Med. Genet. A *161A*, 2652–2655.

Cox, G.F., Bürger, J., Lip, V., Mau, U.A., Sperling, K., Wu, B.-L., and Horsthemke, B. (2002). Intracytoplasmic sperm injection may increase the risk of imprinting defects. Am. J.

Hum. Genet. *71*, 162–164.

de Waal, E., Mak, W., Calhoun, S., Stein, P., Ord, T., Krapp, C., Coutifaris, C., Schultz, R.M., and Bartolomei, M.S. (2014). In vitro culture increases the frequency of stochastic epigenetic errors at imprinted genes in placental tissues from mouse concepti produced through assisted reproductive technologies. Biol. Reprod. *90*, 22.

DeBaun, M.R., Niemitz, E.L., and Feinberg, A.P. (2003). Association of in vitro fertilization with Beckwith-Wiedemann syndrome and epigenetic alterations of LIT1 and H19. Am. J. Hum. Genet. *72*, 156–160.

Denomme, M.M., Zhang, L., and Mann, M.R.W. (2011). Embryonic imprinting perturbations do not originate from superovulation-induced defects in DNA methylation acquisition. Fertil. Steril. *96*, 734–738.e2.

Doornbos, M.E., Maas, S.M., McDonnell, J., Vermeiden, J.P.W., and Hennekam, R.C.M. (2007). Infertility, assisted reproduction technologies and imprinting disturbances: a Dutch study. Human Reproduction *22*, 2476–2480.

Fauque, P., Jouannet, P., Lesaffre, C., Ripoche, M.-A., Dandolo, L., Vaiman, D., and Jammes, H. (2007). Assisted Reproductive Technology affects developmental kinetics, H19 Imprinting Control Region methylation and H19 gene expression in individual mouse embryos. BMC Dev. Biol. *7*, 116.

Gardner, D.K., and Schoolcraft, W.B. (1999). Towards Reproductive Certainty: Fertility and Genetics Beyond 1999: The Plenary Proceedings of the 11th Congress on In Vitro Fertilization and Human Reproductive Genetics (eds Jansen, R. & Mortimer, D.) Ch. 47, 378–388 (Parthenon Pub. Group, 1999)

Geuns, E., De Rycke, M., Van Steirteghem, A., and Liebaers, I. (2003). Methylation imprints of the imprint control region of the SNRPN-gene in human gametes and preimplantation embryos. Hum. Mol. Genet. *12*, 2873–2879.

Geuns, E., De Temmerman, N., Hilven, P., Van Steirteghem, A., Liebaers, I., and De Rycke, M. (2007). Methylation analysis of the intergenic differentially methylated region of DLK1-GTL2 in human. Eur. J. Hum. Genet. *15*, 352–361.

Gicquel, C., Gaston, V., Mandelbaum, J., Siffroi, J.-P., Flahault, A., and Le Bouc, Y. (2003). In vitro fertilization may increase the risk of Beckwith-Wiedemann syndrome related to the abnormal imprinting of the KCN1OT gene. Am. J. Hum. Genet. *72*, 1338–1341.

Hajj, El, N., Trapphoff, T., Linke, M., May, A., Hansmann, T., Kuhtz, J., Reifenberg, K., Heinzmann, J., Niemann, H., Daser, A., et al. (2011). Limiting dilution bisulfite (pyro)sequencing reveals parent-specific methylation patterns in single early mouse embryos and bovine oocytes. Epigenetics *6*, 1176–1188.

Halliday, J., Oke, K., Breheny, S., Algar, E., and Amor, D.J. (2004). Beckwith-Wiedemann syndrome and IVF: a case-control study. Am. J. Hum. Genet. *75*, 526–528.

Hardy, K., Stark, J., and Winston, R.M.L. (2003). Maintenance of the inner cell mass in human blastocysts from fragmented embryos. Biol. Reprod. *68*, 1165–1169.

Hiura, H., Okae, H., Miyauchi, N., Sato, F., Sato, A., Van De Pette, M., John, R.M., Kagami, M., Nakai, K., Soejima, H., et al. (2012). Characterization of DNA methylation errors in patients with imprinting disorders conceived by assisted reproduction technologies. Hum. Reprod. *27*, 2541–2548.

Horike, S., Mitsuya, K., Meguro, M., Kotobuki, N., Kashiwagi, A., Notsu, T., Schulz, T.C., Shirayoshi, Y., and Oshimura, M. (2000). Targeted disruption of the human LIT1 locus defines a putative imprinting control element playing an essential role in Beckwith-Wiedemann syndrome. Hum. Mol. Genet. *9*, 2075–2083.

Ibala-Romdhane, S., Al-Khtib, M., Khoueiry, R., Blachère, T., Guérin, J.F., and Lefèvre, A. (2011). Analysis of H19 methylation in control and abnormal human embryos, sperm and oocytes. Eur. J. Hum. Genet. *19*, 1138–1143.

Kagami, M., Nagai, T., Fukami, M., Yamazawa, K., and Ogata, T. (2007). Silver-Russell syndrome in a girl born after in vitro fertilization: partial hypermethylation at the differentially methylated region of PEG1/MEST. J Assist Reprod Genet *24*, 131–136.

Kalra, S.K., and Barnhart, K.T. (2011). In vitro fertilization and adverse childhood outcomes: what we know, where we are going, and how we will get there. A glimpse into what lies behind and beckons ahead. Fertil. Steril. *95*, 1887–1889.

Khoueiry, R., Ibala-Romdhane, S., Al-Khtib, M., Blachère, T., Lornage, J., Guérin, J.F., and Lefèvre, A. (2012). Abnormal methylation of KCNQ1OT1 and differential methylation of H19 imprinting control regions in human ICSI embryos. Zygote 1–10.

Lammers, T.H.M., van Haelst, M.M., Alders, M., and Cobben, J.M. (2012). Het Silver-Russell-syndroom in Nederland. Tijdschr. Kindergeneeskunde *80*, 86–91.

Lennerz, J.K., Timmerman, R.J., Grange, D.K., DeBaun, M.R., Feinberg, A.P., and Zehnbauer, B.A. (2010). Addition of H19 "loss of methylation testing" for Beckwith-Wiedemann syndrome (BWS) increases the diagnostic yield. J Mol Diagn *12*, 576–588.

Lim, D., Bowdin, S.C., Tee, L., Kirby, G.A., Blair, E., Fryer, A., Lam, W., Oley, C., Cole, T., Brueton, L.A., et al. (2009). Clinical and molecular genetic features of Beckwith-Wiedemann syndrome associated with assisted reproductive technologies. Hum. Reprod. *24*, 741–747.

Ludwig, M., Katalinic, A., Gross, S., Sutcliffe, A., Varon, R., and Horsthemke, B. (2005). Increased prevalence of imprinting defects in patients with Angelman syndrome born to subfertile couples. J. Med. Genet. *42*, 289–291.

Maher, E.R., Afnan, M., and Barratt, C.L. (2003a). Epigenetic risks related to assisted reproductive technologies: epigenetics, imprinting, ART and icebergs? Human Reproduction *18*, 2508–2511.

Maher, E.R., Brueton, L.A., Bowdin, S.C., Luharia, A., Cooper, W., Cole, T.R., Macdonald, F., Sampson, J.R., Barratt, C.L., Reik, W., et al. (2003b). Beckwith-Wiedemann syndrome and assisted reproduction technology (ART). J. Med. Genet. *40*, 62–64.

Maher, E.R. (2005). Imprinting and assisted reproductive technology. Hum. Mol. Genet. *14 Spec No 1*, R133–R138.

Mann, M.R.W., Lee, S.S., Doherty, A.S., Verona, R.I., Nolen, L.D., Schultz, R.M., and Bartolomei, M.S. (2004). Selective loss of imprinting in the placenta following preimplantation development in culture. Development *131*, 3727–3735.

Market-Velker, B.A., Denomme, M.M., and Mann, M.R.W. (2012). Loss of genomic imprinting in mouse embryos with fast rates of preimplantation development in culture. Biol. Reprod. *86*, 143–1–16.

Market-Velker, B.A., Zhang, L., Magri, L.S., Bonvissuto, A.C., and Mann, M.R.W. (2010). Dual effects of superovulation: loss of maternal and paternal imprinted methylation in a dose-dependent manner. Hum. Mol. Genet. *19*, 36–51.

Mascarenhas, M.N., Flaxman, S.R., Boerma, T., Vanderpoel, S., and Stevens, G.A. (2012). National, regional, and global trends in infertility prevalence since 1990: a systematic analysis of 277 health surveys. PLoS Med. *9*, e1001356.

Okun, N., and Sierra, S. (2014). Pregnancy outcomes after assisted human reproduction. J Obstet Gynaecol Can *36*, 64–83.

Rijnders, P.M., and Jansen, C.A. (1998). The predictive value of day 3 embryo morphology regarding blastocyst formation, pregnancy and implantation rate after day 5 transfer following in-vitro fertilization or intracytoplasmic sperm injection. Human Reproduction *13*, 2869–2873.

Rivera, R.M., Stein, P., Weaver, J.R., Mager, J., Schultz, R.M., and Bartolomei, M.S. (2008). Manipulations of mouse embryos prior to implantation result in aberrant expression of imprinted genes on day 9.5 of development. Hum. Mol. Genet. *17*, 1–14.

Rossignol, S., Steunou, V., Chalas, C., Kerjean, A., Rigolet, M., Viegas-Pequignot, E., Jouannet, P., Le Bouc, Y., and Gicquel, C. (2006). The epigenetic imprinting defect of patients with Beckwith-Wiedemann syndrome born after assisted reproductive technology is not restricted to the 11p15 region. J. Med. Genet. *43*, 902–907.

Savage, T., Peek, J., Hofman, P.L., and Cutfield, W.S. (2011). Childhood outcomes of assisted reproductive technology. Hum. Reprod. *26*, 2392–2400.

Shi, X., Chen, S., Zheng, H., Wang, L., and Wu, Y. (2014). Abnormal DNA Methylation of Imprinted Loci in Human Preimplantation Embryos. Reprod Sci.

Sjöblom, P., Menezes, J., Cummins, L., Mathiyalagan, B., and Costello, M.F. (2006). Prediction of embryo developmental potential and pregnancy based on early stage morphological characteristics. Fertil. Steril. *86*, 848–861.

Sutcliffe, A.G., Peters, C.J., Bowdin, S., Temple, K., Reardon, W., Wilson, L., Clayton-Smith, J., Brueton, L.A., Bannister, W., and Maher, E.R. (2006). Assisted reproductive therapies and imprinting disorders--a preliminary British survey. Human Reproduction *21*, 1009–1011.

Testart, J., Lassalle, B., Belaisch-Allart, J., Hazout, A., Forman, R., Rainhorn, J.D., and Frydman, R. (1986). High pregnancy rate after early human embryo freezing. Fertil. Steril. *46*, 268–272.

Turan, N., Ghalwash, M.F., Katari, S., Coutifaris, C., Obradovic, Z., and Sapienza, C. (2012). DNA methylation differences at growth related genes correlate with birth weight: a molecular signature linked to developmental origins of adult disease? BMC Med Genomics *5*, 10.

Turner, C.L.S., Mackay, D.M., Callaway, J.L.A., Docherty, L.E., Poole, R.L., Bullman, H., Lever, M., Castle, B.M., Kivuva, E.C., Turnpenny, P.D., et al. (2010). Methylation analysis of 79 patients with growth restriction reveals novel patterns of methylation change at imprinted loci. Eur. J. Hum. Genet. *18*, 648–655.

Van Buggenhout, G., and Fryns, J.-P. (2009). Angelman syndrome (AS, MIM 105830). Eur. J. Hum. Genet. *17*, 1367–1373.

van Montfoort, A.P.A., Hanssen, L.L.P., de Sutter, P., Viville, S., Geraedts, J.P.M., and de Boer, P. (2012). Assisted reproduction treatment and epigenetic inheritance. Human Reproduction Update *18*, 171–197.

Weksberg, R., Shuman, C., and Beckwith, J.B. (2010). Beckwith-Wiedemann syndrome. Eur. J. Hum. Genet. *18*, 8–14.

Ørstavik, K.H., Eiklid, K., van der Hagen, C.B., Spetalen, S., Kierulf, K., Skjeldal, O., and Buiting, K. (2003). Another case of imprinting defect in a girl with Angelman syndrome who was conceived by intracytoplasmic semen injection. Am. J. Hum. Genet. *72*, 218–219.

Chapter 3

3 Superovulation disrupts mitochondria in mouse oocytes and preimplantation embryos

3.1 Introduction

Mitochondria are vital for oocyte and preimplantation embryo developmental competence. This has been perpetually demonstrated over the years in multiple different species, including mouse and human [reviewed in (Chappel, 2013; Schatten et al., 2014; Van Blerkom, 2011)]. Consequently, in the assisted reproductive technology (ART) field, fertility clinics around the world have been exploring experimental techniques that target mitochondria to improve IVF success. For example, three-parent mitochondrial replacement therapy (MRT) was approved for human clinical investigation in the United Kingdom on February 3rd, 2015. This technique has emerged to bypass inheritance of mitochondrial disease from affected mothers to offspring by injecting the pronuclei of intended parents into an enucleated donor oocyte (Reinhardt et al., 2013). Furthermore, AUGMENT (for autologous germline mitochondrial energy transfer), a novel and controversial technique, is currently being offered in one city in North America, first originating at the Toronto Centre for Advanced Reproductive Technology (TCART) clinic, in addition to being offered in London, Japan, Panama, Spain, Turkey and Dubai (Motluk, 2015) (http://www.augmenttreatment.com/#find-a-clinic). This technique injects patient-matched mitochondria obtained from a population of cells existing within the woman's ovarian cortex into the oocyte at the time of intracytoplasmic sperm injection (ICSI) (Motluk, 2015; Tilly and Sinclair, 2013; Woods and Tilly, 2015). The idea behind AUGMENT is to supplement the mitochondrial pool in oocytes from women of advanced reproductive age or in couples with multiple failed rounds of infertility treatments (Motluk, 2015; Woods and Tilly, 2015). The world's first AUGMENT baby was born in Toronto in April of 2015. However, despite this success, there are still many unanswered questions regarding the risks these treatments pose to the resulting offspring. Furthermore, little research has been conducted to determine what effects common ART treatments, such as ovarian stimulation, have on the oocyte and preimplantation embryo during *in vitro* development.

The mature human MII oocyte contains about 100,000 to 400,000 mitochondria (Cummins, 2002; Jansen, 2000; Jansen and de Boer, 1998; Jansen and Burton, 2004), which is similar to the number originally identified in mouse eggs ($92,500 \pm 7000$) (Pikó and Matsumoto, 1976). In somatic cells the number of mitochondria vary depending on ATP requirements but are orders of magnitude lower than the MII oocyte, ranging from 265 ± 40 in mouse fibroblasts to 308 ± 47 in human lung fibroblasts (Robin and Wong, 1988). The mitochondrial complement in the MII oocyte is derived from approximately 10-20 mitochondria in primordial germ cells (PGCs), which increases during oocyte growth through mitochondrial DNA replication and biogenesis (Cummins, 2002; Jansen, 2000; St John et al., 2010; Van Blerkom, 2011). The resultant mitochondrial population in MII oocytes represents the only source of mitochondria in resulting offspring.

Given the large size of the mature oocyte, adequate mitochondria numbers and proper mitochondrial distribution are necessary to fulfill spatial ATP requirements. In the mouse, bursts of ATP production coincide with perinuclear mitochondrial translocation throughout meiotic maturation, specifically during germinal vesicle breakdown (GVBD), metaphase I (MI) spindle migration, MI to MII transition, and polar body (PB) extrusion (Van Blerkom, 1991; Yu et al., 2010). At the MII ovulated stage, some reports suggest mitochondria organize to the perinuclear region (Calarco, 1995; Kan et al., 2011; Nagai et al., 2006), while others indicate mitochondria are homogeneously distributed throughout the cytoplasm (Tokura et al., 1993; Van Blerkom, 2004; Yu et al., 2010). In addition, a subcortical ring of high potential mitochondria is necessary for sperm penetration and consequently fertilization and meiotic maturation (Van Blerkom and Davis, 2007).

Upon oocyte meiotic maturation, mitochondrial DNA replication ceases and does not resume until post-implantation (Larsson et al., 1998; Pikó and Chase, 1973; Pikó and Taylor, 1987; Thundathil et al., 2005). This absence of mitochondrial DNA replication during cleavage stages of embryogenesis has been confirmed in mice (Ebert et al., 1988; Larsson et al., 1998; Pikó and Chase, 1973; Pikó and Taylor, 1987), rats (Meziane et al., 1989), pigs (Kameyama et al., 2007), and frogs (Shourbagy et al., 2006). Although mitochondrial numbers are anticipated to remain relatively constant within the preimplantation embryo, paradoxically after fertilization, this means that the mitochondrial complement per blastomere halves with each cell division in concert with an increased demand for ATP (Van

Blerkom, 2009; 2011).   Spatial distribution of mitochondria is also important throughout preimplantation development.   In mouse and human, mitochondria predominantly exhibit perinuclear localization in 1-cell (Tokura et al., 1993; Van Blerkom, 2000; Van Blerkom et al., 2000; Van Blerkom, 2009; Zhao et al., 2009) and 2-cell (Tokura et al., 1993; Van Blerkom et al., 2000; Van Blerkom, 2009; Wilding et al., 2001) embryos.   During cell cleavage, symmetrical segregation of mitochondria surrounding the pronuclei in 1-cell embryos and between blastomeres of 2-cell to 8-cell embryos is associated with enhanced developmental competence (Van Blerkom et al., 2000). By comparison, asymmetric distribution of mitochondria in early cleavage embryos can result in arrested division and lysis (Van Blerkom et al., 2000).   Beyond the 8-cell stage, mitochondria segregate differentially between outer and inner blastomeres (Van Blerkom et al., 2000) to ultimately establish a higher mitochondrial content in trophectoderm (TE) cells compared to inner mass cells (Assou et al., 2006; Houghton, 2006; St John et al., 2010; Thundathil et al., 2005).   This asymmetric distribution is likely required during cavitation to power the sodium-potassium adenosine triphosphatase (Na^+/K^+-ATPase) pump, which is present on the basolateral surface of TE cells, to enable blastocoel cavity formation (Houghton, 2006; Van Blerkom, 2008).

Although numerous studies have analyzed mitochondrial dynamics during gametogenesis and preimplantation development, this knowledge is based on oocytes and embryos obtained through assisted reproductive technologies (ARTs).   However, ART treatments coincide with critical time points where mitochondria are highly replicative and drastically increase in numbers during oogenesis, distributed to provide stage-specific spatial ATP requirements, and sustained in a non-replicative state during preimplantation development. Few studies in mouse and human have described negative effects of ARTs on mitochondrial dynamics and function, with most focusing on oocyte freezing (Demant et al., 2012; Jones et al., 2004; Lei et al., 2014; Manipalviratn et al., 2011; Martino et al., 2013; Wilding et al., 2001; Zander-Fox et al., 2013; Zhao et al., 2009).   These studies also have the confounding effects of superovulation/ovarian stimulation. Finally, there is an emerging interest in the role mitochondria play in epigenetic gene regulation (Martinez-Pastor et al., 2013; Rathmell and Newgard, 2009; Wallace, 2010; Wallace and Fan, 2010; Wellen et al., 2009).   More specifically, mitochondria provide the cell with its source of ATP, which powers chromatin-remodeling complexes and is needed for conversion of methionine to S-

adenosylmethionine (SAM), the cells sole methyl donor required for histone and DNA methylation (Martinez-Pastor et al., 2013; Wallace, 2010). Additionally acetyl-coA required for histone acetylation is mainly derived from citrate, a byproduct derived solely from the mitochondria through the tricarboxylic acid (TCA) cycle (Wallace, 2010; Wallace and Fan, 2010; Wellen et al., 2009). Therefore, disruptions in mitochondrial numbers, dynamics and/or function could lead to perturbations in epigenetic gene regulation.

Here, I investigated, for the first time, the effect of ovarian stimulation on mitochondrial levels, distribution, and function in mouse oocytes and preimplantation embryos under control and stimulated conditions. As a detailed analysis of mitochondrial properties throughout all stages of preimplantation development has not been obtained, I analyzed mitochondrial dynamics in oocytes, and 1-cell, 2-cell, 4-cell, 8-cell, morula- and blastocyst-stage embryos. To assess if mitochondrial perturbation coincides with disrupted DNA methylation, I investigated levels of CHDH, an inner mitochondrial membrane enzyme required in the betaine pathway of methylation production, in control embryos and embryos obtained after hormone stimulation. Overall, the results of this novel study improves our knowledge of mitochondrial dynamics in control oocytes and preimplantation embryos, in addition to providing insight on the effect of hormone treatment on mitochondrial dynamics.

3.2   Materials and Methods

3.2.1   Ethics Statements, source of animals

Experiments were performed in compliance with the guidelines set by the Canadian Council for Animal Care and the policies and procedures approved by the University of Western Ontario Council on Animal Care.

3.2.2   Oocyte and embryo collection

Metaphase II (MII) oocytes were collected from C57BL6/CAST7p6 [B6(CAST7p6)] x C57BL/6 (Charles River) F1 females at 6-8 weeks of age. These females have a *Mus musculus castaneous* (CAST) chromosome 7 and partial regions of chromosome 6 on a C57BL/6 (B6) background. To obtain spontaneously ovulated oocytes, untreated females were examined for estrus and at noon the following day, the oviduct/ampulla was dissected and flushed in warmed M2 media (Sigma) to retrieve cumulus-oocyte-complexes. For

superovulated oocytes, females were injected intraperitoneally (ip) with 6.25 IU or 10 IU equine chorionic gonadotropin (eCG) (Intervet Canada), followed 44-48 hours later by 6.25 IU or 10 IU human chorionic gonadotropin (hCG) (Intervet Canada), respectively. Hormone concentrations of 6.25 IU and 10 IU were considered low and high hormone dosages, respectively. At noon the following day, superovulated cumulus-oocyte-complexes were flushed into warmed M2 media. Spontaneous and superovulated oocytes were washed in 2-3 drops of M2 media containing 0.3 mg/mL hyaluronidase (Sigma) under mineral oil (Sigma) to denude surrounding cumulus cells. Pronuclear to blastocyst-stage embryos were derived from control and hormone-treated B6(CAST7p6) females crossed to B6 males. Embryos were retrieved from oviducts/uteri at 0.5 days postcoitum (dpc) (1-cell), 1.5 dpc (2-cell), 2 dpc (4-cell) and 2.5 dpc (8-cell), 3 dpc (morula) and 3.5 dpc (blastocyst).

3.2.3   Total mitochondrial quantification

To analyze total mitochondrial pools, at least 40 spontaneously ovulated, hormone-treated oocytes and ~20 1-cell, 2-cell, morula and blastocyst-stage embryos from control and hormone-treated females were stained with 0.250 µM Mitotracker® Green FM (Molecular Probes, Invitrogen) in M2 media under mineral oil for 30 minutes at 37°C and 5% CO_2 in air. Following this, DNA was stained in M2 drops containing Hoechst 33342 (1:200 dilution) for 15 minutes at 37°C and 5% CO_2 in air. For imaging, individual oocytes and embryos were immediately transferred to 4 µL M2 drops under mineral oil in glass bottom dishes (MatTek Corporation). The Olympus FluoViewTM FV1000 coupled to the IX81 Motorized Inverted System Microscope (IX2 series) confocal scanning microscope was used to obtain live cell images compiled of Z stacks of 4 µm slices. During image acquisition the microscope was kept warm at 37°C. To maintain consistent fluorescence intensity values between samples imaged on different days, acquisition parameters were identical for all oocytes (filter, 490 HV; Gain, 1; Offset, 2%), and embryos (filter, 445 HV; Gain, 2; Offset 2%). Determination of total Mitotracker green signal intensity was done using Volocity 6.3 Image Analysis Software (Perkin Elmer). For quantification, each oocyte or embryo was outlined to create a region of interest (ROI). The ROI for MII oocytes included all cytoplasm contained within the cortex and excluded the polar body, while the ROI for embryos included the area encased in the zona pellucida to maintain consistency between embryos. Mean total Mitotracker

fluorescence was calculated from the fluorescence intensity of all samples within a group and is represented in relative fluorescence units (RFU). A minimum of 3 females were used for both oocyte and embryo collections, for all control and hormone treatment groups.

3.2.4   Active mitochondrial quantification

To analyze the active mitochondrial pools and the localization of active mitochondria, at least 40 spontaneously ovulated and hormone-treated oocytes were stained with Mitotracker® Red CMXRos (Molecular Probes, Invitrogen) at a final concentration of 0.250 μM in M2 media under mineral oil for 30 minutes at 37°C and 5% CO_2 in air. Subsequently, DNA was stained in M2 drops containing Hoechst 33342 (1:200 dilution) for 15 minutes at 37°C and 5% CO_2 in air. For preimplantation embryos, a minimum of 20 control and hormone-treated 1-cell, 2-cell, 4-cell, 8-cell, morula and blastocyst-stage embryos were stained using the same parameters as oocytes. Individual oocytes and embryos were immediately transferred to 4 μL M2 drops under mineral oil in glass bottom dishes for imaging. Confocal images were obtained using identical acquisition parameters for all Mitotracker red MII oocytes, 1-cell and 2-cell embryos (filter, 400 HV; Gain, 1; Offset, 2%) and Mitotracker red 4-cell, 8-cell, morula- and blastocyst-stage embryos (filter, 370 HV; Gain, 1; Offset, 2%). Mean total Mitotracker red fluorescence was calculated as described above for Mitotracker green using Volocity. At least 3 females were used for both spontaneous and superovulated oocyte and embryo collections.

3.2.5   Quantification of blastocyst cell number and blastocyst volume

Cell counting for blastocysts embryos was performed using Hoechst staining and was done from the top to the bottom of each embryo Z-stack using images from the Olympus FluoViewTM FV1000 system (Market-Velker et al., 2012). Blastocyst cavity volume was calculated using two perpendicular measurements of blastocyst cavity length (μm) obtained with Volocity software. Then lengths were then averaged and halved to determine an average radius, and cavity volume was calculated using the formula for a sphere.

3.2.6   Quantification of superoxide levels

Superoxide accumulation in control and 10 IU blastocysts was determined by live cell immunofluorescence staining with 5 μM MitoSOX Red (Molecular Probes, Invitrogen) for

30 minutes at 37°C and 5% CO_2 in air, followed by DNA detection via Hoechst 33342 (1:200 dilution) staining for 15 minutes at 37°C and 5% CO_2 in air. Following imaging as described above, mean total MitoSOX Red fluorescence was calculated. At least 3 females were used for both control and hormone-treated oocyte and embryo collections.

3.2.7   Immunohistochemistry

For immunohistochemistry analyses, control and hormone-treated embryos were flushed into warmed M2 medium, washed in 1X PBS and fixed in 4% PFA for 30 minutes. Following fixation, embryos were permeabilized for 40 minutes in 0.5% Triton-X-100 (Sigma) in 1X PBS, blocked for 1 hour in 5% normal goat serum (NGS) (Jackson ImmunoResearch), and incubated with 1:50 anti-Tom20 FL-145 (Santa Cruz Biotechnology), 1:100 CHDH (Proteintech), or 1:200 histone 3 lysine 9 dimethylation (H3K9me2) (Abcam) overnight at 4°C. The next day, embryos were washed three times in antibody dilution buffer (ADB, 0.005% Triton-X-100 and 1% NGS in 1X PBS), incubated with appropriate secondary antibody in ADB (1:200) for 1 hour followed by Hoechst 33342 (1:200 dilution) staining for 20 minutes. Embryos were then washed 3 times before imaging in 4 μL M2 drops under mineral oil in glass bottom dishes. Negative controls without primary antibody incubation were processed with experimental groups.

3.2.8   Statistical analyses

Significant differences in total mitochondrial distribution for MII oocytes and active mitochondrial distribution in MII oocytes, 1-cell and 2-cell embryos were analyzed using one-way ANOVA followed by the nonparametric Kolmogorov-Smirnov (KS) test to analyze differences between pairs. The nonparametric KS test was used to analyze distribution differences between the control and treatment groups for total mitochondria in 1-cell and 2-cell embryos and active mitochondria in 4-cell, 8-cell, morula and blastocyst embryos. Statistics for fluorescence intensity analyses for total mitochondria in MII oocytes and active mitochondria in MII oocytes, 1-cell and 2-cell embryos were performed using one-way ANOVA followed by Student's t-test, while Student's t-test was used to identify significance between control and hormone-treated 1-cell, 2-cell (total mitochondria, CHDH intensity) 4-cell, 8-cell (active mitochondria), morula and blastocyst embryos (total and active mitochondria, CHDH and H3K9me2 [blastocysts]). All mean fluorescence intensity bar

graph values are presented as mean ± standard error of the mean (SEM). A p-value of p<0.01 was considered to be statistically significant.

3.3   Results

3.3.1   Superovulation disrupted total and active mitochondrial pool and active mitochondrial distribution in MII ovulated oocytes

Adequate mitochondrial numbers and mitochondrial activity are required for successful meiotic maturation (Yu et al., 2010). To investigate the effects of superovulation on the total mitochondrial pool in MII ovulated oocytes, live-cell immunofluorescence data was first obtained for 50 spontaneous, 57 6.25 IU superovulated and 62 10 IU superovulated oocytes using Mitotracker green and Hoechst 33342 staining. Mitotracker green stains all mitochondria membranes irrespective of respiratory status and thus is a measure of the total mitochondrial pool. Compared to control and the 6.25 IU groups, the total mitochondrial pool was significantly decreased in the 10 IU high hormone treatment group (Figure 3-1A).

Since the high hormone dose disrupted the total mitochondrial pool in oocytes, this may result in a concomitant decrease in the pool of active mitochondria. I therefore assessed the active mitochondria pool in oocytes using Mitotracker red imaging in 48 spontaneously ovulated, 68 6.25 IU superovulated and 67 10 IU superovulated oocytes. Mitotracker red is a dye that specifically stains mitochondria that are actively respiring through oxidative phosphorylation, since its accumulation is dependent on oxidation. Compared to spontaneous controls, a significant decrease in the respiring mitochondrial pool was present at both 6.25 IU and 10 IU hormone dosages (Figure 3-1B).

As mitochondria are dynamic organelles and translocate to different regions of the cytoplasm in oocytes and early embryos, I assessed the distribution of total mitochondria in spontaneous and superovulated oocytes. Three distinct distribution patterns were observed, perinuclear, homogenous, and clustered aggregates, with the latter either to one side of the chromosomes or as clumps dispersed throughout the cytoplasm (Figure 3-1C). With respect to total mitochondria, the majority of spontaneous, 6.25 IU, and 10 IU superovulated oocytes had perinuclear mitochondrial localization (86%, 77%, and 77% oocytes, respectively), with low percentages of oocytes exhibiting homogenous (2%, 5% and 8%, respectively) and

clustered aggregate (12%, 18% and 15%, respectively) patterns (Figure 3-1C). These distributions were not significantly different. Of note is that within the clustered distribution category, oocytes possessed mitochondria that were clustered proximal to the DNA (75% spontaneous; 36% 6.25 IU; 50% 10 IU), distal to the DNA (12.5% spontaneous; 43% 6.25 IU; 40% 10 IU), or in aggregates throughout the cytoplasm (12.5% spontaneous; 21% 6.25 IU; 10% 10 IU) (Figure 3-1D). These distributions were not significantly different, although 6.25 IU and 10 IU oocytes trended toward decreased proximal clustering.

Perinuclear translocation of active mitochondria during oogenesis is essential for oocyte competence (Calarco, 1995; Nagai et al., 2006; Van Blerkom, 1991; Yu et al., 2010). Therefore, I analyzed whether actively respiring mitochondria were correctly localized to the perinuclear region in spontaneous oocytes, and whether superovulation disrupted this organization (Figure 3-1E). Similar to total mitochondrial distribution, perinuclear, homogenous, and clustered aggregate patterns were observed for active mitochondria. However, unlike total mitochondria, distribution of active mitochondria was predominantly perinuclear (92% oocytes; 4% homogenous; 4% clustered) in spontaneous oocytes, while 6.25 IU and 10 IU hormone-treated oocytes had significantly decreased perinuclear localization (50%, 60%) and increased homogenous (26%, 22%) and clustered aggregate (24%, 18%) distributions, respectively (Figure 3-1E). Within the clustered distribution category, oocytes had mitochondrial clusters proximal to the DNA (100% spontaneous; 62% 6.25 IU; 58% 10 IU), distal to DNA (0% spontaneous; 38% 6.25 IU; 30% 10 IU), and in clustered aggregates throughout the cytoplasm (0% spontaneous; 0% 6.25 IU; 8% 10 IU) (Figure 3-1F). These patterns were not significantly different, although 6.25 IU, and 10 IU superovulated oocytes seemed to exhibit decreased proximal clustering compared to controls.

Overall, oocytes obtained after high-hormone treatment exhibited a significant decrease in both the total mitochondrial and active mitochondrial pools. In contrast, the low hormone dose group exhibited a decreased pool of active mitochondria only. Total mitochondria were correctly localized to the perinuclear region in spontaneous, 6.25 IU and 10 IU oocytes. However, active mitochondria were mislocalized as a result of both low and high hormone treatment, displaying increased homogenous and clustered aggregate patterns and decreased perinuclear accumulation.
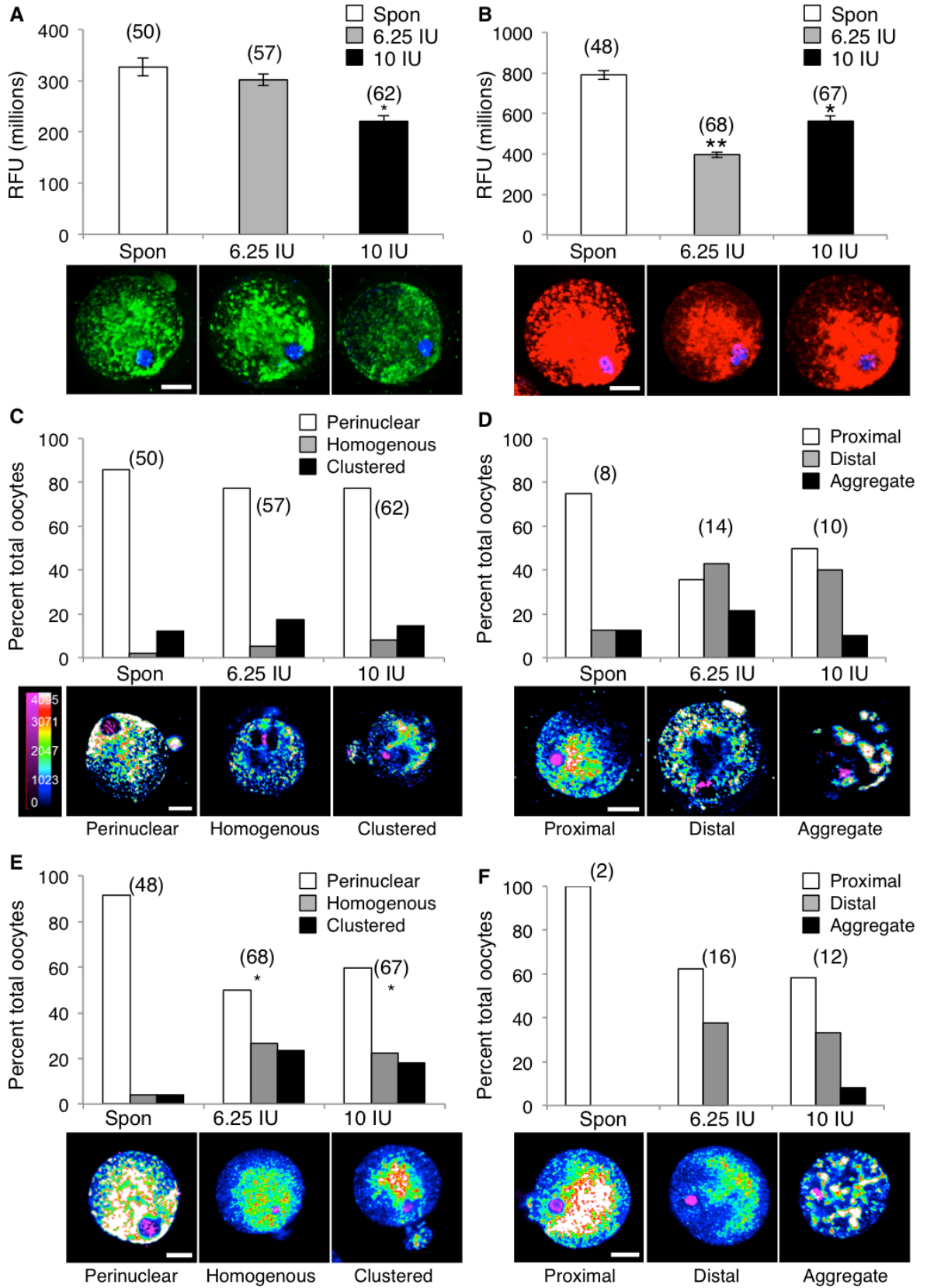
Figure 3-1: Superovulation disrupts mitochondria in MII ovulated oocytes

(A) The total mitochondrial pool, calculated from average total Mitotracker green fluorescence intensity in oocytes, was significantly decreased in the 10 IU hormone treatment group. (B) The active mitochondrial pool, calculated using total Mitotracker red fluorescence intensity in oocytes, was significantly decreased in both 6.25 IU and 10 IU hormone treated groups. (C) Distribution of total mitochondria in spontaneously ovulated (Spon), 6.25 IU and 10 IU superovulated oocytes was predominantly perinuclear, with a small percentage of oocytes displaying homogenous and clustered aggregate patterns. Quantification of distributions is represented as percentage of total oocytes analyzed. (D) With respect to the clustered total mitochondrial distribution, spontaneously ovulated oocytes primarily displayed mitochondrial clustering proximal to the DNA, while the 6.25 IU and 10 IU superovulated oocytes exhibited mitochondrial clustering proximal to the DNA, distal to the DNA, or in clustered aggregates throughout the cytoplasm. (E) Distribution of active mitochondria in spontaneously ovulated oocytes was a perinuclear ring. 6.25 IU and 10 IU superovulated oocytes displayed perinuclear localization in addition to aberrant homogenous and clustered aggregate patterns. Quantification of distributions is depicted as percentage of total oocytes. (F) For clustered active mitochondrial distribution, spontaneously ovulated oocytes displayed mitochondrial clustering proximal to the DNA, while the 6.25 IU and 10 IU superovulated oocytes exhibited mitochondrial clustering proximal to the DNA as well as distal to the DNA and/or in clustered aggregates throughout the cytoplasm. Representative images are shown. Quantification of mitochondrial fluorescence intensity was calculated as the mean relative fluorescence units (RFU) in millions ± SEM for each oocyte group. Numbers in parentheses indicate total number of oocytes analyzed per group. Asterisks (*) indicate significant differences where $p < 0.01$ determined by one-way ANOVA followed by nonparametric Kolmogorov-Smirnov test. DAPI DNA staining, blue (A, B) or magenta (C-F); Mitotracker green staining of total mitochondria, green (A); Mitotracker red staining of active mitochondria, red (B); white scale bar, 20 μm. Pseudocolour imaging was applied to analyze mitochondrial distribution (C-F). Pseudocolour scale is shown in panel C.

3.3.2 Total mitochondrial pool was stable throughout preimplantation development

To determine whether a decreased total mitochondrial pool persisted in early cleavage-stage embryos following superovulation, control and 10 IU 1-cell and 2-cell embryos were stained with Mitotracker green and subjected to live-cell immunofluorescence. The 6.25 IU low hormone group was not analyzed, as no significant decrease was observed in oocytes, and since mitochondria DNA does not replicate post-ovulation and mitochondrial numbers are anticipated to decrease by approximately half with successive cell division (Larsson et al., 1998; Pikó and Chase, 1973; Pikó and Taylor, 1987). At the 1-cell and 2-cell stage, no significant difference in the total mitochondrial pool was detected in the control and 10 IU treatment groups (Figure 3-2A, B). I next analyzed the distribution of total mitochondria within individual blastomeres of 1-cell and 2-cell embryos. Both the control and 10 IU superovulated groups exhibited a homogenous distribution at the 1-cell stage (Figure 3-2C) and perinuclear distribution at the 2-cell stage (Figure 3-2D). Since there was no change in total mitochondrial numbers at the 1-cell and 2-cell stages, I proceeded to analyze the total mitochondrial pool at the morula and blastocyst stages using Mitotracker green. No significant difference in the total mitochondrial pool was observed between morula (Figure 3-3A) and blastocysts (Figure 3-3B) in the control and 10 IU hormone-treated groups. Overall, 10 IU hormone-treated 1-cell, 2-cell, morula and blastocyst-stage embryos displayed similar total mitochondrial pools to their control counterparts. These results indicate that the total mitochondrial pool during preimplantation development is relatively stable following superovulation.

3.3.3 Total mitochondria distribution is unchanged throughout preimplantation development

Symmetrical mitochondrial distribution between blastomeres in early preimplantation embryos is important for competence (Van Blerkom et al., 2000). A previous study indicated that human 1-cell to 8-cell preimplantation embryos with an uneven distribution of mitochondria were developmentally compromised (Van Blerkom et al., 2000). To analyze whether superovulation alters the symmetrical distribution of mitochondria surrounding pronuclei in 1-cell embryos and between blastomeres in 2-cell embryos, embryos from control and 10 IU hormone-treated females were classified as either having symmetrical

(even) or asymmetrical (uneven) mitochondrial segregation. For 1-cell pronuclear embryos, this was analyzed as the distribution of mitochondria surrounding the pronuclei. The majority of 1-cell and 2-cell embryos in the both control and hormone-treated groups exhibited a symmetrical distribution of mitochondria surrounding pronuclei in 1-cell embryos (Figure 3-E) or between blastomeres of 2-cell embryos (Figure 3-2F), respectively, with no significant differences between groups (Figure 3-2E, F). Overall, mitochondrial localization was predominantly symmetrical in both control and hormone-treated 1-cell and 2-cell embryos.
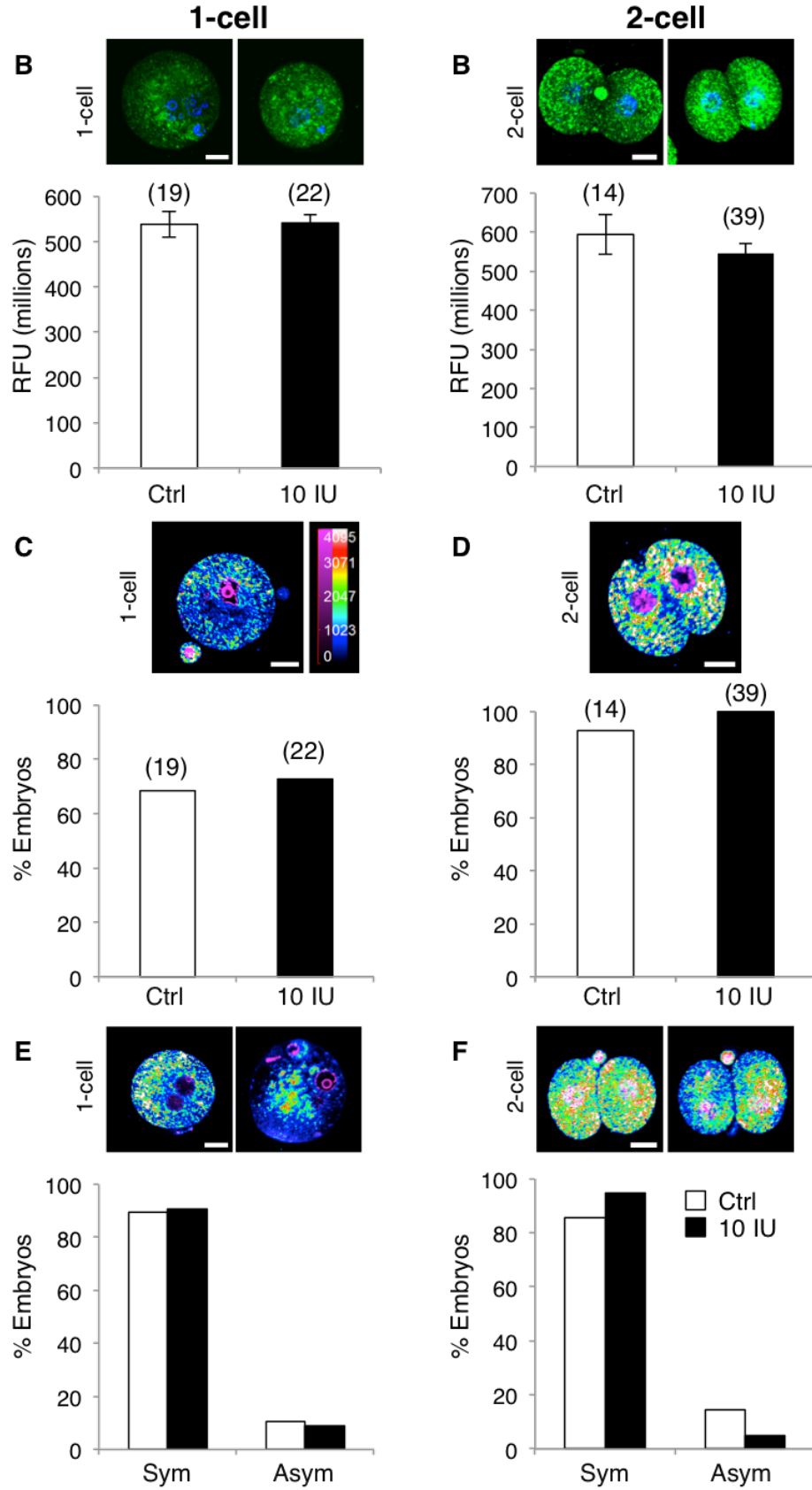
1-cell

2-cell

B 1-cell

B 2-cell

(19) (22)

RFU (millions)

Ctrl   10 IU

(14) (39)

RFU (millions)

Ctrl   10 IU

C 1-cell

D 2-cell

(19) (22)

% Embryos

Ctrl   10 IU

(14) (39)

% Embryos

Ctrl   10 IU

E 1-cell

F 2-cell

% Embryos

Sym   Asym

% Embryos

□ Ctrl
■ 10 IU

Sym   Asym

Figure 3-2: Total mitochondrial pool and distribution in 1-cell and 2-cell embryos

(A, B) Total mitochondrial pool quantification, calculated using Mitotracker green relative fluorescence units (RFU) (millions ± SEM), in 1-cell (A) and 2-cell (B) stage control (Ctrl) and 10 IU hormone-treated embryos. (C, D) Representative pseudocolour conversion slices and quantification of the percent of total embryos showing a homogenous distribution of total mitochondria at the 1-cell stage (C) and a perinuclear distribution of total mitochondria at the 2-cell stage (D). (E, F) Representative pseudocolour images and percentage of total embryos with a symmetrical (even segregation) or asymmetrical (uneven segregation) distribution of total mitochondria surrounding pronuclei at the 1-cell stage (E) and between blastomeres at the 2-cell stage (F) are shown. DAPI DNA staining, blue (A, B) or magenta (C-F); Mitotracker green staining of total mitochondria, green (A, B); Mitotracker green staining, pseudocolour (C-F). Pseudocolour scale is shown in panel C; numbers in brackets indicates the total number of embryos analyzed per Spon and 10 IU treatment groups; white scale bar is 20 μm.
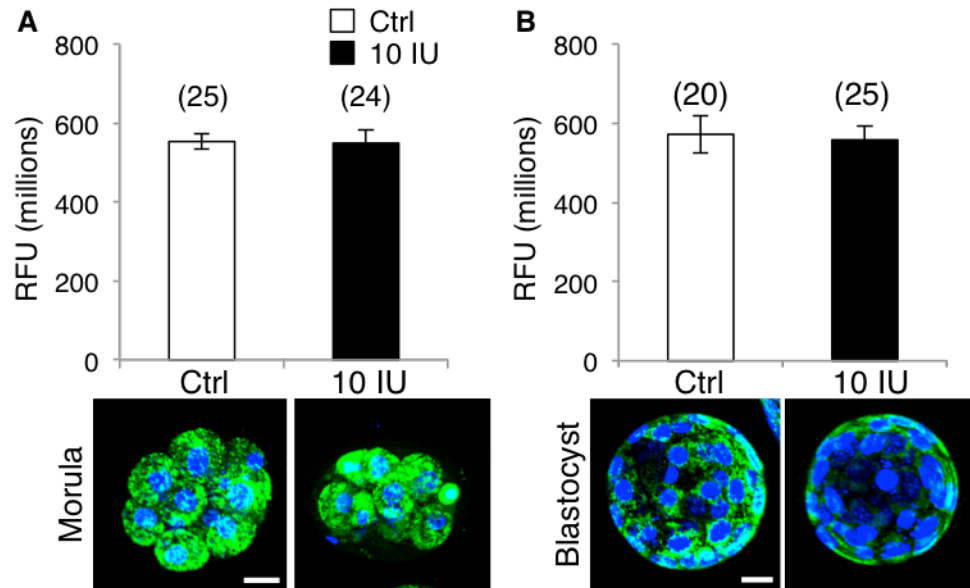
Figure 3-3: Total mitochondrial pool in morula- and blastocyst-stage embryos

Total mitochondrial pool quantification was measured as Mitotracker green relative fluorescence units (RFU) (millions ± SEM) in control (Ctrl) and 10 IU hormone-treated morula (A) and blastocysts (B). Representative Z-stack images are shown. DAPI DNA staining, blue; Mitotracker green staining of total mitochondria, green. Numbers in parentheses indicate total number of embryos analyzed per group; scale bar is 20 μm.

3.3.4 Superovulation affected mitochondrial activity but not mitochondrial organization at early cleavage stages

In addition to total mitochondria pools, I next investigated if the active mitochondrial pool is perturbed in superovulated early cleavage embryos. Compared to controls, the decreased active mitochondrial pool in superovulated oocytes persisted in 1-cell (Figure 3-4A) and 2-cell (Figure 3-4B) embryos in the hormone groups. This effect was dose-dependent. However, no significant difference was seen in the active mitochondrial pool between 4-cell (Figure 3-4C) or 8-cell (Figure 3-4D) embryos in control and 10 IU groups.

Since perinuclear accumulation of active mitochondria was disrupted in superovulated oocytes, I evaluated distribution of active mitochondria in cleavage embryos. Similar to perinuclear active mitochondria in control oocytes (91.6%; Figure 1-1E), the majority of 1-cell (100%; Figure 3-5A) and 2-cell (93.3%; Figure 3-5B) embryos in the untreated group maintained perinuclear distribution. Beginning at the 4-cell stage, active mitochondria move to a cortical arrangement in 4-cell (100%; Figure 3-5C) and 8-cell (81.5%; Figure 3-5D) embryos. Embryos in superovulated groups displayed a statistically similar perinuclear distribution to the controls at 1-cell (96.4% 6.25 IU, 82.9% 10 IU; Figure 3-5A) and 2-cell (93.3% 6.25 IU, 85.7% 10 IU; Figure 3-5B) stages, and a primarily cortical distribution at the 4-cell (95.2% 10 IU, Figure 3-5C) and 8-cell (81.6% 10 IU, Figure 3-5D) stages. Thus, active mitochondrial distribution defects in superovulated oocytes were no longer evident in blastomeres of superovulated 1-cell, 2-cell, 4-cell and 8-cell embryos.

Symmetrical distribution of mitochondria exists in competent early cleavage embryos (Van Blerkom et al., 2000). To determine if superovulation resulted in asymmetric distribution of mitochondria surrounding pronuclei of the 1-cell embryo and between blastomeres of cleavage stage embryos, embryos were classified as having symmetric or asymmetric distribution. The majority of 1-cell (81.8% control, 100% 6.25 IU, 94.3% 10 IU; Figure 3-6A), 2-cell (90% control, 93.3% 6.25 IU, 82.1% 10 IU; Figure 3-6B), and 4-cell (95.2% control, 90.5% 10 IU; Figure 3-6C) embryos in the control and hormone groups displayed a statistically similar symmetrical distribution of active mitochondria. Although not statistically significant, compared to controls (92.6%, Figure 3-6D), the symmetrical distribution in 10 IU 8-cell embryos (73.7%) was slightly decreased.
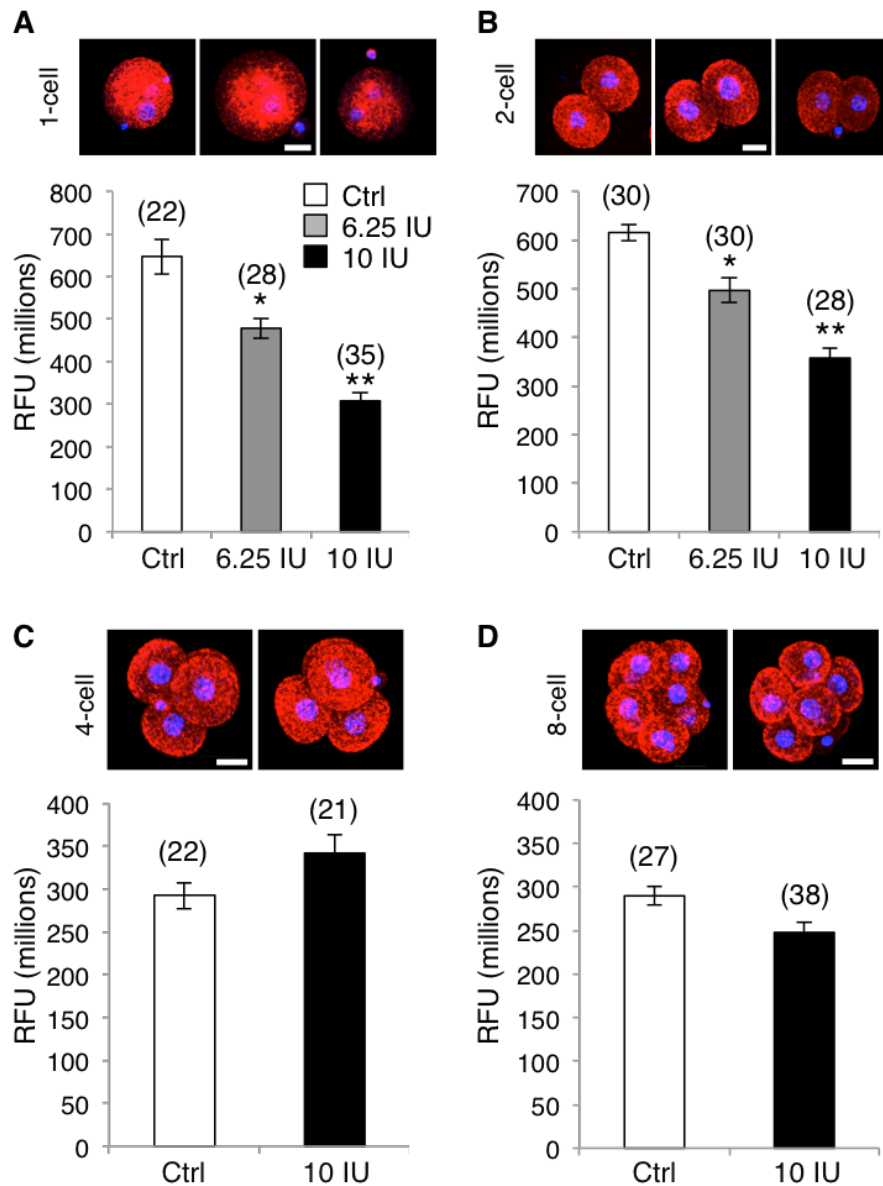
Figure 3-4: Active mitochondrial pool in early cleavage stage embryos

Active mitochondrial pool quantification in 1-cell (A), 2-cell (B), 4-cell (C) and 8-cell (D) early cleavage stage embryos. Representative Z-stack images are shown. Quantification of active mitochondrial pool was calculated as the mean total Mitotracker red fluorescence units (RFU in millions ± SEM). Numbers in parentheses indicate the total number of embryos analyzed. DAPI DNA staining, blue; Mitotracker red staining of active mitochondria, red; scale bar, 20 μm; Ctrl, control.
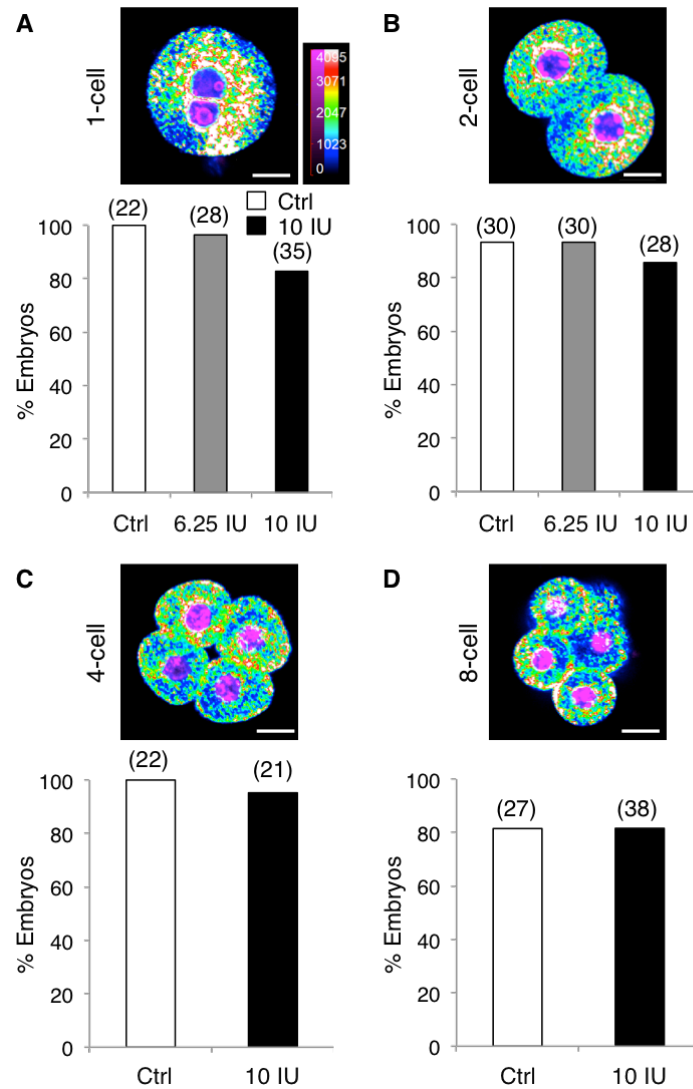
Figure 3-5: Active mitochondrial distribution in early preimplantation embryos

Representative pseudocolour conversion slices of embryos showing active mitochondria moving from a perinuclear distribution at the 1-cell (A) and 2-cell (B) stage to a cortical distribution at the 4-cell (C) and 8-cell (D) stages. This occurred in both control (Ctrl) and 10 IU embryos. Quantification of perinuclear (A, B) and cortical (C, D) staining is represented as the percentage of total embryos analyzed. DAPI DNA staining, magenta; Mitotracker red staining, pseudocolour (scale in panel A). Numbers in brackets indicate the total number of embryos analyzed per group and the scale bar is 20 μm.
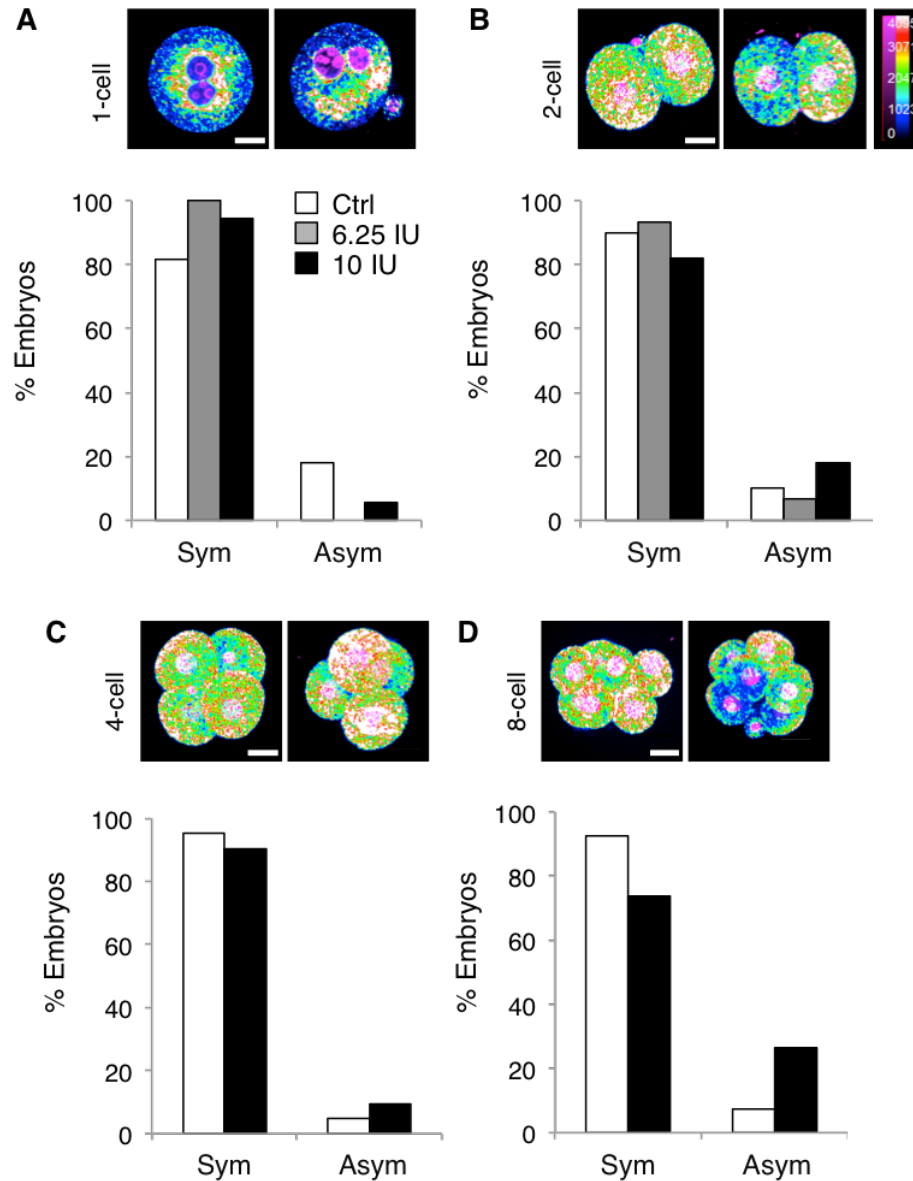
Figure 3-6: Mitochondrial segregation between pronuclei and blastomeres in early preimplantation embryos

Embryos at the 1-cell (A), 2-cell (B), 4-cell (C), and 8-cell (D) stage were classified as having symmetrical (Sym, even segregation) or asymmetrical (Asym, uneven segregation) distribution of active mitochondria between blastomeres. Representative pseudocolour image slices of symmetrical and asymmetrical distributions are shown above each graph. Graphs display the percentage of control (Ctrl), 6.25 IU and 10 IU embryos displaying either distribution. The pseudocolour scale is shown in panel B. DAPI DNA staining, magenta; Mitotracker red staining of active mitochondria, pseudocolour; white bar, 20 μm.

Overall, the active mitochondrial pool was significantly reduced in a dose-dependent manner in superovulated 1-cell and 2-cell embryos, but this effect was not observed at 4-cell and 8-cell stages. Furthermore, active mitochondria were correctly localized in control and hormone-stimulated 1-cell to 8-cell embryos, specifically to the perinuclear region at 1-cell and 2-cell stages, to the cortical region at 4-cell and 8-cell stages, and symmetrically around pronuclei and between blastomeres from 1-cell to 8-cell stages. Thus, ovarian stimulation led to reduced active mitochondrial pools up to the 2-cell stage, after which there were no significant differences between control and hormone-stimulated early cleavage embryos.

3.3.5   Superovulation perturbs mitochondria in morula and blastocyst-stage embryos

A previous study on human preimplantation embryos demonstrated asymmetrical mitochondrial distribution in developmentally competent late (12-16 cell) cleavage embryos (Van Blerkom et al., 2000). To determine the effects of superovulation on mitochondrial distribution between blastomeres in morula- and blastocyst-stage embryos, pseudocolour imaging was applied to Mitotracker green and Mitotracker red staining to allow characterization of mitochondrial intensity in individual blastomeres of an embryo. Blastomeres were classified as having low (primarily blue pseudocolour), medium (mostly green/yellow pseudocolour) or high (primarily red/white pseudocolour) amounts of mitochondria (i.e. Mitotracker red, 10 IU morula #84; 12 low; 4 medium; 10 high; Figure 3-7A-J). Since a previous study identified increased levels of total mitochondria in trophectoderm compared to inner cell mass cells at the blastocyst stage (Houghton, 2006), I assessed inner and outer cells separately for total mitochondrial levels and active mitochondria levels. For total mitochondria distribution, in both control and 10 IU groups, inner blastomeres possessed low total mitochondria compared to outer blastomeres. Furthermore, no significant difference was observed in the percent of inner blastomeres with low levels of total mitochondria between control and 10 IU embryos. However, for outer blastomeres, compared to controls, blastomeres of embryos in the 10 IU group exhibited an increased percentage of blastomeres with low total mitochondria in both morula (control 18.3%; 10 IU 31.9%, Figure 3-7K) and blastocysts (control 33.7%; 10 IU 50.2%, Figure 3-7L). Additionally in blastocysts, outer cells in the 10 IU embryo group had significantly decreased high total mitochondria (24.9% control, 8.8% 10 IU; Figure 3-7L).
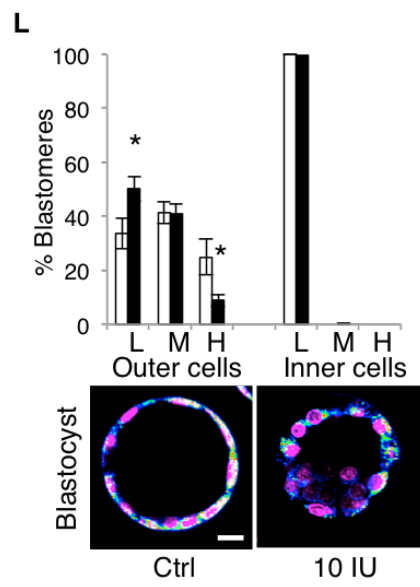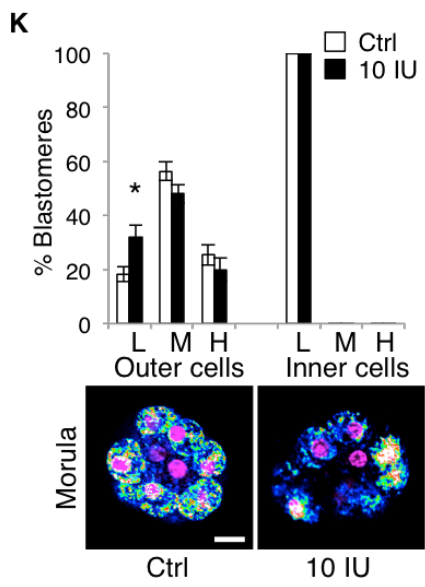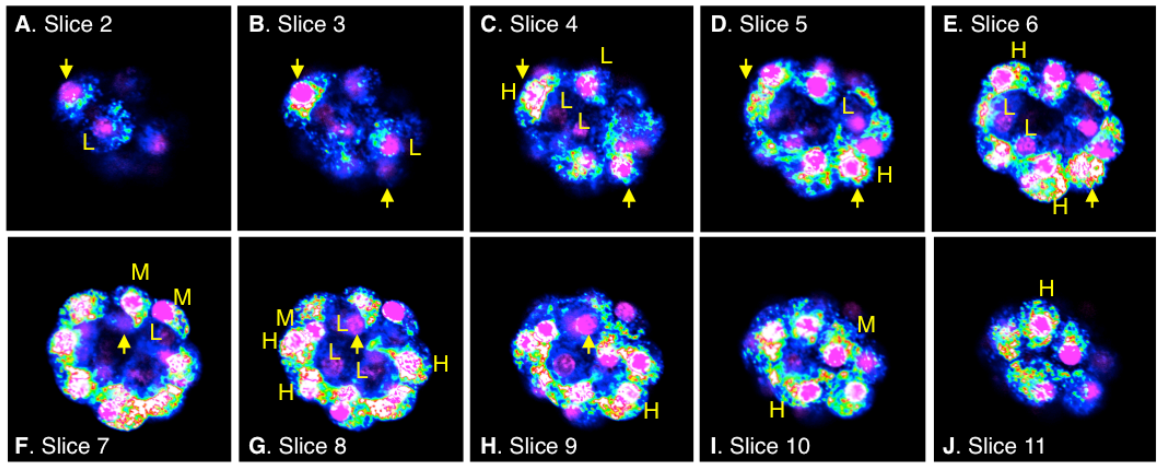
Figure 3-7: Total mitochondrial distribution in morula- and blastocyst-stage embryos

In morula- and blastocyst-stage preimplantation embryos, blastomeres were classified as having low (L, primarily blue pseudocolour), medium (M, mostly green/yellow pseudocolour) or high (H, primarily red/white pseudocolour) amounts of total mitochondria. Individual slices (A-J, example Mitotracker red 10 IU morula #84) of each embryo were analyzed, and each blastomere was followed throughout a subset of slices (see arrows for examples) to determine its classification. (K) Early morula- and (L) blastocyst-stage embryos were divided into inner and outer cells for analysis. Representative morula (K) and blastocyst (L) are shown, with percentage of total blastomeres showing each distribution depicted in each graph. DAPI DNA staining, magenta; (A-J) Mitotracker red staining of active mitochondria, pseudocolour; (K, L) Mitotracker green staining of total mitochondria, pseudocolour; white bar, 20 µm; Ctrl, control. Pseudocolour scale bar is shown under panel J. Asterisks indicate significant differences determined by Student's T-test.

My assessment of mitochondrial activity with Mitotracker Red revealed that morula (Figure 3-8A) and blastocysts (Figure 3-8B) in the 10 IU group had a significant decrease in the active mitochondria pool compared to controls. At the blastomere level, morula and blastocysts in both control and 10 IU groups had an asymmetrical distribution of active mitochondria between outer and inner blastomeres, with inner blastomeres primarily displaying low mitochondrial activity.

For outer blastomeres, compared to the control group, embryos in the 10 IU group displayed a significantly decreased percentage of blastomeres with high mitochondrial activity in morula (control 50.9%; 10 IU 26.8%, Figure 3-8C) and blastocysts (control 53.3%; 10 IU 21.1%, Figure 3-8D). This coincided with a decreased percentage of blastomeres with low (morula control 19.5%; 10 IU 35.2%, Figure 3-8C; blastocysts control 14.5%; 10 IU 34.0% Figure 3-8D) and medium (morula control 29.6%; 10 IU 37.9%, Fig. 8C; blastocysts control 32.2%; 10 IU 44.8%, Figure 3-8D) amounts of active mitochondria in embryos obtained after hormone treatment.

By comparison, inner blastomeres were indistinguishable between control and 10 IU morula-stage embryos (Figure 3-8C). However, inner cells of blastocysts from the 10 IU group displayed a decreased percentage of blastomeres with low amounts of active mitochondria (control 96.6%, 10 IU 89.0%) and an increased percentage of blastomeres with medium amounts of active mitochondria (control 3.4%, 10 IU 10.3%, Figure 3-8D).

On an individual embryo basis, few control morula (7%, Figure 3-9A) and blastocysts (4% Figure 3-9B) had less than 15% of outer blastomeres with high mitochondrial activity. By comparison, in the 10 IU group, approximately half of the morula (44%, Figure 3-9A) and blastocysts (56% Figure 3-9B) had less than 15% of blastomeres with high amounts of active mitochondria.
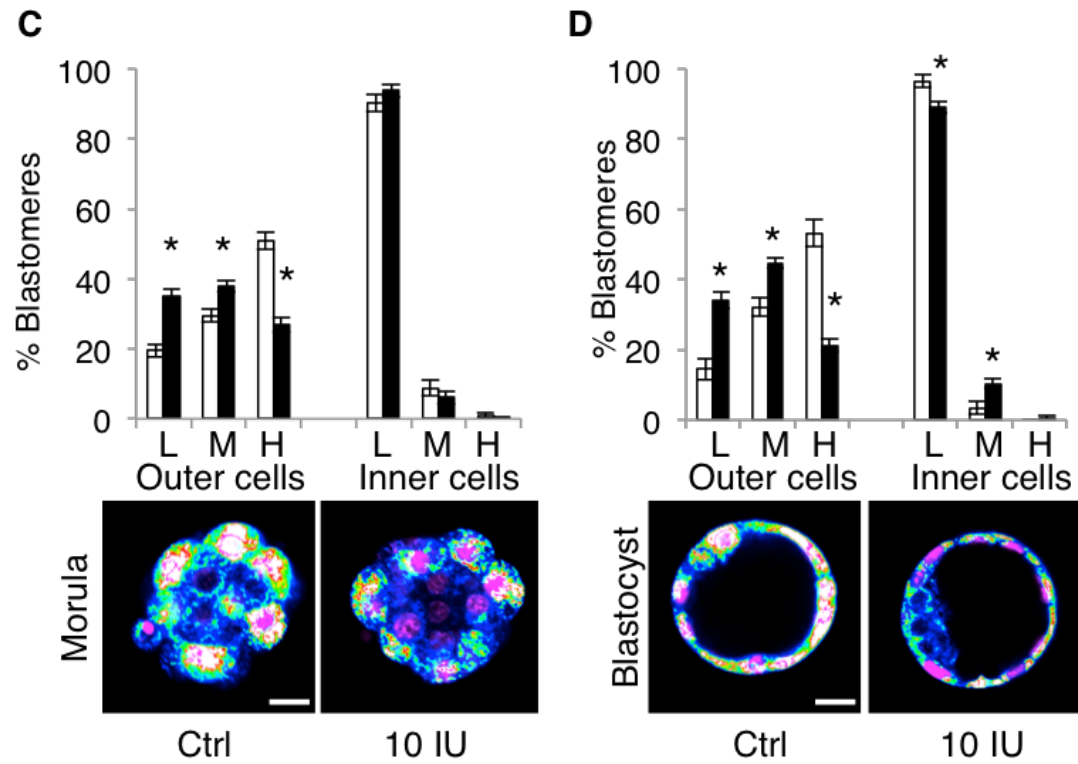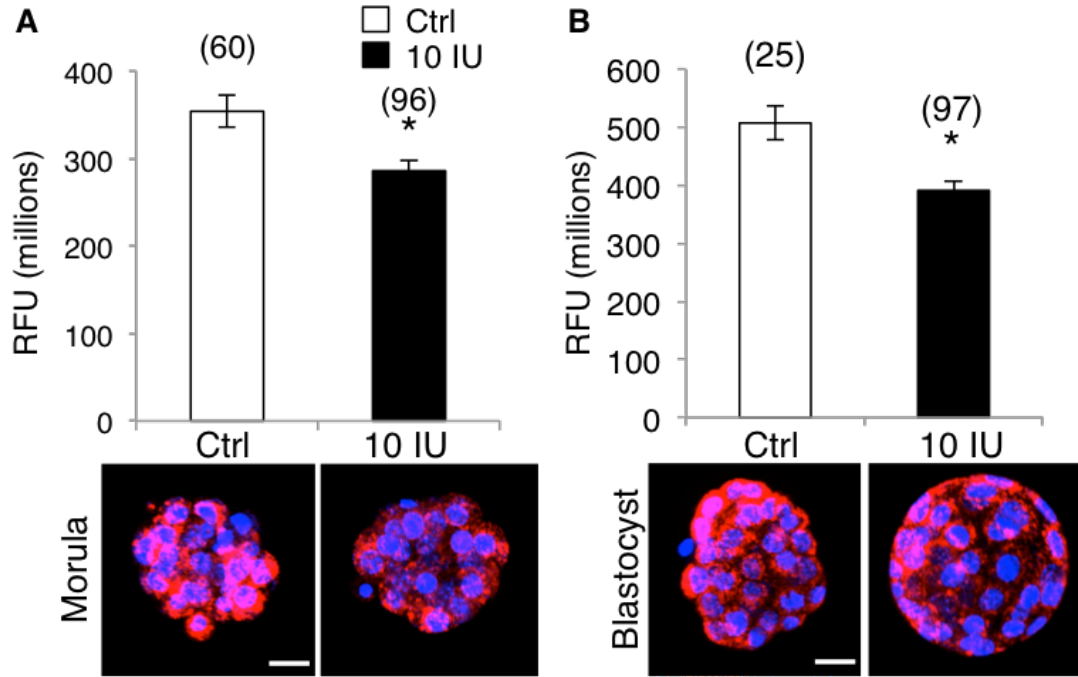
Figure 3-8: Active mitochondria intensity and distribution in morula and blastocysts

Active mitochondrial pool quantification, calculated from total Mitotracker red fluorescence intensity, in morula- (A) and blastocyst-stage (B) control (Ctrl) and 10 IU hormone-treated embryos. Representative Z-stack images are shown along with mean relative fluorescence units (RFU) in millions ± SEM for each group. Active mitochondrial distribution in inner and outer blastomeres of morula (C) and blastocysts (D) depicted as percentage of blastomeres with low (L, primarily blue pseudocolour), medium (M, mostly green/yellow pseudocolour) or high (H, primarily red/white pseudocolour) amounts of active mitochondria. Representative slices are shown. DAPI DNA staining, magenta; Mitotracker red staining of active mitochondria, red (A, B) and pseudocolour (C, D); white bar, 20 μm; Ctrl, control. Pseudocolour scale bar is shown in panel D. Asterisks indicate significant differences.
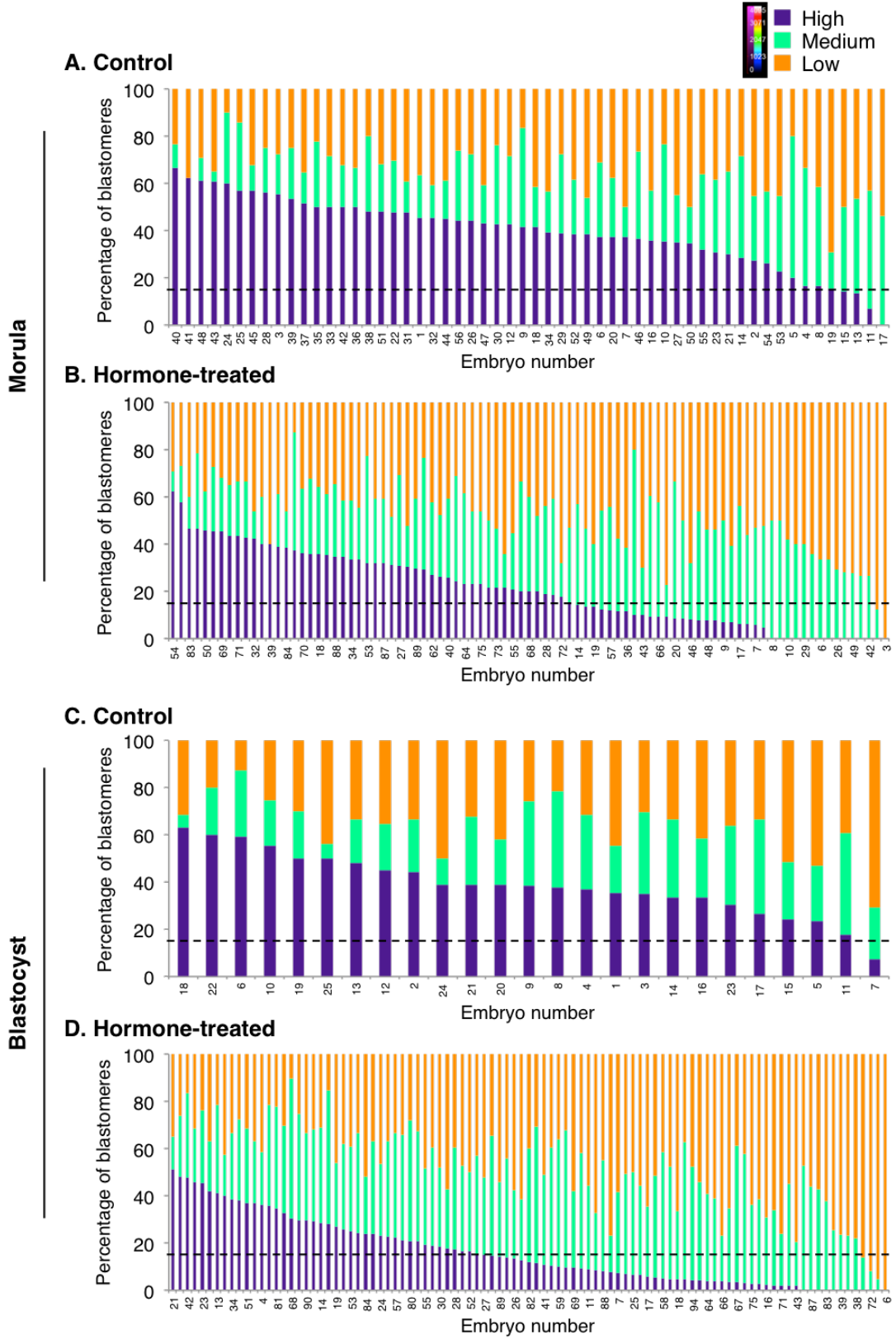
Figure 3-9: Active mitochondrial distribution patterns in individual morula and blastocysts

Distribution of active mitochondria in individual (A) control morula, (B) hormone-stimulated morula, (C) control blastocysts and (D) hormone-stimulated blastocysts. Data is arranged (left to right) in decreasing percentage of blastomeres with high (purple bars), then medium (green bars), then low (orange bars) percentage amounts of active mitochondria. The dotted black line represents where 15% of blastomeres within an embryo have high amounts of active mitochondria.

Since ATP is utilized by the Na^+/K^+-ATPase pump in trophectoderm cells, and this is required for successful cavitation and blastocyst formation (Madan et al., 2007), I assessed cell number (total, inner and outer) (Figure 3-10A) and blastocyst cavity volume (Figure 3-10B) in control and 10 IU blastocysts. Compared to controls, total cell numbers (Figure 3-10C), outer cell numbers and inner cell numbers (Figure 3-10D) were significantly increased in the 10 IU blastocyst group compared to controls, while blastocyst cavity volume was not significantly different (Figure 3-10E).

Overall, late preimplantation embryos exhibited an asymmetrical distribution of both total and active mitochondria. In comparison to control embryos, morula and blastocysts from the 10 IU hormone group exhibited an increase in the proportion of outer cells exhibiting low amounts of mitochondria, both total and active. In addition, high total mitochondria in blastocysts and high active mitochondria in morula and blastocysts were significantly decreased in outer cells of embryos in the 10 IU hormone group. The decrease in active mitochondria in outer cells of blastocysts was not associated with decreased blastocyst cell number or cavity volume.
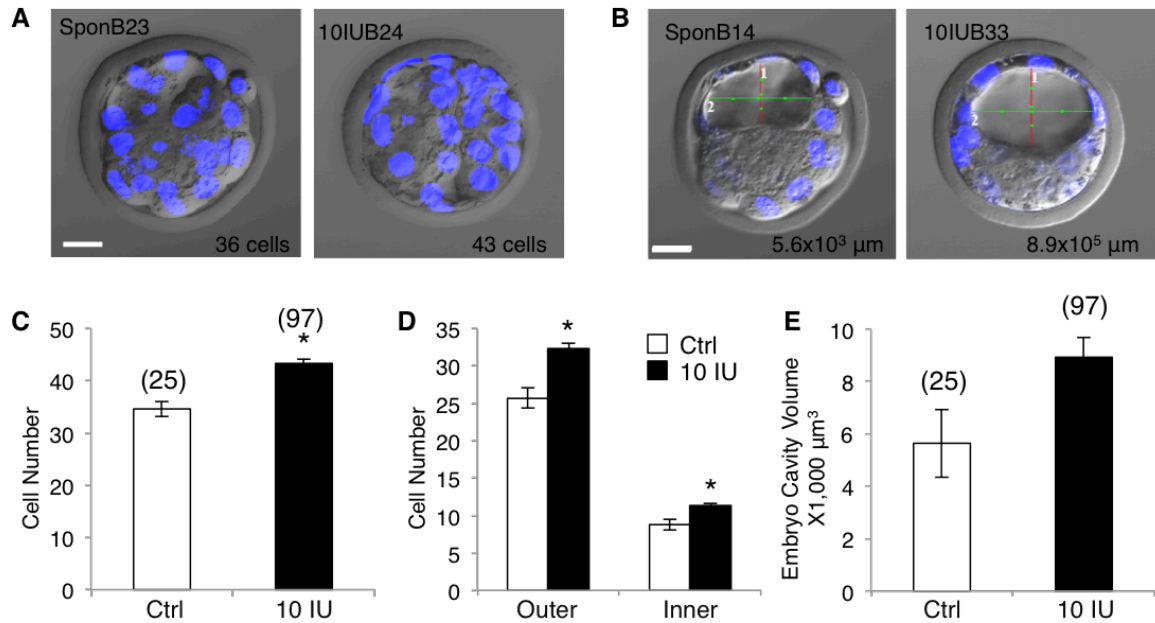
Figure 3-10: Cell number and blastocyst cavity volume

Merge of bright field and DAPI staining for (A) cell counts and (B) blastocyst cavity volume. (C) Total cell number and (D) outer and inner cell numbers and (E) blastocyst cavity volume in control and 10 IU blastocysts. Asterisks indicate significant differences determined by Student's t-test and numbers in parentheses indicate the number of embryos analyzed. DAPI DNA staining, blue; white bar, 20 μm. Representative embryos are shown with embryo number indicated on the top left of bright field images and cell number (A) and cavity volume (B) indicated at the bottom right. Red line (1), horizontal cavity length; green line (2), vertical cavity length.

3.3.6 Superovulation does not alter TOM20 levels but increases superoxide accumulation

To determine if mitochondrial function was affected following ovarian stimulation, levels of the mitochondrial import protein translocase of outer membrane 20 (TOM20) and oxidative stress was assessed. Nuclear-mitochondrial cross talk is vital for proper control of gene expression and mitochondrial function (Woodson and Chory, 2008). Nuclear-encoded proteins are imported into the mitochondria to control its function in response to cellular demand (Jiang and Wang, 2012; Mootha et al., 2003). TOM20 specifically targets the outer mitochondrial membrane and is responsible together with TOM22 to recognize and import cytosolic N-terminal mitochondrial preproteins (Baker et al., 2007; Perry et al., 2008). Since import of nuclear-encoded cytosolic proteins is crucial for mitochondrial function, TOM20 protein expression was analyzed by immunofluorescence in blastocysts from control and 10 IU superovulated females. No significant difference in TOM20 levels was observed between blastocysts in the control and 10 IU hormone groups (Figure 3-11A). Furthermore, there was no difference in the distribution of TOM20 between inner (control 80.0%, 10 IU 79.1%) and outer (control 73.2%, 10 IU 76.7%) blastomeres of these embryos, where the majority displayed medium levels of TOM20 immunofluorescence (Figure 3-11B).

Mitochondrial dysfunction in aged oocytes has been attributed to increased oxidative stress causing oxidative damage (Chappel, 2013; Venkatesh et al., 2010). To assess whether superovulation leads to increased oxidative stress, I analyzed the accumulation of superoxide, a reactive oxygen species (ROS) produced as a byproduct of mitochondrial respiration, using MitoSOX live-cell immunofluorescence. Oxidation of MitoSOX by superoxide produces red fluorescence. Compared to controls, blastocysts in the 10 IU group displayed significantly increased superoxide intensity levels (Figure 3-11C). To identify if accumulation of superoxide is more prevalent in inner or outer cells, pseudocolour imaging was applied and cells were quantified as having low, medium or high superoxide levels. Control blastocysts exhibited low superoxide in both inner (100%) and outer (89.3%) cells (Figure 3-11D). In contrast, while no significant difference in superoxide accumulation was observed between inner cells of control blastocysts versus the 10 IU hormone group (97.5% low, Figure 3-11D), outer cells of the hormone group exhibited a significant increase in blastomeres with medium superoxide levels (37.1%), and decrease in cells with low superoxide levels (58.1%).
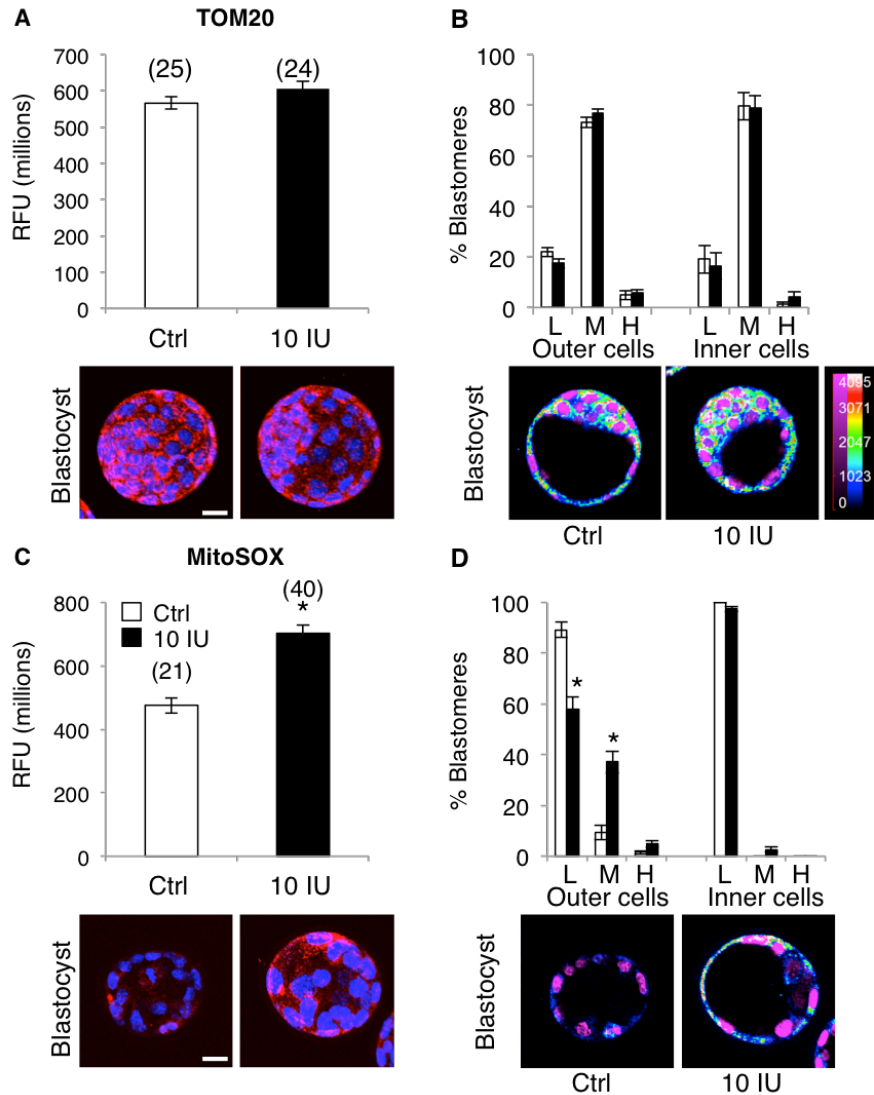
Figure 3-11: TOM20 and superoxide in control and 10 IU blastocysts

(A) TOM20 protein levels in control (Ctrl) and 10 IU blastocysts. Data were analyzed as relative fluorescence units (RFUs) ± SEM. DAPI, blue; TOM20 protein, red. (B) Percentage of outer and inner blastomeres with low (L), medium (M) or high (H) amounts of TOM20 immunofluorescence. (C) MitoSOX staining of superoxide levels in control (Ctrl) and 10 IU blastocysts. Data were analyzed as RFUs ± SEM. (D) Percentage of outer and inner blastomeres with low (L), medium (M) or high (H) superoxide levels. Representative Z-stacks (A, C) and slices (B, D) are shown. Number in parentheses indicate the total number of embryos analyzed. DAPI DNA staining, blue; MitoSOX staining, red; pseudocolour L, primarily blue, pseudocolour M, mostly green/yellow; pseudocolour H, primarily red/white. The pseudocolour scale bar is shown in panel B and the white bars measure 20 μm.

3.3.7   CHDH protein levels

Another function of mitochondria is to produce a proportion of the metabolites required for epigenetic control of nuclear gene expression. For example, methylation groups, provided by the methyl donor S-adenosylmethionine (SAM), in the blastocyst are derived through two 1-carbon metabolic pathways (Ikeda et al., 2012); the folate cycle and the betaine-homocysteine methyltransferase (BHMT) pathway (Zhang et al., 2015). The BHMT pathway requires the enzyme choline dehydrogenase (CHDH). Choline dehydrogenase localizes to the inner mitochondrial membrane where it catalyzes the 2-step conversion of choline to betaine. This specific pathway is active in mouse blastocysts (Anas et al., 2008; Lee et al., 2012). Furthermore, *Chdh* deletion in mouse (Johnson et al., 2010) and a single nucleotide polymorphism in the human *CHDH* that decreases CHDH protein levels (Johnson et al., 2012) perturbs mitochondrial function in sperm and results in decreased sperm motility, indicating a role for CHDH in mitochondrial function. Thus, CHDH dysregulation has the potential to disrupt both mitochondrial function and DNA methylation. Since CHDH is a maternal effect protein, levels were analyzed in fertilized 1-cell embryos by CHDH protein immunofluorescence. There was a significant decrease in CHDH protein immunofluorescence, as measured by total RFUs, in 1-cell embryos derived from 10 IU hormone-treated females compared to controls (Figure 3-12A). I next assessed the levels of CHDH and global H3K9me2, a repressive histone methylation mark, in control and 10 IU blastocysts. In contrast to 1-cell embryos generated after ovarian stimulation, there was no longer a significant difference in CHDH protein levels (Figure 3-12B). Furthermore, global levels of the repressive histone 3 lysine 9 dimethylation (H3K9me2) mark (Figure 3-12C) were unchanged between control and 10 IU blastocysts. Additionally, there was no difference in the distribution of CHDH between inner (control 28.0% high, 62.4% medium; 10 IU 26.0% high, 65.2% medium) and outer (control 71.8% high, 20.9%; 10 IU 71.2% high, 24.2% medium) blastomeres of these embryos, where the majority displayed high or medium levels of CHDH immunofluorescence (Figure 3-12D). Having said this, a greater number of blastocysts, and more stages of preimplantation development, need to assessed for CHDH and H3K9me2 levels in control and hormone treated groups before this analysis is completed.
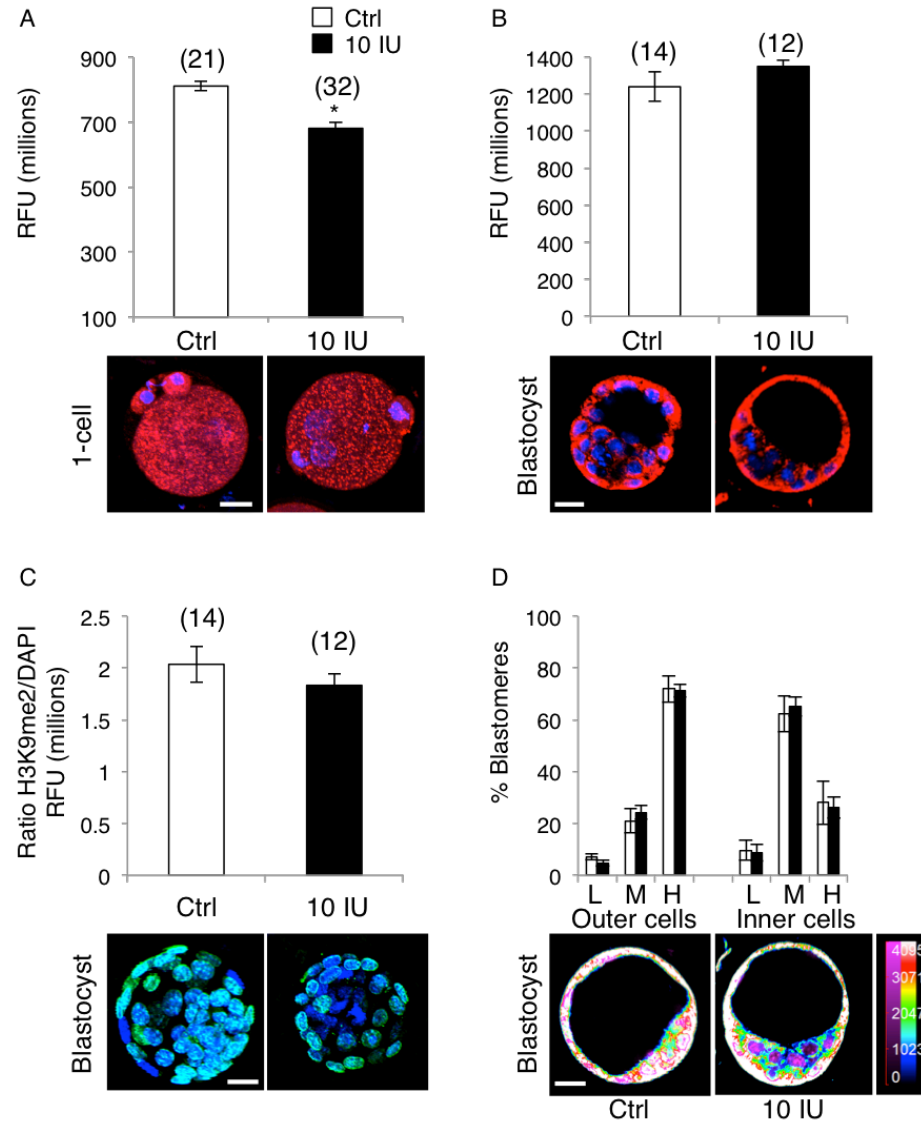
Figure 3-12: CHDH protein in 1-cells and blastocysts in the control and 10 IU groups

(A) CHDH protein levels in 1-cell embryos in the control (Ctrl) and 10 IU groups. (B) CHDH protein levels in blastocysts in Ctrl and 10 IU groups. Data were analyzed as relative fluorescence units (RFUs) ± SEM. DAPI, blue; CHDH protein, red. (C) Global H3K9me2 levels normalized to DAPI RFUs (quantified as total H3K9me2 RFU divided by total DAPI RFU) in blastocysts in the Ctrl and 10 IU groups. DAPI, blue; H3K9me2, green. (D) Percentage of outer and inner blastomeres with low (L), medium (M) or high (H) amounts of CHDH immunofluorescence. Representative Z-stacks (A, C) and slices (B, D) are shown. Number in parentheses indicates the number of embryos analyzed. The pseudocolour scale bar is shown in panel D and white bars measure 20 μm.

3.4 Discussion

My study is the first to report a detailed analysis of total and active mitochondrial pools, location, and distribution in control and hormone-treated oocytes and embryos throughout preimplantation development, specifically from the MII oocyte to the blastocyst stage (Figure 3-13). I showed that high-hormone treatment led to a decrease in the total and active mitochondria pool in oocytes and abnormal accumulation of active mitochondria away from the perinuclear region. Subsequently, the total mitochondrial pool was no longer affected by hormone administration in 1-cell, 2-cell, morula and blastocysts, although the active mitochondria pool was significantly decreased in a dose-dependent manner in 1-cell and 2-cell embryos. This decrease was no longer present in 4-cell and 8-cell embryos in the 10 IU group. With respect to mitochondrial distribution, 1-cell and 2-cell embryos from both control and stimulated females displayed homogenous and perinuclear distribution patterns of total mitochondria, respectively. Furthermore, all embryos, regardless of exogenous hormone administration, displayed perinuclear accumulation of active mitochondria at 1-cell and 2-cell stages and cortical distribution of active mitochondria at 4-cell and 8-cell stages. Finally, late preimplantation embryos exhibit an asymmetrical distribution of both total and active mitochondria. In comparison to control embryos, morula and blastocysts in the hormone-treated group exhibited an increase in the proportion of outer cells with low amounts of both total and active mitochondria. In addition, high total mitochondria in blastocysts and high active mitochondria in morula and blastocysts were significantly decreased in outer cells of embryos in the hormone-treated group. This was accompanied by decreased active mitochondria in morula and blastocysts in the 10 IU hormone group, and increased superoxide in outer cells of 10 IU embryos. Overall, these results indicate that 10 IU hormone stimulation ultimately leads to blastocysts exhibiting abnormal mitochondrial dynamics in outer/TE cells.

156

Analysis	MII oocyte	1-cell	2-cell	4-cell	8-cell	Morula	Blastocyst
Total Mito	↓	=	=	NA	NA	=	=
Active Mito	↓	↓	↓	=	=	↓	↓
Total distribution	P	H	P	NA	NA	↓ Outer	↓ Outer
Active distribution	↓ P ↑ H, Cl	P	P	Co	Co	↓ Outer	↓ Outer
Superoxide	NA	NA	NA	NA	NA	NA	↑ Outer
TOM20	NA	NA	NA	NA	NA	NA	=
CHDH	↓	NA	NA	NA	NA	NA	=

Figure 3-13: Summary of hormone-induced disruption of mitochondrial dynamics

The effects of hormone administration (10 IU) on the total mitochondrial pool (Total Mito, Mitotracker green), the active mitochondrial pool (Active Mito, Mitotracker red), distribution of total mitochondria (Total distribution, Mitotracker green), distribution of active mitochondria (Active distribution, Mitotracker red), superoxide levels (MitoSOX staining), TOM20 immunofluorescence (TOM20) and CHDH levels (CHDH) are summarized. Upwards arrow, increased in 10 IU hormone embryos; downwards arrow, decreased in 10 IU hormone-stimulated embryos; equal sign, no change between hormone and control groups; NA, not analyzed; P, perinuclear; H, homogenous; Cl, clustered; Co, cortical; Outer, outer cells of morula- and blastocyst-stage embryos

It is well documented that oocytes with decreased mitochondria and/or mitochondrial DNA molecules (Murakoshi et al., 2013; Pikó and Taylor, 1987; Reynier et al., 2001; Santos et al., 2006) or a decreased ability to produce ATP (i.e. mitochondrial activity) (Assou et al., 2006; Ge et al., 2012; May-Panloup et al., 2005; Selesniemi et al., 2011; St John et al., 2010; Thouas et al., 2004; Yu et al., 2010) have reduced developmental competence. Furthermore, domains of concentrated respiratory activity in oocytes, as previously observed in differentiated cells (Collins et al., 2002; Diaz et al., 1999), permit local ATP supply and demand for spatially localized processes during oogenesis (Van Blerkom et al., 2002; Yu et al., 2010). Consistent with this, perinuclear accumulation of active mitochondria in mouse, human and porcine is essential for the high-energy consuming processes that occur during oogenesis, namely nuclear and meiotic maturation and polar body extrusion (Nagai et al., 2006; Sun et al., 2001; Tokura et al., 1993; Van Blerkom, 1991; Van Blerkom and Runner, 1984; Van Blerkom et al., 2000; Yu et al., 2010). In this study, I observed a dose-dependent effect of ovarian stimulation on mitochondria in resulting oocytes. In comparison to spontaneously ovulated oocytes, oocytes ovulated after low hormone dose administration had a decrease in the active mitochondrial pool, although the total mitochondrial pool was unchanged. By comparison, high hormone-treated oocytes displayed a decrease in the total mitochondrial pool and as well as a decrease in the active mitochondrial pool. This indicates that a decrease in the total mitochondrial pool could lead to the diminished active mitochondrial pool in the 10 IU hormone group.

Active mitochondrial accumulation at the perinuclear region is required for oocyte maturation (Nagai et al., 2006; Sun et al., 2001; Tokura et al., 1993; Van Blerkom, 1991; Van Blerkom and Runner, 1984; Van Blerkom et al., 2000; Yu et al., 2010). Although total mitochondria in superovulated oocytes maintained a perinuclear organization, the active mitochondria were mislocalized. Superovulated oocytes exhibited increased homogenous and clustered distributions and decreased perinuclear organization in comparison to their spontaneously ovulated counterparts. Effects on the active mitochondria pool and distribution also occurred at the lower hormone dose.

Overall, my results in oocytes indicate that superovulation leads to increased production of oocytes with mitochondrial defects, namely a decreased total mitochondrial pool, active mitochondrial pool, and active mitochondrial localization. These specific defects

have previously been shown to impede successful completion of the second meiotic division of oogenesis and subsequent development. Future studies should confirm this data by analyzing the effect of superovulation on total mitochondrial DNA numbers, total mitochondrial numbers using transmission electron microscopy (TEM), and resulting ATP production. As mitochondria in the mouse and human oocyte are translocated by microtubule structures (Kan et al., 2011; Van Blerkom, 1991; Van Blerkom et al., 2000), it is possible that superovulation disrupts the microtubule network required for successful perinuclear translocation of active mitochondria. In fact, decreased mitochondrial generation of ATP has been shown to cause disassembly of meiotic spindles (Zhang et al., 2006). Furthermore, in mouse and human somatic cells, mitochondrial function and ROS levels/oxidative stress have been implicated in regulating microtubule dynamics (Shi et al., 2010; Wilson and González-Billault, 2015). Thus, it is possible that superovulation induced mitochondrial dysfunction leads to failure to establish microtubule-dependent perinuclear accumulation of mitochondria. Future research should investigate the effect of superovulation on cytoskeletal structures, particularly the microtubule network.

The ability of superovulated oocytes with insufficient numbers of mitochondria to complete meiosis and undergo successful fertilization is compromised in both human (Reynier et al., 2001; Santos et al., 2006) and pig (Shourbagy et al., 2006). By extension generation of ATP is important for oocyte maturation and fertilization (Dumollard et al., 2004; Yu et al., 2010; Zhang et al., 2006). However, completion of meiosis and subsequent fertilization can occur over a wide range of ATP contents, while it is continued embryogenesis and implantation that is compromised in embryos from oocytes with low ATP contents (Van Blerkom et al., 1995). Consistent with these studies, I have shown that superovulation leads to the disruption of the total mitochondrial pool in oocytes, although this was no longer evident in 1-cell and 2-cell embryos, which displayed a similar total mitochondrial pool compared to spontaneous counterparts. However, 1-cell and 2-cell preimplantation embryos continued to exhibit a decrease in the active mitochondrial pool compared to spontaneous counterparts, and this was dose-dependent. This decrease in the hormone-treated group was no longer evident in 4-cell and 8-cell embryos, suggesting that 2-cell embryos with decreased mitochondrial activity may undergo a 2-cell block in development; a phenomenon that was originally observed in cultured embryos and certain

strains of mice (Biggers, 1998). The 2-cell block depends on maternally inherited cytoplasmic factors (Biggers, 1998; Goddard and Pratt, 1983; Muggleton-Harris and Brown, 1988; Zanoni et al., 2009) and is associated with lower ATP and mitochondrial membrane potential (Komatsu et al., 2014; Wang et al., 2009). Two-cell embryos are particularly vulnerable as the mouse embryonic genome is activated at this stage and this process requires ATP (Bianchi and Sette, 2011; Bultman et al., 2006). Therefore, 2-cell embryos generated after ovarian stimulation with reduced mitochondrial activity may be energetically incapable of cleaving to the 4-cell stage. Future studies should be directed towards analyzing mitochondrial dynamics using time-lapse microscopy to determine whether oocytes with decreased total mitochondria do not undergo successful fertilization, and whether 2-cell embryos with decreased mitochondrial activity are unable to divide to the 4-cell stage.

Mouse and human 1-cell and 2-cell embryos display perinuclear accumulation of mitochondria (Tokura et al., 1993; Van Blerkom, 2000; Van Blerkom et al., 2000; Van Blerkom, 2009; Wilding et al., 2001; Zhao et al., 2009). Furthermore, developmentally competent embryos exhibit an even distribution of mitochondria between blastomeres while those that arrest and lyse have an uneven segregation of mitochondria. With regards to mitochondrial distribution in early cleavage embryos, regardless of ovarian stimulation, total mitochondria was homogenous in 1-cell embryos and perinuclear in 2-cell embryos, active mitochondria accumulated at the perinuclear region in 1-cell and 2-cell embryos, while 4-cell and 8-cell embryos exhibited cortical accumulation of active mitochondria. Thus, it is possible that superovulated oocytes that did not establish perinuclear translocation of active mitochondria at the MII stage were unable to complete meiosis and be fertilized to create perinuclear 1-cell embryos. In my study, the distribution of mitochondria around pronuclei and between blastomeres was mostly symmetrical in both control and hormone stimulated zygote to 8-cell embryos, indicating exogenous hormone administration does not lead to an increased frequency of asymmetrically distributed mitochondria. Overall, by 4-cell and 8-cell stages of preimplantation development, embryos generated spontaneously or by ovarian stimulation were indistinguishable with respect to active mitochondrial intensity and distribution.

Adequate amounts of mitochondrial activity throughout preimplantation are required for successful development through to the blastocyst stage (Wakefield et al., 2011; Wilding

et al., 2001). As embryos progress to the morula and blastocyst stages, blastomeres no longer exhibit comparable mitochondrial distributions, with total and active mitochondria preferentially localizing to the outer cells (Houghton, 2006; Van Blerkom et al., 2000). This is further supported by ATP production, oxygen consumption, and amino acid turnover that are significantly increased in blastocyst trophectoderm compared to inner cell mass cells (Houghton, 2006). Additionally, activity of the Na^+/K^+-ATPase, located on the basolateral surface of the trophectoderm cells accounts for 60% of the ATP used in human blastocysts (Houghton et al., 2003). Ultimately, the blastocysts requires ATP-dependent Na^+/K^+-ATPase to drive cavitation and blastocyst formation (Madan et al., 2007). In my study, I also observed a similar unequal mitochondrial distribution in morula and blastocysts in both the control and 10 IU hormone groups. Here, superovulation led to significant alteration in the allocation of mitochondria in the outer blastomeres, with an increased percentage of blastomeres displaying low amounts of total and active mitochondria, and a decreased percentage of cells with high amounts of active mitochondria. This decrease did not coincide with decreased number of cells in blastocysts obtained after hormone treatment, nor did it result in decreased embryo cavity volume, which would be suggestive of defective blastocyst cavitation. Instead, while blastocysts produced after hormone treatment had increased cell numbers, they had similar embryo cavity volumes compared to controls. The increased cell number could be due to a compensatory mechanism accounting for a lower mitochondrial activity in 10 IU hormone-stimulated embryos. Future studies are required to investigate the effect of low mitochondria in outer blastomeres of hormone-treated embryos on downstream measurements such as successful blastocyst hatching, implantation and resulting pregnancy.

Hyperstimulation has previously been shown to result in increased superoxide production in the mouse oocyte (Chao et al., 2005), and increased superoxide increases mitochondrial DNA mutations, which can ultimately affect oxidative phosphorylation and ATP generation (Jacobs et al., 2007; Keefe et al., 1995; Shamsi et al., 2013; Venkatesh et al., 2010). In this study, superovulation led to a significant increase in superoxide accumulation in blastocyst embryos, specifically in the outer blastomeres. Increased mitochondrial superoxide accumulation could result in decreased mitochondrial activity in outer embryonic cells. However, future studies will be required to determine the downstream consequences of this superoxide accumulation. Having said this, superovulation did not seem to impact

nuclear control over mitochondrial function, as measured by both intensity and localization of the mitochondrial import protein TOM20, which was unchanged between control and hormone groups.

In addition to providing the oocyte and preimplantation embryo with the energy required for development, mitochondria also provide the cell with metabolites needed for epigenetic control of gene expression (Martinez-Pastor et al., 2013; Wallace and Fan, 2010). For example, methyl groups for the preimplantation embryo (generated from SAM) are produced in part via the betaine pathway, where choline is catalyzed to betaine in a 2-step process that involves CHDH (Anas et al., 2008; Ikeda et al., 2012; Lee et al., 2012). This reaction occurs in the mitochondria. Therefore, I analyzed the effect of ovarian stimulation on CHDH protein levels. My results indicate that the maternal supply of CHDH protein in fertilized 1-cell embryos is significantly decreased after exogenous hormone treatment compared to controls. Consequently, this could affect the methyl pool available during preimplantation development. By the blastocyst stage, this decrease no longer appeared to be present in the hormone-stimulated group, which showed similar levels of CHDH and the repressive histone methylation mark, H3K9me2, in comparison to controls. Overall, future studies are required to determine the effect of ovarian stimulation on CHDH protein levels throughout preimplantation development, in addition to determining the consequences of decreased CHDH methylation present in 1-cell embryos and subsequent cleavage stage embryos with respect to both DNA and histone methylation.

Current practices to increase success in the ART clinic have begun to target the mitochondria. These include the controversial techniques of mitochondrial replacement therapy and AUGMENT. My study confirms the importance of mitochondria in preimplantation development. Additionally, it points to the greater need to understand the effects that all ARTs treatment modalities have on the mitochondria, as well as the basic science behind new technologies targeting mitochondria in animal models and clinical trials.

3.5   References

Anas, M.-K.I., Lee, M.B., Zhou, C., Hammer, M.-A., Slow, S., Karmouch, J., Liu, X.J., Bröer, S., Lever, M., and Baltz, J.M. (2008). SIT1 is a betaine/proline transporter that is activated in mouse eggs after fertilization and functions until the 2-cell stage. Development *135*, 4123–4130.

Assou, S., Anahory, T., Pantesco, V., Le Carrour, T., Pellestor, F., Klein, B., Reyftmann, L., Dechaud, H., De Vos, J., and Hamamah, S. (2006). The human cumulus--oocyte complex gene-expression profile. Human Reproduction *21*, 1705–1719.

Baker, M.J., Frazier, A.E., Gulbis, J.M., and Ryan, M.T. (2007). Mitochondrial protein-import machinery: correlating structure with function. Trends Cell Biol. *17*, 456–464.

Bianchi, E., and Sette, C. (2011). Post-transcriptional control of gene expression in mouse early embryo development: a view from the tip of the iceberg. Genes (Basel) *2*, 345–359.

Biggers, J.D. (1998). Reflections on the culture of the preimplantation embryo. Int. J. Dev. Biol. *42*, 879–884.

Bultman, S.J., Gebuhr, T.C., Pan, H., Svoboda, P., Schultz, R.M., and Magnuson, T. (2006). Maternal BRG1 regulates zygotic genome activation in the mouse. Genes & Development *20*, 1744–1754.

Calarco, P.G. (1995). Polarization of mitochondria in the unfertilized mouse oocyte. Dev. Genet. *16*, 36–43.

Chao, H.-T., Lee, S.-Y., Lee, H.-M., Liao, T.-L., Wei, Y.-H., and Kao, S.-H. (2005). Repeated ovarian stimulations induce oxidative damage and mitochondrial DNA mutations in mouse ovaries. Annals of the New York Academy of Sciences *1042*, 148–156.

Chappel, S. (2013). The role of mitochondria from mature oocyte to viable blastocyst. Obstet Gynecol Int *2013*, 183024–183024.

Collins, T.J., Berridge, M.J., Lipp, P., and Bootman, M.D. (2002). Mitochondria are morphologically and functionally heterogeneous within cells. Embo J. *21*, 1616–1627.

Cummins, J.M. (2002). The role of maternal mitochondria during oogenesis, fertilization and embryogenesis. Reprod. Biomed. Online *4*, 176–182.

Demant, M., Trapphoff, T., Fröhlich, T., Arnold, G.J., and Eichenlaub-Ritter, U. (2012). Vitrification at the pre-antral stage transiently alters inner mitochondrial membrane potential but proteome of in vitro grown and matured mouse oocytes appears unaffected. Hum. Reprod. *27*, 1096–1111.

Diaz, G., Setzu, M.D., Zucca, A., Isola, R., Diana, A., Murru, R., Sogos, V., and Gremo, F. (1999). Subcellular heterogeneity of mitochondrial membrane potential: relationship with organelle distribution and intercellular contacts in normal, hypoxic and apoptotic cells. J. Cell. Sci. *112 (Pt 7)*, 1077–1084.

Dumollard, R., Marangos, P., FitzHarris, G., Swann, K., Duchen, M., and Carroll, J. (2004). Sperm-triggered [Ca2+] oscillations and Ca2+ homeostasis in the mouse egg have an absolute requirement for mitochondrial ATP production. Development *131*, 3057–3067.

Ebert, K.M., Liem, H., and Hecht, N.B. (1988). Mitochondrial DNA in the mouse preimplantation embryo. J. Reprod. Fertil. *82*, 145–149.

Ge, H., Tollner, T.L., Hu, Z., Da, M., Li, X., Guan, H., Shan, D., Lu, J., Huang, C., and Dong, Q. (2012). Impaired mitochondrial function in murine oocytes is associated with controlled ovarian hyperstimulation and in vitro maturation. Reprod. Fertil. Dev. *24*, 945–952.

Goddard, M.J., and Pratt, H.P. (1983). Control of events during early cleavage of the mouse embryo: an analysis of the '2-cell block'. J Embryol Exp Morphol *73*, 111–133.

Houghton, F.D. (2006). Energy metabolism of the inner cell mass and trophectoderm of the mouse blastocyst. Differentiation *74*, 11–18.

Houghton, F.D., Humpherson, P.G., Hawkhead, J.A., Hall, C.J., and Leese, H.J. (2003). Na+, K+, ATPase activity in the human and bovine preimplantation embryo. Dev. Biol. *263*, 360–366.

Ikeda, S., Koyama, H., Sugimoto, M., and Kume, S. (2012). Roles of one-carbon metabolism in preimplantation period--effects on short-term development and long-term programming--. J. Reprod. Dev. *58*, 38–43.

Jacobs, L., Gerards, M., Chinnery, P., Dumoulin, J., de Coo, I., Geraedts, J., and Smeets, H. (2007). mtDNA point mutations are present at various levels of heteroplasmy in human oocytes. Mol. Hum. Reprod. *13*, 149–154.

Jansen, R.P. (2000). Germline passage of mitochondria: quantitative considerations and possible embryological sequelae. Human Reproduction *15 Suppl 2*, 112–128.

Jansen, R.P., and de Boer, K. (1998). The bottleneck: mitochondrial imperatives in oogenesis and ovarian follicular fate. Molecular and Cellular Endocrinology *145*, 81–88.

Jansen, R.P.S., and Burton, G.J. (2004). Mitochondrial dysfunction in reproduction. Mitochondrion *4*, 577–600.

Jiang, Y., and Wang, X. (2012). Comparative mitochondrial proteomics: perspective in human diseases. J Hematol Oncol *5*, 11.

Johnson, A.R., Craciunescu, C.N., Guo, Z., Teng, Y.-W., Thresher, R.J., Blusztajn, J.K., and Zeisel, S.H. (2010). Deletion of murine choline dehydrogenase results in diminished sperm motility. Faseb J. *24*, 2752–2761.

Johnson, A.R., Lao, S., Wang, T., Galanko, J.A., and Zeisel, S.H. (2012). Choline dehydrogenase polymorphism rs12676 is a functional variation and is associated with changes in human sperm cell function. PLoS ONE *7*, e36047.

Jones, A., Van Blerkom, J., Davis, P., and Toledo, A.A. (2004). Cryopreservation of metaphase II human oocytes effects mitochondrial membrane potential: implications for developmental competence. Human Reproduction *19*, 1861–1866.

Kameyama, Y., Filion, F., Yoo, J.G., and Smith, L.C. (2007). Characterization of mitochondrial replication and transcription control during rat early development in vivo and

in vitro. Reproduction *133*, 423–432.

Kan, R., Yurttas, P., Kim, B., Jin, M., Wo, L., Lee, B., Gosden, R., and Coonrod, S.A. (2011). Regulation of mouse oocyte microtubule and organelle dynamics by PADI6 and the cytoplasmic lattices. Dev. Biol. *350*, 311–322.

Keefe, D.L., Niven-Fairchild, T., Powell, S., and Buradagunta, S. (1995). Mitochondrial deoxyribonucleic acid deletions in oocytes and reproductive aging in women. Fertil. Steril. *64*, 577–583.

Komatsu, K., Iwase, A., Mawatari, M., Wang, J., Yamashita, M., and Kikkawa, F. (2014). Mitochondrial membrane potential in 2-cell stage embryos correlates with the success of preimplantation development. Reproduction *147*, 627–638.

Larsson, N.G., Wang, J., Wilhelmsson, H., Oldfors, A., Rustin, P., Lewandoski, M., Barsh, G.S., and Clayton, D.A. (1998). Mitochondrial transcription factor A is necessary for mtDNA maintenance and embryogenesis in mice. Nat Genet *18*, 231–236.

Lee, M.B., Kooistra, M., Zhang, B., Slow, S., Fortier, A.L., Garrow, T.A., Lever, M., Trasler, J.M., and Baltz, J.M. (2012). Betaine homocysteine methyltransferase is active in the mouse blastocyst and promotes inner cell mass development. J. Biol. Chem. *287*, 33094–33103.

Lei, T., Guo, N., Tan, M.-H., and Li, Y.-F. (2014). Effect of mouse oocyte vitrification on mitochondrial membrane potential and distribution. J. Huazhong Univ. Sci. Technol. Med. Sci. *34*, 99–102.

Madan, P., Rose, K., and Watson, A.J. (2007). Na/K-ATPase beta1 subunit expression is required for blastocyst formation and normal assembly of trophectoderm tight junction-associated proteins. J. Biol. Chem. *282*, 12127–12134.

Manipalviratn, S., Tong, Z.-B., Stegmann, B., Widra, E., Carter, J., and DeCherney, A. (2011). Effect of vitrification and thawing on human oocyte ATP concentration. Fertil. Steril. *95*, 1839–1841.

Market-Velker, B.A., Denomme, M.M., and Mann, M.R.W. (2012). Loss of genomic imprinting in mouse embryos with fast rates of preimplantation development in culture. Biol. Reprod. *86*, 143–1–16.

Martinez-Pastor, B., Cosentino, C., and Mostoslavsky, R. (2013). A Tale of Metabolites: The Cross-Talk between Chromatin and Energy Metabolism. Cancer Discovery *3*, 497–501.

Martino, N.A., Dell'aquila, M.E., Cardone, R.A., Somoskoi, B., Lacalandra, G.M., and Cseh, S. (2013). Vitrification preserves chromatin integrity, bioenergy potential and oxidative parameters in mouse embryos. Reprod. Biol. Endocrinol. *11*, 27.

May-Panloup, P., Chretien, M.F., Jacques, C., Vasseur, C., Malthièry, Y., and Reynier, P. (2005). Low oocyte mitochondrial DNA content in ovarian insufficiency. Human Reproduction *20*, 593–597.

Meziane, el, A., Callen, J.C., and Mounolou, J.C. (1989). Mitochondrial gene expression during Xenopus laevis development: a molecular study. Embo J. *8*, 1649–1655.

Mootha, V.K., Bunkenborg, J., Olsen, J.V., Hjerrild, M., Wisniewski, J.R., Stahl, E., Bolouri, M.S., Ray, H.N., Sihag, S., Kamal, M., et al. (2003). Integrated analysis of protein composition, tissue diversity, and gene regulation in mouse mitochondria. Cell *115*, 629–640.

Motluk, A. (2015). IVF booster offered in Canada but not US. Cmaj *187*, E89–E90.

Muggleton-Harris, A.L., and Brown, J.J. (1988). Cytoplasmic factors influence mitochondrial reorganization and resumption of cleavage during culture of early mouse embryos. Human Reproduction *3*, 1020–1028.

Murakoshi, Y., Sueoka, K., Takahashi, K., Sato, S., Sakurai, T., Tajima, H., and Yoshimura, Y. (2013). Embryo developmental capability and pregnancy outcome are related to the mitochondrial DNA copy number and ooplasmic volume. J Assist Reprod Genet *30*, 1367–1375.

Nagai, S., Mabuchi, T., Hirata, S., Shoda, T., Kasai, T., Yokota, S., Shitara, H., Yonekawa, H., and Hoshi, K. (2006). Correlation of abnormal mitochondrial distribution in mouse oocytes with reduced developmental competence. Tohoku J. Exp. Med. *210*, 137–144.

Perry, A.J., Rimmer, K.A., Mertens, H.D.T., Waller, R.F., Mulhern, T.D., Lithgow, T., and Gooley, P.R. (2008). Structure, topology and function of the translocase of the outer membrane of mitochondria. Plant Physiol. Biochem. *46*, 265–274.

Pikó, L., and Chase, D.G. (1973). Role of the mitochondrial genome during early development in mice. Effects of ethidium bromide and chloramphenicol. J. Cell Biol. *58*, 357–378.

Pikó, L., and Matsumoto, L. (1976). Number of mitochondria and some properties of mitochondrial DNA in the mouse egg. Dev. Biol. *49*, 1–10.

Pikó, L., and Taylor, K.D. (1987). Amounts of mitochondrial DNA and abundance of some mitochondrial gene transcripts in early mouse embryos. Dev. Biol. *123*, 364–374.

Rathmell, J.C., and Newgard, C.B. (2009). Biochemistry. A glucose-to-gene link. Science *324*, 1021–1022.

Reinhardt, K., Dowling, D.K., and Morrow, E.H. (2013). Medicine. Mitochondrial replacement, evolution, and the clinic. Science *341*, 1345–1346.

Reynier, P., May-Panloup, P., Chretien, M.F., Morgan, C.J., Jean, M., Savagner, F., Barriere, P., and Malthièry, Y. (2001). Mitochondrial DNA content affects the fertilizability of human oocytes. Mol. Hum. Reprod. *7*, 425–429.

Robin, E.D., and Wong, R. (1988). Mitochondrial DNA molecules and virtual number of mitochondria per cell in mammalian cells. J. Cell. Physiol. *136*, 507–513.

Santos, T.A., Shourbagy, El, S., and St John, J.C. (2006). Mitochondrial content reflects oocyte variability and fertilization outcome. Fertil. Steril. *85*, 584–591.

Schatten, H., Sun, Q.-Y., and Prather, R. (2014). The impact of mitochondrial function/dysfunction on IVF and new treatment possibilities for infertility. Reprod. Biol. Endocrinol. *12*, 111.

Selesniemi, K., Lee, H.-J., Muhlhauser, A., and Tilly, J.L. (2011). Prevention of maternal aging-associated oocyte aneuploidy and meiotic spindle defects in mice by dietary and genetic strategies. Proceedings of the National Academy of Sciences *108*, 12319–12324.

Shamsi, M.B., Govindaraj, P., Chawla, L., Malhotra, N., Singh, N., Mittal, S., Talwar, P., Thangaraj, K., and Dada, R. (2013). Mitochondrial DNA variations in ova and blastocyst: implications in assisted reproduction. Mitochondrion *13*, 96–105.

Shi, P., Wei, Y., Zhang, J., Gal, J., and Zhu, H. (2010). Mitochondrial dysfunction is a converging point of multiple pathological pathways in amyotrophic lateral sclerosis. J. Alzheimers Dis. *20 Suppl 2*, S311–S324.

Shourbagy, El, S.H., Spikings, E.C., Freitas, M., and St John, J.C. (2006). Mitochondria directly influence fertilisation outcome in the pig. Reproduction *131*, 233–245.

St John, J.C., Facucho-Oliveira, J., Jiang, Y., Kelly, R., and Salah, R. (2010). Mitochondrial DNA transmission, replication and inheritance: a journey from the gamete through the embryo and into offspring and embryonic stem cells. Human Reproduction Update *16*, 488–509.

Sun, Q.Y., Wu, G.M., Lai, L., Park, K.W., Cabot, R., Cheong, H.T., Day, B.N., Prather, R.S., and Schatten, H. (2001). Translocation of active mitochondria during pig oocyte maturation, fertilization and early embryo development in vitro. Reproduction *122*, 155–163.

Thouas, G.A., Trounson, A.O., Wolvetang, E.J., and Jones, G.M. (2004). Mitochondrial dysfunction in mouse oocytes results in preimplantation embryo arrest in vitro. Biol. Reprod. *71*, 1936–1942.

Thundathil, J., Filion, F., and Smith, L.C. (2005). Molecular control of mitochondrial function in preimplantation mouse embryos. Mol. Reprod. Dev. *71*, 405–413.

Tilly, J.L., and Sinclair, D.A. (2013). Germline energetics, aging, and female infertility. Cell Metab *17*, 838–850.

Tokura, T., Noda, Y., Goto, Y., and Mori, T. (1993). Sequential observation of mitochondrial distribution in mouse oocytes and embryos. J Assist Reprod Genet *10*, 417–426.

Van Blerkom, J. (1991). Microtubule mediation of cytoplasmic and nuclear maturation during the early stages of resumed meiosis in cultured mouse oocytes. Proc. Natl. Acad. Sci. U.S.a. *88*, 5031–5035.

Van Blerkom, J. (2000). Intrafollicular influences on human oocyte developmental

competence: perifollicular vascularity, oocyte metabolism and mitochondrial function. Human Reproduction *15*, 173–188.

Van Blerkom, J., and Runner, M.N. (1984). Mitochondrial reorganization during resumption of arrested meiosis in the mouse oocyte. Am. J. Anat. *171*, 335–355.

Van Blerkom, J., Davis, P.W., and Lee, J. (1995). ATP content of human oocytes and developmental potential and outcome after in-vitro fertilization and embryo transfer. Human Reproduction *10*, 415–424.

Van Blerkom, J., Davis, P., and Alexander, S. (2000). Differential mitochondrial distribution in human pronuclear embryos leads to disproportionate inheritance between blastomeres: relationship to microtubular organization, ATP content and competence. Human Reproduction *15*, 2621–2633.

Van Blerkom, J. (2004). Mitochondria in human oogenesis and preimplantation embryogenesis: engines of metabolism, ionic regulation and developmental competence. Reproduction *128*, 269–280.

Van Blerkom, J. (2008). Mitochondria as regulatory forces in oocytes, preimplantation embryos and stem cells. Reprod. Biomed. Online *16*, 553–569.

Van Blerkom, J. (2009). Mitochondria in early mammalian development. Seminars in Cell & Developmental Biology *20*, 354–364.

Van Blerkom, J. (2011). Mitochondrial function in the human oocyte and embryo and their role in developmental competence. Mitochondrion *11*, 797–813.

Van Blerkom, J., and Davis, P. (2007). Mitochondrial signaling and fertilization. Mol. Hum. Reprod. *13*, 759–770.

Van Blerkom, J., Davis, P., Mathwig, V., and Alexander, S. (2002). Domains of high-polarized and low-polarized mitochondria may occur in mouse and human oocytes and early embryos. Human Reproduction *17*, 393–406.

Venkatesh, S., Kumar, M., Sharma, A., Kriplani, A., Ammini, A.C., Talwar, P., Agarwal, A., and Dada, R. (2010). Oxidative stress and ATPase6 mutation is associated with primary ovarian insufficiency. Arch. Gynecol. Obstet. *282*, 313–318.

Wakefield, S.L., Lane, M., and Mitchell, M. (2011). Impaired mitochondrial function in the preimplantation embryo perturbs fetal and placental development in the mouse. Biol. Reprod. *84*, 572–580.

Wallace, D.C. (2010). Bioenergetics and the epigenome: interface between the environment and genes in common diseases. Dev Disabil Res Rev *16*, 114–119.

Wallace, D.C., and Fan, W. (2010). Energetics, epigenetics, mitochondrial genetics. Mitochondrion *10*, 12–31.

Wang, Z., Sun, Z., Chen, Y., and He, F. (2009). A modified cryoloop vitrification protocol in the cryopreservation of mature mouse oocytes. Zygote *17*, 217–224.

Wellen, K.E., Hatzivassiliou, G., Sachdeva, U.M., Bui, T.V., Cross, J.R., and Thompson, C.B. (2009). ATP-citrate lyase links cellular metabolism to histone acetylation. Science *324*, 1076–1080.

Wilding, M., Dale, B., Marino, M., di Matteo, L., Alviggi, C., Pisaturo, M.L., Lombardi, L., and De Placido, G. (2001). Mitochondrial aggregation patterns and activity in human oocytes and preimplantation embryos. Human Reproduction *16*, 909–917.

Wilson, C., and González-Billault, C. (2015). Regulation of cytoskeletal dynamics by redox signaling and oxidative stress: implications for neuronal development and trafficking. Front Cell Neurosci *9*, 381.

Woods, D.C., and Tilly, J.L. (2015). Autologous Germline Mitochondrial Energy Transfer (AUGMENT) in Human Assisted Reproduction. Semin. Reprod. Med. *33*, 410–421.

Woodson, J.D., and Chory, J. (2008). Coordination of gene expression between organellar and nuclear genomes. Nat Rev Genet *9*, 383–395.

Yu, Y., Dumollard, R., Rossbach, A., Lai, F.A., and Swann, K. (2010). Redistribution of mitochondria leads to bursts of ATP production during spontaneous mouse oocyte maturation. J. Cell. Physiol. *224*, 672–680.

Zander-Fox, D., Cashman, K.S., and Lane, M. (2013). The presence of 1 mM glycine in vitrification solutions protects oocyte mitochondrial homeostasis and improves blastocyst development. J Assist Reprod Genet *30*, 107–116.

Zanoni, M., Garagna, S., Redi, C.A., and Zuccotti, M. (2009). The 2-cell block occurring during development of outbred mouse embryos is rescued by cytoplasmic factors present in inbred metaphase II oocytes. Int. J. Dev. Biol. *53*, 129–134.

Zhang, B., Denomme, M.M., White, C.R., Leung, K.-Y., Lee, M.B., Greene, N.D.E., Mann, M.R.W., Trasler, J.M., and Baltz, J.M. (2015). Both the folate cycle and betaine-homocysteine methyltransferase contribute methyl groups for DNA methylation in mouse blastocysts. Faseb J. *29*, 1069–1079.

Zhang, X., Wu, X.Q., Lu, S., Guo, Y.L., and Ma, X. (2006). Deficit of mitochondria-derived ATP during oxidative stress impairs mouse MII oocyte spindles. Cell Res. *16*, 841–850.

Zhao, X.-M., Fu, X.-W., Hou, Y.-P., Yan, C.-L., Suo, L., Wang, Y.-P., Zhu, H.-B., Dinnyés, A., and Zhu, S.-E. (2009). Effect of vitrification on mitochondrial distribution and membrane potential in mouse two pronuclear (2-PN) embryos. Mol. Reprod. Dev. *76*, 1056–1063.

Chapter 4

4 Discussion

4.1 General overview

Infertility has risen to 16% of Canadian couples, tripling since 1984 (5.4%) (Bushnik et al., 2012). Similar numbers exist in the United States, with infertility affecting more than 10% of adult women (6.1 million) and 9% (4.7 million) of adult males, representing 10 to 15% of couples (Chandra et al., 2013). Due to rising rates of infertility, many couples are seeking medically assisted reproductive technologies (ARTs). Thus, it is becoming increasingly important for researchers to investigate the effects of these techniques on the manipulated oocyte and preimplantation embryo.

The developmental competence and health of the preimplantation embryo is dependent on successful completion of coordinated molecular processes that occur during early gamete and embryo development. Two of these pathways include DNA methylation reprogramming (Macdonald and Mann, 2014) and mitochondrial dynamics (Van Blerkom, 2011). Here, I investigated (a) the effects of ARTs on imprinted DNA methylation in human preimplantation embryos, and (b) the effect of ovarian stimulation on mitochondrial dynamics in mouse oocytes and preimplantation embryos. Although these pathways are distinct, based on my data, I propose that ARTs predispose trophectoderm cells of preimplantation embryos to aberrant imprinted methylation and mitochondrial defects.

4.1.1 Human ART embryos display a high frequency of imprinted methylation errors

Genomic imprinting disorders occur at an increased prevalence in the population of children conceived by ARTs (Okun and Sierra, 2014). Thus, numerous animal models have investigated the impact of ARTs on imprint establishment in oocytes and maintenance in preimplantation embryos [reviewed in (Denomme and Mann, 2012)]. One benefit of using the mouse as a model is that it allows for controlled studies of the effects of individual ART procedures without issues of confounding infertility. Major findings from mouse studies indicate that imprinted methylation is disrupted by superovulation (Hajj et al., 2011; Market-Velker et al., 2010b), *in vitro* fertilization (IVF) (Fauque et al., 2010), *in vitro* embryo culture

(Li et al., 2005; Mann et al., 2004; Market-Velker et al., 2010a; 2012) and cryopreservation (Cheng et al., 2014). Abnormal imprinted methylation occurs in 10-90% of ART preimplantation embryos (Fauque et al., 2007; Hajj et al., 2011; Market-Velker et al., 2010b; 2012).

In contrast, due to the limited availability of and ethical issues associated with the use of human gametes and preimplantation embryos, very few studies have analyzed imprinted DNA methylation in the human, with the majority of studies utilizing human embryos not suitable for embryo transfer (Chen et al., 2010; Geuns et al., 2003; 2007; Ibala-Romdhane et al., 2011; Khoueiry et al., 2012; Shi et al., 2014). To uncover the discrepancy between imprinted DNA methylation errors in mouse preimplantation embryos and human ART children, I evaluated individual, good to high quality, day 3 and blastocyst stage human preimplantation embryos for imprinted methylation at *SNRPN, KCNQ1OT1* and *H19*. I specifically analyzed these regions because they are associated with the three imprinting disorders showing increased prevalence (1 in 5,000 children) in the ART population (Okun and Sierra, 2014). The experimental design I used allowed for analysis of more than one gene per embryo in addition to comparing short and extended embryo culture. The human embryos used were subjected to the combined effect of multiple ARTs, namely ovarian stimulation, IVF/ICSI, *in vitro* embryo culture, and cryopreservation. Importantly, these embryos were suitable for transfer but instead were donated for research after patients no longer needed embryos for their treatment. Overall, I observed a similar frequency of imprinted methylation errors in the donated human embryos to that observed in mouse (Fauque et al., 2007; Hajj et al., 2011; Market-Velker et al., 2010b; 2012) and other studies of poor quality human preimplantation embryos (Chen et al., 2010; Geuns et al., 2003; 2007; Ibala-Romdhane et al., 2011; Khoueiry et al., 2012; Shi et al., 2014). Imprinted methylation in similar good to high-quality human preimplantation embryos has only been analyzed in two previous studies with small embryo numbers (14 blastocysts (Khoueiry et al., 2012), 5 blastocysts (Ibala-Romdhane et al., 2011) compared to the 24 day 3 embryos and 29 blastocysts analyzed here). Therefore, my results are of clinical relevance as the embryos analyzed are representative of cleavage-stage and blastocyst-stage embryos that could be transferred to patients with the potential of future pregnancy. Overall, these results indicate

that good quality, transferrable human ART preimplantation embryos possess a frequency of imprinted methylation errors similar to that previously reported in the mouse.

Studies in the mouse permit controlled analysis of the effects of individual ARTs on resulting imprinted DNA methylation, without the confounding effects of inherent infertility. The results of these studies generally indicate that increasing the number of ART procedures exacerbates imprinting errors (de Waal et al., 2015; Fauque et al., 2007; Market-Velker et al., 2010a; Rivera et al., 2008). However, discrepancy in the field exists with regards to whether it is the infertility treatment or inherent infertility itself that results in abnormal imprinted methylation (Doornbos et al., 2007; Ludwig et al., 2005; Strawn et al., 2010). Notably, I identified two embryos possessing abnormal imprinted methylation that were generated using donor sperm due to male factor infertility. In these cases, inherent infertility is bypassed as embryos were generated with oocytes and sperm from a fertile man and woman. Although this is small subset of embryos, it provides support for ART-induced errors, presumably in the absence of inherent infertility.

Taken together, I have identified similar imprinted DNA methylation abnormalities at the *SNRPN, KCNQ1OT1* and *H19* ICRs in human embryos to that observed in the mouse. Importantly, extending analyses to both day 3 cleavage and blastocyst stage embryos allowed me to conclude that continued culture to the blastocyst stage does not seem to pose greater risks for imprinting perturbations, although analyses during subsequent development would be required to confirm this result.

4.1.2 Ovarian stimulation disrupts mitochondria in mouse oocytes and preimplantation embryos

The vital role mitochondria have in establishing developmental competence of the oocyte and preimplantation embryo, and consequently IVF success, has fueled the design of new techniques aimed at improving or reconstituting the mitochondrial pool in oocytes and embryos in IVF clinics worldwide (Meldrum et al., 2016; Reinhardt et al., 2013; Wolf et al., 2015; Woods and Tilly, 2015). These techniques are experimental, and very few studies have been performed to examine their safety. Additionally, the effects of standard ART protocols on mitochondria have not been fully discerned. Here, I specifically demonstrated

that the most commonly used, indispensable treatment modality, ovarian stimulation, led to mitochondrial disruption in oocytes and preimplantation embryos.

To extend my analysis of the effects of ARTs on the oocyte and preimplantation embryo, I analyzed the effects of ovarian stimulation on mitochondria in mouse oocytes and throughout preimplantation development. Ovarian stimulation is implemented to increase the number of follicles recruited for ovulation during assisted reproduction. The doses of exogenous hormones that accompany ovarian stimulation are administered during oogenesis, and coincide with the crucial time-points of drastic mitochondrial replication, biogenesis, respiration, and mitochondrial localization changes. Consequently, this ART procedure has the potential to disrupt mitochondria in the mature, ovulated MII oocyte. I specifically identified that ovarian stimulation with exogenous hormones leads to a decrease in both total and active mitochondrial pools, and an increase in the percentage of ovulated oocytes displaying abnormal active mitochondrial localization. These results are consistent with previous studies, which showed that ovarian stimulation disrupted mitochondrial DNA copy numbers and mitochondrial membrane potential in ovulated oocytes (Combelles and Albertini, 2003; Ge et al., 2012; Gibson et al., 2005).

Analysis of embryos obtained after exogenous hormone treatment at later stages of preimplantation development indicated that mitochondrial perturbations caused by ovarian stimulation preferentially occurred in the outer trophectoderm cells. In both morula and blastocyst-stage embryos, I reported a decrease in high amounts of active mitochondria in outer cells and a concomitant increase in the percentage of outer blastomeres inheriting low amounts of active mitochondria. I also saw increased superoxide in outer cells of hormone-stimulated embryos compared to controls. Increased oxidative damage could increase mitochondrial DNA damage, consequently affecting respiration and ATP generation (Jacobs et al., 2007; Keefe et al., 1995; Shamsi et al., 2013; Venkatesh et al., 2010). However, this remains to be determined.

Finally, I investigated the effects of hormone treatment on choline dehydrogenase (CHDH) levels. CHDH links mitochondria to epigenetic regulation as it catalyzes the conversion of choline into betaine aldehyde at the inner mitochondrial membrane. This substrate is required for production of s-adenosylmethionine (SAM), the cells methyl donor,

through the betaine pathway (Anas et al., 2008; Ikeda et al., 2012; Lee et al., 2012). I identified a significant decrease in CHDH levels in hormone stimulated 1-cell embryos compared to controls. However, this decrease no longer appeared to be present in hormone-stimulated blastocysts compared to controls. Furthermore, there appeared to be no difference in global levels of the repressive histone mark, histone 3 lysine 9 dimethylation (H3K9me2), in blastocysts in the 10 IU group compared to controls. Thus, my results suggest that ovarian stimulation may lead to the disruption of mitochondrial control of epigenetic regulation in cleavage stage embryos, but this requires further investigation.

Overall, I have shown that ovarian stimulation alone, as an existing and indispensable ART procedure, leads to the disruption of mitochondria in the outer/trophectoderm cells of resultant morula- and blastocyst-stage embryos. As respiration in the outer/trophectoderm cells is critical for blastocyst formation and hatching (Larsson et al., 1998; Madan et al., 2007; Watson et al., 2004), future studies are required to investigate the downstream effects of this disruption.

4.1.3   Contributions to the field of reproductive biology

Overall, my work presented in this thesis advances the field of reproductive biology with the following novel findings: (a) ARTs disrupt imprinted methylation at the *SNRPN*, *KCNQ1OT1* and *H19* imprinting control regions (ICRs) in day 3 and blastocyst-stage, good to high quality, human embryos; (b) this occurs at a similar frequency to that observed in the mouse; (c) extended culture from the day 3 to blastocyst stage did not pose a greater risk for imprinting errors compared to short culture; (d) mitochondria were also disrupted by ARTs, specifically ovarian stimulation, resulting in decreased active mitochondrial pools, and mitochondrial localization defects as well as increased superoxide levels in the outer/trophectoderm cells of morula- and blastocyst-stage embryos; and (e) ovarian stimulation also leads to decreased CHDH protein levels in 1-cell embryos produced after hormone treatment; however, this decrease no longer appeared to be present in blastocyst-stage embryos in the 10 IU group. This research is relevant to the human clinic and demonstrates the need to establish a mechanistic basis for the validation of optimal techniques and procedures that will ensure the generation of healthy, viable embryos for infertile couples.

4.2   ARTs and the trophectoderm

The results of my thesis suggest that the trophectoderm is a selective target of ART-induced defects.   Specifically, in the first aim of this thesis, I demonstrated that human embryos produced through the use of multiple ARTs in the human IVF clinic exhibit a high frequency of abnormal imprinted DNA methylation.   However, disparity still exists with regards to the frequency of imprinting errors in human preimplantation embryos (6-89% embryos) (Chen et al., 2010; Geuns et al., 2003; 2007; Ibala-Romdhane et al., 2011; Khoueiry et al., 2012; Shi et al., 2014; White et al., 2015) compared to the frequencies of imprinting errors reported in ART children (~1 in 5,000 children) (Okun and Sierra, 2014). In the second aim of my thesis, I demonstrated that ovarian stimulation alone disrupted mitochondrial dynamics in mouse oocytes and preimplantation embryos. This resulted in a decreased amount of active mitochondria and increased superoxide production in outer/trophectoderm cells of blastocysts obtained after hormone stimulation.   Thus, ARTs affected two important components of early embryogenesis: imprinted DNA methylation maintenance and mitochondrial function. Hence, I hypothesize that the connection between these results is that ARTs-induced disruptions selectively occur within the trophectoderm.

One explanation for the discrepancy between imprinting errors in human embryos compared to resulting children could be that blastomeres with aberrant imprinted methylation are preferentially relegated to the trophectoderm lineage. In support of this, many studies in mouse have reported a selective loss of imprinted methylation and/or imprinted expression in the placenta compared to the embryo in midgestation mouse embryos following superovulation (Fortier et al., 2008; 2014) or preimplantation development in culture (de Waal et al., 2014; Khosla et al., 2001; Mann et al., 2004; Rivera et al., 2008). A recent study in mouse found that ART procedures reduced fetal and placental growth at midgestation, reduced DNA methylation at *H19, Kcnq1ot1* and *Snrpn* ICRs in the placenta, suppressed placental expression of paternally expressed imprinted genes that enhance fetal growth, and upregulated placental expression of maternally expressed imprinted genes that repress fetal growth (Li et al., 2016).   In humans, placentas from a group of successful IVF/ICSI pregnancies displayed abnormal *H19/IGF2* expression compared to placentas from natural conceptions (Sakian et al., 2015; Turan et al., 2010). If imprinted methylation errors in human ART preimplantation embryos preferentially arise in the trophectoderm rather than

embryonic cells, this would explain the reduced frequency of imprinting disorders in the resulting child.

A greater frequency of imprinted methylation errors in trophectoderm and placenta could lead to failed implantation or aberrant placental and fetal growth. The essential role of imprinted genes in placental function and fetal growth has been established in the mouse [reviewed in (Tunster et al., 2013)]. A correlation between imprinted gene expression in the placenta and resulting fetal growth was recently demonstrated in human, where increased or decreased placental expression of specific imprinted genes was correlated with large or small for gestational age infants (Kappil et al., 2015). Thus, relegation of imprint abnormalities to the trophectoderm could account for the increased frequencies of IUGR, low birth weight, small for gestational age (Okun and Sierra, 2014) or large for gestational age (Hansen and Bower, 2014; Ishihara et al., 2014; Korosec et al., 2014; 2016; Li et al., 2014; Pinborg et al., 2014; Sazonova et al., 2012; Wennerholm et al., 2013) in ART children. Consistent with this, abnormal imprinted gene methylation or expression has been detected in IUGR (Gonzalez-Rodriguez et al., 2016; López-Abad et al., 2016; Madeleneau et al., 2015; McMinn et al., 2006) and low birth weight/ small for gestational age (Bouwland-Both et al., 2013; Kanber et al., 2009) placentas compared to controls. In my study, patients who donated their frozen embryos had received a fresh embryo transfer from the same cycle of which the donated frozen embryos were obtained. Resulting information was available regarding live birth rate and pregnancy outcomes. Consistent with growth restriction and overgrowth being associated with aberrant methylation or expression of imprinted genes, 45% of newborns from patients in my study were outside clinically normal birth weight, with 1 high (>4000g), 5 low (<2500g), 1 very low (<1500g) and 1 extremely low (<1000g). This may suggest that the high frequency of imprinted DNA methylation errors in remaining day 3 cleavage and blastocyst embryos could lead to a range of effects regarding placental development and growth. While risk of multiples increases the risk of low birth weight, it should be noted that one of the very low birth weight infants and one of the high birth weight infants were singletons, resulting in 2 out of 9 (22%) singletons under/above clinically normal birth weight. This increased risk of low birth weight (Helmerhorst et al., 2004; Jackson et al., 2004; Okun and Sierra, 2014; Reddy et al., 2007; Savage et al., 2011; Schieve et al., 2002; Sunderam et al., 2014; 2015; Wisborg et al., 2010) and large for gestational age

(Hansen and Bower, 2014; Ishihara et al., 2014; Korosec et al., 2014; 2016; Li et al., 2014; Pinborg et al., 2014; Sazonova et al., 2012; Wennerholm et al., 2013) in singletons of ART pregnancies has been previously reported.

In addition to imprinted genes playing a role in placental function, mitochondrial studies also indicate a specific role for mitochondria in the trophectoderm. Trophectoderm cells of blastocysts exhibit increased mitochondrial content, ATP production, oxygen consumption, and amino acid turnover compared to cells in the inner cell mass (Assou et al., 2006; Houghton, 2006; Houghton et al., 2003; Thundathil et al., 2005). Increased mitochondrial activity in the trophectoderm lineage is required to activate the Na^+/K^+ ATPase, which accounts for 60% of the ATP used in human blastocysts (Houghton et al., 2003) and is required for cavity formation (Madan et al., 2007). I also observed in untreated, control embryos preferential total and active mitochondrial localization to trophectoderm cells in morula and blastocysts, indicating that this is a consistent process that normally occurs during preimplantation development. Ovarian stimulation led to a disruption in the mitochondria content of outer/trophectoderm cells, specifically resulting in decreased active mitochondrial pools and increased superoxide levels in outer/trophectoderm cells of morula and blastocysts. This indicates that the disruption was initiated when blastomeres adopted inner and outer cell identity, as outer morula cells will be specified to the trophectoderm lineage (Artus and Chazaud, 2014).

Consistent with these observations, ART-induced mitochondrial defects have been demonstrated preferentially in the placental cell lineage (Thouas et al., 2006; Wakefield et al., 2011). Specifically, embryos cultured in media containing low concentrations of a mitochondrial inhibitor had reduced placental but not fetal growth (Wakefield et al., 2011), while mitochondrial dysfunction in mouse oocytes lead to a decrease in trophectoderm cell number (Thouas et al., 2006). Although the consequences of perturbed mitochondrial function in trophectoderm cells is unknown, like imprinted DNA methylation errors, mitochondrial disruption in the placenta has been implicated in growth restriction of the developing fetus. Data from human IUGR placentas demonstrate a significant decrease in the expression of genes involved in mitochondrial function and oxidative phosphorylation, specifically affecting 3 out of 5 complexes of the respiratory chain (Madeleneau et al., 2015). Lower mitochondrial DNA content and higher placental superoxide dismutase activity, likely

to counteract oxidative damage, has also been observed in small for gestational age pregnancies (Díaz et al., 2014). Finally in the mouse, mutation of a subunit of complex II of the respiratory chain induced ROS production and resulted in excessive apoptosis leading to low birth weight and growth retardation (Ishii et al., 2011). Overall, ART induced disruption of imprinted DNA methylation and mitochondria could be preferentially occurring in the outer/trophectoderm cells of the blastocyst embryo, and I propose this would lead to failed implantation or aberrant placental function and consequently, abnormal fetal growth.

4.2.1 Potential link between ART-induced disruption of mitochondria and imprinted DNA methylation

The role of mitochondria in epigenetic regulation is a recently emerging area of interest. The relationship between mitochondria and chromatin arises through the metabolic products of energy consumption, as numerous intermediate epigenetic metabolites are produced by mitochondrial utilization of carbon sources to generate ATP (Castegna et al., 2015; Martinez-Pastor et al., 2013; Wallace, 2010; Wallace and Fan, 2010) (Figure 4-1). First, histone acetylation and corresponding active chromatin depends on the availability of the acetyl-coA substrate. In mammals, the majority of acetyl-coA is derived from the precursor citrate, which is produced solely by the mitochondria as a byproduct of the tricarboxylic acid (TCA) cycle and converted into acetyl-coA by the nuclear-encoded enzyme ATP-citrate lyase (ACL) (Martinez-Pastor et al., 2013; Wellen et al., 2009) (Figure 4-1A). The ACL-catalyzed generation of acetyl-coA from citrate is required for histone acetylation (Wellen et al., 2009). In contrast to histone acetylation, histone deacetylation and corresponding repressive chromatin exhibits a metabolic influence through histone deacetylase (HDAC) activity and nicotinamide adenine dinucleotide (NAD^+), another product of mitochondrial metabolism (Carafa et al., 2016; Martinez-Pastor et al., 2013) (Figure 4-1B). DNA and histone methylation are also regulated by mitochondrial-produced metabolites (Martinez-Pastor et al., 2013). During preimplantation development, two 1-carbon metabolic pathways, the betaine pathway (Figure 1-4C) and the folate cycle (Figure 4-1D), are required to produce methionine and ultimately S-adenosylmethionine (SAM) (Ikeda et al., 2012). S-adenosylmethionine (SAM), the universal methyl donor for histone and DNA methylation, is produced from methionine by S-adenosylmethionine transferase (MAT) (Lu, 2000). This reaction requires ATP, the product of mitochondrial respiration (Lu,

2000; Martinez-Pastor et al., 2013; Teperino et al., 2010) (Figure 4-1E). The reverse reaction, or removal of methyl groups from histone proteins, is catalyzed by histone demethylases (HDMs), which require two metabolites [flavin adenine dinucleotide (FAD$^+$) (Anand and Marmorstein, 2007) and α-ketoglutarate (Tsukada et al., 2006)], that are produced during the TCA cycle (Martinez-Pastor et al., 2013; Teperino et al., 2010) (Figure 4-1F). Finally, the end product of cellular respiration, ATP, is required as a substrate for histone phosphorylation in addition to powering ATP-dependent chromatin remodeling complexes (Runge et al., 2016). Thus, it is likely that fluctuations in mitochondrial respiration impact epigenetic dynamics. As the oocyte provides the preimplantation embryo with its only source of mitochondria during preimplantation development, and mitochondria provide the preimplantation embryo with its source of epigenetic metabolites, it is possible epigenetic control of imprint maintenance during preimplantation development is dependent on mitochondrial respiration. Overall, I would anticipate that decreased mitochondrial respiration, and consequently decreased ATP, would force blastomeres to allocate their metabolites to processes vital for immediate survival (i.e. DNA replication, transcription, cell division, and cavitation in blastocyst-stage embryos). This would have the net effect of reducing the metabolite pool required for proper epigenetic control of gene expression, for example, imprinted DNA methylation.
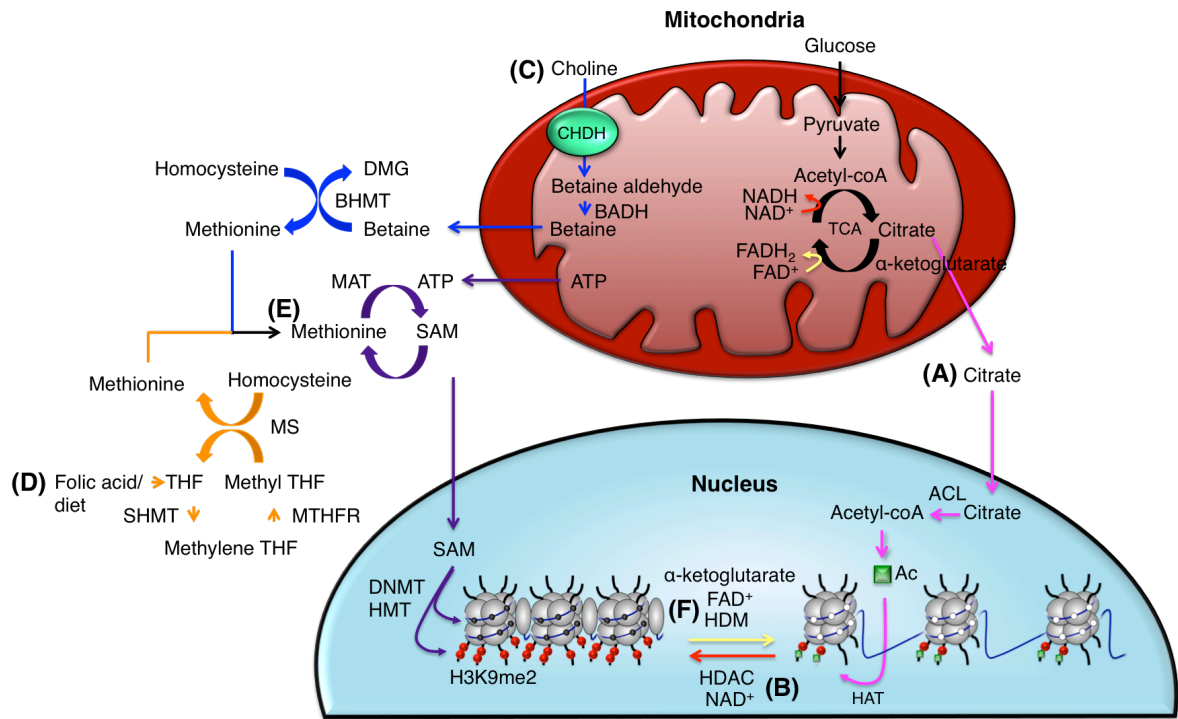
Figure 4-1: Mitochondria and epigenetics

The relationship between mitochondria and nuclear epigenetic regulation is mediated through intermediate metabolites produced during mitochondrial respiration. (A, pink arrows) Citrate, produced through the tricarboxylic acid cycle (TCA), is converted to acetyl-coA by ATP citrate lyase (ACL). Histone acetyltransferases (HATs) catalyze the addition of acetyl groups (green square) to histones for formation of active chromatin. (B, red arrow) Histone deacetylation requires histone deacetylases (HDACs) and nicotinamide adenine dinucleotide (NAD$^+$), a metabolite from the TCA cycle, to remove acetyl groups. In preimplantation embryos, two 1-carbon metabolism pathways are involved in generation of methionine and ultimately S-adenosylmethionine (SAM), the universal methyl donor. (C, blue arrows) In the first pathway, choline is converted into betaine aldehyde by the inner mitochondrial membrane enzyme choline dehydrogenase (CHDH, green circle). Betaine aldehyde is subsequently converted into betaine in the mitochondrial matrix by betaine aldehyde dehydrogenase (BADH). Betaine-homocysteine S-methyltransferase (BHMT) then converts betaine and homocysteine to dimethylglycine (DMG) and methionine, respectively. (D, orange arrows) In the folate pathway, folic acid is reduced to tetrahydrofolate (THF), which is converted to methylene tetrahydrofolate (methylene THF) by serine hydroxymethyltransferase (SHMT). Methylene tetrahydrofolate reductase (MTHFR) catalyzes methylene THF conversion to methyl THF, and methionine synthase converts methyl THF and homocysteine to THF and methionine, respectively. (E, purple arrows) Finally, methionine from both pathways is converted into S-adenosylmethionine (SAM) by S-adenosylmethionine transferase (MAT) and ATP. SAM is the methyl donor for DNA methylation (white circle; unmethylated CpGs; black circles, methylated CpGs) and histone (i.e. H3K9me2) methylation (red square). (F, yellow arrow) Demethylation by histone demethylases (HDMs) involves substrates flavin adenine dinucleotide (FAD$^+$, utilized in the TCA cycle) and α-ketoglutarate, an intermediate in the TCA cycle.

A few studies have directly analyzed the effect of mitochondrial disruption on epigenetic control of nuclear gene expression. Depletion of mitochondrial DNA resulted in significant DNA methylation changes at a number of genes (Smiraglia et al., 2008), in addition to decreasing the presence of multiple acetylation marks of histone H3, H2B and H4 (Martínez-Reyes et al., 2016). A further relationship between mitochondria and epigenetics was demonstrated in *Dnmt1o*-deficient placentas (Himes et al., 2015). These placentas were characterized by swollen mitochondria with abnormal cristae, and exhibited metabolomic profiles indicative of mitochondrial dysfunction (Himes et al., 2015). I hypothesized that ovarian stimulation-induced disruption of mitochondria consequently leads to aberrant epigenetic regulation. Specifically, I demonstrated that CHDH, a mitochondrial membrane protein involved in production of SAM during preimplantation development (Ikeda et al., 2012; Zhang et al., 2015), was significantly decreased in the 1-cell 10 IU hormone stimulated group. By the blastocyst stage, there was no apparent difference in CHDH levels or the repressive histone 3 lysine 9 dimethylation (H3K9me2) mark in 10 IU blastocysts compared to controls. Future studies are needed to investigate downstream effects of CHDH disruption in 1-cell and subsequent cleavage stage embryos, in addition to determining the effects of ARTs on other mitochondrial metabolites involved in epigenetic regulation.

4.3   Translating results to the human ART clinic

The results that I obtained in this thesis are relevant to the human ART clinic. Of particular relevance are the findings I obtained regarding imprinted methylation after extended culture to the blastocyst stage. Specifically, I was the first to analyze imprinted methylation at two different stages of preimplantation development: the day 3 cleavage and the blastocyst stage. Recently, there has been movement towards elective single embryo transfer (eSET) in ART to decrease the rate of multiple births (Maheshwari et al., 2011; Styer et al., 2016). Furthermore, the advent of one free cycle of ART funding specifically in Ontario requires that a single embryo be transferred in patients ≤35 years of age (Motluk, 2016). Consequently, many fertility clinics will culture embryos from good prognosis patients to the blastocyst stage to help identify the best embryo for transfer based on rate of development and morphological grading (Blake et al., 2007; Gardner et al., 2000; Gleicher et al., 2015; Glujovsky et al., 2012; Ubaldi et al., 2015). The data I obtained in this study support additional culture to the blastocyst stage. Specifically, the presence of methylation

errors in both day 3 (76%) and blastocyst (50%) stage embryos indicated that methylation errors already exist in ~6 to 8-cell cleavage embryos, and extending culture to the blastocyst stage of development does not appear to pose an increased risk for imprinted methylation errors.

Human fertility clinics implement supraphysiological exogenous hormone doses in addition to using multiple ART procedures to generate preimplantation embryos for transfer to mothers. The overall live birth rate after ART is 25% per egg retrieval and 29% per embryo transfer in Canada (Human Assisted Reproduction 2014) and 39.4% per embryo transfer in the United States (Sunderam et al., 2015)]. Furthermore, the incidence of low birth weight (29.1% ART, 8% non-ART) and preterm birth (33.6% ART, 11.4% non-ART) is higher in the ART population than among all infants in the total birth population of the United States (Sunderam et al., 2015). As the embryos analyzed in this study were transferrable but frozen for future cycles, the results here are applicable to the human clinic. The high frequency of imprinted DNA methylation abnormalities that I reported might provide one explanation for the birth rates between 25%-39% and increased incidences of fetal growth abnormalities in the ART population. Mild stimulation and minimizing the number of ARTs used in human IVF could be beneficial, as additional studies in the mouse have also demonstrated dose-dependent effects of hormone-stimulation on imprinted DNA methylation (Market-Velker et al., 2010b) as well as confounding effects of multiple ARTs on imprinted DNA methylation errors (de Waal et al., 2015; Fauque et al., 2007; Market-Velker et al., 2010a; Rivera et al., 2008). The same is true for mitochondrial dynamics throughout human IVF. My research along with others demonstrates that ARTs disrupt mitochondrial numbers, activity, membrane potential and distribution in the oocyte and preimplantation embryo (Acton et al., 2004; Amoushahi et al., 2013; Combelles and Albertini, 2003; Ge et al., 2012; Gibson et al., 2005; Lee et al., 2006; Lei et al., 2014; Manipalviratn et al., 2011; Wilding et al., 2001; Zander-Fox et al., 2013; Zhao et al., 2011a; 2011b; 2009). Minimizing the hormone dose and number of ART techniques may minimize effects to mitochondria during IVF. Furthermore, with the recent advent of novel procedures in human ART designed to alter mitochondrial sources by nuclear transfer into donor oocytes (Reinhardt et al., 2013; Wolf et al., 2015) or injecting mitochondria from ovarian cortex cells

into the oocyte during ICSI (Woods and Tilly, 2015), it is important to continue studies on mitochondria with regards to both pre-existing and novel ART methods.

4.4   Future directions

4.4.1   ARTs and imprinted DNA methylation in human preimplantation embryos

During preimplantation development in the mouse, recruitment of protein complexes to ICRs is required to ensure maintenance of DNA methylation when the remainder of the genome undergoes genome-wide DNA demethylation (Denomme and Mann, 2013). These maternal effect protector proteins include DPPA3 (Nakamura et al., 2007; 2012), DNMT1o and DNMT1s (Cirio et al., 2008a; 2008b; Hirasawa et al., 2008), and ZFP57 (Li et al., 2008; Quenneville et al., 2011; Zuo et al., 2012). As I reported similar disruptions to imprinted DNA methylation in the human preimplantation embryo to those reported in mouse, the next steps would be to determine the mechanism behind this disruption. Specifically, I would assess the maternal factors that regulate imprinted methylation maintenance in donated human preimplantation embryos. First, I would analyze whether *DPPA3*/DPPA3 mRNA and protein are present in donated human zygotes. As *DPPA3* transcript has been detected in human oocytes (Goto et al., 2002; Kobayashi et al., 2012; Yan et al., 2013), I expect that the role of this protein in protecting imprinted domains from active DNA demethylation from the 1-cell to 2-cell stage is conserved. Co-localization of DPPA3 and H3K9me2 (Nakamura et al., 2007; 2012) in human zygotes would be conducted by immunofluorescence to identify whether DPPA3 and H3K9me2 preferentially localize to the maternal pronucleus to protect imprinted domains from active DNA demethylation, and whether a subset of human embryos display mislocalization. Mislocalization of DPPA3 and H3K9me2 in human zygotes would suggest that the imprinted methylation errors I observed in day 3 human preimplantation embryos originates at the first cleavage division. Next, I would assess the *DNMT1o/s* mRNA and DNMT1o/s protein levels at all stages of preimplantation development in donated human embryos. The presence of these mRNAs and proteins has been confirmed in human oocytes and preimplantation embryos (Huntriss et al., 2004; Okae et al., 2014; Petrussa et al., 2014). Therefore, I would specifically analyze nuclear localization of DNMT1o/s in early cleavage-stage embryos and separately, in inner/outer cell nuclei of later-stage preimplantation embryos. Finally, I would analyze the *ZFP57* expression and ZFP57 protein levels in

donated human preimplantation embryos. Although *ZFP57* mRNA was not present in human oocytes (Okae et al., 2014), levels were detected in human morula (Yan et al., 2013). Additionally, the fact that mouse and human ZFP57 proteins are interchangeable in maintaining imprinted DNA methylation in mouse indicates conservation of this protein (Takikawa et al., 2013). In mouse, ZFP57 is required for imprint maintenance at the 8-cell stage of preimplantation development (Denomme and Mann, 2013; Li et al., 2008; Quenneville et al., 2011). Therefore I would concentrate analyses of ZFP57 to later stages of preimplantation development. Again, I would assess nuclear localization of ZFP57 beginning at the 8-cell stage and separately in inner and outer nuclei of morula and blastocysts. Overall, I would anticipate a disruption in DPPA3 and/or DNMT1o/s localization during early cleavage development to account for the aberrant imprinted DNA methylation I identified in day 3 embryos. Furthermore, I would also expect to see preferential loss of DNMT1o/s and/or ZFP57 in the outer nuclei of donated human morula and blastocysts.

4.4.2   ARTs and mitochondria

My second aim was to analyze the effect of an indispensable ART treatment, ovarian stimulation, on mitochondrial pools, localization, and function during preimplantation development. I identified that ovarian stimulation led to decreased active mitochondrial pools and increased superoxide levels in the outer cells of morula and blastocyst-stage embryos. Mitochondrial activity in control and hormone-stimulated embryos was assessed at all stages of preimplantation development. However, embryos were recovered at distinct stages and not followed throughout the course of cleavage development. Consequently, this analysis would benefit from time-lapse imaging of embryos and mitochondria throughout the course of preimplantation development, for multiple reasons. Using this technique, mitochondrial dynamics could be linked to specific embryo characteristics such as failed fertilization and embryonic cleavage. From my results, I hypothesized that hormone-stimulated oocytes with decreased total mitochondria pool cannot be fertilized to generate zygotes. This hypothesis could be tested using time-lapse imaging. Specifically, MitoTracker green-stained oocytes would be subjected to live-cell imaging, after which sperm would be injected using ICSI and successful fertilization of individual oocytes could be examined with time-lapse imaging. Next, I hypothesized that hormone-treated 2-cell embryos with decreased active

mitochondrial pool undergo a 2-cell block in development. Using time-lapse microscopy, I would test this hypothesis by assessing the ability of hormone-stimulated 2-cell embryos with decreased mitochondrial activity to cleave to the 4-cell stage. This finding would indicate that sufficient energy is required for 2-cell embryos to activate the embryonic genome and bypass a 2-cell block in development. The use of time-lapse during subsequent cleavage development will help to identify the segregation patterns of mitochondria in later-stage preimplantation embryos. Specifically as 8-cell and morula-stage embryos divide, orientation of the plane of cleavage will determine whether a blastomere will give rise to an inner (inner cell mass) and outer (trophectoderm) cell (asymmetric cleavage), or two outer (trophectoderm) cells (symmetric cleavage) (Artus and Chazaud, 2014). I would therefore use time-lapse imaging to analyze the segregation of mitochondria with respect to the orientation of division. In the hormone-treated groups, which exhibit a decrease in the percentage of outer blastomeres inheriting high mitochondria, I would expect to see an abnormal segregation of mitochondria during symmetric cleavage generating two outer cells. Specifically, I anticipate that distribution of mitochondria in this scenario will be reminiscent of asymmetric cleavage, where one cell inherits less mitochondria than the other.

Investigation of the downstream consequences of abnormal mitochondrial dynamics in trophectoderm cells of blastocysts should also be assessed. Specifically, I would assess whether blastocysts with abnormal mitochondria in trophectoderm cells are able to undergo blastocyst hatching and implantation. To analyze whether hormone-stimulated embryos with aberrant mitochondria in the trophectoderm exhibit decreased hatching rates, control and 10 IU blastocysts would be subjected to live-cell Mitotracker red imaging and subsequently cultured until hatching is complete or embryos degenerate. To analyze post-implantation development of blastocysts, control and hormone-stimulated embryos would be subjected to live-cell Mitotracker red imaging then transferred to pseudopregnant females. Specifically, recipient females would randomly receive embryos with abnormal mitochondria in one uterine horn and control embryos in the other. Implantation rates will be calculated as the number of implantation sites compared to the number of embryos transferred, and this will be compared for uterine horns containing embryos with abnormal mitochondria versus control embryos along with fetal and placental analysis.

Recent experimental infertility treatments have been aimed at replacing existing oocyte mitochondria in an attempt to bypass inheritance of mitochondrial disease or enhance IVF success (Chappel, 2013; Reinhardt et al., 2013; Wolf et al., 2015; Woods and Tilly, 2015). These techniques are already implemented in human IVF with little supporting research performed to assess their safety. The need for investigation of these techniques has been acknowledged by few research groups, and a recent study examining replacement of mitochondria through nuclear transfer between a donor and recipient oocyte found that mitochondrial heteroplasmy leads to reversion to the disease phenotype (Yamada et al., 2016). This further emphasizes the need to carefully analyze these treatments. Since I have shown that ovarian stimulation alone leads to mitochondrial disruption, it is essential that these new techniques be scrutinized. To study the effects of mitochondrial replacement therapy, AUGMENT and CoQ10 administration on mitochondrial dynamics, I would first use time-lapse imaging to assess the activity and distribution of mitochondria throughout preimplantation development after each treatment. This would be completed using a mouse model. Specifically, oocytes generated using each treatment will be fertilized and cultured to the blastocyst stage while being subjected to time-lapse Mitotracker red imaging. Treatment groups would be compared to spontaneously obtained zygotes cultured to the blastocyst stage and subjected to Mitotracker time-lapse imaging. Additionally with respect to AUGMENT, I would assess mitochondrial morphology in injected oocytes and throughout preimplantation development using transmission electron microscopy to assess whether mitochondria are structurally underdeveloped and elongate to mature forms first in trophectoderm cells of blastocysts (Motta et al., 2000; Pikó and Chase, 1973; Van Blerkom et al., 1973). If I find that this is not the case, it will mean that mitochondria injected during AUGMENT are not morphologically equivalent to mitochondria in a mature oocyte.

4.4.3   Establishing a connection between the effects ARTs on mitochondria and imprinted DNA methylation

Together, the results presented in my thesis suggest that ARTs might affect processes specifically in the trophectoderm. This is supported by the discrepancy between the high frequency of imprinted methylation errors in human preimplantation embryos and low penetrance of imprinting disorders in resultant ART children; mitochondrial abnormalities in the trophectoderm of hormone-stimulated blastocysts; and the seeming role of imprinted

gene regulation and mitochondria respiration in placental insufficiency. Overall, I propose that decreased mitochondrial activity in trophectoderm cells of blastocysts derived from hormone-treated females causes abnormal imprinted DNA methylation. I hypothesize that this would be due to decreased availability of metabolites/epigenetic molecules produced as products of mitochondrial respiration. In support of this, I identified decreased CHDH protein levels in 1-cell embryos in the hormone-stimulated group. This decrease no longer appeared to be present in blastocysts in the hormone-stimulated group and did not correspond with diminished global H3K9me2 levels in blastocysts. Therefore, to further test the effect of ovarian stimulation on mitochondrial control of epigenetic regulation, I would analyze CHDH protein levels throughout all stages of preimplantation development to determine whether embryonic genome activation at the 2-cell stage compensates for the decreased maternally-derived CHDH in 1-cell embryos. Additionally, rather than analyzing the effect of ovarian stimulation on global methylation levels as I did using H3K9me2 immunofluorescence analyses, I would analyze the effect of ovarian stimulation-induced mitochondrial disruption on gene-specific DNA methylation. Specifically, blastocysts in the control and 10 IU treated group would be subjected to live-cell Mitotracker red imaging and then trophectoderm and inner cell mass would be isolated separately to single trophectoderm/epiblast cells, which would be subjected to the bisulfite mutagenesis and sequencing assay. Imprinted methylation would be tested at the *Snrpn, Kcnq1ot1* and *H19* imprinted domains for both maternal and paternal alleles in hormone-stimulated embryos with normal mitochondria, hormone-stimulated embryos with abnormal mitochondria, and control untreated embryos. Abnormal imprinted methylation in trophectoderm but not epiblast samples would indicate that imprinted methylation errors predominantly occur in the trophectoderm lineage. Furthermore, if this occurs in the group of embryos with abnormal mitochondria, a correlation between decreased mitochondrial activity and imprinted methylation errors in the trophectoderm can be made.

If the above results indicate a linkage between mitochondria and imprinted DNA methylation in the trophectoderm, I would assess postimplantation development of normal and affected embryos. Embryos with normal and aberrant mitochondria will be transferred to separate uterine horns of recipient females. Downstream postimplantation development would be then be assessed separately for fetal and placental parameters as previously

described (Wakefield et al., 2011). Additionally, imprinted DNA methylation and expression would be assessed. Overall, I would anticipate that embryos obtained after hormone stimulation with decreased mitochondrial activity in trophectoderm cells display decreased fetal and placental weights and abnormal imprinted regulation compared to controls. This would mean that ART-induced effects occurring in the trophectoderm disrupt both mitochondria and imprinted DNA methylation, ultimately resulting in abnormal growth of the embryo through placental insufficiencies.

4.5 Conclusions

The use of assisted reproductive technologies has rapidly increased since the first human success story in 1978 (Steptoe and Edwards, 1978). The treatment modalities used by infertile couples to conceive their own biological child are continually growing in number. It is therefore imperative that research be conducted to assess any negative consequences of these techniques on the oocyte, preimplantation embryo, and resulting children. Work in this thesis has specifically provided insight on the effects of ARTs on two critical components of successful development: imprinted DNA methylation maintenance and mitochondrial dynamics. Specifically, I have shown that imprinted DNA methylation is disrupted in human preimplantation embryos, and ovarian stimulation alone leads to perturbations in mitochondrial dynamics in mouse oocytes and embryos. These two affected pathways may converge, and future studies are required to delineate whether these effects are (1) specific to the trophectoderm cell lineage, and (2) whether ART-induced mitochondrial dysfunction alters epigenetic signatures such as imprinted DNA methylation.

4.6 References

Acton, B.M., Jurisicova, A., Jurisica, I., and Casper, R.F. (2004). Alterations in mitochondrial membrane potential during preimplantation stages of mouse and human embryo development. Mol. Hum. Reprod. *10*, 23–32.

Amoushahi, M., Salehnia, M., and HosseinKhani, S. (2013). The effect of vitrification and in vitro culture on the adenosine triphosphate content and mitochondrial distribution of mouse pre-implantation embryos. Iran. Biomed. J. *17*, 123–128.

Anand, R., and Marmorstein, R. (2007). Structure and mechanism of lysine-specific demethylase enzymes. J. Biol. Chem. *282*, 35425–35429.

Anas, M.-K.I., Lee, M.B., Zhou, C., Hammer, M.-A., Slow, S., Karmouch, J., Liu, X.J.,

Bröer, S., Lever, M., and Baltz, J.M. (2008). SIT1 is a betaine/proline transporter that is activated in mouse eggs after fertilization and functions until the 2-cell stage. Development *135*, 4123–4130.

Artus, J., and Chazaud, C. (2014). A close look at the mammalian blastocyst: epiblast and primitive endoderm formation. Cell. Mol. Life Sci. *71*, 3327–3338.

Assou, S., Anahory, T., Pantesco, V., Le Carrour, T., Pellestor, F., Klein, B., Reyftmann, L., Dechaud, H., De Vos, J., and Hamamah, S. (2006). The human cumulus--oocyte complex gene-expression profile. Human Reproduction *21*, 1705–1719.

Blake, D.A., Farquhar, C.M., Johnson, N., and Proctor, M. (2007). Cleavage stage versus blastocyst stage embryo transfer in assisted conception. Cochrane Database Syst Rev CD002118.

Bouwland-Both, M.I., van Mil, N.H., Stolk, L., Eilers, P.H.C., Verbiest, M.M.P.J., Heijmans, B.T., Tiemeier, H., Hofman, A., Steegers, E.A.P., Jaddoe, V.W.V., et al. (2013). DNA methylation of IGF2DMR and H19 is associated with fetal and infant growth: the generation R study. PLoS ONE *8*, e81731.

Bushnik, T., Cook, J.L., Yuzpe, A.A., Tough, S., and Collins, J. (2012). Estimating the prevalence of infertility in Canada. Hum. Reprod. *27*, 738–746.

Carafa, V., Rotili, D., Forgione, M., Cuomo, F., Serretiello, E., Hailu, G.S., Jarho, E., Lahtela-Kakkonen, M., Mai, A., and Altucci, L. (2016). Sirtuin functions and modulation: from chemistry to the clinic. Clin Epigenet *8*, 61.

Castegna, A., Iacobazzi, V., and Infantino, V. (2015). The mitochondrial side of epigenetics. Physiol. Genomics *47*, 299–307.

Chandra, A., Copen, C.E., and Stephen, E.H. (2013). Infertility and impaired fecundity in the United States, 1982-2010: data from the National Survey of Family Growth. Natl Health Stat Report 1–18–1pfollowing19.

Chappel, S. (2013). The role of mitochondria from mature oocyte to viable blastocyst. Obstet Gynecol Int *2013*, 183024–183024.

Chen, S.-L., Shi, X.-Y., Zheng, H.-Y., Wu, F.-R., and Luo, C. (2010). Aberrant DNA methylation of imprinted H19 gene in human preimplantation embryos. Fertil. Steril. *94*, 2356–8–2358.e1.

Cheng, K.-R., Fu, X.-W., Zhang, R.-N., Jia, G.-X., Hou, Y.-P., and Zhu, S.-E. (2014). Effect of oocyte vitrification on deoxyribonucleic acid methylation of H19, Peg3, and Snrpn differentially methylated regions in mouse blastocysts. Fertil. Steril. *102*, 1183–1190.e1183.

Cirio, M.C., Martel, J., Mann, M., Toppings, M., Bartolomei, M., Trasler, J., and Chaillet, J.R. (2008a). DNA methyltransferase 1o functions during preimplantation development to preclude a profound level of epigenetic variation. Dev. Biol. *324*, 139–150.

Cirio, M.C., Ratnam, S., Ding, F., Reinhart, B., Navara, C., and Chaillet, J.R. (2008b). Preimplantation expression of the somatic form of Dnmt1 suggests a role in the inheritance of genomic imprints. BMC Dev. Biol. *8*, 9.

Combelles, C.M.H., and Albertini, D.F. (2003). Assessment of oocyte quality following repeated gonadotropin stimulation in the mouse. Biol. Reprod. *68*, 812–821.

de Waal, E., Mak, W., Calhoun, S., Stein, P., Ord, T., Krapp, C., Coutifaris, C., Schultz, R.M., and Bartolomei, M.S. (2014). In vitro culture increases the frequency of stochastic epigenetic errors at imprinted genes in placental tissues from mouse concepti produced through assisted reproductive technologies. Biol. Reprod. *90*, 22.

de Waal, E., Vrooman, L.A., Fischer, E., Ord, T., Mainigi, M.A., Coutifaris, C., Schultz, R.M., and Bartolomei, M.S. (2015). The cumulative effect of assisted reproduction procedures on placental development and epigenetic perturbations in a mouse model. Hum. Mol. Genet. *24*, 6975–6985.

Denomme, M.M., and Mann, M.R.W. (2012). Genomic imprints as a model for the analysis of epigenetic stability during assisted reproductive technologies. Reproduction *144*, 393–409.

Denomme, M.M., and Mann, M.R.W. (2013). Maternal control of genomic imprint maintenance. Reprod. Biomed. Online *27*, 629–636.

Díaz, M., Aragonés, G., Sánchez-Infantes, D., Bassols, J., Pérez-Cruz, M., de Zegher, F., Lopez-Bermejo, A., and Ibáñez, L. (2014). Mitochondrial DNA in placenta: associations with fetal growth and superoxide dismutase activity. Horm Res Paediatr *82*, 303–309.

Doornbos, M.E., Maas, S.M., McDonnell, J., Vermeiden, J.P.W., and Hennekam, R.C.M. (2007). Infertility, assisted reproduction technologies and imprinting disturbances: a Dutch study. Human Reproduction *22*, 2476–2480.

Fauque, P., Jouannet, P., Lesaffre, C., Ripoche, M.-A., Dandolo, L., Vaiman, D., and Jammes, H. (2007). Assisted Reproductive Technology affects developmental kinetics, H19 Imprinting Control Region methylation and H19 gene expression in individual mouse embryos. BMC Dev. Biol. *7*, 116.

Fauque, P., Mondon, F., Letourneur, F., Ripoche, M.-A., Journot, L., Barbaux, S., Dandolo, L., Patrat, C., Wolf, J.-P., Jouannet, P., et al. (2010). In vitro fertilization and embryo culture strongly impact the placental transcriptome in the mouse model. PLoS ONE *5*, e9218.

Fortier, A.L., Lopes, F.L., Darricarrère, N., Martel, J., and Trasler, J.M. (2008). Superovulation alters the expression of imprinted genes in the midgestation mouse placenta. Hum. Mol. Genet. *17*, 1653–1665.

Fortier, A.L., McGraw, S., Lopes, F.L., Niles, K.M., Landry, M., and Trasler, J.M. (2014). Modulation of imprinted gene expression following superovulation. Molecular and Cellular Endocrinology *388*, 51–57.

Gardner, D.K., Lane, M., Stevens, J., Schlenker, T., and Schoolcraft, W.B. (2000). Blastocyst

score affects implantation and pregnancy outcome: towards a single blastocyst transfer. Fertil. Steril. *73*, 1155–1158.

Ge, H., Tollner, T.L., Hu, Z., Da, M., Li, X., Guan, H., Shan, D., Lu, J., Huang, C., and Dong, Q. (2012). Impaired mitochondrial function in murine oocytes is associated with controlled ovarian hyperstimulation and in vitro maturation. Reprod. Fertil. Dev. *24*, 945–952.

Geuns, E., De Rycke, M., Van Steirteghem, A., and Liebaers, I. (2003). Methylation imprints of the imprint control region of the SNRPN-gene in human gametes and preimplantation embryos. Hum. Mol. Genet. *12*, 2873–2879.

Geuns, E., De Temmerman, N., Hilven, P., Van Steirteghem, A., Liebaers, I., and De Rycke, M. (2007). Methylation analysis of the intergenic differentially methylated region of DLK1-GTL2 in human. Eur. J. Hum. Genet. *15*, 352–361.

Gibson, T.C., Kubisch, H.M., and Brenner, C.A. (2005). Mitochondrial DNA deletions in rhesus macaque oocytes and embryos. Mol. Hum. Reprod. *11*, 785–789.

Gleicher, N., Kushnir, V.A., and Barad, D.H. (2015). Is it time for a paradigm shift in understanding embryo selection? Reprod. Biol. Endocrinol. *13*, 3.

Glujovsky, D., Blake, D., Farquhar, C., and Bardach, A. (2012). Cleavage stage versus blastocyst stage embryo transfer in assisted reproductive technology. Cochrane Database Syst Rev CD002118.

Gonzalez-Rodriguez, P., Cantu, J., O'Neil, D., Seferovic, M.D., Goodspeed, D.M., Suter, M.A., and Aagaard, K.M. (2016). Alterations in expression of imprinted genes from the H19/IGF2 loci in a multigenerational model of intrauterine growth restriction (IUGR). Am. J. Obstet. Gynecol. *214*, 625.e1–625.e11.

Goto, T., Jones, G.M., Lolatgis, N., Pera, M.F., Trounson, A.O., and Monk, M. (2002). Identification and characterisation of known and novel transcripts expressed during the final stages of human oocyte maturation. Mol. Reprod. Dev. *62*, 13–28.

Hajj, El, N., Trapphoff, T., Linke, M., May, A., Hansmann, T., Kuhtz, J., Reifenberg, K., Heinzmann, J., Niemann, H., Daser, A., et al. (2011). Limiting dilution bisulfite (pyro)sequencing reveals parent-specific methylation patterns in single early mouse embryos and bovine oocytes. Epigenetics *6*, 1176–1188.

Hansen, M., and Bower, C. (2014). The impact of assisted reproductive technologies on intra-uterine growth and birth defects in singletons. Semin Fetal Neonatal Med *19*, 228–233.

Helmerhorst, F.M., Perquin, D.A.M., Donker, D., and Keirse, M.J.N.C. (2004). Perinatal outcome of singletons and twins after assisted conception: a systematic review of controlled studies. Bmj *328*, 261.

Himes, K.P., Young, A., Koppes, E., Stolz, D., Barak, Y., Sadovsky, Y., and Chaillet, J.R. (2015). Loss of inherited genomic imprints in mice leads to severe disruption in placental

lipid metabolism. Placenta *36*, 389–396.

Hirasawa, R., Chiba, H., Kaneda, M., Tajima, S., Li, E., Jaenisch, R., and Sasaki, H. (2008). Maternal and zygotic Dnmt1 are necessary and sufficient for the maintenance of DNA methylation imprints during preimplantation development. Genes & Development *22*, 1607–1616.

Houghton, F.D. (2006). Energy metabolism of the inner cell mass and trophectoderm of the mouse blastocyst. Differentiation *74*, 11–18.

Houghton, F.D., Humpherson, P.G., Hawkhead, J.A., Hall, C.J., and Leese, H.J. (2003). Na+, K+, ATPase activity in the human and bovine preimplantation embryo. Dev. Biol. *263*, 360–366.

Huntriss, J., Hinkins, M., Oliver, B., Harris, S.E., Beazley, J.C., Rutherford, A.J., Gosden, R.G., Lanzendorf, S.E., and Picton, H.M. (2004). Expression of mRNAs for DNA methyltransferases and methyl-CpG-binding proteins in the human female germ line, preimplantation embryos, and embryonic stem cells. Mol. Reprod. Dev. *67*, 323–336.

Ibala-Romdhane, S., Al-Khtib, M., Khoueiry, R., Blachère, T., Guérin, J.F., and Lefèvre, A. (2011). Analysis of H19 methylation in control and abnormal human embryos, sperm and oocytes. Eur. J. Hum. Genet. *19*, 1138–1143.

Ikeda, S., Koyama, H., Sugimoto, M., and Kume, S. (2012). Roles of one-carbon metabolism in preimplantation period--effects on short-term development and long-term programming--. J. Reprod. Dev. *58*, 38–43.

Ishihara, O., Araki, R., Kuwahara, A., Itakura, A., Saito, H., and Adamson, G.D. (2014). Impact of frozen-thawed single-blastocyst transfer on maternal and neonatal outcome: an analysis of 277,042 single-embryo transfer cycles from 2008 to 2010 in Japan. Fertil. Steril. *101*, 128–133.

Ishii, T., Miyazawa, M., Onodera, A., Yasuda, K., Kawabe, N., Kirinashizawa, M., Yoshimura, S., Maruyama, N., Hartman, P.S., and Ishii, N. (2011). Mitochondrial reactive oxygen species generation by the SDHC V69E mutation causes low birth weight and neonatal growth retardation. Mitochondrion *11*, 155–165.

Jackson, R.A., Gibson, K.A., Wu, Y.W., and Croughan, M.S. (2004). Perinatal outcomes in singletons following in vitro fertilization: a meta-analysis. Obstet Gynecol *103*, 551–563.

Jacobs, L., Gerards, M., Chinnery, P., Dumoulin, J., de Coo, I., Geraedts, J., and Smeets, H. (2007). mtDNA point mutations are present at various levels of heteroplasmy in human oocytes. Mol. Hum. Reprod. *13*, 149–154.

Kanber, D., Buiting, K., Zeschnigk, M., Ludwig, M., and Horsthemke, B. (2009). Low frequency of imprinting defects in ICSI children born small for gestational age. Eur. J. Hum. Genet. *17*, 22–29.

Kappil, M.A., Green, B.B., Armstrong, D.A., Sharp, A.J., Lambertini, L., Marsit, C.J., and

Chen, J. (2015). Placental expression profile of imprinted genes impacts birth weight. Epigenetics *10*, 842–849.

Keefe, D.L., Niven-Fairchild, T., Powell, S., and Buradagunta, S. (1995). Mitochondrial deoxyribonucleic acid deletions in oocytes and reproductive aging in women. Fertil. Steril. *64*, 577–583.

Khosla, S., Dean, W., Reik, W., and Feil, R. (2001). Culture of preimplantation embryos and its long-term effects on gene expression and phenotype. Human Reproduction Update *7*, 419–427.

Khoueiry, R., Ibala-Romdhane, S., Al-Khtib, M., Blachère, T., Lornage, J., Guérin, J.F., and Lefèvre, A. (2012). Abnormal methylation of KCNQ1OT1 and differential methylation of H19 imprinting control regions in human ICSI embryos. Zygote 1–10.

Kobayashi, H., Sakurai, T., Sato, S., Nakabayashi, K., Hata, K., and Kono, T. (2012). Imprinted DNA methylation reprogramming during early mouse embryogenesis at the Gpr1-Zdbf2 locus is linked to long cis-intergenic transcription. FEBS Lett. *586*, 827–833.

Korosec, S., Ban Frangez, H., Verdenik, I., Kladnik, U., Kotar, V., Virant-Klun, I., and Vrtacnik Bokal, E. (2014). Singleton pregnancy outcomes after in vitro fertilization with fresh or frozen-thawed embryo transfer and incidence of placenta praevia. Biomed Res Int *2014*, 431797.

Korosec, S., Frangez, H.B., Steblovnik, L., Verdenik, I., and Bokal, E.V. (2016). Independent factors influencing large-for-gestation birth weight in singletons born after in vitro fertilization. J Assist Reprod Genet *33*, 9–17.

Larsson, N.G., Wang, J., Wilhelmsson, H., Oldfors, A., Rustin, P., Lewandoski, M., Barsh, G.S., and Clayton, D.A. (1998). Mitochondrial transcription factor A is necessary for mtDNA maintenance and embryogenesis in mice. Nat Genet *18*, 231–236.

Lee, M.B., Kooistra, M., Zhang, B., Slow, S., Fortier, A.L., Garrow, T.A., Lever, M., Trasler, J.M., and Baltz, J.M. (2012). Betaine homocysteine methyltransferase is active in the mouse blastocyst and promotes inner cell mass development. J. Biol. Chem. *287*, 33094–33103.

Lee, S.T., Oh, S.J., Lee, E.J., Han, H.J., and Lim, J.M. (2006). Adenosine triphosphate synthesis, mitochondrial number and activity, and pyruvate uptake in oocytes after gonadotropin injections. Fertil. Steril. *86*, 1164–1169.

Lei, T., Guo, N., Tan, M.-H., and Li, Y.-F. (2014). Effect of mouse oocyte vitrification on mitochondrial membrane potential and distribution. J. Huazhong Univ. Sci. Technol. Med. Sci. *34*, 99–102.

Li, B., Chen, S., Tang, N., Xiao, X., Huang, J., Jiang, F., Huang, X., Sun, F., and Wang, X. (2016). Assisted Reproduction Causes Reduced Fetal Growth Associated with Downregulation of Paternally Expressed Imprinted Genes That Enhance Fetal Growth in Mice. Biol. Reprod. *94*, 45.

Li, T., Vu, T.H., Ulaner, G.A., Littman, E., Ling, J.-Q., Chen, H.-L., Hu, J.-F., Behr, B., Giudice, L., and Hoffman, A.R. (2005). IVF results in de novo DNA methylation and histone methylation at an Igf2-H19 imprinting epigenetic switch. Mol. Hum. Reprod. *11*, 631–640.

Li, X., Ito, M., Zhou, F., Youngson, N., Zuo, X., Leder, P., and Ferguson-Smith, A.C. (2008). A maternal-zygotic effect gene, Zfp57, maintains both maternal and paternal imprints. Developmental Cell *15*, 547–557.

Li, Z., Wang, Y.A., Ledger, W., and Sullivan, E.A. (2014). Birthweight percentiles by gestational age for births following assisted reproductive technology in Australia and New Zealand, 2002-2010. Hum. Reprod. *29*, 1787–1800.

López-Abad, M., Iglesias-Platas, I., and Monk, D. (2016). Epigenetic Characterization of CDKN1C in Placenta Samples from Non-syndromic Intrauterine Growth Restriction. Front Genet *7*, 62.

Lu, S.C. (2000). S-Adenosylmethionine. Int. J. Biochem. Cell Biol. *32*, 391–395.

Ludwig, M., Katalinic, A., Gross, S., Sutcliffe, A., Varon, R., and Horsthemke, B. (2005). Increased prevalence of imprinting defects in patients with Angelman syndrome born to subfertile couples. J. Med. Genet. *42*, 289–291.

Macdonald, W.A., and Mann, M.R.W. (2014). Epigenetic regulation of genomic imprinting from germ line to preimplantation. Mol. Reprod. Dev. *81*, 126–140.

Madan, P., Rose, K., and Watson, A.J. (2007). Na/K-ATPase beta1 subunit expression is required for blastocyst formation and normal assembly of trophectoderm tight junction-associated proteins. J. Biol. Chem. *282*, 12127–12134.

Madeleneau, D., Buffat, C., Mondon, F., Grimault, H., Rigourd, V., Tsatsaris, V., Letourneur, F., Vaiman, D., Barbaux, S., and Gascoin, G. (2015). Transcriptomic analysis of human placenta in intrauterine growth restriction. Pediatr. Res. *77*, 799–807.

Maheshwari, A., Griffiths, S., and Bhattacharya, S. (2011). Global variations in the uptake of single embryo transfer. Human Reproduction Update *17*, 107–120.

Manipalviratn, S., Tong, Z.-B., Stegmann, B., Widra, E., Carter, J., and DeCherney, A. (2011). Effect of vitrification and thawing on human oocyte ATP concentration. Fertil. Steril. *95*, 1839–1841.

Mann, M.R.W., Lee, S.S., Doherty, A.S., Verona, R.I., Nolen, L.D., Schultz, R.M., and Bartolomei, M.S. (2004). Selective loss of imprinting in the placenta following preimplantation development in culture. Development *131*, 3727–3735.

Market-Velker, B.A., Fernandes, A.D., and Mann, M.R.W. (2010a). Side-by-side comparison of five commercial media systems in a mouse model: suboptimal in vitro culture interferes with imprint maintenance. Biol. Reprod. *83*, 938–950.

Market-Velker, B.A., Denomme, M.M., and Mann, M.R.W. (2012). Loss of genomic

imprinting in mouse embryos with fast rates of preimplantation development in culture. Biol. Reprod. *86*, 143–1–16.

Market-Velker, B.A., Zhang, L., Magri, L.S., Bonvissuto, A.C., and Mann, M.R.W. (2010b). Dual effects of superovulation: loss of maternal and paternal imprinted methylation in a dose-dependent manner. Hum. Mol. Genet. *19*, 36–51.

Martinez-Pastor, B., Cosentino, C., and Mostoslavsky, R. (2013). A Tale of Metabolites: The Cross-Talk between Chromatin and Energy Metabolism. Cancer Discovery *3*, 497–501.

Martínez-Reyes, I., Diebold, L.P., Kong, H., Schieber, M., Huang, H., Hensley, C.T., Mehta, M.M., Wang, T., Santos, J.H., Woychik, R., et al. (2016). TCA Cycle and Mitochondrial Membrane Potential Are Necessary for Diverse Biological Functions. Molecular Cell *61*, 199–209.

McMinn, J., Wei, M., Schupf, N., Cusmai, J., Johnson, E.B., Smith, A.C., Weksberg, R., Thaker, H.M., and Tycko, B. (2006). Unbalanced placental expression of imprinted genes in human intrauterine growth restriction. Placenta *27*, 540–549.

Meldrum, D.R., Casper, R.F., Diez-Juan, A., Simón, C., Domar, A.D., and Frydman, R. (2016). Aging and the environment affect gamete and embryo potential: can we intervene? Fertil. Steril. *105*, 548–559.

Motluk, A. (2016). Ontario funds one cycle of IVF--while supplies last. Cmaj *188*, E32.

Motta, P.M., Nottola, S.A., Makabe, S., and Heyn, R. (2000). Mitochondrial morphology in human fetal and adult female germ cells. Human Reproduction *15 Suppl 2*, 129–147.

Nakamura, T., Arai, Y., Umehara, H., Masuhara, M., Kimura, T., Taniguchi, H., Sekimoto, T., Ikawa, M., Yoneda, Y., Okabe, M., et al. (2007). PGC7/Stella protects against DNA demethylation in early embryogenesis. Nat. Cell Biol. *9*, 64–71.

Nakamura, T., Liu, Y.-J., Nakashima, H., Umehara, H., Inoue, K., Matoba, S., Tachibana, M., Ogura, A., Shinkai, Y., and Nakano, T. (2012). PGC7 binds histone H3K9me2 to protect against conversion of 5mC to 5hmC in early embryos. Nature *486*, 415–419.

Okae, H., Chiba, H., Hiura, H., Hamada, H., Sato, A., Utsunomiya, T., Kikuchi, H., Yoshida, H., Tanaka, A., Suyama, M., et al. (2014). Genome-wide analysis of DNA methylation dynamics during early human development. PLoS Genet *10*, e1004868.

Okun, N., and Sierra, S. (2014). Pregnancy outcomes after assisted human reproduction. J Obstet Gynaecol Can *36*, 64–83.

Petrussa, L., Van de Velde, H., and De Rycke, M. (2014). Dynamic regulation of DNA methyltransferases in human oocytes and preimplantation embryos after assisted reproductive technologies. Mol. Hum. Reprod. *20*, 861–874.

Pikó, L., and Chase, D.G. (1973). Role of the mitochondrial genome during early development in mice. Effects of ethidium bromide and chloramphenicol. J. Cell Biol. *58*,

357–378.

Pinborg, A., Henningsen, A.A., Loft, A., Malchau, S.S., Forman, J., and Andersen, A.N. (2014). Large baby syndrome in singletons born after frozen embryo transfer (FET): is it due to maternal factors or the cryotechnique? Hum. Reprod. *29*, 618–627.

Quenneville, S., Verde, G., Corsinotti, A., Kapopoulou, A., Jakobsson, J., Offner, S., Baglivo, I., Pedone, P.V., Grimaldi, G., Riccio, A., et al. (2011). In embryonic stem cells, ZFP57/KAP1 recognize a methylated hexanucleotide to affect chromatin and DNA methylation of imprinting control regions. Molecular Cell *44*, 361–372.

Reddy, U.M., Wapner, R.J., Rebar, R.W., and Tasca, R.J. (2007). Infertility, assisted reproductive technology, and adverse pregnancy outcomes: executive summary of a National Institute of Child Health and Human Development workshop. pp. 967–977.

Reinhardt, K., Dowling, D.K., and Morrow, E.H. (2013). Medicine. Mitochondrial replacement, evolution, and the clinic. Science *341*, 1345–1346.

Rivera, R.M., Stein, P., Weaver, J.R., Mager, J., Schultz, R.M., and Bartolomei, M.S. (2008). Manipulations of mouse embryos prior to implantation result in aberrant expression of imprinted genes on day 9.5 of development. Hum. Mol. Genet. *17*, 1–14.

Runge, J.S., Raab, J.R., and Magnuson, T. (2016). Epigenetic Regulation by ATP-Dependent Chromatin-Remodeling Enzymes: SNF-ing Out Crosstalk. Curr. Top. Dev. Biol. *117*, 1–13.

Sakian, S., Louie, K., Wong, E.C., Havelock, J., Kashyap, S., Rowe, T., Taylor, B., and Ma, S. (2015). Altered gene expression of H19 and IGF2 in placentas from ART pregnancies. Placenta *36*, 1100–1105.

Savage, T., Peek, J., Hofman, P.L., and Cutfield, W.S. (2011). Childhood outcomes of assisted reproductive technology. Hum. Reprod. *26*, 2392–2400.

Sazonova, A., Källen, K., Thurin-Kjellberg, A., Wennerholm, U.-B., and Bergh, C. (2012). Obstetric outcome in singletons after in vitro fertilization with cryopreserved/thawed embryos. Hum. Reprod. *27*, 1343–1350.

Schieve, L.A., Meikle, S.F., Ferre, C., Peterson, H.B., Jeng, G., and Wilcox, L.S. (2002). Low and very low birth weight in infants conceived with use of assisted reproductive technology. N. Engl. J. Med. *346*, 731–737.

Shamsi, M.B., Govindaraj, P., Chawla, L., Malhotra, N., Singh, N., Mittal, S., Talwar, P., Thangaraj, K., and Dada, R. (2013). Mitochondrial DNA variations in ova and blastocyst: implications in assisted reproduction. Mitochondrion *13*, 96–105.

Shi, X., Chen, S., Zheng, H., Wang, L., and Wu, Y. (2014). Abnormal DNA Methylation of Imprinted Loci in Human Preimplantation Embryos. Reprod Sci.

Smiraglia, D.J., Kulawiec, M., Bistulfi, G.L., Gupta, S.G., and Singh, K.K. (2008). A novel role for mitochondria in regulating epigenetic modification in the nucleus. Cancer Biol. Ther.

7, 1182–1190.

Steptoe, P.C., and Edwards, R.G. (1978). Birth after the reimplantation of a human embryo. Lancet *2*, 366.

Strawn, E.Y., Jr, Bick, D., and Swanson, A. (2010). Is it the patient or the IVF? Beckwith-Wiedemann syndrome in both spontaneous and assisted reproductive conceptions. Fertil. Steril. *94*, 754.e1–754.e2.

Styer, A.K., Luke, B., Vitek, W., Christianson, M.S., Baker, V.L., Christy, A.Y., and Polotsky, A.J. (2016). Factors associated with the use of elective single-embryo transfer and pregnancy outcomes in the United States, 2004-2012. Fertil. Steril.

Sunderam, S., Kissin, D.M., Crawford, S.B., Folger, S.G., Jamieson, D.J., and Barfield, W.D. (2014). Assisted reproductive technology surveillance - United States, 2011. MMWR Surveill Summ *63 Suppl 10*, 1–28.

Sunderam, S., Kissin, D.M., Crawford, S.B., Folger, S.G., Jamieson, D.J., Warner, L., Barfield, W.D., Centers for Disease Control and Prevention (CDC) (2015). Assisted Reproductive Technology Surveillance - United States, 2013. MMWR Surveill Summ *64*, 1–25.

Takikawa, S., Wang, X., Ray, C., Vakulenko, M., Bell, F.T., and Li, X. (2013). Human and mouse ZFP57 proteins are functionally interchangeable in maintaining genomic imprinting at multiple imprinted regions in mouse ES cells. Epigenetics *8*, 1268–1279.

Teperino, R., Schoonjans, K., and Auwerx, J. (2010). Histone methyl transferases and demethylases; can they link metabolism and transcription? Cell Metab *12*, 321–327.

Thouas, G.A., Trounson, A.O., and Jones, G.M. (2006). Developmental effects of sublethal mitochondrial injury in mouse oocytes. Biol. Reprod. *74*, 969–977.

Thundathil, J., Filion, F., and Smith, L.C. (2005). Molecular control of mitochondrial function in preimplantation mouse embryos. Mol. Reprod. Dev. *71*, 405–413.

Tsukada, Y.-I., Fang, J., Erdjument-Bromage, H., Warren, M.E., Borchers, C.H., Tempst, P., and Zhang, Y. (2006). Histone demethylation by a family of JmjC domain-containing proteins. Nature *439*, 811–816.

Tunster, S.J., Jensen, A.B., and John, R.M. (2013). Imprinted genes in mouse placental development and the regulation of fetal energy stores. Reproduction *145*, R117–R137.

Turan, N., Katari, S., Gerson, L.F., Chalian, R., Foster, M.W., Gaughan, J.P., Coutifaris, C., and Sapienza, C. (2010). Inter- and intra-individual variation in allele-specific DNA methylation and gene expression in children conceived using assisted reproductive technology. PLoS Genet *6*, e1001033.

Ubaldi, F.M., Capalbo, A., Colamaria, S., Ferrero, S., Maggiulli, R., Vajta, G., Sapienza, F., Cimadomo, D., Giuliani, M., Gravotta, E., et al. (2015). Reduction of multiple pregnancies in

the advanced maternal age population after implementation of an elective single embryo transfer policy coupled with enhanced embryo selection: pre- and post-intervention study. Hum. Reprod. *30*, 2097–2106.

Van Blerkom, J., Manes, C., and Daniel, J.C. (1973). Development of preimplantation rabbit embryos in vivo and in vitro. I. An ultrastructural comparison. Dev. Biol. *35*, 262–282.

Van Blerkom, J. (2011). Mitochondrial function in the human oocyte and embryo and their role in developmental competence. Mitochondrion *11*, 797–813.

Venkatesh, S., Kumar, M., Sharma, A., Kriplani, A., Ammini, A.C., Talwar, P., Agarwal, A., and Dada, R. (2010). Oxidative stress and ATPase6 mutation is associated with primary ovarian insufficiency. Arch. Gynecol. Obstet. *282*, 313–318.

Wakefield, S.L., Lane, M., and Mitchell, M. (2011). Impaired mitochondrial function in the preimplantation embryo perturbs fetal and placental development in the mouse. Biol. Reprod. *84*, 572–580.

Wallace, D.C. (2010). The epigenome and the mitochondrion: bioenergetics and the environment. Genes & Development *24*, 1571–1573.

Wallace, D.C., and Fan, W. (2010). Energetics, epigenetics, mitochondrial genetics. Mitochondrion *10*, 12–31.

Watson, A.J., Natale, D.R., and Barcroft, L.C. (2004). Molecular regulation of blastocyst formation. Animal Reproduction Science *82-83*, 583–592.

Wellen, K.E., Hatzivassiliou, G., Sachdeva, U.M., Bui, T.V., Cross, J.R., and Thompson, C.B. (2009). ATP-citrate lyase links cellular metabolism to histone acetylation. Science *324*, 1076–1080.

Wennerholm, U.-B., Henningsen, A.-K.A., Romundstad, L.B., Bergh, C., Pinborg, A., Skjaerven, R., Forman, J., Gissler, M., Nygren, K.-G., and Tiitinen, A. (2013). Perinatal outcomes of children born after frozen-thawed embryo transfer: a Nordic cohort study from the CoNARTaS group. Hum. Reprod. *28*, 2545–2553.

White, C.R., Denomme, M.M., Tekpetey, F.R., Feyles, V., Power, S.G.A., and Mann, M.R.W. (2015). High Frequency of Imprinted Methylation Errors in Human Preimplantation Embryos. Sci Rep *5*, 17311.

Wilding, M., Dale, B., Marino, M., di Matteo, L., Alviggi, C., Pisaturo, M.L., Lombardi, L., and De Placido, G. (2001). Mitochondrial aggregation patterns and activity in human oocytes and preimplantation embryos. Human Reproduction *16*, 909–917.

Wisborg, K., Ingerslev, H.J., and Henriksen, T.B. (2010). In vitro fertilization and preterm delivery, low birth weight, and admission to the neonatal intensive care unit: a prospective follow-up study. Fertil. Steril. *94*, 2102–2106.

Wolf, D.P., Mitalipov, N., and Mitalipov, S. (2015). Mitochondrial replacement therapy in

reproductive medicine. Trends Mol Med *21*, 68–76.

Woods, D.C., and Tilly, J.L. (2015). Autologous Germline Mitochondrial Energy Transfer (AUGMENT) in Human Assisted Reproduction. Semin. Reprod. Med. *33*, 410–421.

Yamada, M., Emmanuele, V., Sanchez-Quintero, M.J., Sun, B., Lallos, G., Paull, D., Zimmer, M., Pagett, S., Prosser, R.W., Sauer, M.V., et al. (2016). Genetic Drift Can Compromise Mitochondrial Replacement by Nuclear Transfer in Human Oocytes. Cell Stem Cell *18*, 749–754.

Yan, L., Yang, M., Guo, H., Yang, L., Wu, J., Li, R., Liu, P., Lian, Y., Zheng, X., Yan, J., et al. (2013). Single-cell RNA-Seq profiling of human preimplantation embryos and embryonic stem cells. Nat. Struct. Mol. Biol. *20*, 1131–1139.

Zander-Fox, D., Cashman, K.S., and Lane, M. (2013). The presence of 1 mM glycine in vitrification solutions protects oocyte mitochondrial homeostasis and improves blastocyst development. J Assist Reprod Genet *30*, 107–116.

Zhang, B., Denomme, M.M., White, C.R., Leung, K.-Y., Lee, M.B., Greene, N.D.E., Mann, M.R.W., Trasler, J.M., and Baltz, J.M. (2015). Both the folate cycle and betaine-homocysteine methyltransferase contribute methyl groups for DNA methylation in mouse blastocysts. Faseb J. *29*, 1069–1079.

Zhao, X.-M., Du, W.-H., Wang, D., Hao, H.-S., Liu, Y., Qin, T., and Zhu, H.-B. (2011a). Effect of cyclosporine pretreatment on mitochondrial function in vitrified bovine mature oocytes. Fertil. Steril. *95*, 2786–2788.

Zhao, X.-M., Du, W.-H., Wang, D., Hao, H.-S., Liu, Y., Qin, T., and Zhu, H.-B. (2011b). Recovery of mitochondrial function and endogenous antioxidant systems in vitrified bovine oocytes during extended in vitro culture. Mol. Reprod. Dev. *78*, 942–950.

Zhao, X.-M., Fu, X.-W., Hou, Y.-P., Yan, C.-L., Suo, L., Wang, Y.-P., Zhu, H.-B., Dinnyés, A., and Zhu, S.-E. (2009). Effect of vitrification on mitochondrial distribution and membrane potential in mouse two pronuclear (2-PN) embryos. Mol. Reprod. Dev. *76*, 1056–1063.

Zuo, X., Sheng, J., Lau, H.-T., McDonald, C.M., Andrade, M., Cullen, D.E., Bell, F.T., Iacovino, M., Kyba, M., Xu, G., et al. (2012). Zinc finger protein ZFP57 requires its co-factor to recruit DNA methyltransferases and maintains DNA methylation imprint in embryonic stem cells via its transcriptional repression domain. J. Biol. Chem. *287*, 2107–2118.

Appendices

Copyright Release

White, C.R., Denomme, M.M., Tekpetey, F.R., Feyles, V., Power, S.G.A., and Mann, M.R.W. (2015). High Frequency of Imprinted Methylation Errors in Human Preimplantation Embryos. Sci Rep *5*, 17311.

From: Nature Permissions
To: Carlee White
RE: Permission to Use Copyrighted Material in a Doctoral Thesis
Date: June 17th, 2016 at 4:21 AM

Dear Carlee,

Thank you for contacting Nature Publishing Group. As an author, you have the right to use this manuscript and figures, as per the licence-to-publish you signed:
Ownership of copyright in the article remains with the Authors, and provided that, when reproducing the Contribution or extracts from it, the Authors acknowledge first and reference publication in the Journal, the Authors retain the following non-exclusive rights:a) To reproduce the Contribution in whole or in part in any printed volume (book or thesis) of which they are the author(s).
b) They and any academic institution where they work at the time may reproduce the Contribution for the purpose of course teaching.
c) To post a copy of the Contribution as accepted for publication after peer review (in Word or Tex format) on the Authors' own web site or institutional repository, or the Authors' funding body's designated archive, six months after publication of the printed or online edition of the Journal, provided that they also give a hyperlink from the Contribution to the Journals web site.
d) To reuse figures or tables created by them and contained in the Contribution in other works created by them.

The above use of the term 'Contribution' refers to the author's own version, not the final version as published in the Journal.

Kind Regards,

Claire Smith

Senior Rights Assistant
SpringerNature

Copyright Release

White, C.R., Macdonald, W.A., and Mann, M.R.W. (2016). Conservation of DNA Methylation Programming Between Mouse and Human Gametes and Preimplantation Embryos. Biol. Reprod; doi: 10.1095/biolreprod.116.140319

From: Production Desk
To: Carlee White
RE: Permission to Use Copyrighted Material in a Doctoral Thesis
Date: August 1st, 2016 at 2:42 PM

Dear Carlee:

Thank you for your email. Since you are an author on the paper in question, you do not need to secure written permission from SSR. It is SSR policy that authors may reuse their own work provided that the source paper is cited specifically. This information is found in the "Copyright Transfer" section of the Biology of Reproduction Authorship form, "The SSR, in turn, grants to each author the right of republication in any work of which she/he is the author or editor, subject only to giving proper credit to the original journal publication of the article."

Please let us know if you have additional questions.

Sincerely,

Katina Ashworth

Biology of Reproduction
Managing Editor's Office

Curriculum Vitae

Carlee Rees White

EDUCATION

Ph.D., Biochemistry and Developmental Biology   09/2011-present
Western University, Schulich School of Medicine and Dentistry, London, Ontario. Assisted reproductive technologies disrupt genomic imprinting in human and mitochondria in mouse embryos.

Bachelor of Science, honors specialization in genetics   09/2007-04/2011
With distinction, Western Scholars, with Thesis, Changing substrate specificity of *Arabidopsis thaliana* AROGENATE DEHYDRATASES (ADTs), 2007-2011.

Pauline Johnson Collegiate and Vocational School Diploma   09/2003-06/2007
Honor roll, Governor General's Bronze Medal Award

SCHOLARSHIPS AND AWARDS

Scholarships
- Ontario Graduate Scholarship/Queen Elizabeth II Graduate Scholarship in Science and Technology (OGS/QEII), Ph.D., 2013-2016
- CIHR Reproduction, Early development, and the Impact on Health (REDIH) Scholarship- PhD, 2011-2015- declined scholarships
- Canadian Institute of Health Research (CIHR) Master's Award: Frederick Banting and Charles Best Canada Graduate Scholarships, M.Sc., 2012-2013
- OGS/QEIIGSST, 2012/2013- declined
- Ontario Graduate Scholarship (OGS)- Master's, 2011/2012
- Western Graduate Research Scholarship (WGRS), 2011-2015
- Queen Elizabeth II Aiming for the Top Scholarship, 2007-2011
- UWO In-Course Scholarship Year IV, 2011

Awards
- Runner up, 2015 Lawson Leadership Award
- First Prize oral presentation- 2014 Paul Harding Research Awards Day, 05/15/2014.
- Second Prize oral presentation- 47th Annual Southwestern Ontario Reproductive Biology Meeting (SORB), 05/02/2014
- Collaborative Graduate Program in Developmental Biology Student Award, 2011/2012
- Western Scholars, The University of Western Ontario, 2011
- Western Undergraduate Research Forum Top Oral Presentation- Thesis student, 2011
- Dean's Honor Roll, The University of Western Ontario, 2007-Present.

WORK EXPERIENCE

The Fertility Clinic, London Health Sciences Centre (LHSC)   11/2014-present
REI Technologist
- Sperm preparation for IVF/ICSI, oocyte retrieval, insemination (IVF and ICSI), embryo transfer, embryo culture, oocyte and embryo vitrification and warming
- Sperm analyses for initial program assessments (viscosity, sperm count, viability, morphology, motility and progression), sperm preparation for intrauterine insemination (IUI) and donor insemination (DI), and sperm freeze/thaw

Summer Research Student (Dr. Mellissa Mann)   05/11-08/11
Children's Health Research Institute (CHRI)
- Developed techniques to isolate mouse oocytes and preimplantation embryos
- Vitrification of mouse oocytes and embryos
- Single embryo bisulfite mutagenesis protocol

Research Thesis (Dr. Susanne Kohalmi)   09/2010-04/2011
- PCR technique to introduce random point mutations into a family of plant enzymes
- Cloning in *E. coli* and yeast homologous recombination

PEER REVIEWED PUBLICATIONS
1. **Carlee R. White**, William A. MacDonald and Mellissa R.W. Mann. (2016). Conservation of DNA Methylation Programming Between Mouse and Human Gametes and Preimplantation Embryos, Biol. Reprod. Published July 27th, 2016; doi: 10.1095/biolreprod.116.140319
2. **Carlee R. White**, Michelle M. Denomme, Francis R Tekpetey, Valter Feyles, Stephen GA Power and Mellissa R.W. Mann (2015). High frequency of imprinted methylation errors in human preimplantation embryos. *Scientific Reports* **5**, 17311; doi: 10.1038/srep17311
3. William A. MacDonald, Saqib S. Sachani, **Carlee R. White** and Mellissa R.W.Mann. (2016). A role for chromatin topology in imprinted domain regulation. *Biochemistry and cell biology* **94**, 1-13.
4. Baohua, Zhang, Michelle M. Denomme, **Carlee R. White,** Kit-Ye Leung, Martin B. Lee, Nicholas D. E. Greene, Mellissa R. W. Mann, Jaquetta M. Trasler, and Jay M. Baltz (2014). Both the folate cycle and betaine-homocysteine methyltransferase contribute methyl groups for DNA methylation in mouse blastocysts. *FASEB* **2(29)**, 1-11.
5. Alfonso Gutierrez Adan, **Carlee R. White**, Ann Van Soom, Mellissa R. W. Mann (2014). Why we should not select the faster embryo: lessons from mice and cattle. *Reproduction, Fertility and* Development, DOI: 10.1071/RD14216
6. Michelle M Denomme, **Carlee R White**, Carolina Gillio-Meina, William A MacDonald, Bonnie J Deroo, Gerald M Kidder, Mellissa RW Mann (2012). Compromised fertility disrupts Peg1 but not Snrpn and Peg3 imprinted methylation acquisition in mouse oocytes. *Frontiers in Genetics* **3 (129)**, 1-11.

MANUSCRIPTS SUBMITTED OR IN PREPARATION

1. Charles A. Ishak, Aren Marshall, Daniel T. Passos, **Carlee R. White**, Matthew J. Cecchini, Sara Ferwati, William A. Macdonald, Christopher J. Howlett, Ian D. Welch, Seth M. Rubin, Mellissa R. W. Mann, and Frederick A. Dick. An RB-EZH2 complex mediates cell cycle independent silencing of repetitive DNA sequences, manuscript under review (submitted to Molecular Cell April 19, 2016)
2. **Carlee R. White** and Mellissa R.W. Mann. Superovulation leads to disruption in mitochondrial pools, dynamics and function in mouse oocytes and preimplantation embryos, manuscript in preparation.
3. Saqib S. Sachani, Lauren S. Landschoot, Liyue Zhang, **Carlee R. White**, William A. MacDonald, Michael C. Golding and Mellissa, R.W. Mann. Nucleoporin-mediated regulation of a genomic imprinted domain, manuscript in preparation.

PUBLISHED ABSTRACTS

1. **Carlee R. White** and Mellissa R.W. Mann. Effects of Superovulation on Mitochondrial Distribution and Genomic Imprint Maintenance in Mouse Oocytes and Preimplantation Embryos. Society for the Study of Reproduction (SSR) Meeting 2014.
2. **Carlee R. White** and Mellissa R.W. Mann. Effects of Oocyte Vitrification on Genomic Imprinting. Society of the Study of Reproduction (SSR) Meeting 2013

PRESENTATIONS

1. **Carlee R. White** and Mellissa R.W. Mann. The effect of superovulation on mitochondria in mouse oocytes and preimplantation embryos. REDIH Meeting, Ottawa, ON, December 2nd, 2015, Oral.
2. **Carlee R. White**, Michelle M. Denomme, Francis R Tekpetey, Valter Feyles, Stephen GA Power and Mellissa R.W. Mann. High frequency of imprinted methylation errors in human preimplantation embryos. REDIH Meeting, Ottawa, Ontario, June 2nd, 2015, Oral.
3. **Carlee R. White**, Michelle M. Denomme, Francis R Tekpetey, Valter Feyles, Stephen GA Power and Mellissa R.W. Mann. High frequency of imprinted methylation errors in human preimplantation embryos. Paul Harding Research Day, London, Ontario, May 13th, 2015, Oral.
4. **Carlee R. White**, Michelle M. Denomme, Francis R Tekpetey, Valter Feyles, Stephen GA Power and Mellissa R.W. Mann. High frequency of imprinted methylation errors in human preimplantation embryos. SORB Research Day, Hamilton, ON, May 1st, 2015, Oral.
5. **Carlee R. White** and Mellissa R.W.Mann. Effects of superovulation on mitochondrial distribution and genomic imprint maintenance in mouse oocytes and preimplantation embryos. SSR 2014 Meeting, Grand Rapids, Michigan, July 20th, 2014, Oral.
6. **Carlee R. White** and Mellissa R.W.Mann. Effects of superovulation on mitochondrial distribution and genomic imprint maintenance in mouse oocytes and preimplantation embryos. Epigenetics, Eh! Meeting, London, Ontario, June 25th 2014, Poster.
7. **Carlee R. White** and Mellissa R.W.Mann. Effects of superovulation on mitochondrial distribution and genomic imprint maintenance in mouse oocytes and preimplantation

embryos. REDIH Meeting, Ottawa, Ontario, June 3rd, 2014, Poster.

8. **Carlee R. White** and Mellissa R.W.Mann. Effects of superovulation on mitochondrial distribution and genomic imprint maintenance in mouse oocytes and preimplantation embryos. Collaborative Program in Developmental Biology Annual Meeting, May 30th 2014, Poster

9. **Carlee R. White** and Mellissa R.W.Mann. Effects of superovulation on mitochondrial distribution and genomic imprint maintenance in mouse oocytes and preimplantation embryos. Paul Harding Research Day, London, Ontario, May 14th, 2014, Oral

10. **Carlee R. White** and Mellissa R.W.Mann. Effects of superovulation on mitochondrial distribution and genomic imprint maintenance in mouse oocytes and preimplantation embryos. SORB Research day, May 2nd, 2014, Oral.

11. **Carlee R. White** and Mellissa R.W.Mann. Effects of superovulation on mitochondrial distribution and genomic imprint maintenance in mouse oocytes and preimplantation embryos. London Health Research Day, March 18th, 2014. Poster.

12. **Carlee R. White** and Mellissa R.W. Mann. Effects of Oocyte Vitrification on Genomic Imprinting. Society of the Study of Reproduction (SSR) 2013 Meeting, Montreal, Quebec, July 24th, 2013, Poster.

13. **White, C.R**., and Mann, M.R. Effects of assisted reproductive technologies on cytoplasmic lattices, maternal mitochondria and genomic imprint maintenance in mouse. Reproduction, Early Development, and the Impact on Health Meeting, London, Ontario, June 13th, 2013, Poster.

14. **White, C.R**., and Mann, M.R. Effects of assisted reproductive technologies on cytoplasmic lattices, maternal mitochondria and genomic imprint maintenance in mouse. Developmental Biology Research Day, London, Ontario, May 30th, 2013, Poster.

15. **White, C.R**., and Mann, M.R. Effects of assisted reproductive technologies on cytoplasmic lattices, maternal mitochondria and genomic imprint maintenance in mouse. Department of Obstetrics and Gynaecology Paul Harding Research Day, London, Ontario, May 1st, 2013, Poster

16. **White, C.R**., and Mann, M.R Effects of assisted reproductive technologies (ARTs) on maternal mitochondria and genomic imprint maintenance in mouse. Reproduction, Early Development, and the Impact on Health Meeting, Ottawa, Ontario, December 6th, 2012, Poster.

17. **White, C.R**., and Mann, M.R. Investigating the effects of vitrification on imprint establishment in oocytes and maintenance in preimplantation embryos. Reproduction, Early Development, and the Impact on Health Meeting, Ottawa, Ontario, June 21st, 2012, Poster.

18. **White, C. R**., and Mann, M.R. The effects of vitrification on imprint establishment in oocytes and maintenance in preimplantation embryos. Developmental Biology Research Day, London, Ontario, May 31st, 2012, Poster.

19. **White, C. R**., and Mann, M.R. The effects of vitrification on imprint establishment in oocytes and maintenance in preimplantation embryos. Department of Obstetrics and Gynaecology Paul Harding Research Day, London, Ontario, May 9th, 2012, Poster.

20. **White, C. R**., and Mann, M.R. The effects of vitrification on imprint establishment in oocytes and maintenance in preimplantation embryos. Great Lakes Mammalian Development meeting, April 14th, 2012, Poster.

21. **White, C. R**., and Mann, M.R. The effects of vitrification on imprint establishment in oocytes and maintenance in preimplantation embryos. Reproduction, Early Development, and the Impact on Health meeting, December 2011, Poster.
22. **White, C.R**., and Kohalmi, S.E. Changing substrate specificity of *Arabidopsis thaliana* AROGENATE DEHYDRATASES (ADTs), Ontario Biology Day, May 2011, Oral presentation.
23. **White, C.R**., and Kohalmi, S.E. Changing substrate specificity of *Arabidopsis thaliana* AROGENATE DEHYDRATASES (ADTs), Western Undergraduate Research Forum, May 2011, Oral presentation.
24. **White, C.R**., and Kohalmi, S.E. Changing substrate specificity of *Arabidopsis thaliana* AROGENATE DEHYDRATASES (ADTs), Western Biology Day, May 2011, Oral presentation.

TEACHING

Mentorship
- Taylor Smith, Co-op College Student (Fleming College)- 05/15-08/14
- Dorothy Kessler, Co-op High School Student- 02/12-06/12

Tutoring
- Third Year Genetics Tutor, The University of Western Ontario- 2013
- Second Year Genetics Tutor, The University of Western Ontario- 2012
- Emily Thomson, High School Calculus Student- 2010

SERVICE

Committees
- Canadian Fertility and Andrology Society (CFAS) member- 2015-present
- CFAS ART Lab SIG Junior executive member- 2015-present
- REDIH training program member- 2011-present
- Lawson Association of Fellows and Students (LAFS)- 2012-present
- Developmental Biology Student Representative- 2013-present
- CHRI Journal Club- 2011- present
- CHRI Student Seminar Series - 2011- present
- Society for the Study of Reproduction- 2013-2015
- CHRI student representative at Partner's in Research awards dinner- 2013
- CHRI Change Bandits for Children's- 2012-2013
- Member of the Society of Developmental Biology (SDB)- 2012
- Member of the Society of the Study of Reproduction (SSR)- 2013
- Volunteer, Shinerama- 2007
- Western Soccer Club- 2007-2008
- National Pee-wee Fast pitch Championship- tournament scorekeeper- 2006

Extracurricular activities
- London United Recreational Soccer League, London, Ontario- 2015-present

- Stratford Co-ed Soccer League, Stratford, Ontario- 2014-present
- London Women's Indoor Soccer League, London, Ontario- 2013-present
- Kensal Park Women's Soccer League, London, Ontario- 2013-2015
- Intramural Outdoor Soccer, The University of Western Ontario- 2012-present
- London Hospital's Co-ed Slo-pitch League (LHCSL)- 2012-2014
- Intramural Volleyball, The University of Western Ontario- 2008-2013
- Intramural Beach Volleyball, The University of Western Ontario- 2012-2013
- Intramural Inner Tube Water Polo, The University of Western Ontario- 2011-2012
- London Volley's Co-Ed Volleyball League- 2011
- Intramural Indoor Soccer, The University of Western Ontario- 2009-2011
- Rotary Brantford Classic Run - 2010
- Ontario Women's Soccer League (OWSL)- 2009-2010
- Intramural Dodgeball- 2009/2010
- Intramural Basketball, The University of Western Ontario- 2007-2008
- Royal Conservatory of Music, level 7 piano (level 6 theory)